UNIVERSITY OF CALIFORNIA
RIVERSIDE

Analysis of the *S. cerevisiae* Telomere Capping Protein Stn1's Function in Global DNA Replication and S phase Checkpoint Control

A Dissertation submitted in partial satisfaction
of the requirements for the degree of

Doctor of Philosophy

in

Cell, Molecular, and Developmental Biology

by

Hovik J. Gasparyan

August 2013

Dissertation Committee:

Dr. Connie Nugent, Chairperson
Dr. Jeffery Bachant
Dr. Morris Maduro
Dr. Yinsheng Wang

The Dissertation of Hovik J. Gasparyan is approved:

_____

_____

_____

_____

Committee Chairperson

University of California, Riverside

ACKNOWLEDGEMENTS

The work presented in this dissertation would not have been possible without the endless patience, support, guidance, encouragement, and friendship I have received from numerous people over the last seven years.

First, I would like to thank my major professor, Dr. Connie Nugent, for being an excellent mentor. When I came to UC Riverside as a graduate student in the fall of 2006, I had virtually no experience working in a molecular biology laboratory. However, Connie was incredibly generous in allowing me to join her lab. Because of her outstanding guidance and continual patience with my many shortcomings in the lab, I feel that I have mastered many techniques in a variety of disciplines, including molecular biology, cell biology, biochemistry, and genetics. Additionally, Connie has taught me how to work independently and think critically when analyzing data, designing and executing experiments, and reading scientific literature. I believe that these qualities are absolutely essential for a successful scientific career. For these reasons and much, much more, I am truly grateful to Connie for her never-ending support and guidance.

I also owe a tremendous debt of gratitude to Dr. Jeff Bachant for his mentorship throughout my graduate career. Jeff not only served on my guidance committee and chaired my qualifying exam, he has also been directly involved in the development of my thesis project. Jeff always contributes valuable insights in our weekly lab meetings, constantly providing a unique perspective and challenging me to explore new ideas. His expertise in the DNA replication and checkpoint fields have been an invaluable resource for my graduate work.

I would also like to thank Dr. Morris Maduro for serving on both my dissertation and qualifying exam committees. Despite working in an unrelated field, Morris always imparts valuable advice and helpful suggestions in our meetings, providing a fresh point of view. He is extremely supportive, continually encouraging me to have high expectations in my scientific career through perseverance and hard work.

I'm greatly appreciative for Dr. Yinsheng Wang's generous offer to serve on my dissertation committee on such short notice. Additionally, I would like to thank two faculty members outside of UCR, Oscar Aparicio and Wenyi Feng, for providing both intellectual and technical assistants on this project.

Throughout my time in Connie's lab, I've been very fortunate in having had a wonderful set of labmates as my colleagues. When I started working for Connie, Ruben Petreaca, Ling Xu and Vanessa Small were all senior graduate students in the lab. All three were extremely encouraging, welcoming me into their research group. I'm especially grateful to Ruben, for taking time out of his busy schedule to train me. Additionally, I would like to thank the graduate students that joined Connie's lab after me; Hank Hsieh, Chris Caridi, Tim Ngo and Tim Tran. All of them have been incredibly supportive, and constantly provide valuable intellectual contributions. Furthermore, I am deeply appreciative for the numerous talented undergraduates in our lab, as well as the members of Jeff Bachant's lab, for both their scientific contributions and friendship.

Lastly, I want to extend a very special thanks to my family and friends for all their love, support and patience. Thanks mom, dad, Srpouhi (and family), grandparents, uncles and aunts, cousins, and Graciel. I love you guys! I couldn't have done it without you!

DEDICATION

I dedicate this dissertation to my grandparents, who instilled in me, from a very young age, the virtues of hard work, diligence, respect and integrity.

ABSTRACT OF THE DISSERTATION

Analysis of the *S. cerevisiae* Telomere Capping Protein Stn1's Function in Global DNA Replication and S phase Checkpoint Control

by

Hovik J. Gasparyan

Doctor of Philosophy, Graduate Program in Cell, Molecular, and Developmental Biology
University of California, Riverside, August 2013
Dr. Connie Nugent, Chairperson

Telomeres, the nucleoprotein structures that comprise the natural ends of eukaryotic chromosomes, play a critical role in maintaining genomic stability. Their essential function is to cap chromosome ends, thus preventing these natural ends from being inappropriately fused to one-another or repaired by resection/recombination. Telomeres are distinct from internal DNA double-stranded breaks because they do not elicit a DNA damage checkpoint response. In addition to their capping function, telomeres also help overcome the DNA end-replication problem. Because all DNA polymerases synthesize only in the 5' to 3' direction and require a pre-existing 3' hydroxyl group as a primer, the most terminal portion of a chromosome cannot be completely duplicated. Through the concerted actions of two enzymes, telomerase and DNA polymerase alpha (Pol-α), telomeres are able to facilitate complete and faithful duplication of the entire genome. Both the capping of ends and their complete replication are integral in maintaining genomic stability. In the budding yeast *S. cerevisiae*, three proteins, Cdc13, Stn1 and Ten1, participate in both the capping and replication of telomeres. The three proteins are

hypothesized to form a heterotrimeric complex (CST), which binds to chromosome termini, forming a physical cap. Furthermore, Cdc13 has been shown to physically interact with telomerase, and all three CST components interact with Pol-α. Genetic analysis suggests that these interactions are critical for efficient replication of telomeres. Current models within the field propose that Cdc13 first recruits telomerase to the chromosome end, which uses an intrinsic RNA template to elongate one of the DNA strands. Then, Pol-α is recruited to the end, which "fills-in" the complementary strand to achieve full duplication of the telomere. There are several outstanding questions within this model. 1) How is the switch between telomerase dependent elongation and Pol-α dependent fill-in synthesis regulated? 2) Are these two events temporally separated, or are they coordinated? 3) Does the CST complex simply recruit Pol-α to the end, or does it facilitate its catalytic activity? 4) Can the CST complex regulate Pol-α dependent synthesis at non-telomeric sites throughout the genome? The majority of research presented in this dissertation examines the hypothesis that Stn1 can facilitate global DNA replication in budding yeast. Using a variety of genetic, biochemical, cellular and molecular biology approaches, we demonstrate that Stn1 has newly discovered roles in DNA metabolism in addition to its previously characterized function at the telomere. In chapter 3, we analyze the functional significance of the interactions between the CST complex and Pol-α, in both telomere capping and length regulation. The results demonstrate that multiple redundant interactions between the capping and replication complexes reinforce each other, thereby generating functional telomeres.

TABLE OF CONTENTS

LIST OF FIGURES

Introduction

Chapter 1

Chapter 2

Chapter 3

LIST OF TABLES

Chapter 1

Chapter 2

Chapter 3

Introduction

Telomere Capping and Chromosome End Replication: Two Sides of the Same Coin

Before DNA was identified as the genetic material of cells and its structure was determined, experiments in Barbara McClintock's and Hermann Muller's labs demonstrated that telomeres have very unique and specialized properties. Discoveries by these early pioneers of molecular genetics revealed that telomeres afford protection to chromosomes. Without these stabilizing "caps" chromosomes would either get completely lost or undergo fusion events (Muller, 1938; McClintock 1938; McClintock, 1941). From these observations, it was inferred that telomeres function to prevent the natural ends of chromosomes from being recognized as damage, thus functioning as an "anti-checkpoint" (Michelson *et al*, 2005). In the absence of telomeres, cells sense chromosome ends as being broken (Sandell and Zakian, 1993), and attempt to repair them via non-homologous end joining (NHEJ). This leads to the creation of di-centric chromosomes, which break as cells attempt to segregate them during mitosis (Mieczkowski *et al*, 2003; Pobiega and Marcand, 2010). These profound discoveries early in the history of molecular biology highlighted the fundamental role of telomeres in ensuring the integrity of a cell's genetic material.

In addition to their end-protection function, telomeres were found to facilitate the replication of chromosome ends. When James Watson and Francis Crick reported the structure of DNA in their landmark paper in 1953, they proposed an elegant model for its replication. Watson and Crick determined that a DNA molecule is comprised of two strands of nucleotides, base-paired to one-another in a complementary fashion, with the

strands wrapped around each other forming an anti-parallel double-helix (Watson and Crick, 1953). They hypothesized that during DNA replication the two strands could denature, and serve as templates for the synthesis of two new strands. This semi-conservative model of DNA replication was later shown to be correct (Meselson and Stahl, 1958); however, a critical problem was realized. Since polymerases synthesize DNA in only one direction and require an RNA primer, the most terminal portion of a linear DNA molecule could not be replicated, on at least one of the strands (Watson, 1972; Olovnikov, 1973). If the end of a chromosome was blunt or contained a 5' overhang, the product generated by lagging strand synthesis would be shorter than the parental strand after removal of the terminal primer. However, if chromosome end contained a 3' overhang, as was later shown to be the case (Henderson and Blackburn, 1989), then the product generated by leading strand synthesis would be shorter than the parental strand (Lingner *et al*, 1995). Because of this "end-replication problem", cells that maintain their genomes on linear chromosomes would lose a small amount of genetic information with each replication cycle (Figure 0-1).

The end-replication problem has several important implications regarding cell division and proliferation. First, it was postulated that in order for cells to grow and divide for a substantial number of generations, they must have a means to counteract the gradual erosion occurring at chromosome ends. This mechanism would have to exist in all unicellular eukaryotes, and at least in the germline cells of metazoans. Second, in the somatic cells of higher eukaryotes, the inability to maintain the ends of chromosomes could serve as a molecular clock, that could be a determinant of aging. According to this

model, cells have a limited replicative capacity, which in turn limits the number of division cycles they can undergo. Experiments carried out by Leonard Hayflick demonstrated that human fetal cells could only be cultured for approximately 50 generations before the population would senesce (Hayflick, 1965). This observation, now referred to as the "Hayflick limit", suggested that without a counteracting mechanism, the gradual erosion of telomeres caused by the end-replication problem would eventually lead to cell death. Interestingly, a small fraction of the cells in the culture were able to escape senescence, and essentially become immortalized. Although the precise mechanism by which cells maintain their telomeres was not known during this time, this finding provided insights to a better understanding of tumor formation and cancer. By circumventing the end replication problem, cancerous cells are able to replicate indefinitely and become immortalized (Feldser *et al*, 2003; Verdun and Karlseder, 2007).

The mechanism by which cells maintain their chromosome ends was discovered in 1985 in the Blackburn lab. Using the ciliated protozoan *Tetrahymena thermophila* as their model system, the Blackburn group was able to demonstrate that these cells contained an enzyme capable of adding terminal repetitive sequences to a linear DNA molecule (Greider and Blackburn, 1985). This enzyme, now termed telomerase, functions as a reverse transcriptase. Telomerase uses an intrinsic RNA template to catalyze the addition of repetitive G-rich sequences to the 3' ends of chromosomes (Singer and Gottschling, 1994; Lingner *et al*, 1997b). The complementary C-rich strand is subsequently synthesized by DNA polymerase alpha (Pol-α) and DNA polymerase delta (Adams and Holm, 1996; Diede and Gottschling, 1999; Adams-Martin *et al*, 2000; Qi

and Zakian 2000). Through the activity of these two enzymes, cells are able to counteract the gradual erosion of chromosome ends, and overcome the end-replication problem.

Telomerase is a ubiquitous enzymes found in nearly all eukaryotes, from ciliates and yeasts to plants and animals (Cech and Lingner, 1997; Vega *et al*, 2003). The telomeric sequence itself has diverged somewhat throughout the course of evolution, but the strand terminating with 3' is always enriched in guanine (G-strand) and the complementary 5' strand is enriched in cytosine (C-strand). The 3' end is always longer than the 5' end in all species, resulting in a G-strand overhang (Chakhparonian and Wellinger, 2003). Cloning heterologous telomeric sequences from ciliates or mammals onto the ends of yeast chromosomes is sufficient to cap the ends, suggesting that end-protection is not an inherent property of the specific telomere sequence of an organism (Szostak and Blackburn, 1982**;** Shampay *et al*, 1984; Henning *et al*, 1998). Rather, telomere capping is achieved by the connexus of proteins that assemble onto the chromosome end. The telomeric DNA sequence functions to recruit the appropriate proteins to protect the ends. Although different eukaryotes have evolved distinct mechanisms to cap their telomeres, end protection appears to be fairly dynamic, with unique sets of challenges throughout the cell cycle. Intriguingly, in nearly every species, the capping complexes appear to also function in telomere replication, suggesting that these two processes are inherently related (Gilson and Géli, 2007; de Lange, 2009; Giraud-Panis *et al*, 2010; Price *et al*, 2010; Sampathi and Chai, 2011; Stewart *et al*, 2011).

Telomere capping by single-stranded DNA binding proteins

The telomeric DNA of all eukaryotes is comprised of both single-stranded and duplex regions. The very ends of chromosomes terminate with a 3' single-stranded G-rich overhang (Wellinger and Sen, 1997). The length of this overhang varies among species, ranging from 10-15 nucleotides in yeasts and ciliates to >100 in mammals (Chakhparonian and Wellinger, 2003). The overhang serves as a binding site for distinct sets of telomere capping proteins in different species (Figure 0-2). One such protein initially discovered in the budding yeast *S. cerevisiae* is Cdc13. *CDC13* was first identified in Hartwell's cell division cycle screens as a gene that when mutated, elicits a *RAD9* dependent DNA damage checkpoint response (Garvik *et al*, 1995). Analysis of the type and location of the damage responsible for checkpoint activation revealed that *cdc13-1* mutants accumulated aberrant amounts of telomeric single-stranded DNA (ssDNA). Through both *in vitro* and *in vivo* studies, Cdc13 was shown to have a very specific telomeric ssDNA binding activity (Nugent *et al*, 1996; Lin and Zakian, 1996; Lin *et al*, 2001). In its absence, the 5' ends of chromosomes undergo exonucleolytic degradation in the telomere to centromere direction. The extent of this degradation is normally limited by the DNA damage checkpoint, but can extend internally up to 30kB, far beyond the telomeric repeats and subtelomeric elements (Garvik and Hartwell, 1995; Booth *et al*, 2001). These findings implied that the essential function of Cdc13 is to cap the ends of chromosomes, protecting against inappropriate exonucleolytic activities.

In addition to Cdc13, two other end-binding proteins, Stn1 and Ten1, function to protect against nucleolytic degradation of telomeres in budding yeast. *STN1* is an

essential gene that was identified as a dosage suppressor of the *cdc13-1* mutation (Grandin *et al*, 1997). Similarly, *TEN1* was isolated in a screen as a dosage suppressor of a conditional *stn1* mutation (Grandin *et al*, 2001). Loss of function of either Stn1 or Ten1 leads to compromised end-protection, causing aberrant accumulation of terminal ssDNA, similar to *cdc13* mutants (Grandin *et al*, 1997; Grandin *et al*, 2001; Petreaca *et al*, 2007; Puglisi *et al*, 2008; Xu *et al*, 2009). Mutations within *STN1* or *TEN1* also lead to the formation of extrachromosomal telomeric circles (t-circles) in some budding yeast species, implying that these proteins normally prevent recombination at telomeres (Iyer *et al*, 2005; Sun *et al*, 2009; Basenko *et al*, 2010). Whether Cdc13 functions to prevent t-circle formation remains to be seen. In addition to their genetic interactions, Cdc13, Stn1 and Ten1 all appear to interact physically, as assessed by two-hybrid analysis (Grandin *et al*, 2001; Petreaca *et al*, 2006; Petreaca *et al*, 2007; Puglisi *et al*, 2008; Xu *et al*, 2009). Stn1 and Ten1 have also been crystallized as a complex from several species of yeasts (Sun *et al*, 2009; Gelinas *et al*, 2009), but a direct *in vitro* interaction with Cdc13 has not been demonstrated to date. The crystal structure of the Cdc13 DNA binding domain has been solved (Mitton-Fry *et al*, 2002; Mitton-Fry *et al*, 2004), and structural prediction algorithms implicate the existence of multiple oligonucleotide/oligosaccharide binding (OB-fold) domains throughout the protein (Theobald and Wuttke, 2004). Superimposition of the Cdc13-Stn1-Ten1 predicted structure upon the replication protein A (RPA) crystal structure reveals remarkably conserved domain architecture (Sun *et al*, 2009; Gelinas *et al*, 2009). This has lead to the suggestion that Cdc13, Stn1 and Ten1

may form a heterotrimeric RPA-like complex, termed the CST complex, at telomeres (Gao *et al*, 2007; Paschini *et al*, 2010).

Until recently, the CST capping proteins were only thought to exist in budding yeast species. *S. pombe* and mammalian cells use an entirely different protein, Pot1, to cap their ends (Baumann and Cech, 2001). Although Pot1 contains two OB-fold domains and associates with the telomeric 3' overhang, it is not an ortholog of the budding yeast Cdc13 (Theobald and Wuttke, 2004). The two proteins do not share similar structural features or sequence homology, and use differential mechanisms to associate with DNA (Lei *et al*, 2004). However, Pot1 functions to cap the ends of telomeres in a manner analogous to Cdc13. Fission yeast cells lacking Pot1 rapidly lose their telomeric sequences due to exonucleolytic degradation, and activate a DNA damage response (Baumann and Cech, 2001). Amazingly, some *pot1*$^{-}$ cells are able to survive by circularizing their chromosomes. Similarly, mammalian cells deficient for POT1 accumulate DNA damage foci containing γH2AX, 53BP1 and MDC1 at their telomeres, and activate the ATR (Mec1) checkpoint response (Wu *et al*, 2006; Denchi and de Lange, 2007; Hockemeyer *et al*, 2007). These observations initially led to the speculation that fission yeast and higher eukaryotes utilized a different strategy from budding yeast to execute chromosome end protection. However, CST-like proteins have been discovered in many species within the last few years.

STN1 and *TEN1* homologs were first identified in *S. pombe* by sequence alignment and structural prediction algorithms (Martin *et al*, 2007). Although the primary amino acid sequences have diverged significantly through evolution, Stn1 and Ten1 from

various species display remarkable conservation of their three-dimensional structures (Horvath, 2011). As in budding yeast, Stn1 and Ten1 in *S. pombe* physically interact, and localize to telomeres. Deletion of either gene leads to rapid loss of telomeric sequence, and circularization of chromosomes similar to *POT1* deletion (Martin *et al*, 2007). Stn1 and Ten1 do not physically interact with Pot1, supporting the idea that Pot1 is not an ortholog of Cdc13 (Martin *et al*, 2007). To date, no *CDC13* homolog has been reported in *S. pombe*. These findings indicating that fission yeast have evolved to utilize two separate end-capping mechanisms to protect their telomeres.

Shortly after the discovery of *STN1* and *TEN1* in fission yeast, CST-like proteins were reported in the flowering plant *Arabidopsis thaliana* (Song *et al*, 2008; Surovtseva *et al*, 2009). The *STN1* homolog appears to be fairly conserved, but *CDC13* has diverged significantly, and is therefore termed *CTC1* (conserved telomere maintenance component 1). No *TEN1* homolog has been reported in plants as of this writing. Both STN1 and CTC1 localize to telomeres, as assessed by fluorescence microscopy. Mutations in *stn1* and *ctc1* lead to loss of telomeric DNA sequences and generation of t-circles. Mutant cells also display chromosome end-to-end fusions, which lead to the generation of di-centric chromosomes and anaphase bridges during mitosis (Song *et al*, 2008; Surovtseva *et al*, 2009). These processes result in the activation of an ATR-dependent DNA damage checkpoint, and stimulate apoptosis in some cells (Amiard *et al*, 2011; Boltz *et al*, 2012). In addition to the CST capping proteins, plant cells also contain multiple paralogs of the *POT1* gene. However, plant POT1 appears to function as part of the telomerase

holoenzyme, rather than a capping component (Cifuentes-Rojas *et al*, 2011). This highlights how dynamic and rapidly evolving telomere capping can be.

In parallel with the findings from plants, mammalian cells were also shown to contain a CST complex (Wan *et al*, 2009; Miyake *et al*, 2009; Surovtseva *et al*, 2009). Homologs for *STN1* and *TEN1* have been identified, and as with plants, the largest component is called *CTC1*. Although *STN1* (*OBFC1*) and *CTC1* had been encountered in older studies as DNA Pol-α accessory proteins, they were not recognized as homologs of the yeast telomere capping proteins until much later (Goulian and Heard, 1990; Goulian *et al*, 1990; Casteel *et al*, 2009). All three proteins within the mammalian CST complex physically interact and associate with telomeric ssDNA. Knocking down expression of *CTC1* or *STN1* results in degradation of the telomeric C-strand, and stimulates formation of telomeric DNA damage foci (Miyake *et al*, 2009; Surovtseva *et al*, 2009). The CST complex appears to function independently of POT1 in telomere capping, as knocking down both *STN1* and *POT1* causes a synergistic induction of DNA damage foci (Miyake *et al*, 2009). Interestingly, both POT1 and STN1 have been shown to interact physically with TPP1, one of the bridging factors within the shelterin complex that connects ssDNA binding proteins to duplex DNA binding proteins (Hockemeyer *et al*, 2007; Wang *et al*, 2007; Xin *et al*, 2007; Wan *et al*, 2009). More recently, CTC1 was found to interact with POT1 through co-immunoprecipitation experiments (Wu *et al*, 2012). These findings indicate that the CST complex may be more intimately associated with shelterin than was initially anticipated.

Capping contributions of duplex binding proteins

The majority of the telomere sequence in eukaryotes is comprised of double-stranded DNA (dsDNA). Several distinct classes of telomeric dsDNA binding proteins have been identified, each working in parallel with ssDNA binding proteins to facilitate chromosome end protection. In *S. cerevisiae*, the major dsDNA binding protein is Rap1, along with its two interacting factors Rif1 and Rif2 (Lustig *et al*, 1990; Hardy *et al*, 1992; Wotton and Shore, 1997). At the telomere, the Rap1-Rif1-Rif2 complex functions in both length regulation and capping (Chen *et al*, 2011). In addition to its role at telomeres, Rap1 functions in regulating transcription (Shore and Nasmyth, 1987). Although *RAP1* is an essential gene, its function at the telomere has been dissected using a C-terminal truncation allele, which fails to interact with Rif1 and Rif2 (Marcand *et al*, 1997b). *Rap1* mutants display increased chromosome end-to-end fusions, suggesting a role in inhibiting NHEJ (Pardo and Marcand, 2005). Intriguingly, Rap1 appears to inhibit telomeric NHEJ through two genetically distinct, separable pathways. One pathway requires interaction with Rif2 through Rap1's C-terminal domain, whereas a second pathway functions through the central domain, and is independent of Rif1 and Rif2 (Marcand *et al*, 2008). The Rap1-Rif1-Rif2 complex also appears to function in blocking resection of ends (Bonetti *et al*, 2010; Vodenicharov *et al*, 2010; Anbalagan *et al*, 2011). This function was not fully appreciated until recently, possibly because loss of capping following inactivation of the Rap1-complex does not lead to activation of a robust DNA damage response. Rap1's role in telomere capping is more prominent in G1, whereas the CST complex is required for capping in S and G2/M phases of the cell cycle (Bonetti *et al*,

2010; Vodenicharov *et al*, 2010). Interestingly, *cdc13 rif1* and *stn1 rif1* double mutants show a synthetic capping defect, accumulating telomeric single-stranded DNA even when arrested in G2, suggesting that the CST and Rap1 complexes make independent contributions to end protection (Anbalagan *et al*, 2011).

Telomeres in budding yeast also associate with a second dsDNA binding protein, the Ku70/80 heterodimer (Ku) (Gravel *et al*, 1998). Ku has numerous functions in DNA metabolic processes, including promotion of NHEJ and inhibition of homologous recombination at breaks, regulation of the timing of origin firing, heterochromatin formation, telomere length regulation, and chromosome end capping (Fisher and Zakian 2005; Ribes-Zamora *et al*, 2007). The two subunits of Ku are obligate binding partners, which localize to either double strand breaks or the ends of the duplex region of telomeres. Deletion of either subunit renders the complex non-functional. Ku mutants display increased telomeric ssDNA and have a synthetic phenotype when combined with c*dc13* mutants (Nugent *et al*, 1998; Polotnianka *et al*, 1998). As with the *cdc13-1* mutant, the extent of telomeric ssDNA accumulation in *yku70*-Δ cells is normally limited by the DNA damage checkpoint. In the absence of checkpoint activity, resection can extend several thousand base-pairs into the chromosome (Maringele and Lydall, 2002). Ku functions in an independent, parallel pathway with the Rap1 complex to cap telomeres in G1 (Bonetti *et al*, 2010; Vodenicharov *et al*, 2010). This implies that budding yeast utilize at least three distinct strategies to protect their chromosome ends against the diverse array of nucleolytic activities they encounter through the cell cycle.

In *S. pombe*, the Rap1 protein does not directly bind to telomeric DNA. Rather, it localizes to chromosome ends through an interaction with Taz1, the major telomere dsDNA binding protein in fission yeast (Cooper *et al*, 1997; Kanoh and Ishikawa, 2001). Taz1 also directly interacts with Rif1, independent of its interaction with Rap1 (Kanoh and Ishikawa, 2001). No Rif2 ortholog exists in fission yeast or other eukaryotes outside of budding yeast family. Taz1 has a role in regulation of telomere length, which is partially dependent on both Rap1 and Rif1 (Miller *et al*, 2005; Dehé *et al*, 2012). Taz1 also functions in blocking chromosome end-to-end fusions. This role in telomeric NHEJ inhibition requires Rap1, but is not dependent on Rif1 (Ferreira and Cooper 2001). *S. pombe* chromosome ends are also bound by the Ku complex. Ku's role at fission yeast telomeres is not well characterized, but as in budding yeast, it is proposed to inhibit recombination and exonucleolytic activities at chromosome ends (Baumann and Cech, 2000; Tomita *et al*, 2003). One striking difference between telomere capping in fission yeast as compared with budding yeast is that the dsDNA binding proteins in *S. pombe* physically interact with ssDNA binding proteins. Rap1 associates with Poz1, and Pot1 binds to Tpz1. Poz1 and Tpz1 in turn interact with each other, completing a bridge between the duplex telomeric DNA and the 3' single-stranded overhang (Miyoshi *et al*, 2008). Poz1, Tpz1 and Ccq1 (a Tpz1 interacting factor) all function in end protection. Deletion of $tpz1^{+}$ results in rapid loss of telomeric DNA, and chromosome circularization. Moreover, $poz1^{-}$ $ccq1^{-}$ double mutants phenocopy this telomere protection defect; however, either single mutant is still sufficient for telomere capping, indicating that Poz1

and Ccq1 have overlapping or redundant functions in end protection (Miyoshi *et al*, 2008).

In mammalian cells, the single-stranded overhang can invade the duplex region, forming a structure called a "t-loop". The DNA sequence of mammalian telomeres has a precise TTAGGG repeat, allowing the ssDNA overhang to hybridize completely to the upstream duplex DNA. Because of this, t-loop formation is relatively straightforward in mammalian cells, and these structures can be observed microscopically (Griffith *et al*, 1999). The formation of a t-loop organizes the telomeric chromatin in a manner that promotes interaction between ssDNA and dsDNA binding proteins, analogous to the situation in fission yeast. Six proteins (POT1, TPP1, TIN2, TRF1, TRF2 and RAP1) assemble into a telomere capping complex called shelterin (Palm and de Lange, 2008). POT1 is the only protein within the complex that directly binds to ssDNA. The other five members either bind to dsDNA directly, or associate with the complex through protein-protein interactions.

TRF1 and TRF2, which are homologs of *S. pombe* Taz1, directly bind to the duplex DNA. Both proteins form homodimers, and associate with the telomeric repeats through their C-terminal myb domains (Broccoli *et al*, 1997). Both proteins have roles in telomere capping and length regulation. TRF1 deletion triggers a DNA damage response at telomeres, as assessed by activation of the checkpoint kinases CHK1 and CHK2 (Martinez *et al*, 2009). Similarly, deletion of TRF2 results in rapid and extensive chromosome end-to-end fusions, and accumulation of telomeric DNA damage foci (van Steensel *et al*, 1998). Unlike loss of POT1 which activates an ATR dependent checkpoint,

loss of TRF2 results in an ATM dependent checkpoint response (Denchi and de Lange, 2007). Interestingly, loss of TRF2 does not result in degradation of telomeric DNA. This implies that POT1 protects against exonucleolytic activities which would cause ssDNA accumulation, whereas TRF2 prevents the chromosome ends from being recognized as breaks. The exact nature by which TRF2 inhibits chromosome fusions has not been determined, but one possible mechanism may be through telomeric chromatin re-organization. TRF2 has been shown to induce positive supercoiling of telomeric DNA *in vitro*, which may enhance strand invasion and facilitate t-loop formation (Amiard *et al*, 2007). Thus, TRF2 may prevent the ends of chromosomes from being recognized as substrates for NHEJ.

Mammalian telomeres also associate with RAP1, but as with fission yeast, the protein does not bind DNA directly. Rather, RAP1 localizes to telomeres through an interaction with TRF2 (Bae and Baumann, 2007). RAP1 appears to protect telomeres through two independent pathways. First, it functions in concert with TRF2 to inhibit NHEJ (Sarthy *et al*, 2009). Second, RAP1 represses homology directed repair of telomeres, in a TRF2 independent manner (Sfeir *et al*, 2010). The two other shelterin components, TIN2 and TPP1, appear to function as accessory factors in helping TRF1, TRF2 and POT1 protect chromosome ends. TIN2 can bind to both TRF1 and TRF2 simultaneously, and functions to stabilize the association of these proteins on telomeric DNA (Ye *et al*, 2004). Similarly, TPP1, the homolog of *S. pombe* Tpz1, associates with POT1 and enhances its protective activity (Hockemeyer *et al*, 2007). TPP1 and TIN2 also interact with each other, bridging the ssDNA and dsDNA telomere binding proteins. This

association of the shelterin components results in the physical stabilization of telomeric chromatin, thus preventing the t-loop from spontaneously unraveling. The entire web of interactions to achieve telomere capping in *S. cerevisiae*, *S. Pombe*, and mammalian cells is summarized in Figure 0-2.

Telomere length regulation: telomerase-dependent elongation and C-strand fill-in synthesis

While telomere capping proteins ensure that chromosome ends are not degraded or processed aberrantly as breaks, they also play a critical role in controlling the length of the telomere repeat sequences. The repeat length varies widely in different organisms, ranging from ~300bp in budding yeast to >10,000bp in plant and mammalian cells (Chakhparonian and Wellinger, 2003). However, within a specific organism, telomere length is maintained within a relatively narrow range. Almost all eukaryotes utilize the telomerase enzyme to synthesize the G-rich strand when telomeres become short. The mechanisms that regulate telomerase access and activity at chromosome ends vary among species, but in nearly all cases, telomere capping proteins are integrally involved in these processes.

In budding yeast, the telomerase holoenzyme is comprised of three protein subunits (Est1, Est2 and Est3), and an RNA template (TLC1) (Lundblad and Szostak, 1989; Singer and Gottschling, 1994; Lendvay *et al*, 1996). The Est2 subunit contains the catalytic activity, whereas Est1 and Est3 are accessory factors (Lingner *et al*, 1997b; Evans and Lundblad, 1999; Hughes *et al*, 2000). All four components are required for

telomere maintenance *in vivo*, but Est2 and TLC1 alone are sufficient for elongation of a telomeric seed *in vitro* (Lingner *et al*, 1997a). Telomerase can get recruited to chromosome ends through two genetically separable pathways. First, in the G1 phase of the cell cycle, the Ku80 protein can recruit telomerase through an interaction with TLC1 (Fisher *et al*, 2004). Although this pathway is not essential for telomere maintenance, disruption of the Ku80-TLC1 interaction does lead to a moderate telomere shortening phenotype (Stellwagen *et al*, 2003). The more prominent means for recruiting telomerase to the chromosome end is achieved through an interaction between Est1 and Cdc13 (Nugent *et al*, 1996). Cdc13 recruits Est1 to telomeres in late S phase, facilitating access of the telomerase holoenzyme to ends (Pennock *et al*, 2001; Taggart *et al*, 2002). Disrupting this interaction leads to continual telomere shortening and eventually senescence, resembling a telomerase null mutation (Nugent *et al*, 1996).

Telomerase is not recruited to every chromosome end within each S phase. Rather, the accessibility is somewhat stochastic, with the shortest ends most likely to be extended (Teixeira *et al*, 2004; Chang *et al*, 2007). Cells utilize a "counting" mechanism, dependent on the number of Rap1 proteins associated with each end to maintain a homeostatic telomere length (Marcand *et al*, 1997a). Chromosome ends that are shorter, and thus have fewer Rap1 molecules bound, more efficiently recruit Cdc13, Est1, Est2 and the checkpoint kinase Tel1, which stimulates telomerase activity (Bianchi and Shore, 2007b; Chang et at., 2007; Hector *et al*, 2007; Sabourin *et al*, 2007). Furthermore, Rif1 and Rif2 inhibit telomerase activity at long ends by blocking Tel1 association (Hirano *et*

al, 2009). This creates an auto-regulatory feedback inhibition loop, allowing telomere length to be maintained in a relatively narrow size range (Marcand *et al*, 1999).

Telomere length regulation also appears to be tightly coupled to DNA replication. Both Cdc13 and telomerase interact with the single-stranded DNA binding protein RPA (Luciano *et al*, 2012). Chromosome ends containing short telomeres are replicated at an earlier point in S phase, allowing them to associate with Cdc13 and telomerase more efficiently. The earlier replication is caused by the activation of normally dormant origins found within the subtelomeric Y' and X-elements, rather than by rapid fork progression from more internal, early-firing origins (Bianchi and Shore, 2007a). Consistent with this finding, deletion of Ku results in telomere shortening, and earlier firing of telomere proximal replication origins (Cosgrove *et al*, 2002). This effect can be suppressed by mutations which restore telomere length, indicating that the early firing is directly related to the length of the telomere tract (Lian *et al*, 2011). Telomere addition at an artificially shortened end requires passage of a replication fork as a prerequisite (Dionne and Wellinger, 1998; Marcand *et al*, 2000), and is dependent on the activities of DNA Pol-α-primase and Pol-δ (Diede and Gottschling, 1999). Therefore, the earlier replication of short telomeres gives these ends a greater window of time for elongation by telomerase.

After telomerase extends the G-rich strand, Pol-α synthesizes the complementary C-rich strand. G and C-strand synthesis appears to be coupled in ciliated protozoa, via a physical interaction between telomerase and the lagging strand machinery (Fan and Price, 1997; Ray *et al*, 2002). However, no such interaction has been observed in budding yeast. Rather, Pol-α is thought to be recruited to chromosome termini through interactions with

the CST complex. Cdc13 directly interacts with the catalytic subunit, Pol1 (Qi and Zakian 2000; Sun *et al*, 2011), and Stn1 binds to Pol12, the regulatory B subunit (Grossi *et al*, 2004; Petreaca *et al*, 2006). Disrupting the Pol-α function leads to telomere elongation, usually accompanied by increased terminal ssDNA (Carson and Hartwell, 1985; Adams and Holm, 1996; Adams-Martin *et al*, 2000; Qi and Zakian 2000; Grossi *et al*, 2004). This observation suggests that although G-strand and C-strand synthesis are not directly coupled in *S. cerevisiae*, the two processes are tightly coordinated (Chandra *et al*, 2001). In the absence of efficient C-strand fill-in synthesis, telomerase over-extends the G-strand, leading to elongated, single-stranded chromosome termini.

Telomere length regulation in *S. pombe* is very similar to budding yeast, but a few minor differences will be highlighted here. As with ciliates, telomerase physically interacts with the lagging strand machinery in fission yeast, thus coupling G and C-strand synthesis (Dahlén *et al*, 2003). Telomerase is recruited to chromosome ends via an interaction between Est1 and Ccq1 (Tomita and Cooper, 2008; Moser *et al*, 2011; Yamazaki *et al*, 2012; Webb and Zakian, 2012). Deletion of ccq1 leads to telomere shortening, followed by activation of the checkpoint kinase Chk1 (Tomita and Cooper, 2008). Unlike capping mutants which tend to cause circularization of chromosomes in *S. pombe*, Ccq1 mutants are able to maintain linear chromosomes through an ALT-like recombination dependent pathway (Tomita and Cooper, 2008). The checkpoint kinases Tel1 (ATM) and Rad3 (ATR) promote the Ccq1-Est1 interaction through phosphorylation of the Thr93 residue of Ccq1. Thr93 appears to be the major Tel1/Rad3 target site, as ccq1-T93A mutants fail to interact with Est1, and display a telomere

shortening phenotype (Moser *et al*, 2011; Yamazaki *et al*, 2012). The Ccq1-Est1 interaction is proposed to stabilize the association of the telomerase catalytic subunit, Trt1, with Est1, and thus facilitate formation of the telomerase holoenzyme (Webb and Zakian, 2012). The interactions between Ccq1, Est1 and Trt1, and the dynamics of their regulation by Tel1/Rad3 are directly analogous to the roles of Cdc13, Est1, Est2 and Tel1 in *S. cerevisiae*.

In mammalian cells, TRF1 and TRF2 regulate telomere length in a manner analogous to the budding yeast Rap1-Rif1-Rif2 complex. Both proteins are negative regulators of telomerase, and overproduction of either one leads to a telomere shortening phenotype. Conversely, loss of function or dominant negative alleles cause telomere elongation (van Steensel and de Lange, 1997; Smogorzewska *et al*, 2000). The exact mechanism by which TRF1 and TRF2 control telomere length is yet to be determined, but neither protein affects telomerase levels in the cell. One model consistent with these findings proposes that TRF1/TRF2 stimulate t-loop formation, thus sequestering the free 3' terminus away, making it inaccessible for extension by telomerase (Smogorzewska *et al*, 2000). Additionally, TRF1 has been proposed to affect telomere length through regulating access of POT1 to the chromosome end (Loayza and de Lange, 2003). Telomerase is recruited to mammalian chromosome ends through an interaction with the POT1-TPP1 subcomplex of shelterin. POT1 was initially found to be a positive regulator of telomere length, but the mechanism by which it elongated telomeres was not known for some time (Colgin *et al*, 2003). Later studies demonstrated that TPP1, rather than POT1, recruits telomerase to the chromosome end. This recruitment is mediated through

an interaction between the catalytic subunit of telomerase, TERT1, and the OB-fold domain of TPP1 (Wang *et al*, 2007; Xin *et al*, 2007). Interestingly, TPP1 and POT1 both appear to enhance telomerase processivity, leading to increased telomere repeat addition. *In vitro* telomere extension assays have shown that individually, each protein contributes positively to telomerase activity; however, as a complex, POT1-TPP1 has a synergistic effect on telomerase processivity (Wang *et al*, 2007). In support of this idea, TPP1 binding to POT1 enhances the complexes association with the telomeric ssDNA overhang, forming a functional module for efficient telomerase recruitment and activation (Xin *et al*, 2007).

C-strand fill-in synthesis appears to be uncoupled from telomerase-dependent G-strand extension in mammalian cells (Zhao *et al*, 2009). However, the mechanistic details of the fill-in synthesis process have not been well characterized to date. The mammalian CST complex has been implicated in limiting excessive G-strand elongation, and promoting C-strand fill-in synthesis (Chen *et al*, 2012; Huang *et al*, 2012; Wang *et al*, 2012). Recent studies have shown that STN1 interacts with TPP1 (Wan *et al*, 2009), and CTC1 binds POT1 (Wu *et al*, 2012). These findings imply that the mammalian CST complex may limit telomere elongation by blocking the association between POT1-TPP1 and telomerase (Chen *et al*, 2012). However, it is also possible that CST directly inhibits telomerase activity. The exact nature of how the CST complex regulates the switch from G-strand extension to C-strand fill-in synthesis still remains elusive, even in yeast model systems. As with budding yeast, the fill-in synthesis at mammalian telomeres is catalyzed by Pol-α (Dai *et al*, 2010). Surprisingly, knockdown of STN1 causes an increase in Pol-α

binding to telomeres; however, the telomeres remain single stranded, presumably from a failure to execute fill-in synthesis (Huang *et al*, 2012). This finding has led to the model in which STN1 modulates the fill-in synthesis activity of Pol-α, rather than its localization at telomeres.

DNA replication across the genome: origin licensing, firing, and fork progression

To maintain the integrity of its genetic material, a cell must faithfully replicate each of its chromosomes precisely once per cell division cycle. The duplicated copies of the genome must then be accurately partitioned to the daughter cells in mitosis. Replication of the genome is a very tightly regulated process. The mechanistic details of DNA replication and their spatio-temporal regulation are highly conserved across all eukaryotic species. These processes have been studied most extensively in *S. cerevisiae*. This section will discuss the fundamentals of eukaryotic DNA replication and its regulation through the cell cycle, highlighting key experimental findings from budding yeast along with insights gleaned from *in vitro* reconstitution experiments.

DNA replication is initiated from specific sites on chromosomes, termed "origins". Each chromosome contains multiple origins of replication, distributed randomly across its length. The first replication origin was identified from budding yeast via cloning experiments. A small restriction fragment from chromosome IV was isolated and subcloned into a plasmid. The presence of this new segment of DNA allowed autonomous replication of the plasmid in yeast cells transformed with the episome (Stinchcomb *et al*, 1979). This observation was the first confirmation in a eukaryotic cell

of Jacob, Brenner and Cuzin's classic replicon hypothesis, which states in part, "any genetic element capable of autonomous replication must possess an origin of replication" (Jacob *et al*, 1963).

Many additional origins of replication were identified in the 1980's and 90's using similar cloning approaches. However, in 2001, two groups mapped out nearly every autonomous replication sequence (ARS) within the budding yeast genome, using modern genomic tools. One group performed ChIP of ORC and MCM, two complexes known to associate with replication origins, across the genome (Wyrick *et al*, 2001). Approximately 80% of the predicted sites were confirmed to behave as ARSs in this study. A second group used Meselson and Stahl's classic isotope density transfer approach, combined with hybridization to genomic microarrays to monitor where replication occurs over time (Raghuraman *et al*, 2001). These two complementary approaches produced a topographical map of both the position and timing of chromosomal replication in budding yeast.

Origin firing is a stochastic process; origins vary in both the timing and efficiency with which they fire. However, these parameters are determined on a population level, and are strictly probabilistic. On a cellular level, one can only predict that an early efficient origin has a higher likelihood of firing than a late, inefficient one (Patel *et al*, 2006). Multiple variables contribute to the replication timing profile of an origin. One of the first factors identified was chromatin context. A series of elegant cloning experiments demonstrated that transposing an early firing ARS element into the heterochromatic subtelomeres rendered it late firing. Conversely, cloning a late firing origin onto a

plasmid advanced its replication timing (Ferguson and Fangman, 1992). These findings imply that the timing of origin firing is not an intrinsic property of a specific ARS element, but a consequence arising from its position within the genome.

In addition to global chromatin context, cis-acting factors adjacent to an origin can also determine its timing. Deletion of ARS adjacent sequences can alter the timing of the nearby origin (Friedman *et al*, 1996). Furthermore, trans acting factors such as histone remodeling protein, transcription factors and even telomere binding proteins can influence the replication timing profile on a global scale (Knott *et al*, 2009; Hayano *et al*, 2012; Knott *et al*, 2012; Tazumi *et al*, 2012). These observations have led to the current model, which claims that the timing of origin firing depends on the sub-nuclear organization of chromatin. According to this model, a limiting set of replication factors are concentrated within a specific region in the nucleus, thus giving the origins within this domain the highest probability of firing (Mantiero *et al*, 2011; Aparicio, 2013). Chromatin organization is dependent on a wide variety of factors, including DNA binding proteins, transcription factors, histone remodeling complexes, and nuclear anchoring proteins. Consequentially, many of these factors which have been implicated in affecting the replication timing profile of the genome may do so indirectly by altering chromatin organization.

All replication origins have the capacity to fire, but not every one is used in each S phase (Patel *et al*, 2006). If a specific origin does not fire, it will be replicated passively from a nearby origin that did initiate. It is imperative that once an origin has either fired or been replicated passively, it does not reinitiate a second time until the next S phase.

Doing so could result in aneuploidy, chromosomal breakage and gross chromosomal rearrangements, all of which contribute to genome instability (Dahmann *et al*, 1995).

Each fired origin produces two replication forks, which progress bi-directionally. At each fork, the leading strand in synthesized continuously by a single polymerase molecule. In contrast, the lagging strand is synthesized discontinuously in multiple pieces, termed Okazaki fragments. Each Okazaki fragment requires priming by Pol-α-primase, followed by elongation by a more processive polymerase (Burgers, 2009). In most eukaryotes, Pol-δ and Pol-ε are essential for DNA replication. However, for a long time, it was not known whether each polymerase is responsible for synthesizing a specific strand, or if both are required for leading and lagging strand synthesis. This problem was resolved in 2007 through an elegant genetic experiment in budding yeast. A reporter gene was cloned adjacent to an early efficient replication origin in two orientations. One orientation would cause it to be replicated via leading strand synthesis, whereas the second would cause it to be replicated via lagging strand synthesis. By compromising the fidelity of Pol-ε and measuring the rate of point mutations in the reporter gene, the Kunkel group was able to demonstrate that Pol-δ synthesizes the lagging strand, while Pol-ε synthesizes the leading strand (Pavlov *et al*, 2006; Purssel *et al*, 2007)

Eukaryotic cells have evolved a highly proficient mechanisms to ensure their DNA is replicated only once per cell cycle. In late M phase, the origin recognition complex (ORC) is loaded onto specific DNA sequences called origins of replication, which can potentially initiate replication during S phase (Bell and Stillman, 1992). Then, in the G1 phase, the Cdc6 and Cdt1 proteins recruit and load the MCM2-7 DNA

replicative helicase complex (MCM complex) onto ORC bound chromatin (Liang *et al*, 1995; Tanaka and Diffley, 2002; Chen *et al*, 2007). During this period, the MCM complex is in an inactive state. Assembly of the ORC and MCM proteins on origins forms a pre-replicative complex (pre-RC). Pre-RC formation "licenses" replication origins, potentiating them to fire (Diffley *et al*, 1994; Donavan *et al*, 1997). At the onset of S phase, the replication machinery is assembled at pre-RC bound origins. Then, two protein kinases, CDK and DDK (Dbf4 dependent kinase, comprised of the Dbf4 regulatory subunit and Cdc7 catalytic subunit), trigger initiation of DNA replication (Labib, 2010; Masai *et al*, 2010). This temporal separation between the licensing and firing steps of replication ensures that each origin can initiate only once per cell cycle.

Assembly of all the components required for origin firing is a very complex and dynamic process. Although the details of replisome assembly are not yet entirely known, biochemical and genetic experiments have deciphered the major events in the initiation phase of DNA replication. After the MCM helicase is loaded onto origins, both CDK and DDK phosphorylate several residues on the complex (Masai *et al*, 2000; Masai *et al*, 2006; Sheu and Stillman 2006; Devault *et al*, 2008). This allows two replisome components, Sld3 and Cdc45, to associate with the MCMs (Yabuuchi *et al*, 2006). In a temporally separate step, CDK phosphorylates Sld3 and a related protein, Sld2 (Tanaka *et al* 2007; Zegerman and Diffley, 2007). This then allows recruitment of yet additional replisome components, such as Dpb11, MCM10, and the GINS complex (Heller *et al*, 2011). To generate a fully active helicase complex, MCM2-7 associates with Cdc45 and GINS, forming the CMG complex (Aparicio *et al*, 1997; Takayama *et al*, 2003). Once the

CMG complex is assembled at an origin, DNA unwinding initiates, and the Pol-α-primase complex is brought in through interactions with Mcm10 (Homesley *et al*, 2000; Ricke and Beilinsky, 2006). This completes assembly of the replisome, and DNA synthesis begins. The major steps in the initiation of DNA replication are summarized in Figure 0-3.

In addition to the core components listed above, several non-essential proteins associate with the replisome during the elongation phase to ensure proper fork progression. One such protein is Mrc1, which was initially identified as a mediator of the replication checkpoint (Alcasabas *et al*, 2001). Mrc1 was shown to travel with the replication fork, ensuring replisome stability (Osborn and Elledge 2003; Szyjka *et al*, 2005). Specifically, Mrc1 bridges Pol-ε to the MCM complex, to ensure coupling of leading strand synthesis to the unwinding activities of the helicases (Lou *et al*, 2008). Similarly, the Ctf4 protein was recently found to associate with Pol-α and fullfil an analogous function on the lagging strand (Gambus *et al*, 2009). Interestingly, although neither *MRC1* nor *CTF4* is essential for viability, deletion of both genes is synthetic lethal (Tong *et al*, 2001; Gambus *et al*, 2009). This suggests that cells can tolerate uncoupling between the MCM helicases and one, but not both replicating strands of a fork, indicating that cells have evolved robust mechanisms with redundant backup pathways to ensure efficient replication of their genome.

Replicating chromosome termini: end-processing and replication fork dynamics through telomeres

Telomere replication presents a unique set of challenges for a cell. Most notably, telomeres are replicated unidirectionally. The most distal origin on a chromosome will produce the terminal fork responsible for replicating the telomere (Raghuraman *et al*, 2001). This final fork must replicate the end of the chromosome in its entirety. Unlike internal replication forks which can potentially be rescued by nearby origins, if the terminal fork collapses, the end of the chromosome will remain un-replicated. Therefore, lesions in telomeres are more likely to lead to replication fork stalling or collapse. Compounding these problems, DNA polymerases are more predisposed to stalling at telomeres because of the repetitive nature of the sequence (Ivessa *et al*, 2003; Makovets *et al*, 2004; Anand *et al*, 2011). Studies from budding yeast show that as a replication fork approaches the telomeric repeat sequence, it will briefly pause. Longer telomeres illicit a more robust pause, and this effect depends on the chromatin context. Internal telomere tracts induce a significantly weaker fork pause. Interestingly, the pause response appears to be independent of telomeric chromatin binding factors, such as Rap1, Rif1, Rif2, Sir2 and Sir3 (Makovets *et al*, 2004). The exact cause of these fork stalling events are not well understood.

As cells complete replication of their telomeres, two distinct types of ends are generated. A chromosome end replicated via leading strand synthesis will produce a blunt-end product. Conversely, its sister chromatid generated via lagging strand synthesis will terminate in a 3’ overhang (Figure 0-1). The two distinct structures are processed

differentially to reconstitute the normal 3' overhang found at chromosome termini (Faure *et al*, 2010). The chromosome end synthesized by the leading strand must undergo a 5' to 3' resection event on the C-rich strand to generate the 3' overhang. These end processing events, which occur in late S phase, are inherently coupled to semi-conservative replication of telomeres. In contrast, the end produced by lagging strand synthesis may require replication fork independent priming and fill-in activities to ensure its complete synthesis (Figure 0-4).

S. cerevisiae telomeres terminate in a short 3' overhang, which persists throughout the cell cycle. However, the size of the overhang is not constant. Current models estimate that for most of the cell cycle the G-tail is ~10-15 nucleotides in length. As cells replicate their telomeres in late S phase, the size of the overhang increases to >30 nucleotides (Wellinger *et al*, 1993). This increase in length is not a result of telomerase dependent extension, as *TLC1* deficient cells also display elongated G-tails in late S phase (Dionne and Wellinger, 1996). Furthermore, the increase in G-tail length requires passage of a replication fork through the telomere (Dionne and Wellinger, 1998). This suggests that the increased terminal ssDNA is a result of either degradation by a nuclease in late S/G2, or incomplete synthesis of the C-strand. A replication fork moving through a telomere may alter the terminal chromatin structure, making the end more accessible to nucleases. Alternatively, as a replication fork approaches the end of a chromosome, leading and lagging strand synthesis may become uncoupled (Moser *et al*, 2009). Because the lagging strand is synthesized discontinuously, such an uncoupling event can generate excess telomeric ssDNA (Figure 0-4). These two models are not mutually

exclusive, and it is likely that both processes contribute to the increase in overhang length in late S phase.

Chromosome ends synthesized by the leading strand terminate with a blunt end, and require processing by the Mre11-Rad50-Xrs2 (MRX) complex to generate the 3' overhang (Larrivée *et al*, 2004; Takata *et al*, 2005). MRX possesses intrinsic endonuclease and helicase activities, and enhances the processivity of a multitude of exonucleases. In the absence of functional MRX, neither Cdc13 nor telomerase are recruited to chromosome ends generated by leading strand synthesis. In contrast, ends generated via lagging strand synthesis do not require MRX activity for Cdc13 and telomerase binding (Faure *et al*, 2010). Furthermore, telomere addition at a "seed" adjacent to an HO induced double strand break also requires MRX processing (Diede and Gottschling, 2001). These observations suggest that MRX activity is a prerequisite to generate the terminal 3' overhang on telomeres synthesized by the leading strand. However, it is not known whether MRX is the only nuclease required for end processing, or if other nucleases are also necessary for proper generation of the 3' overhang.

Chromosome end processing activities are regulated in a cell cycle dependent manner by the Cdk1 kinase. Uncapped telomeres undergo C-strand resection during G2/M phase, but not during G1 or S. Inhibiting Cdk1 function suppresses resection in these capping mutants, suggesting that the nucleases/helicases responsible for telomere C-strand degradation are activated by the Cdk1 kinase (Vodenicharov and Wellinger, 2006; Xu *et al*, 2009). Even when a chromosome end is capped, Cdk1 dependent processing activities are necessary to generate a functional 3' overhang. Blocking Cdk1

prevents telomere addition at a critically short telomere seed adjacent to an HO break (Frank *et al*, 2006). Genetic analysis has revealed that Cdk1 activity is required for a very early step in telomere addition, most likely in the generation of the 3' overhang. The exact substrate that Cdk1 phosphorylates to promote telomere addition remains unknown, but it is likely that there are multiple key targets. For example, in addition to generating the 3' overhang, Cdk1 also phosphorylates Cdc13 to promote telomere addition (Li *et al*, 2009; Tseng *et al*, 2009). These findings demonstrate that Cdk1 is intimately involved in regulating the complex interplay between end replication, C-strand resection, telomere elongation and capping.

As with budding yeast, telomere replication and chromosome end processing are tightly coordinated in fission yeast. ChIP data has revealed that leading and lagging strand polymerase localization to chromosome ends is temporally separated, suggesting that replication of the two daughter telomeres is uncoupled (Moser *et al*, 2009). The end generated by lagging strand synthesis is replicated later in S phase than the leading end. In conjunction with this, Pot1, Stn1 and telomerase all associate with telomeres in late S phase as the lagging end is replicated. These findings suggest that replication of the telomere is a prerequisite for the end processing events that allow telomerase to bind to the end. Replication fork passage through *S. pombe* telomeres is facilitated by Taz1. In *taz1*$^{-}$ mutants, forks are much more prone to stalls and collapses (Miller *et al*, 2006). This characteristic is independent of the orientation and location of the telomere tract, suggesting that Taz1 can generally promote replication fork movement through regions of the genome prone to stalling. Interestingly, *taz1*$^{-}$ mutants also affect end processing

and telomerase dependent extension. Mutant strains display elongated 3' overhangs, and misregluation in the timing of telomere extension (Dehé *et al*, 2012). Unlike WT cells which extend their telomeres in late S/G2, *taz1*$^{-}$ mutants are able to elongate their ends much earlier in S phase. An intriguing model that encompasses all these phenotypes proposes that fork stalling in *taz1*$^{-}$ mutants leads to incomplete replication of the telomere. These partially replicated products are generated at an earlier point in S phase, and serve as substrates for resection and telomerase dependent elongation. Hence, the premature telomere elongation in *taz1*$^{-}$ cells directly stems from Taz1's role in end replication.

Resection of the telomeric C-strand has not been well characterized in fission yeast. The Mre11-Rad50-NBS1 (MRN, homologous to the budding yeast MRX) complex is required for generation of the 3' overhang (Tomita *et al*, 2003). ChIP data demonstrates that MRN localizes to telomeres with similar timing as the leading strand polymerases, implying that it resects the blunt end generated by leading strand synthesis (Moser *et al*, 2009). Interestingly, the nuclease activity of MRN is dispensable for generation of the 3' overhang (Tomita *et al*, 2003). This suggests that MRN either recruits or activates another nuclease to produce the telomeric G-tail. The key nuclease may be Dna2, an endonuclease which normally processes double strand breaks and removes RNA primers on the lagging strand during replication (Tomita *et al*, 2004). The coordination of telomere replication, end processing and telomerase dependent extension, and the means by which they are regulated remains elusive in *S. pombe*. Taz1 appears to be directly involved in all three processes. However, it is not known whether Cdk1 is the

key regulator that controls the dynamics of telomere metabolism, as in budding yeast, or if fission yeast has evolved another mechanism to coordinate these processes.

Mammalian telomere replication occurs throughout S phase, mainly from origins situated within the subtelomere. Each end is synthesized at a specific time, suggesting that replication follows a chromosome specific, rather than universal program (Drosopoulos *et al*, 2012). Both TRF1 and TRF2, homologs of the fission yeast Taz1, promote efficient fork progression through telomeres. TRF1 recruits the BLM and RTEL1 helicases to telomeres during replication to prevent fork stalling and chromosome breakage (Sfeir *et al*, 2009). Furthermore, recent work has shown that Timeless, a replisome component involved in fork stability, physically interacts with TRF1 to ensure complete replication of telomeres (Leman *et al*, 2012). TFR2 has a more enigmatic role in facilitating telomere replication. Normally, it is thought to recruit the Apollo nuclease after replication to generate the 3' overhang (Wu *et al*, 2012). However, TRF2 also brings in Apollo during S phase to relieve the topological stress generated as telomeres are replicated (Ye *et al*, 2010). Together, both TRF1 and TRF2 maintain fork integrity as chromosome ends are replicated.

In addition to TRF1 and TRF2, POT1 and the CST complex have also been implicated in facilitating telomere replication. POT1 may not normally function in replication, but its role becomes apparent in the absence of the WRN helicase. WRN couples the leading and lagging strand during telomere replication. Cells deficient for this helicase fail to completely synthesize the lagging telomere, but fully replicate the leading strand (Crabbe *et al*, 2004). When POT1 is inactivated in this context, both leading and

lagging telomeres remain unreplicated (Arnoult *et al*, 2009). This suggests that POT1 is required for efficient leading strand synthesis when telomere replication becomes uncoupled. Conversely, several reports indicate that the mammalian CST complex functions to facilitate lagging strand synthesis of telomeres (Gu *et al*, 2012; Wang *et al*, 2012; Wu *et al*, 2012). Loss of either CTC1 or STN1 leads to increased telomeric ssDNA, specifically on ends generated via lagging strand synthesis. This implies that CST has a role in promoting C-strand synthesis.

As with yeasts, mammalian chromosomes have differential end-processing requirements for telomeres generated via leading vs. lagging strand synthesis. In the absence of telomerase, lagging ends have longer G-overhangs than leading ends. However, when telomerase is active, both types of ends have elongated G-tails (Chai *et al*, 2006). This suggests that telomerase preferentially extends ends generated by leading strand synthesis to produce the 3' overhang. Furthermore, leading ends require resection of the C-strand by multiple exonucleases to generate the G-overhang. Both EXO1 and Apollo, through its interaction with TRF2, are required to resect the 5' ends of telomeres generated by leading strand synthesis (Wu *et al*, 2012). On ends replicated by lagging strand synthesis, the terminal primer is positioned ~70-100 nucleotides internal to the chromosome end. The 3' overhang on lagging ends is almost completely mature by mid S phase, but removal of the final primer occurs in late S phase (Chow *et al*, 2012). Lagging ends also require exonucleolytic processing, which is EXO1 dependent, but Apollo independent (Wu *et al*, 2012). These resection and fill-in activities also appear to be

regulated by the CDK1 kinase, but the specific mechanistic details remain to be elucidated (Dai *et al*, 2010; Dai *et al*, 2012).

The S phase checkpoint: controlling timing of origin firing and fork stability

Cells have evolved robust mechanisms to ensure the integrity of their genetic material. Telomeres function to maintain genomic stability by facilitating end replication, and capping chromosome termini to prevent inappropriate processing events. Chromosomal replication is very tightly regulated in a cell cycle dependent manner to ensure accurate and faithful duplication of the genome. If cells encounter problems that threaten the fidelity of their genome, they can activate a checkpoint response. Checkpoints are surveillance mechanisms that arrest the cell cycle in response to genotoxic stress, thereby affording cells additional time to repair damage to the genome (Hartwell and Weinert, 1989). Work done over the last 25 years has revealed the existence of four separate checkpoints within the cell cycle: the G1 DNA damage checkpoint, the intra-S phase or replication checkpoint, the G2/M DNA damage checkpoint, and the mitotic spindle assembly checkpoint (Elledge, 1996). This section will introduce the S phase checkpoint, discussing key experimental findings from the last two decades that have led to our current understanding of its organization and regulation in *S. cerevisiae*.

Genetic screens performed in the 1970's and 80's in budding and fission yeast identified a large number of genes required for cellular survival after treatment with DNA damaging agents. The identified genes could be grouped into two categories; one class

encodes proteins involved in repair of DNA damage, while the second class encodes proteins that "sense" damaged DNA and arrest the cell cycle. These observations eventually led to the discovery of cellular checkpoints, and an understanding of how DNA repair processes are coupled to the cell cycle control machinery (Hartwell and Weinert, 1989; Enoch *et al*, 1992). During S phase, DNA is extremely vulnerable to damaging drugs or replication inhibitors. If cells are challenged with such agents, they activate the S phase checkpoint, which is a multi-faceted response to replicative stress. When the checkpoint is activated, DNA replication slows down, late firing origins are repressed, repair factors are activated, and deoxyribonucleotide triphosphate (dNTP) production increases (Segurado and Tercero, 2009; Labib and De Piccoli, 2011). The ultimate role of the S phase checkpoint is to allow efficient recovery from replicative stress, by preserving the integrity of replication forks and preventing their catastrophic collapse (Desany *et al*, 1998; Branzei and Foiani, 2010).

In budding yeast, two essential kinases, Mec1 and Rad53, regulate activation of the S phase checkpoint (Allen *et al*, 1994; Weinert *et al*, 1994). In response to replicative stress or DNA damage occurring in S phase, these kinases slow down the rate of DNA synthesis (Paulovich and Hartwell, 1995). Genetic analysis revealed that Mec1 functions upstream of Rad53 in checkpoint activation (Sanchez *et al*, 1996; Zhao *et al*, 1998). Mec1 functions as a "sensor" of DNA damage or replication stress to broadcast the checkpoint signal, while Rad53 functions as an "effector" kinase that modulates the downstream responses of the checkpoint.

Multiple proteins contribute to the effective "sensing" of DNA lesions and efficient recruitment/activation of Mec1. The first such protein identified was Pol-ε (Navas *et al*, 1995). Current models hypothesize that during DNA replication, Pol-ε is coupled to the MCM helicase complex through the bridging protein Mrc1, thereby coordinating DNA unwinding and synthesis activities (Lou *et al*, 2008). Thus, if replication forks encounter barriers to synthesis, uncoupling of the helicases and polymerases will lead to the accumulation of long tracks of single-stranded DNA. Mec1, along with its accessory factor Ddc2, recognizes RPA coated ssDNA as the primary substrate for activation of the S phase checkpoint (Paciotti *et al*, 2000; Zou and Elledge, 2003). This mechanism of S phase checkpoint activation is also conserved in higher eukaryotes (Cortez *et al*, 2001).

A second pathway has also been shown to be important for activation of the S phase checkpoint through Mec1. This pathway requires the replication protein Dpb11, Pol-α, and the Ddc1-Mec3-Rad17 checkpoint clamp (Majka *et al*, 2006a; Majka *et al*, 2006b; Navadgi-Patil and Burgers, 2008; Yan and Michael, 2009a). The current model predicts that Dpb11 binds to ssDNA arising at stalled replication forks, and recruits both Pol-α and the checkpoint clamp. Pol-α then synthesizes short stretches of DNA, generating the 5' junction between single-stranded and duplex DNA necessary for loading of the checkpoint clamp (Yan and Michael, 2009a, Yan and Michael, 2009b). Assembly of this complex then allows efficient activation of Mec1 through interactions with the C-terminus of Dpb11 (Mordes *et al*, 2008; Navadgi-Patil and Burgers, 2008; Pfander and Diffley, 2011).

When the Mec1 kinase is activated in response to stalled forks or DNA lesions in S phase, it phosphorylates two key downstream targets, Mrc1 and Rad53 (Osborn and Elledge, 2003; Naylor *et al*, 2009). As discussed earlier, Mrc1 functions as a general DNA replication factor, ensuring efficient fork progression (Szyjka *et al*, 2005). However, it was initially identified as a mediator of the replication checkpoint, required for Mec1 dependent activation of Rad53 in response to replication stress (Alcasabas *et al*, 2001). Mrc1, along with its associated co-factors Tof1 and Csm3, function as a fork pausing complex, helping prevent catastrophic collapse when replication forks encounter lesions (Katou *et al*, 2003; Bando *et al*, 2009). When forks do stall, Mec1 phosphorylates Mrc1 on multiple sites (Osborn and Elledge, 2003). This phosphorylated form of Mrc1 then greatly enhances Mec1 dependent phosphorylation of Rad53 (Chen and Zhou, 2009). The Mec1 phosphorylation then allows further auto-phosphorylation of Rad53, thereby amplifying the checkpoint signal (Pellicioli *et al*, 1999). This ensures a rapid and efficient block of cell cycle progression, and activation of the appropriate repair pathways.

Once Rad53 is activated, it phosphorylates multiple key downstream substrates to execute the S phase checkpoint response. The first protein identified as a target of Rad53 was Dun1 (Allen *et al*, 1994). Dun1 itself is a kinase, which upregulates dNTP levels in cells in response to replicative stress (Zhou and Elledge, 1993). It does so by phosphorylating and inactivating Sml1, an inhibitor of the ribonucleotide reductase (RNR) enzyme (Zhao *et al*, 1998). Interestingly, deletion of Sml1 allows bypass of both Rad53 and Mec1, indicating that the essential role of these kinases is to regulate dNTP levels, to ensure complete and efficient replication of the genome during S phase (Zhao *et*

al, 1998). Recent findings support this model, demonstrating that increase of dNTP levels by either *SML1* deletion or RNR overproduction promotes increased DNA synthesis in the presence of the replication inhibiting drug hydroxyurea (HU), thereby allowing efficient recovery of stalled fork (Poli *et al*, 2012).

In addition to upregulating dNTP levels, Rad53 also represses firing of late origins in response to replicative stress caused by HU, or DNA breaks caused by methyl methanesulfonate (MMS) (Santocanale and Diffley, 1998; Shirahige *et al*, 1998). The exact target(s) required for this repression were not known for some time, but genetic and biochemical interactions between Rad53 and DDK indicated that Cdc7 or Dbf4 could be the key regulatory switch (Weinreich and Stillman, 1999; Duncker *et al*, 2002). In support of this, experiments performed using *Xenopus* egg extracts demonstrated that the S phase checkpoint targets DDK to block replication in the presence of damaged DNA (Costanzo *et al*, 2003). More recently, several reports have confirmed that Rad53 phosphorylates Dbf4 on multiple residues to block firing of late replication origins (Lopez-Mosqueda *et al*, 2010; Zegerman and Diffley, 2010; Duch *et al*, 2011). However, these studies showed Rad53 also phosphorylates Sld3 on multiple sites after exposure to HU or MMS. Phosphorylation of both proteins is necessary to block firing of late origins, but neither one alone is sufficient (Lopez-Mosqueda *et al*, 2010; Zegerman and Diffley, 2010; Duch *et al*, 2011). Interestingly, *sld3 dbf4* double mutants that are unable to repress late origin firing are still significantly more HU and MMS resistant than *rad53* mutants, indicating that Rad53 has other essential checkpoint targets.

Rad53 is also thought to maintain the integrity of replication forks arising from early origins, by preventing their catastrophic collapse when cells experience DNA damage. 2-dimensional gel electrophoresis analysis and isotope density transfer experiments have shown that in the absence of Rad53, cells treated with HU or MMS continue synthesizing DNA, and experience elevated levels of fork collapse (Lopes *et al*, 2001; Tercero and Diffley, 2001). Furthermore, electron microscopy analysis reveals that *rad53* mutants have a high incidence of hemi-replicated molecules, large tracks of ssDNA and elevated rates of fork reversal (Sogo *et al*, 2002). More recently, genomic microarray analysis has revealed that in *rad53* mutants, ssDNA accumulates around all origins in cells treated with HU, most likely as a result of forks stalling or collapsing (Feng *et al*, 2006).

The exact mechanism by which Rad53 suppresses formation of aberrant structures at stalled forks is not completely understood, but two general models can be invoked; Rad53 may prevent the formation of such structures through a nucleolytic dependent mechanism, or promote their resolution through recombination mediated processes. These models are not mutually exclusive, and current evidence indicates that both processes are important for fork stability when cells suffer replicative stress. In response to DNA damage, Rad53 phosphorylates the Exo1 exonuclease to modulate its activity (Morin *et al*, 2008). At DNA breaks or uncapped telomeres, Exo1 activity is inhibited; however, at stalled forks, Exo1 activity is required to prevent fork reversals, which could form potentially deleterious "chicken-foot" structures (Cotta-Ramusino *et al*, 2005; Morin *et al*, 2008). Intriguingly, *exo1* deletion partially suppresses the DNA damage

sensitivity of *rad53* mutants, suggesting that in the absence of checkpoint regulation, Exo1 may inappropriately process stalled forks or damaged DNA (Segurado and Diffley, 2008). In *S. pombe*, the Rad53 homolog, Cds1, has been shown to modulate the activity of two additional nucleases, Mus81 and Dna2 (Froget *et al*, 2008; Hu *et al*, 2012). Both nucleases are hypothesized to cleave DNA at stalled forks, thereby counteracting their reversal. Whether Rad53 regulates the activity of additional nucleases in *S. cerevisiae* remains to be determined.

How the replication checkpoint regulates recombination to maintain fork integrity is less well characterized. Early genetic analysis indicated that Rad55 may be a key target of the S phase checkpoint in preventing fork collapse (Bashkirov *et al*, 2000). Rad55, along with its associated cofactor Rad57, promotes formation of Rad51 filaments on ssDNA, which is a key intermediate that forms in nearly all recombination processes. More recently, mass spectrometry analysis has confirmed that in response to stalled forks, Rad53 phosphorylates Rad55 to promote recombination (Herzberg *et al*, 2006). Furthermore, in *S. pombe*, Cds1 phosphorylates the Mcm4 subunit of the MCM helicase complex at stalled forks in response to HU (Bailis *et al*, 2008). This modification is hypothesized to stabilize stalled forks, and facilitate their restart through recombination. Whether Rad53 regulates recombination at stalled forks in an analogous manner in budding yeast is currently unknown. Although the mechanistic details are still being deciphered, current models hypothesize that the replication checkpoint blocks recombination at DNA breaks, but promotes it at stalled forks to prevent their collapse (Alabert *et al*, 2009). Thus, by modulating the complex interplay of recombination and

resection, Rad53 maintains replication fork stability without inappropriately stimulating these processes elsewhere in the genome.

Until recently, it was assumed that in *rad53* mutants experiencing replicative stress, the majority of stalled forks collapse, and such cells cannot restart replication after recovery. However, several pieces of data indicate that this hypothesis is incorrect. One study found that in order to restart stalled replication forks, Rad53 must be de-phosphorylated by the Psy2-Pph3 phosphatase (Szyjka *et al*, 2008). This suggests that the S phase checkpoint is actually inhibitory to fork restart, and must be inactivated after recovery from replicative stress to allow resumption DNA synthesis. Furthermore, genome wide microarray analysis reveals that *rad53* mutants can recover from transient HU treatment and complete the majority of DNA synthesis; however, they fail to bi-orient sister chromatids correctly, and undergo lethal mitotic catastrophes (Feng *et al*, 2009). Consistent with these findings, biochemical analysis reveals that in *mec1*Δ or *rad53*Δ cells treated with HU, the replisome remains intact (De Piccoli *et al*, 2012). This indicates that the S phase checkpoint targets replisome function, rather than stability, to ensure efficient recovery and completion of DNA synthesis after replicative stress. A recent study in fission yeast supports this model, showing that *cds1*$^{-}$ and *mrc1*$^{-}$ mutants are able to continue DNA synthesis, both during HU exposure and after washout, but undergo catastrophic fork collapse during recovery (Sabatinos *et al*, 2012).

Work done in the last two decades is finally beginning to reveal the details of how the S phase checkpoint is organized and regulated. Although the replication checkpoint is much more complex and dynamic than was initially anticipated, an integrated picture is

starting to emerge. Our current understanding of the S phase checkpoint in *S. cerevisiae* is summarized in Figure 0-5.

Do telomeric proteins contribute to global DNA replication?

All eukaryotic cells face a similar set of challenges in telomere capping and replication; yet the mechanistic details of how these challenges are resolved has diverged significantly through evolution. Interestingly, nearly all telomeric proteins from evolutionarily divergent species appear to have dual functions in telomere capping and end replication, reinforcing the idea that these two processes are inherently coupled. Since both processes are essential for maintaining genomic stability, cells have evolved multiple redundant pathways to ensure the integrity of their chromosome ends. The redundancies inherent within these processes allow a fair amount of flexibility in telomere capping and replication. As an example, the budding yeast Cdc13 protein was initially thought to be absolutely essential for capping. However, in recent years, multiple groups have been able to bypass the telomere capping function of Cdc13, using at least three genetically distinct pathways (Larrivée and Wellinger, 2006; Petreaca *et al*, 2006; Zubko and Lydall, 2006; Dewar and Lydall, 2010; Ngo and Lydall, 2010). Furthermore, no Cdc13 ortholog has been discovered in fission yeast to date, suggesting that the protein may have been lost through evolution. These findings highlight the dynamic plasticity in the evolution of chromosome end protection.

Because of the inherent redundancies in chromosome end protection coupled with their rapid evolution, many telomeric proteins have acquired secondary functions in

genome maintenance and DNA metabolism. For example, under come conditions, *S. cerevisiae* Cdc13 can bind to double strand breaks and promote repair via telomere addition (Zhang and Durocher, 2010). Normally, the checkpoint kinase Mec1 phosphorylates Cdc13 to block its association with broken ends, thus promoting error-free recombination-dependent repair. However, if the broken ends are unable to be repaired via recombination or NHEJ pathways, the Pph3 phosphatase can dephosphorylate Cdc13, thus promoting repair through telomere addition. It is not known if Stn1, Ten1, or other telomeric proteins function in double strand break repair or recombination at non-telomeric sites. However, given the similar sets of processing requirements at telomeres and double strand breaks, it would not be surprising to discover that telomeric proteins have adopted secondary roles in these processes.

In recent years, a growing body of evidence is starting to suggest that telomeric proteins not only facilitate chromosome end replication, but also function as general replication factors throughout the genome. Although the mechanistic details have yet to be uncovered, multiple lines of evidence suggest that the CST complex has a direct role in promoting Pol-α dependent DNA synthesis at non-telomeric sites. CTC1 and STN1 from mammalian cells were initially identified as DNA polymerase alpha accessory factors, even before being recognized as orthologs of the yeast CST complex components (Goulian and Heard, 1990; Goulian *et al*, 1990). These studies suggested that *in vitro*, AAF-132(CTC1) and AAF-44(STN1) function to both stimulate the primase and polymerase activities of Pol-α, and increase its affinity to the DNA template. Immunostaining experiments from live cells also showed that these proteins co-localize

with PCNA during S phase, indicating that CTC1 and STN1 have a role in general replication (Casteel *et al*, 2009). Additionally, an *in vitro* study demonstrated that in various phylogenetically distinct yeast species, Cdc13 can bind to non-telomeric, G-rich DNA templates, albeit with a lower binding affinity than it does to telomeric DNA (Mandell *et al*, 2011). Although further work needs to be done to explore the functional consequences of the binding, this observation suggests that Cdc13 in yeast may also have a role in general replication.

More recently, two studies in metazoans have begun to shed some light on the mechanistic details of how the CST complex facilitates global DNA replication. Work in *Xenopus laevis* shows that immunodepletion of Stn1 in egg extracts severely compromises synthesis of a single-stranded template (Nakaoka *et al*, 2012). However, synthesis of a primed template is unaffected, indicating that in *X. laevis*, the CST complex has a role in priming single-stranded templates. A caveat with this work is that addition of recombinant Stn1 failed to rescue the replication defect in the depleted extracts, potentially indicating that another factor may have also been depleted. In conjunction with these findings, a second study demonstrated that mammalian cells in which STN1 has been knocked down have a reduction in recovery of DNA replication after exposure to hydroxyurea (Stewart *et al*, 2012). This compromised recovery results from a failure to activate late-firing and dormant origins, rather than from problems in restarting stalled forks. These findings support a model in which the CST complex facilitates Pol-α dependent priming both at telomeres and other challenging regions, to promote efficient and complete replication of the genome.

The replicative roles of Stn1 and Ten1 have not been characterized in *S. pombe* to date. Therefore, it is unknown if these proteins have any extra-telomeric functions in DNA replication. However, both Rif1 and Taz1 were recently shown to be regulators of global replication timing in fission yeast, lending additional support to the hypothesis that telomeric proteins have adopted roles in DNA metabolism throughout the genome (Hayano *et al*, 2012; Tazumi *et al*, 2012). Deletion of Rif1 allows bypass of the replication activating kinase Hsk1 (homolog of the budding yeast Cdc7), and causes normally repressed origins to fire under stressful replication conditions (Hayano *et al*, 2012). Interestingly, origins that normally fire early in S phase are activated later and less efficiently in the absence of Rif1. This suggests that Rif1 controls the temporal replication profile throughout the genome in fission yeast. A second study revealed a very similar role for Taz1 in regulating the timing of origin firing (Tazumi *et al*, 2012). Taz1 appears to be a negative regulator of origin firing; deletion mutants inappropriately activate late origins in the presence of damage, whereas artificially localizing Taz1 to an early firing origin causes it to fire later. Rif1 and Taz1 are likely to function through two distinct mechanisms to regulate origin firing since taz1 mutants cannot bypass Hsk1. Furthermore, Rif1 is able to regulate replication timing both positively and negatively, whereas Taz1 only represses origin firing. These findings underscore the theme that, within a single species, multiple telomeric proteins/complexes have evolved independently to take on secondary roles in DNA metabolism.

Overview of the projects presented in this dissertation

Current models propose that in budding yeast, the CST complex has multiple roles in telomere maintenance. It functions as a physical cap, preventing exonucleolytic degradation, recombination and fusion of telomeres, and it facilitates efficient replication of chromosome ends by modulating the activities of telomerase and Pol-α. Part of the work presented in this dissertation shows that one of the components within the complex, Stn1, has additional roles in facilitating DNA replication at non-telomeric sites in the genome. In Chapter 1, I show that when Stn1 is overproduced, it interferes with the S phase checkpoint response, by interfering with the checkpoint's control of origin firing and fork progression under DNA damaging conditions (Gasparyan *et al*, 2009). This function is dependent of interaction between Stn1 and Pol12, the regulatory subunit of Pol-α. I conclude this chapter by demonstrating that Stn1 interferes with the checkpoint at a step upstream of MCM helicase function, and in a pathway either downstream of, or parallel to the DDK.

In Chapter 2, I explore genetic interactions between Stn1 and DDK. I demonstrate that *STN1* is a dosage suppressor of the temperature sensitive *cdc7-1* and *dbf4-1* mutations, and show that *stn1 cdc7* and *stn1 dbf4* double mutants have synthetic interactions, likely caused by defects in completing DNA replication. I demonstrate that this defect is not a result of reduced origin firing or fork progression on a whole genome level, but more likely caused by replication problems arising at repetitive sequences, such as the rDNA locus. Genetic analysis reveals that *stn1* mutants require the post-replicative

repair (PRR) pathway for viability, suggesting that Stn1 functions in facilitating replication or repair processes at damaged sites.

In Chapter 3, I analyze the role of the CST complex and Pol-α in telomere capping and length regulation. I show a genetic interaction between a *cdc13* and *pol12* mutant which leads to temperature sensitivity, HU sensitivity, and telomere capping defects. Furthermore, I demonstrate that Ten1 physically interacts with Pol12, although this interaction is likely to be indirect. These findings reinforce the hypothesis that the CST complex and Pol-α function together in telomere maintenance. I also characterize the telomeric phenotypes of a variety of temperature sensitive *ten1* mutants generated in our lab (Xu *et al*, 2009). Using the yeast two hybrid assay, I show that most of these mutants are unable to interact with Cdc13 and Stn1, both at permissive and restrictive temperatures. I show that the mutants have a severe telomere elongation phenotype, which can be partially suppressed by *STN1* overexpression or *rad9* deletion, but not with *exo1* deletion.

The work presented in this dissertation highlights the complex and dynamic nature of maintaining genomic stability. Although the CST complex was proposed to cap telomeres over 10 years ago, the exact details of how it functions, and how it is regulated throughout the cell cycle are still not completely understood. A theme that has begun to emerge recently within the telomere capping field hypothesizes that Cdc13, Stn1 and Ten1 do not necessarily always function as a complex; each protein may function independently from the other two partners, in either telomere metabolism, or other

processes in genome maintenance. A large portion of my work has focused on trying to understand Stn1's role in facilitating replication at non-telomeric sites.

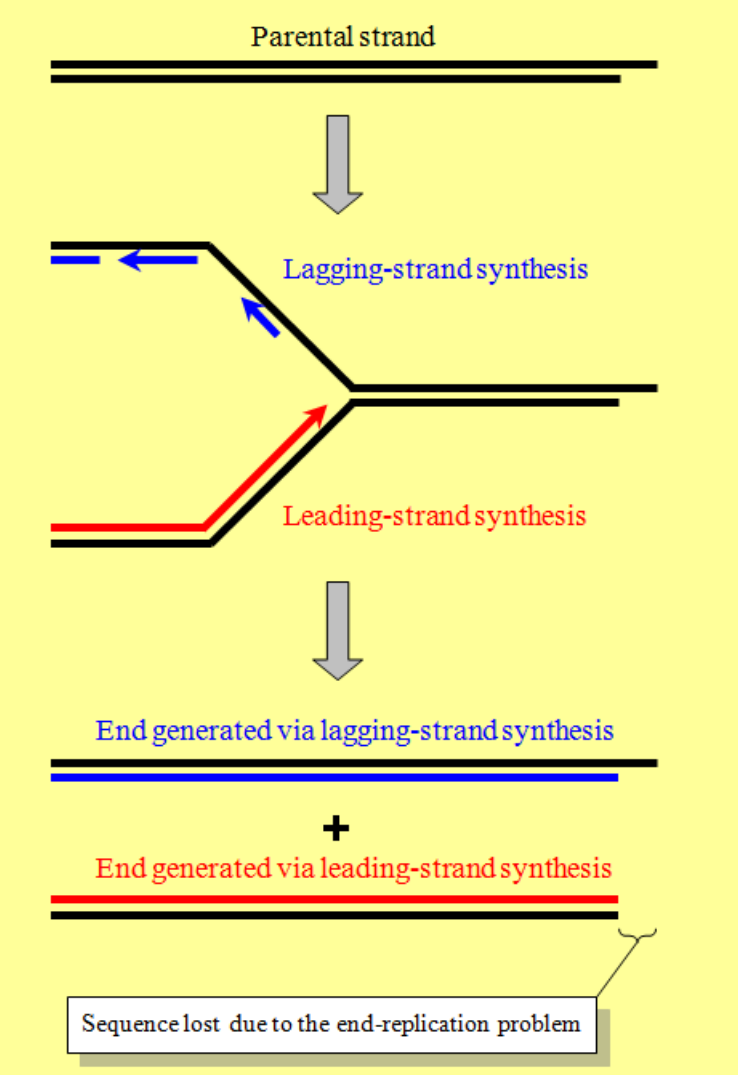

Figure 0-1: The end-replication problem

Replication of a linear chromosome will generated two distinct products. The leading strand, shown in red, will be synthesized continuously to the end of the template. This will generate a blunt end that is slightly shorter than the parent molecule. Conversely, the lagging strand, shown in blue, will be synthesized discontinuously in multiple fragments. It will generate an overhang similar to the parental molecule.

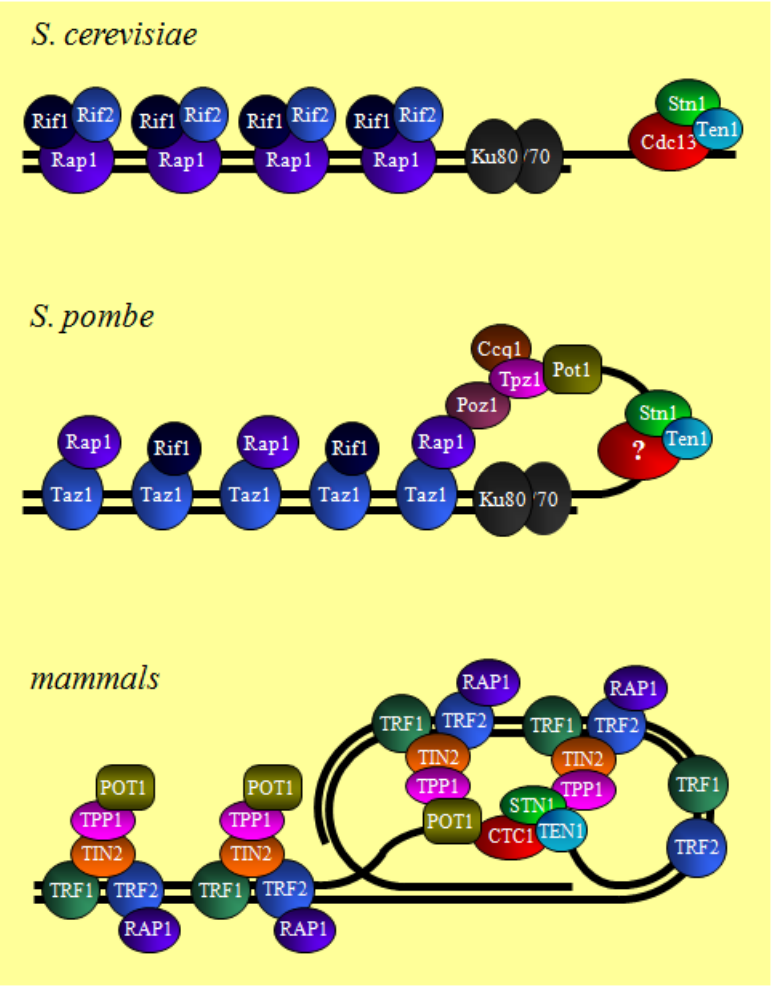

Figure 0-2: Telomere capping strategies among various species

Budding yeast, fission yeast and mammalian cells each use distinct, yet related strategies to cap their telomeres. In all three systems, ssDNA binding proteins associate with the terminal portion of the G-rich strand to form a physical cap. These complexes work in conjunction with dsDNA binding proteins to block resection and prevent NHEJ of chromosome ends. In *S. cerevisiae*, the ssDNA and dsDNA bound proteins appear to work independently, through separate pathways. In *S. pombe* and mammalian cells, the ssDNA and dsDNA bound proteins physically interact to form a functional cap. Furthermore, in mammalian cells, the terminal 3' overhang invades the upstream duplex region, generating a "t-loop" structure which is hypothesized to facilitate telomere capping.

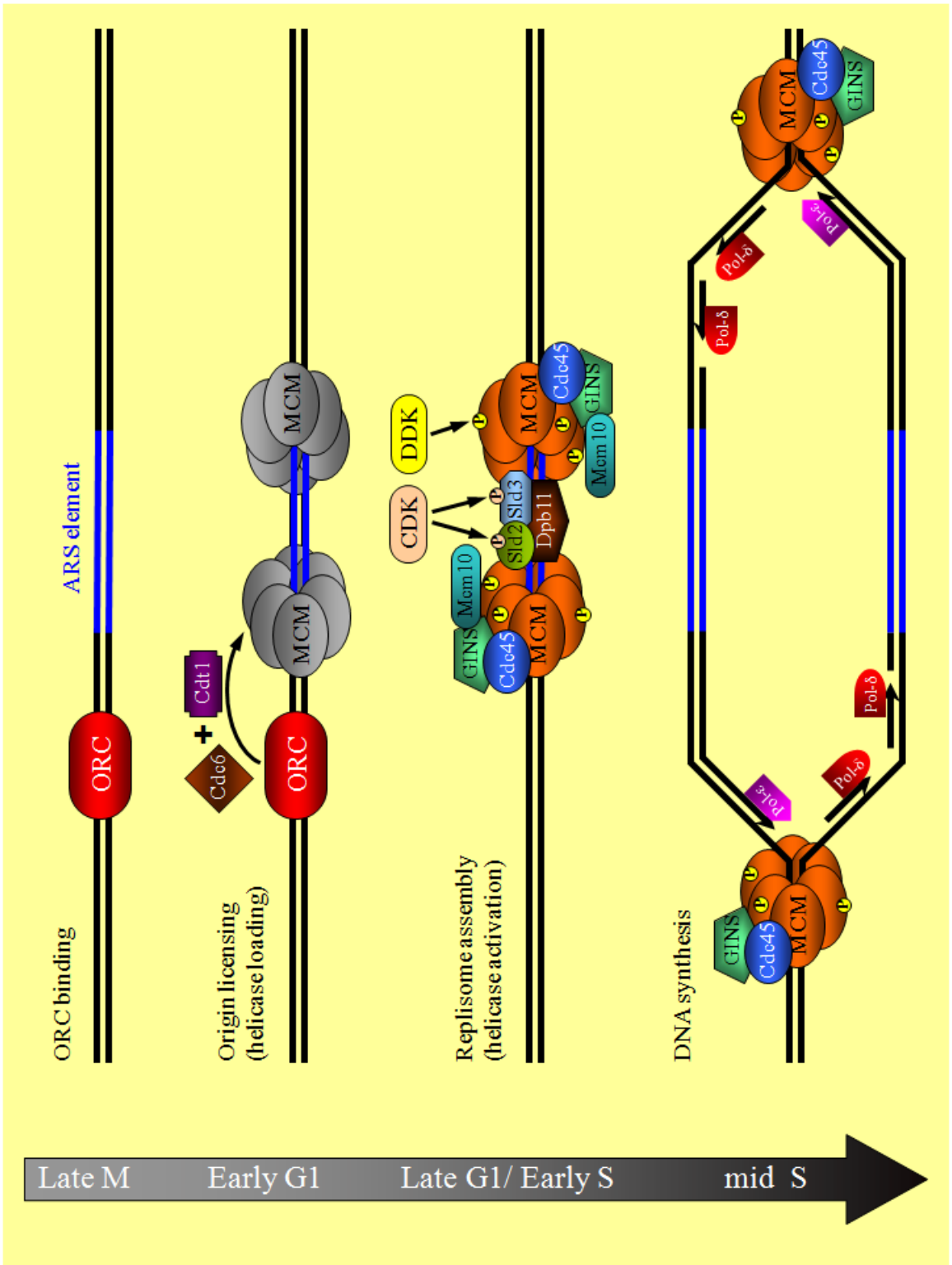
ORC binding
ARS element
ORC
Origin licensing
(helicase loading)
Cdt1
Cdc6
ORC
MCM
Replisome assembly
(helicase activation)
DDK
CDK
GINS
Mcm10
Cdc45
MCM
Sld2
Sld3
Dpb11
DNA synthesis
Pol-δ
Pol-ε
Late M
Early G1
Late G1/ Early S
mid S

Figure 0-3: Initiation of DNA replication

DNA replication initiates from specifically defined origin sequences termed “ARS” elements, or Autonomously Replicating Sequences. In late M phase of the cell cycle, the Origin Recognition Complex (ORC) associates with ARS elements, designating these sequences as potential origins of replication. In early G1, the Cdt1 and Cdc6 proteins load the MCM helicase complex onto ORC bound chromatin, thereby “licensing” the origins. In late G1/ early S phase, a large number of proteins associate at the origin, forming a replisome. During this time, the CDK and DDK kinases phosphorylate several key components within the replisome to stimulate unwinding of duplex DNA by the MCM helicases. DNA polymerases then use the unwound ssDNA as a template for synthesis.

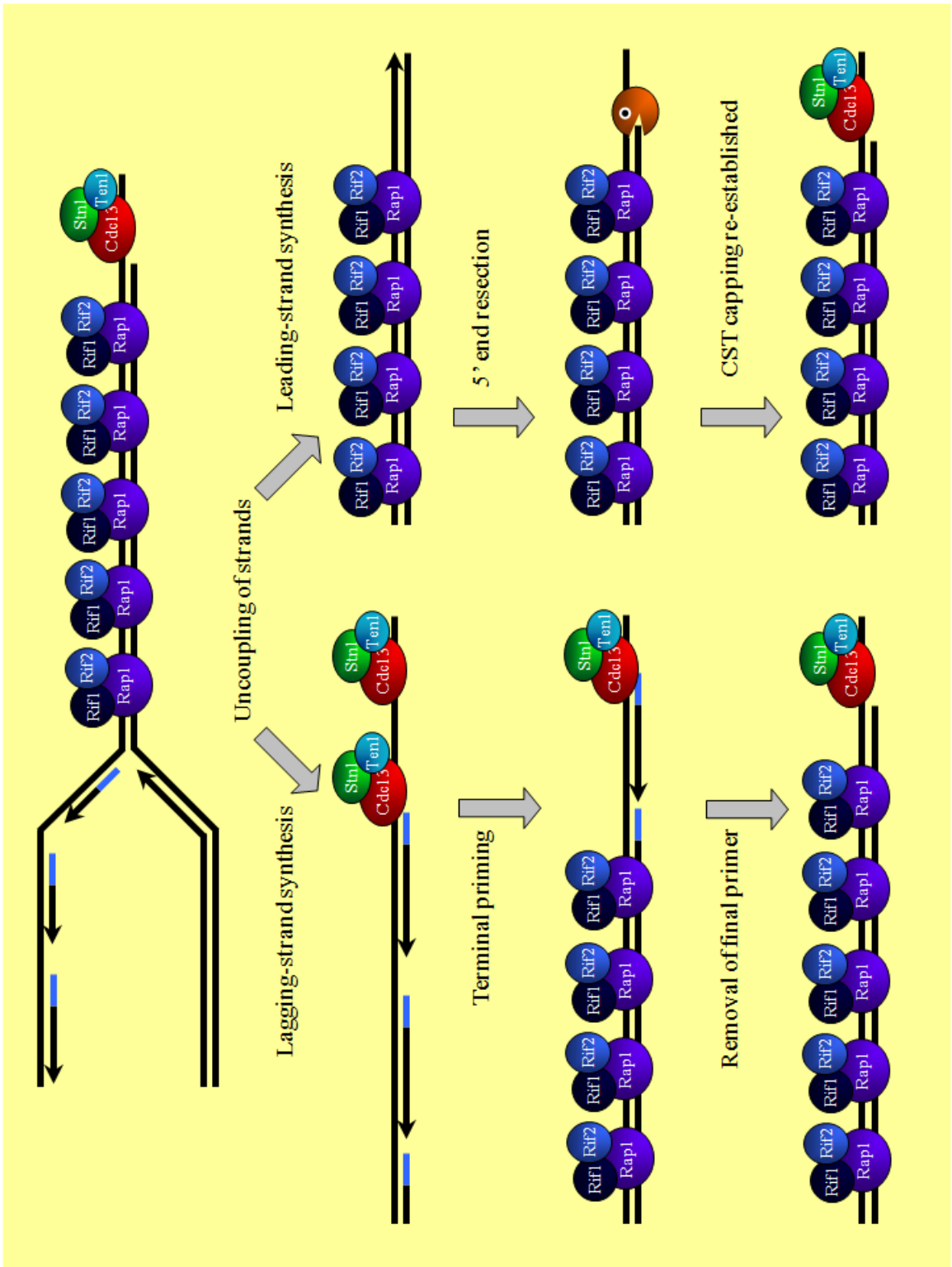
Stn1
Ten1
Cdc13
Rif1
Rif2
Rap1
Uncoupling of strands
Leading-strand synthesis
Lagging-strand synthesis
5' end resection
Terminal priming
CST capping re-established
Removal of final primer

Figure 0-4: Chromosome end replication in *S. cerevisiae*

As a replication fork approaches the end of a chromosome, leading strand and lagging strand synthesis become uncoupled. The leading strand is synthesized to the end of the template, generating a blunt end. This product requires MRX dependent processing of the C-strand to generate the 3' overhang, onto which the CST complex binds. The lagging strand is synthesized discontinuously, in multiple Okazaki fragments. Removal of the terminal primer yields a 3' overhang. Therefore, no MRX activity is required for CST binding to the lagging strand.

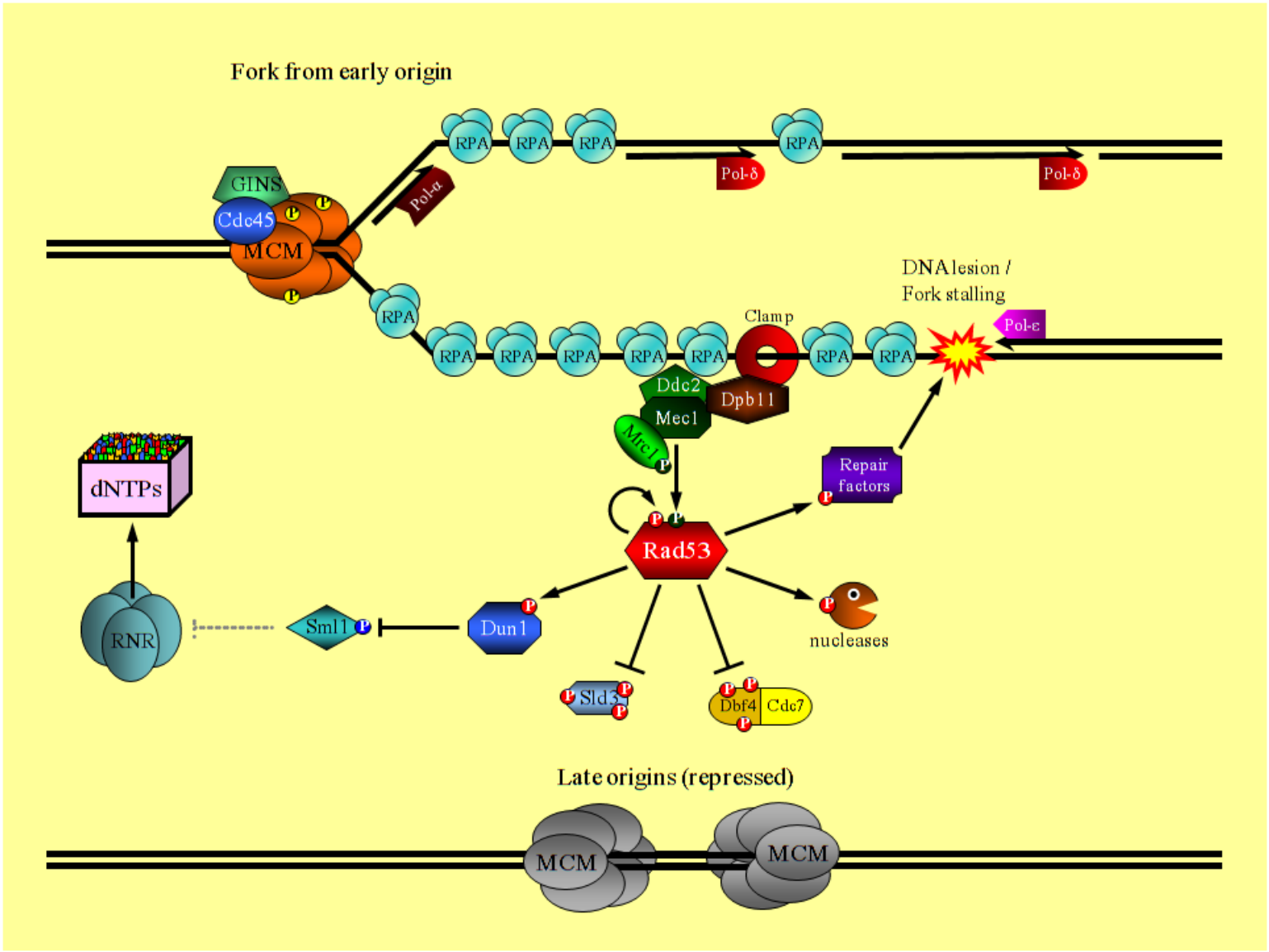
Fork from early origin
RPA
Pol-δ
GINS
Cdc45
MCM
Pol-α
DNA lesion /
Fork stalling
Clamp
Pol-ε
Ddc2
Dpb11
Mec1
Mrc1
dNTPs
Repair
factors
Rad53
RNR
Sml1
Dun1
nucleases
Sld3
Dbf4
Cdc7
Late origins (repressed)
MCM

Figure 0-5: The S phase checkpoint response in *S. cerevisiae*

When a cell encounters replication stress or DNA lesions during S phase, it activates the intra S phase checkpoint. Depletion of deoxyribonucleotides or damage on the template strand can stall DNA polymerases, uncoupling helicase and synthesis activities. This leads to the accumulation of ssDNA behind the replication fork, which gets coated with the ssDNA binding protein RPA. The Mec1 kinase is recruited to RPA coated ssDNA through its accessory factor DDC2. Additionally, Dpb11 and the checkpoint clamp are required to activate Mec1. Upon its activation, Mec1 first phosphorylates Mrc1, which then stimulates phosphorylation of Rad53. Rad53 then autophosphorylates itself on additional residues to become fully active. Once activated, Rad53 has multiple downstream targets, all of which help maintain the integrity of replication forks. Phosphorylation of Dun1 leads to inactivation of the RNR inhibitor Sml1, which then causes an increase in cellular dNTP levels; phosphorylation of Sld3 and Dbf4 prevent firing of late replication origins; phosphorylation of nucleases (including Exo1) counteracts fork reversal; phosphorylation of repair factors (including Rad55) allows recombination dependent restart of stalled forks. The ultimate function of the S phase checkpoint is to allow survival and recovery from replicative stress, by preventing catastrophic collapse of replication forks.

Chapter 1

Stn1 overproduction interferes with S phase checkpoint execution by stimulating replication in the presence of DNA damage

Abstract

In budding yeast, the CST complex is thought to participate in both telomere capping and chromosome end replication. The capping function the CST complex, and especially of Cdc13, are relatively well characterized; however, its replicative role is poorly understood. Physical interactions have been identified between Cdc13 and Pol1, as well as Stn1 and Pol12. This data, along with genetic evidence has led to the model where the CST facilitates replication of telomeres. However, the mechanistic details of this process have yet to be resolved, and many outstanding questions remain. For example, does Pol-α dependent synthesis of the telomeric C-strand occur as a replication fork passes through the telomere, or is it temporally separated from semi-conservative replication? Does the CST complex simply recruit Pol-α to telomeres, or does it stimulate the catalytic activity? Are the multiple interactions between CST and Pol-α redundant, or does each one serve a specific function? Are all components of the CST complex necessary to recruit/activate Pol-α? Can CST function elsewhere in the genome to facilitate Pol-α dependent replication, or is this function limited to telomeres? In this chapter, we present evidence that when Stn1 is overproduced, it can stimulate Pol-α dependent DNA replication throughout the genome. We first show that Stn1 overproduction leads to extreme HU and MMS sensitivity, and demonstrate that these phenotypes result from a defect in the execution of the S phase checkpoint. While exploring the nature of this defect, we discovered that Stn1 interferes with the checkpoint at step downstream of Rad53 activation, but requires functional Pol-α. Stn1 overproducing cells are deficient in all tested downstream readouts of the S phase

checkpoint, including sensitivity to replication inhibitors, failure to restrain elongation of the mitotic spindle in the presence of DNA damage, and inability to repress firing of late origins in response to replication stress. Amazingly, compromising *POL12* function suppresses these defects, suggesting that Stn1's ability to interfere with the checkpoint and facilitate replication in the presence of DNA damage requires fully functional Pol-α. Furthermore, we find that the *STN1* checkpoint phenotype is dependent on a functional MCM helicase complex, but does not require DDK function. These findings imply that *STN1* may have a role in promoting general DNA replication throughout the genome. An important consideration is that Stn1 is overproduced in these experiments; therefore, our findings may simply reflect the protein's normal role at telomeres, which becomes transplanted throughout the genome when Stn1 is overproduced.

Introduction

STN1 was first discovered as a dosage suppressor of *cdc13-1* temperature sensitivity (Grandin *et al*, 1997). This finding, along with its ability to physically interact with Cdc13 indicated that Stn1 functions to cap telomeres. Indeed, loss of function *stn1* mutants do have high levels of telomeric ssDNA, consistent with a capping defect (Grandin *et al*, 1997; Petreaca *et al*, 2007; Puglisi *et al*, 2008). In addition to protecting against exonucleolytic degradation, studies have shown that Stn1 physically interacts with Pol12, suggesting that it has an secondary role in telomere replication (Grossi *et al*, 2004; Petreaca *et al*, 2006). Current models hypothesize that after telomerase extends the G-strand, Pol-α is brought to the chromosome end via interactions with Stn1 and Ten1 to synthesize the complementary C-strand (Qi and Zakian, 2000); however, the mechanistic details of this process and its regulation are poorly understood.

One of the major unknown facets in this model is when Stn1 brings in Pol-α to replicate telomeres; does the interaction occur as a fork passes through the telomere, or is it temporally separated from semi-conservative replication? In an attempt to address this, Puglisi *et al* used a truncation mutant of *stn1* in the telomere healing experiment, to ask if extension a critically short telomere in the absence of replication requires Stn1 function. They found that the *stn1* mutant is capable of healing the telomeric seed, to an even greater extent that wild type cells (Puglisi *et al*, 2008). This led them to conclude that Stn1 influences the efficiency of telomerase during telomere elongation. Unfortunately, these experiments were performed in cycling cells rather than G2 arrested cells; therefore, no conclusions can be drawn about Stn1's ability to promote C-strand synthesis

independent of semi-conservative replication. Additionally, the strains used in these experiments were *RAD52*$^{+}$, and thus could potentially extend the shortened telomere arm through recombination mediated processes.

Another critical unanswered question about Stn1's role in facilitating telomere replication is whether it performs this function independently, or as part of a complex with Cdc13. This has been addressed in part somewhat indirectly in *CDC13* bypass experiments. Multiple different genetic alterations can bypass the essential function of *CDC13* (Larrivée and Wellinger, 2006; Petreaca *et al*, 2006; Zubko and Lydall, 2006; Dewar and Lydall, 2010; Ngo and Lydall, 2010). Most of these are either dependent on recombination, which drastically alters the terminal structure of chromosomes, or require changes to Stn1 and Ten1; however, Ngo and Lydall showed that deletion of *RAD9*, *EXO1* and *SGS1* allows very efficient bypass of *CDC13*, without altering telomere structure (Ngo and Lydall, 2010). Such strains maintain telomere integrity remarkably well, allowing Stn1 and Ten1's contribution to telomere replication to be studied independent of Cdc13. The fact that these strains do not show elevated levels of single-stranded telomeric DNA indicates that both the capping and replication functions are largely intact. This suggests that Stn1's role in facilitating telomere replication does not require Cdc13. However, it should be noted that in the absence of Cdc13, these strains are unable to recruit telomerase to chromosome ends, and therefore senesce. Thus, without telomerase dependent extension of the G-strand, there is no opportunity for C-strand fill in synthesis. Thus, any contribution Stn1 makes to telomere replication in this context must occur in conjunction with passage of the fork during semi-conservative replication.

An alternative means to bypass *CDC13*'s essential function is overproduction of the N-terminus of Stn1, along with full length Ten1 (Petreaca *et al*, 2006). In this background, bypass is dependent on a functional interaction between Stn1 and Pol12. This finding implies that Stn1 does have a Cdc13 independent role in recruiting or activating Pol-α at the telomere, and this function becomes essential in the absence of Cdc13.

A third important question regarding Stn1's role in promoting Pol-α dependent replication is whether this function is only limited to telomeres, or can it be used as a mechanism to facilitate DNA synthesis elsewhere in the genome? Several observations suggest that Stn1 may in fact have a more global role in stimulating DNA replication globally. First, early work from mammalian cells found that two previously unidentified proteins, AAF-132 and AAF-44, associate with Pol-α, and stimulate its catalytic activity (Goulian and Heard, 1990; Goulian *et al*, 1990). Further characterization showed that these proteins co-localize with PCNA on chromatin, and their knockdown results in significant reduction of bulk DNA replication (Casteel *et al*, 2009). It should be noted that in these studies, AAF-132 and AAF-44 were overproduced. When Ctc1 and Stn1 were identified in mammalian cells, it was realized that they are the same genes as AAF-132 and AAF-44, respectively (Miyake *et al*, 2009; Surovtseva *et al*, 2009). Further support for Stn1 having a role in promoting replication at non-telomeric sites comes from *in vitro* experiments using *Xenopus* egg extracts. Nakaoka *et al* found that extracts in which Stn1 was depleted are unable to catalyze synthesis using a single-stranded plasmid as a template (Nakaoka *et al*, 2012). Unfortunately, adding back recombinant Stn1 failed to rescue this phenotype, potentially suggesting that other replication factors may have

also been immuno-depleted. These findings are also consistent with data showing after Stn1 is knocked down, mammalian cells have diminished ability to recover from replication stress (Stewart *et al*, 20012). This reduced recoverability results from a failure to activate dormant and late firing origins, rather than an inability to restart stalled replication forks.

These findings support the hypothesis that Stn1 can facilitate Pol-α dependent DNA replication throughout the genome, but the mechanism by which this occurs is not known. Here, we show that in budding yeast, when Stn1 is overproduced, it interferes with the S phase checkpoint control of DNA replication. The S phase checkpoint is a response to DNA damage or replication stress that occurs during DNA synthesis. DNA lesions or limiting levels of dNTPs can cause replication forks to stall, resulting in the accumulation of single-stranded DNA (Branzei and Foiani, 2010). The ssDNA binding protein RPA then coats the unreplicated stretches of DNA, and serves as a substrate for checkpoint activation. Through a series of sensors and mediators, the Rad53 effector kinase is activated via phosphorylation. Once activated, Rad53 has numerous downstream targets which function to stabilize replication forks, stimulate production of dNTPs, activate transcription of repair factors, regulate the activity of repair enzymes, repress firing of late replication origins, and block premature elongation of the mitotic spindle (summarized in Figure 0-5).

Since Stn1 can promote Pol-α dependent DNA synthesis at telomeres and potentially elsewhere in the genome, we hypothesized that *STN1* overexpression may override the S phase checkpoint by interfering with control of DNA replication. Normally,

in response to replication stress, the S phase checkpoint phosphorylates two targets, Sld3 and Dbf4, to repress activation of late firing origins (Lopez-Mosqueda *et al*, 2010; Zegerman and Diffley, 2010; Duch *et al*, 2011). This is thought to allow the cell time to repair damage to existing forks, and limit the damage by preventing new fork formation. Here, we show that Stn1 overproduction disrupts the checkpoint at a step downstream of Rad53 activation, in a Dbf4 independent manner. However, this phenotype does require both Pol-α and MCM function. These results have important implications for how Stn1 promotes Pol-α dependent replication at telomeres, which we will discuss.

Results

Stn1 overproducing cells are HU and MMS sensitive

Previous work from our lab and others has shown that overexpression of *STN1* can partially suppress the temperature sensitivity of the *cdc13-1* mutation (Grandin *et al*, 1997; Petreaca *et al*, 2006). To examine which domain of Stn1 is required for this suppression, our lab generated several different truncation alleles encoding either N-terminal or C-terminal portions of the protein. In the course of this investigation, Ruben Petreaca discovered that overexpression of either full length *STN1* or truncations which encode the C-terminus make cells sensitive to the replication inhibitor drug HU, or the DNA damaging agent MMS (Figure 1-1; experiment performed by Ruben Petreaca). Overproduction of the N-terminus alone does not cause a similar sensitivity. Stn1 overproducing cells are remarkably sensitive to these genotoxic agents, dying at concentrations comparable to the *mec1-21* checkpoint mutant.

Spindle elongation in Stn1 overproducing cells

The HU and MMS sensitivity of *STN1* overexpression may be interpreted in two ways. The excess protein may be producing damage in cells, making them extremely susceptible to external genotoxic stress. Alternatively, Stn1 may be interfering with execution of the S phase checkpoint, thereby preventing cells from properly responding to the replication stress and DNA damage caused by these drugs. To distinguish between these possibilities, we examined the spindle morphology of cells overproducing Stn1. In checkpoint deficient cells treated with HU, centromeres are frequently left unreplicated

(Feng *et al*, 2009). This prevents formation of proper bi-polar attachments of the spindle microtubules to kinetochores. Thus as the mitotic spindle exerts a pulling force on chromosomes, there is no counteracting tensile force from a cohered sister centromere to restrain spindle elongation. For this reason, in replication checkpoint deficient strains, a large fraction of cells arrest with elongated mitotic spindles after treatment with HU (Bachant *et al*, 2005; Feng *et al*, 2009). Approximately half of the scored Stn1 overproducing cells treated with HU display elongated mitotic spindles, comparable to the *rad53-21* checkpoint mutant (Figure 1-2; experiment performed by Jeff Bachant). This implies that excess Stn1 can interfere with the S phase checkpoint response, and the severity of the checkpoint disruption is nearly equivalent to disruption or Rad53.

Replication origin firing and fork progression in Stn1 overproducing cells

The data in Figures 1-1 and 1-2 suggest that *STN1* overexpression interferes with the S phase checkpoint. In addition to HU and MMS sensitivity and spindle elongation, one of the hallmarks of S phase checkpoint defective cells is their inability to repress late origin firing and maintain fork stability in response to replication stress (Santocanale and Diffley, 1998; Shirahige *et al*, 1998; Segurado and Tercero 2009). To examine the dynamics of origin firing and replication fork progression in Stn1 overproducing cells, we collaborated with the Aparicio lab at USC to perform a BrdU-ChIP microarray assay (experiment was conducted and data were analyzed by Oscar Aparicio and Alex Rex). In this experiment, cells were synchronously released into S phase in the presence of 0.033% MMS. The newly synthesized DNA was pulse labeled with BrdU for either 0-30

minutes or 30-60 minutes after release. The replication profile was then determined by immuno-precipitating the BrdU and hybridizing to a microarrays covering chromosome VI and the left arm of chromosome III. The signal at each of the pulsed time points is then compared to unlabeled control DNA collected from cells arrested in G1, and replication profiles were generated.

In the first 30 minute pulse, both *STN1* overexpressing and control cells show normal activation of early firing origins, as indicated by elevated BrdU signal over background (Figure 1-3). However, in the 30-60 minute pulse labeled samples, the strains overexpressing *STN1* inappropriately fire late origins in the presence of DNA damage (compare ARS603). Furthermore, replication fork progression is altered in the strains overexpressing *STN1*. ARS305 has been deleted in these strains, leaving an extended track of DNA that will be replicated by a single fork emerging from ARS306. This allows for a convenient way to assess replication fork progression. The control strains are able to efficiently synthesize this region, whereas the *STN1* overexpressing strains have a significantly reduced length of synthesis, indicating a high incidence of fork stalling or collapse events.

Stn1 does not interfere with the DNA damage checkpoint

Since increasing *STN1* dosage disrupts the replication checkpoint, we next asked whether the DNA damage checkpoint of *STN1* overexpressing cells was functional. The DNA damage and replication checkpoints have partially overlapping functions, and significant amounts of crosstalk; both pathways converge on the Rad53 kinase (Allen *et*

al, 1994; Sun *et al*, 1996). Therefore, if Stn1 disrupts the S phase checkpoint at an upstream step, it can also potentially block execution of the DNA damage checkpoint. To test this, we monitored DNA damage checkpoint dependent cell cycle arrest in response to a single HO-induced double-stranded break. Previous work has shown that in the absence of a functional DNA damage checkpoint pathway, cells undergo a lethal mitosis in the presence of broken or damaged DNA and die after one cell division cycle, whereas checkpoint proficient cells are able to arrest, and eventually recover (Weinert *et al*, 1994). To test the functionality of the DNA damage checkpoint, strains containing a galactose inducible HO endonuclease and the HO recognition site were transformed with plasmids overexpressing *STN1*, or a vector control. Cells were plated on galactose media to induce expression of the HO enzyme and generate a double stranded break. The ability of individual cells to arrest the cell cycle in response to the break was monitored. 49 cells of each genotype were micro-manipulated into a 7 x 7 grid on either glucose or galactose plates, and allowed to form microcolonies. At various time points, the number of cells in each microcolony was counted, and the results were plotted as histograms (Figure 1-4; Neil Bhogal helped perform experiment). Both Stn1 and control cells are able to divide normally and form large microcolonies on glucose plates, in the absence of DNA damage. Conversely, both stop dividing and arrest very quickly on galactose media after induction of a double stranded break. Even after 8 hours, more than half of the population remains arrested as single cells for both strains. Microcolonies containing more than 5 cells can be observed only after 20 hours post HO induction in both strains. These results indicate that *STN1* overexpression does not disrupt the DNA damage checkpoint.

Activation of Rad53 in Stn1 overproducing cells

We next asked which part of the checkpoint pathway does *STN1* affect. Normal checkpoint activation begins with the Mec1 sensor kinase detecting single-stranded DNA and activating the Rad53 effector kinase. Rad53 then broadcasts the checkpoint signal, and activates downstream targets to block cell cycle progression and activates the appropriate damage repair pathways (Figure 0-5). To test if the upstream part of the checkpoint is functional in Stn1 overproducing cells, we monitored activation or Rad53 in response to HU and MMS induced replication stress. Rad53 can be activated through two separate pathways (Allen *et al*, 1994; Sun *et al*, 1996). During S phase, the Mrc1 mediator can induce activation of Rad53 in response to replication stress (Alcasabas *et al*, 2001). Additionally, the Rad9 mediator can stimulate Rad53 phosphorylation in response to DNA breaks, activating a DNA damage checkpoint response (Sun *et al*, 1998). Since Stn1 specifically interferes with the S phase checkpoint, we conducted the Rad53 phosphorylation experiments in a *rad9-Δ* background to prevent secondary activation of Rad53 through the DNA damage checkpoint. Cells overexpressing *STN1* or vector control were synchronized in G1, and released into media containing either HU or MMS. The activation of Rad53 was monitored by Western bolt. The phosphorylated form of protein migrates as a higher molecular weight species. The results indicate that Stn1 does not prevent Rad53 activation in response to replication stress (Figure 1-5). The phosphorylated form of Rad53 appears within 30 minutes after HU or MMS treatment, similar to control cells. In contrast, *mrc1-Δ* cells show a significant delay in Rad53 activation, as previously reported (Alcasabas *et al*, 2001). From these results, we

conclude that in Stn1 overproducing cells, Mrc1 dependent activation of Rad53 in response to MMS or HU is not affected; cells are still able to "sense" replication stress and activate the upstream effectors of the checkpoint. These findings suggest that Stn1 blocks execution of the S phase checkpoint response at a step downstream of Rad53 activation. It may do so by either directly blocking the kinase activity of Rad53, or interfering with the regulation of one or more Rad53 substrates. We favor the latter model, because if Stn1 were to block Rad53's kinase function, it would likely also interfere with the DNA damage checkpoint.

Overproduced Stn1 generally associates with chromatin

Having shown that Stn1 does not affect sensing of replication stress, we next asked if it interferes with the checkpoint response by disrupting regulation of downstream target(s) of Rad53. Stn1 has previously been shown to interact with Pol12, the regulatory subunit of Pol-α (Grossi *et al*, 2004; Petreaca *et al*, 2006). Although the functional significance of this interaction is not known, genetic evidence suggests that it may be important for Pol-α dependent replication of telomeres. We hypothesized that when Stn1 is overproduced, it associates with Pol-α via its interaction with Pol12, and interferes with the checkpoint's control of DNA synthesis in the presence of replication inhibitors such as HU or MMS. If this hypothesis is correct, one prediction is that we should see overproduced Stn1 generally associate with chromatin. To test this, we performed chromosome spreads assays in both the presence and absence of HU. Cells were lysed, nuclei were spread on glass slides, and Stn1 was labeled by immunostaining. DNA was

also stained with DAPI, and presence of Stn1 on DNA was determined by fluorescence microscopy. The results show that in both untreated and HU treated samples, excess Stn1 generally binds to chromatin (Figure 1-6; experiment performed by Jeff Julius, analyzed by Jeff Bachant). This indicates that when Stn1 is overproduced, it can mislocalize on chromatin, and interfere with the normal execution of the S phase checkpoint. However, this data does not address whether Stn1 specifically associates with replication origins or sites of damage, or if it binds non-specifically to any DNA sequence.

Disrupting the Stn1-Pol12 interaction suppresses the Stn1 S phase checkpoint defect

After discovering that excess Stn1 can associate with chromatin, we attempted to identify the mechanism for this mislocalization. Although Stn1 can weakly bind to telomeric DNA *in vitro* (Gao *et al*, 2007), we hypothesized that it associates with chromatin via interactions with Pol-α. To test this, we utilized the *pol12-40* loss of function allele, which partially cripples the Stn1-Pol12 interaction (Chiu, 2007). *STN1* was overexpressed in the *pol12-40* mutant background, and chromosome spreads were performed as before. Results show that mislocalization of Stn1 is dependent on a functional Pol12 (Figure 1-6; experiment performed by Jeff Julius, analyzed by Jeff Bachant).

Having shown that the Stn1 mislocalization phenotype depends on having wild type Pol12 protein, we next asked if Pol12 function is required for the checkpoint phenotypes. We overexpressed *STN1* or vector controls in the *pol12-40* mutant background, and assayed for both HU sensitivity and spindle elongation. The *pol12-40*

mutation suppresses both the extreme HU sensitivity and spindle elongation phenotypes caused by *STN1* overexpression (Figure 1-7 A, B). We also performed a Western blot to compare the Stn11 protein abundance in wild type and *pol12-40* strains. We found that the protein accumulates to comparable levels in both backgrounds, suggesting that the suppression in the *pol12-40* background is not simply a result of reduced Stn1 levels (Figure 1-7 C). These data show that the functional *POL12* is required for both the checkpoint phenotype and protein mislocalization, but not the stable accumulation of Stn1 in cells.

A functional MCM helicase complex is required for Stn1 to interfere with the checkpoint

We next tested the genetic requirements for Stn1 to block the replication checkpoint. The data from Figures 1-6 and 1-7 suggest that having functional Pol-α is required for Stn1's ability to interfere with the checkpoint. Therefore, we hypothesized that mutations which reduce replication efficiency may also suppress the checkpoint phenotypes caused by *STN1* overexpression. We screened a collection of alleles with replication defects, and identified two mutants within the MCM helicase complex, *mcm2-1* and *mcm5-1,* which partially suppress the Stn1 checkpoint phenotypes. Both mutant alleles produce hypomorphic proteins which have reduced DNA replication proficiency (Yan et al., 1991; Chen *et al*, 1992). *STN1* overexpression in the *mcm* mutant background allows for slightly better growth on low concentrations of HU, and significantly improved ability to recover from transient exposure to higher HU concentrations (Figure

1-8 A, B). We also analyzed the mitotic spindle elongation phenotype of Stn1 overproducing cells in the *mcm* background. Strikingly, both the *mcm2-1* and *mcm5-1* mutations completely suppress the *STN1* spindle elongation phenotype (Figure 1-8 C). Taken together, these results indicate that *STN1* requires a fully functional MCM helicase complex to block the execution of the replication checkpoint.

We next asked if Stn1 accumulates to high levels in the *mcm* background, and if so, whether it's bound to chromatin. Chromosome spreads were performed as before, and the presence of Stn1 on chromatin was analyzed via fluorescence microscopy for at least 100 nuclei from each sample. Figure 1-9 A shows representative micrographs, and Figure 1-9 B is a quantification of the data. The results indicate that overproduced Stn1 can still generally associate with chromatin in the *mcm* background, in both the presence or absence of HU. To corroborate this finding, a Western blot was performed analyzing Stn1 protein levels in WT and *mcm* cells. The results confirm that overproduced Stn1 accumulates to approximately equivalent levels in both WT and *mcm* mutant backgrounds (Figure 1-9 C).

Stn1 can block the S phase checkpoint response in the absence of Dbf4.

After discovering that Stn1 requires full MCM helicase function to interfere with the S phase checkpoint, we asked if DDK activity was necessary. The DDK complex, composed of the Cdc7 kinase and Dbf4 regulatory subunit, phosphorylates the MCM helicases to initiate DNA unwinding at the onset of S phase. Although both *DBF4* and *CDC7* are required for viability, the *mcm5-bob1* suppressor mutation can bypass their

essential function (Hardy *et al*, 1997). Using this allele, we overexpressed *STN1* in a *dbf4-Δ* background, and assessed the functionality of the S phase checkpoint. We hypothesized that if Stn1 requires a fully functional DDK complex to interfere with the replication checkpoint, deletion of *dbf4* would suppress the *STN1* overexpression phenotypes. We first attempted to analyze the viability of *dbf4-Δ* strains overproducing Stn1 on HU. However, the *dbf4-Δ* strain is HU sensitive on its own, compounding the genetic analysis (Figure 1-10A). Previous work has shown that although *cdc7-Δ* and *dbf4-Δ* strains are sensitive to chronic HU treatment, they are able to recover from transient exposure (Weinreich and Stillman 1999; Ogi *et al*, 2008). Therefore, we tested if *dbf4-Δ* strains overexpressing *STN1* can recover from transient exposure to 200 mM HU. The results indicate that the *dbf4-Δ/ STN1* strain is just as HU sensitive as the *DBF4/ STN1* strain, and both are nearly as sensitive as the *rad53-21* checkpoint mutant (Figure 1-10 B). Consistent with published work, we found that *dbf4-Δ/* vector strain is able to recover from the transient HU exposure. We also analyzed the lengths of mitotic spindles in these strains. We found that a large fraction of Stn1 overproducing cells still have elongated spindles in the absence of Dbf4 (Figure 1-10 C). Taken together, these results show that Stn1 does not require DDK function to block execution of the replication checkpoint.

Discussion

The S phase checkpoint functions to prevent fork collapse and blocks origin firing in the presence of replication stress. Our findings show that Stn1 overproduction interferes with the S phase checkpoint response. We found that Stn1 overproducing cells are able to activate Rad53 with normal kinetics in response to replication stress and DNA damage occurring in S phase, suggesting that the upstream sensory functions of the checkpoint are intact. However, downstream effects of the S phase checkpoint activation are compromised. *STN1* overexpression leads to premature elongation of the mitotic spindle in the presence of HU, diminished fork progression, and failure to block firing of late origins in the presence of MMS. Although these phenotypes appear to be distinct and unrelated, it is likely that they are in fact reflections of a single defect; the inability to repress origin firing in response to replication stress. Additionally, *STN1* overexpression causes extreme sensitivity to HU and MMS, reinforcing the notion that the S phase checkpoint has been disrupted; however, this phenotype is unlikely to be a direct result of the deregulation of origin firing.

Normally, cells shut down firing of late origins in response to HU or MMS, allowing forks from early origins to remain stable and progress slowly (Santocanale and Diffley, 1998; Shirahige *et al*, 1998). In the absence of a functional S phase checkpoint, HU treated cells are unable to repress firing of late origins, and therefore have more forks that can potentially stall or collapse. Additionally, replication checkpoint mutants are unable to induce production of dNTPs, increasing the probability of fork stalling (Allen *et al*, 1994). These problems are thought to be the main reason why S phase checkpoint

mutants show extreme sensitivity to replication inhibitors. How does the S phase checkpoint restrain premature mitotic spindle elongation? Normally, centromeres are replicated early in S phase (Raghuraman *et al*, 2001; Wyrick *et al*, 2001). This allows for timely kinetochore assembly, and the establishment of bipolar attachments to the mitotic spindle (Bachant *et al*, 2005). Thus, in a large fraction S phase checkpoint defective cells, centromeres remain unreplicated due to stalling or collapse of forks from early origins (Feng *et al*, 2009). When the spindle attaches to an unreplicated centromere, there is no sister chromatid to counteract the pulling force. This is thought to be the reason for the premature spindle elongation seen in S phase checkpoint mutants. Thus, fork progression problems, inappropriate late origin firing and mitotic spindle elongation phenotypes of Stn1 overproducing cells (or any S phase checkpoint mutants) all arise from a failure to regulate replication. The HU sensitivity phenotypes, however, does not directly arise from the failure to regulate firing or late replication origins. In *mrc1Δ* mutants, or *sld3 dbf4* double mutants which are resistant to Rad53 phosphorylation, late replicating origins are activated in the presence of HU or MMS (Alcasabas *et al*, 2001; Lopez-Mosqueda *et al*, 2010; Zegerman and Diffley, 2010). However, these cells are significantly more resistant to HU and MMS than *rad53* mutants or *STN1* overexpressing cells. This suggests that the extreme sensitivity to DNA replication inhibitors is caused by additional checkpoint defects in these strains.

Why are Stn1 overproducing cells more sensitive to replication inhibitors than *mrc1Δ* mutants or other strains which fire late replication origins in the presence of HU/MMS? The most straightforward explanation for this observation is that in addition

to defects in regulating origin firing, *STN1* overexpression disrupts other processes required for viability when cells experience replication stress. For example, the S phase checkpoint regulates a variety of nucleases, helicases, and other repair factors to stabilize stalled replication forks (Figure 0-5). When Stn1 is overproduced, it may interfere with the normal processing events required to stabilize such forks, thus leading to the extreme HU and MMS sensitivity phenotype. This is consistent with the current understanding of the S phase checkpoint, which claims that its essential function is to allow efficient recovery from replicative stress, by preserving the integrity of replication forks and preventing their catastrophic collapse (Desany *et al*, 1998; Branzei and Foiani, 2010). Thus, mutants which simply disrupt the temporal program of replication origin firing but do not affect fork stability are more HU and MMS resistant than those that completely eliminate all functions of the S phase checkpoint. In *mrc1Δ* mutants, late firing origins become de-repressed; however, once replication forks encounter lesions which produce DNA double stranded breaks, the Rad9 dependent DNA damage checkpoint becomes activated, and phosphorylates Rad53 (Alcasabas *et al*, 2001). Rad53 can then target the appropriate repair factors to prevent the accumulation of additional fork problems.

How does Stn1 overproduction interfere with checkpoint regulation of DNA replication? To answer this question, we must first consider Stn1's role in facilitating telomere replication. The current model in the field is that Stn1 either recruits or activates Pol-α via interaction with Pol12, to promote synthesis of the telomeric C-strand. There are still many unanswered questions about the details of this process. For example, it is not known if this activity occurs in conjunction with normal passage of the replication

fork, or is a temporally separate event. Along those lines, it is also not yet known whether fill-in synthesis of the telomeric C-strand requires DDK and MCM function, or any other replisome component. Starting from what was known, we hypothesized that when *STN1* is overexpressed, it overrides checkpoint control of DNA replication by inappropriately activating Pol-α via its interaction with Pol12. We found that weakening the Pol12-Stn1 interaction with the *pol12-40* mutant allele suppressed the checkpoint phenotype, by preventing Stn1 mislocalization. This finding suggests that the mechanism by which Stn1 promotes telomere replication is most likely the same one that leads to the checkpoint defect.

Does Stn1 override the checkpoint's control of DNA synthesis through the standard replication initiation pathway of origin firing? The finding that Stn1's checkpoint phenotype is dependent of MCM function, but does not required the DDK complex implies that Stn1 does not interfere with control of DNA replication through the canonical DDK dependent origin activation pathway; rather, it may do so by stimulating *de novo* priming and elongation of a single-stranded template. Such a scenario would required MCM helicases for elongation, but would be independent of DDK activity. This would be consistent with findings from experiments preformed using *Xenopus* egg extracts, where it has been shown that Stn1 is required for replication of a single-stranded plasmid (Nakaoka *et al*, 2012). Replication using a ssDNA molecule as a template requires recruitment of Pol-α and *de novo* priming independent of replisome assembly. Thus, it is very likely that Stn1 overrides the checkpoint's regulation of DNA replication through such a pathway.

From the Stn1 overproduction data, we can infer some details about the organization of the S phase checkpoint. Previous reports have identified the DDK complex as a target of Rad53, which regulates late origin firing (Lopez-Mosqueda *et al*, 2010; Zegerman and Diffley, 2010; Duch *et al*, 2011). However, determining whether Rad53's phosphorylation of Dbf4 interferes with the function of the MCM complex has not been shown. In theory, this can be determined by using the *mcm5-bob1* allele to bypass *DBF4*/*CDC7*, and asking if the checkpoint is required to survive replication stress and restrain spindle elongation; however, the DDK cannot be deleted when *RAD53* function is compromised, thus preventing this type of genetic analysis (Dohrmann *et al*, 1999). When the S phase checkpoint is disrupted by overexpressing *STN1*, cells can still tolerate deletion of *Dbf4* using the *mcm5-bob1* suppressor allele. We can use this genetic background to then ask if we can restore some functionality to the checkpoint. Our results show that even in the absence of Dbf4, Stn1 overproduction interferes with the checkpoint response leading to HU sensitivity and premature spindle elongatoin. Thus, from this result, we can conclude that in addition to the Dbf4 dependent block to late origin activation, there must be additional checkpoint targets required to restrain the elongation of the spindle in response to HU.

An important consideration when interpreting these data is that Stn1 is overproduced in all of our experiments. Therefore, it is possible that the observations we've made are not representative of normal function of Stn1 in cells; we've created an artificial situation where the telomeric function of Stn1 has been transplanted elsewhere in the genome. However, several observations indicate that Stn1 does in fact have a

normal role in controlling DNA replication at non-telomeric sites. As mentioned previously, the mammalian homolog of Stn1 (AAF42) was initially discovered as a Pol-α accessory factor (Goulian and Heard, 1990; Goulian *et al*, 1990; Casteel *et al*, 2009). Further characterization of Stn1 in human cells has shown that it does in fact promote firing of dormant origins throughout the genome after recovery from replication stress (Stewart *et al*, 2012). Lastly, we will show in the next chapter that *stn1* loss of function mutants have defects in global DNA synthesis when combined with DDK mutants. Therefore, our results from the overproduction studies are likely to reflect a normal function of Stn1.

Materials and Methods

Strains and plasmids

All strains used in this chapter are listed in Table 1-1, and all plasmids used are listed in Table 1-2. Yeast strains were grown and propagated following standard procedures (Sherman, 2002).

Serial dilution plating assays

Cells of the indicated genotype were inoculated from single colonies grown on selective plates, and incubated for 3 days at 30°C (or 4 days at 23°C for temperature sensitive strains). For each strain, 10-fold serial dilutions from the same initial concentration of cells were done in a 96-well microtiter dish, and stamped onto appropriate plates. Plates were incubated for 3-4 days at the indicated temperatures.

Spindle length measurements

Cells of the indicated genotype were synchronized in G1 by arresting with alpha factor pheromone. The cells were then washed and released into fresh media containing 200mM HU. After 2.5 hours, cells were collected. For strains containing the Spc42-GFP marker, cells were suspended in stop buffer (1mM NaN_3, 10mM EDTA, 200mM NaCl), DNA was stained with DAPI, and spindles were analyzed by fluorescence microscopy. The distance between spindle poles (as indicated by GFP spots) of at least 100 large-budded cells/ strain were measured using the Metamorph software.

For strains not tagged with the Spc42-GFP marker, spindles were analyzed by tubulin immunofluorescence. 10^7-10^8 cells were fixed in 3.7% formaldehyde for 4 hours, permeabilized with 70% ethanol for 1 hour, and spheroplasted for 1 hour with Zymolyase solution (0.1M $NaPO_4$, 1.2M sorbitol pH7.5, 25mM BME, 5mg/mL Zymolyase 100T). The spheroplasted cells were incubated with primary antibody (rat anti-tubulin, YOL1/34 from Accurate Scientific) at a 1:50 dilution in PBS containing 1mg/ml BSA at 4°C overnight with gentle rocking. The primary antibody was washed out, and cells were treated with secondary antibody (FITC-conjugated goat anti-rat from Sigma) at a 1:100 dilution of in PBS containing 1mg/ml BSA for 1 hour at room temperature with gentle rocking. Cells were then resuspended in PBS, DNA was stained with DAPI, and spindles were analyzed by fluorescence microscopy. The spindles of at least 100 large-budded cells were measured using the Metamorph software.

BrdU-IP microarray experiments

BrdU-IP microarray experiments were performed in the laboratory of Dr. Oscar Aparicio at the University of Southern California, following previously described protocols (Vigiani *et al*, 2010), with minor modifications. The indicated strains containing the BrdU-Inc construct were synchronized in G1 by arresting with alpha factor pheromone. The cells were then washed and released into fresh media containing 800 µg/mL BrdU (Sigma) and 0.033% MMS where indicated. Cells were harvested at the indicated time points and lysed by bead-beating in lysis buffer (100mM Tris pH8.0, 50mM EDTA, 1% SDS). DNA was collected using standard phenol/chloroform

extraction procedures, precipitated with 95% ethanol, resuspended 100μL of 1x TE, and sheared by sonication. Samples were treated with RNase for 1 hour at 37°C and proteinase K for 1 hour at 50°C. DNA was cleaned up over columns (Qiagen), eluted with 50μL of elution buffer, and the concentrations were measured on a nanodrop. For each sample, 1μg of DNA was used for the IP, and 1μg was saved as a "reference".

IP's were performed by combining 1μg of sample DNA, 50μg salmon sperm DNA, 10μL of 10x PBS and H_2O to a final volume of 100μL, heating samples to 95°C to denature DNA, cooling on ice, adding 900μL of IP buffer (1x PBS + 0.05% triton-X), 10μL of anti-BrdU antibody (Invitrogen) at a 1:500 dilution, and 20μL of protein A/G magnetic beads. Samples were incubated at 4°C for 2 hours with gentle rocking, washed 4 times with 1mL of IP buffer, and eluted with 50μL of elution buffer. Samples were cleaned up over columns (Qiagen), eluted with 10μL of elution buffer, and the concentrations were measured on a nanodrop. Samples were then amplified with the GenomePlex Whole Genome Amplification kit (Sigma).

After amplification, samples were subjected to Klenow extension for 4 hours at 37°C. 500ng of each sample was conjugated with Cy5 fluorophore (GE Healthcare) to label immunoprecipitated DNA or Cy3 fluorophore (GE Healthcare) to label whole genomic "reference" DNA. 1 μg of "reference" DNA and 1 μg of immunoprecipitated sample were combined, dried in a SpeedVac (Thermo), resuspended in 10 mM EDTA, and denatured for 2 minutes. Samples were suspended in prewarmed (50°C) hybridization buffer (30% formamide, 5x SSC, 0.1% SDS, 100 μg/mL salmon sperm DNA), and hybridized to microarrays for 18 hours at 50°C. Slides were washed with

gentle shaking in 1x SSC, 0.1% SDS, 1mM DTT for 5 min, submerged several times in 0.2x SSC, 1 mM DTT, and washed 2 times for 3 min in 0.1x SSC, 1mM DTT. Slides were dried by centrifugation for 45 seconds in a microcentrifuge and scanned in an Axon scanner using Genepix 5.0 to capture and save the images.

Microcolony formation assay

Cells of the indicated genotype were grown to logarithmic phase in 5mL of YPD at 30°C, and spotted onto either YP-glucose or YP-galactose plates. The strains encode a galactose-inducible HO endonuclease, and an HO recognition sequence cloned within the genome. Plating cells onto media containing galactose induces expression of the endonuclease, thus generating a double-stranded break. 49 cells from each plate were micro-manipulated into a 7 x 7 grid, and incubated at 30°C for 16 hours. At the indicated time points, the number of cells in each microcolony was counted.

Protein methods

To detect Rad53 phosphorylation, 25mL of cells per time point were grown to logarithmic phase, synchronized in G1 by arresting with alpha factor pheromone, then washed and released into fresh media containing 200mM HU or 0.03% MMS. Cells were harvested at the indicated time points and lysed by bead beating in 300µL of 20% trichloroacetic acid (TCA) containing protease inhibitors (1µg/mL leupeptin, 2µg/mL aprotinin, 15µg/mL benzamindine, 100µg/mL PMSF, 10µg/mL pepstatin). Lysates were centrifuged for 10 minutes at 3,000rpm in 4°C to pellet proteins, and TCA was removed.

Protein pellets were resuspended in 200µL of equal parts 1M Tris base and Buffer A (25mM HEPES pH 7.5, 5mM $MgCl_2$, 50mM KCl, 10% glycerol, 0.5% Triton X-100), and protease inhibitors were supplemented. 100µL of 20% SDS and 60µL of Laemmli sample buffer (50mM Tris pH6.8, 2% SDS, 10% glycerol, 0.1M DTT, 0.01% bromophenol blue) were added to each sample, and the protein preparations were boiled at 95°C for 5 minutes. 100µL of each lysate was loaded and separated on a 10% 30:0.39 acrylamide/bisacrylamide gel, and proteins were transferred to a nitrocellulose membrane. Western blots were performed using standard procedures. The primary antibody (goat anti-Rad53 from Santa Cruz Biotechnology) was used at a 1:1,000 dilution in PBS containing 1mg/mL BSA, while the secondary antibody (HRP-conjugated donkey anti-goat from Santa Cruz Biotechnology) was used at a 1:10,000 dilution in PBS containing 1mg/mL BSA.

To detect Stn1-HA protein levels, 25mL of cells of the indicated genotype were grown to logarithmic phase. Cells were harvested by centrifugation and lysed by bead beating in 300µL of 20% trichloroacetic acid (TCA) containing protease inhibitors (1µg/mL leupeptin, 2µg/mL aprotinin, 15µg/mL benzamindine, 100µg/mL PMSF, 10µg/mL pepstatin). Lysates were centrifuged for 10 minutes at 3000rpm in 4°C to pellet proteins, and TCA was removed. Protein pellets were resuspended in 200µL of equal parts 1M Tris base and Buffer A (25mM HEPES pH 7.5, 5mM $MgCl_2$, 50mM KCl, 10% glycerol, 0.5% Triton X-100), and protease inhibitors were supplemented. 100µL of 20% SDS and 60µL of Laemmli sample buffer (50mM Tris pH6.8, 2% SDS, 10% glycerol, 0.1M DTT, 0.01% bromophenol blue) were added to each sample, and the protein

preparations were boiled at 95°C for 5 minutes. 100µL of each lysate was loaded and separated on a 10% polyacrylamide gel, and proteins were transferred to a nitrocellulose membrane. Western blots were performed using standard procedures. The primary antibody (mouse anti-HA, 12CA5 from Roche) was used at a 1:1,000 dilution in PBS containing 3% non-fat dry milk, while the secondary antibody (HRP-conjugated goat anti-mouse from Chemicon) was used at a 1:25,000 dilution in PBS containing 3% non-fat dry milk.

Chromosome spreads

To detect the presence of Stn1-HA on chromatin, 5mL of cells of the indicated genotype were grown to logarithmic phase in appropriate selective media, in triplicates. Cells were harvested and resuspended in 1mL ZK buffer (25mM Tris pH7.5, 0.8M KCl) supplemented with 40µL of 1M DTT, incubated for 2 minutes at room temperature. Samples were spheroplasted by addition of 5µL of zymolyase solution (20mg/mL zymolyase 100T, 2% glucose, 50mM Tris pH7.5) and 2µL of BME, and incubated for 15 minutes at 30°C. The spheroplasted cells were washed with ice cold MES solution (1M Sorbitol, 0.1M MES pH6.5, 1mM EDTA, 0.5mM $MgCl_2$), then resuspended in 300µL of MES solution. 20µL of the cells were spotted onto a glass slide, followed by addition of 40µL of PFA solution (3% paraformaldehyde, 3.4% sucrose), 80µL of 1% lipsol. After 2 minutes of lysis, an additional 80µL of PFA solution was added, and lysates were spread across the glass slides with a clean glass Pasteur pipette. Slides were dried at room temperature overnight.

Prior to immunostaining, slides were washed with 0.2% photoflo (Kodak) for 30 seconds and TBS for 5 minutes, then blocked with 350μL of TBS containing 10mg/mL BSA for 15 minutes at 4°C. Excess blocking solution was drained, and 80μL of primary antibody (mouse anti-HA, 12CA5 from Roche) was added at a 1:200 dilution in TBS containing 10mg/mL BSA. Cover slips were applied, and slides were incubated at 4°C in a wet chamber overnight. Slides were washed twice with TBS, drained, and 80μL of secondary antibody (FITC-conjugated goat anti-rat from Sigma) was added at a 1:500 dilution in TBS containing 10mg/mL BSA. Cover slips were added, and slides were stored in the dark from this point on. After a 2 hour incubation at 4°C, slides were washed with TBS twice, and dried at room temperature for 4 hours. DNA was stained with DAPI, cover slips were applied, and samples were visualized by fluorescence microscopy. For each sample, at least 100 nuclei were scored for the presence of staining above background fluorescence. Analysis was done using the Metamorph software.

Cell viability assays

5mL of cells of the indicated genotype were grown to logarithmic phase in appropriate selective media at 30°C. Cell concentrations were determined by hemocytometery, and the appropriate volumes corresponding to ~500 cells were plated on YPD plates. HU was added to the cultures to a final concentration of 200mM, and the cultures were grown for up to 9 hours. At the indicated time points, ~500 cells were removed from the cultures and plated on YPD plates. All plates were incubated at 30°C

for 3 days to allow viable cells to form colonies. Colonies were counted, and the fraction of surviving cells relative to the untreated control was plotted on a logarithmic graph.

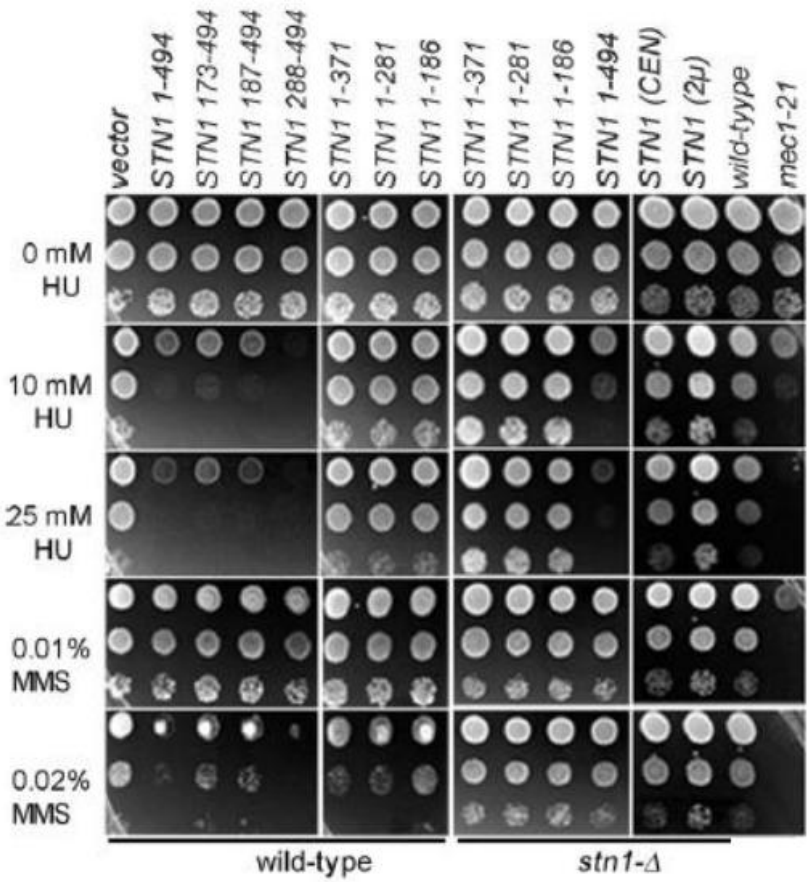

Figure 1-1: Stn1 overproduction makes cells extremely sensitive to replication inhibitors

Cells of the indicated genotype were grown to saturation in selective media for 3 days at 30°C, then 10-fold serial dilutions were stamped onto plates containing HU or MMS. Plates were incubated at 30°C for 3-4 days, then pictures were taken. Overexpression of full-length *STN1* or truncation alleles which encode the C-terminus cause extreme sensitivity to the replication inhibitor drugs. The *mec1-21* checkpoint mutant strain is shown for comparison. Strains used in this figure: hc160 (wild type), hc35 (*stn1-Δ*), hc29 (*mec1-21*). Plasmids used in this figure: pCN416 (*vector*), pCN421 (*STN1*), pCN424 ($STN1^{173-494}$), pCN422 ($STN1^{187-494}$), pCN423 ($STN1^{288-494}$), pCN418 ($STN1^{1-371}$), pCN419 ($STN1^{1-281}$), pCN420 ($STN1^{1-186}$), pCN1 (*CEN-STN1*), pVL1066 (*2μ-STN1*). Figure reproduced from Gasparyan *et al*, 2009 with permission from the publisher.

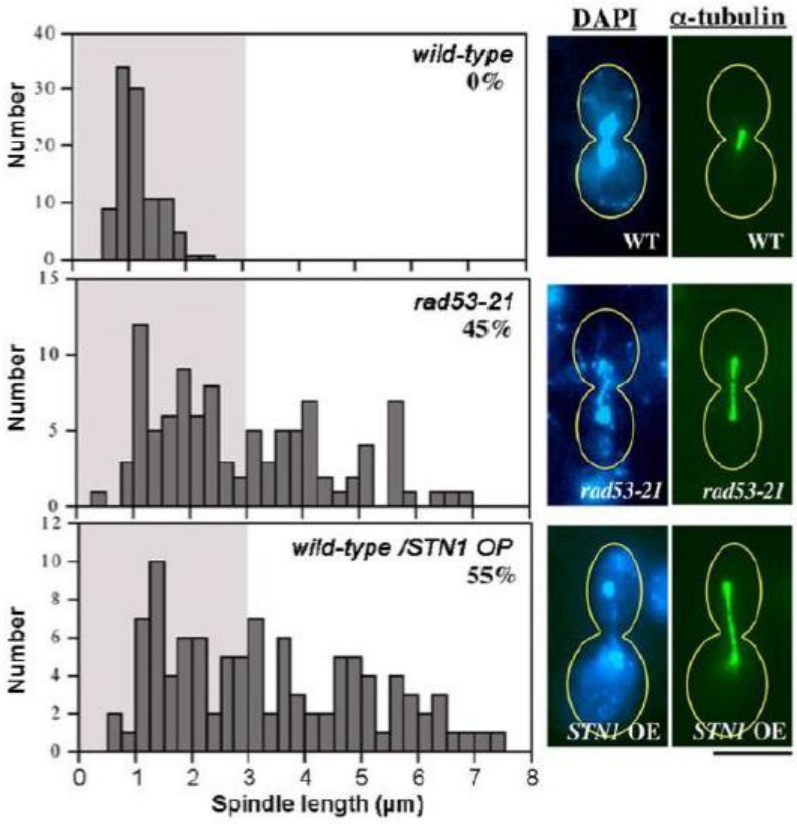

Figure 1-2: Stn1 overproducing cells arrest with elongated mitotic spindles in response to HU treatment

Cells of the indicated genotype were grown to logarithmic phase, arrested in G1, then released into media containing 200mM HU. After 2.5 hours, cells were fixed, spindles were stained with α-tubulin antibody, and DNA was stained with DAPI. The spindle lengths of at least 100 large budded cells from each sample were measured, and the data was plotted on histograms. *STN1* overexpressing cells display spindle elongation comparable to the *rad53-21* checkpoint mutant. Strains used in this figure: hc160 (wild type), hc27 (*rad53-21*). Plasmids used in this figure: pCN421 (*STN1*). Figure reproduced from Gasparyan *et al*, 2009 with permission from the publisher.

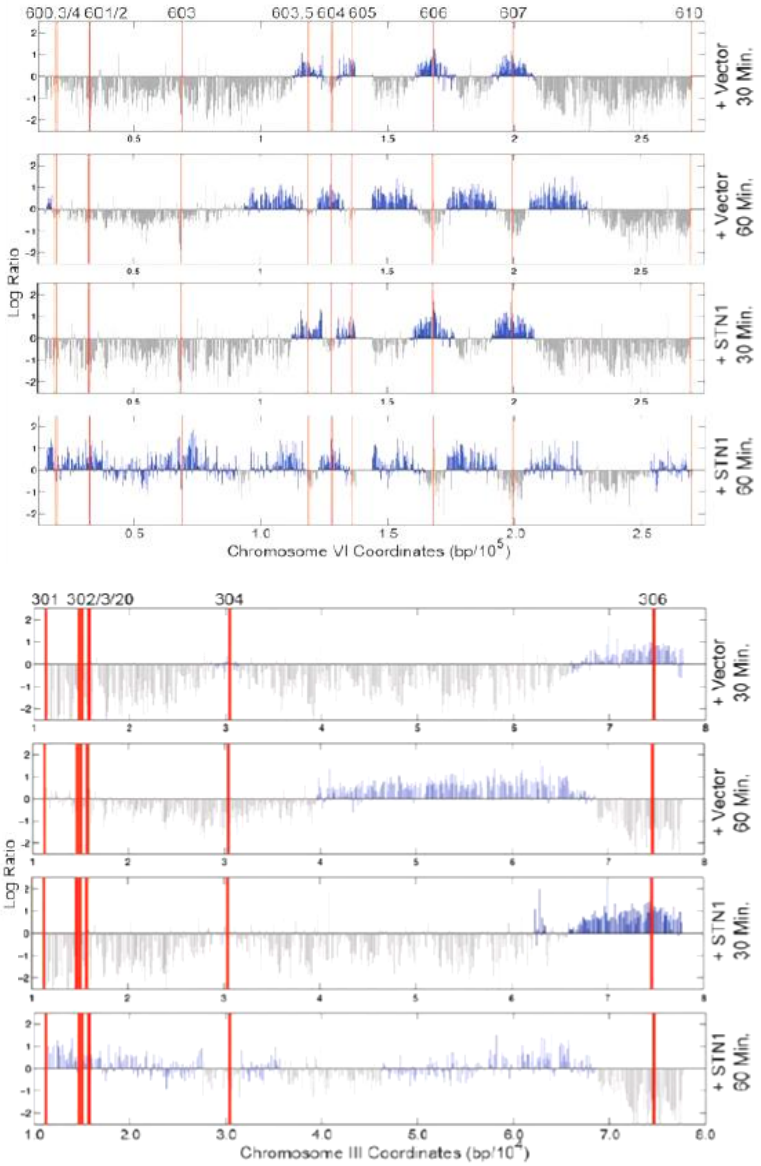

Figure 1-3: Stn1 overproducing cells inappropriately fire late replication origins when treated with MMS

Cells overproducing Stn1 or vector control were arrested in G1, and released into S phase in the presence of 0.033% MMS. Newly synthesized DNA was pulse labeled with BrdU for either 0-30 minutes or 30-60 minutes after release. Labeled DNA was immuno-precipitated with α-BrdU antibodies, and hybridized to a microarray covering chromosome VI and the left arm of chromosome III. The blue peaks represent areas enriched for BrdU, while the thick red lines represent the locations of replication origins. Strains used in this figure: hc2413 (vector), hc2414 (*STN1*). Figure reproduced from Gasparyan *et al*, 2009 with permission from the publisher.

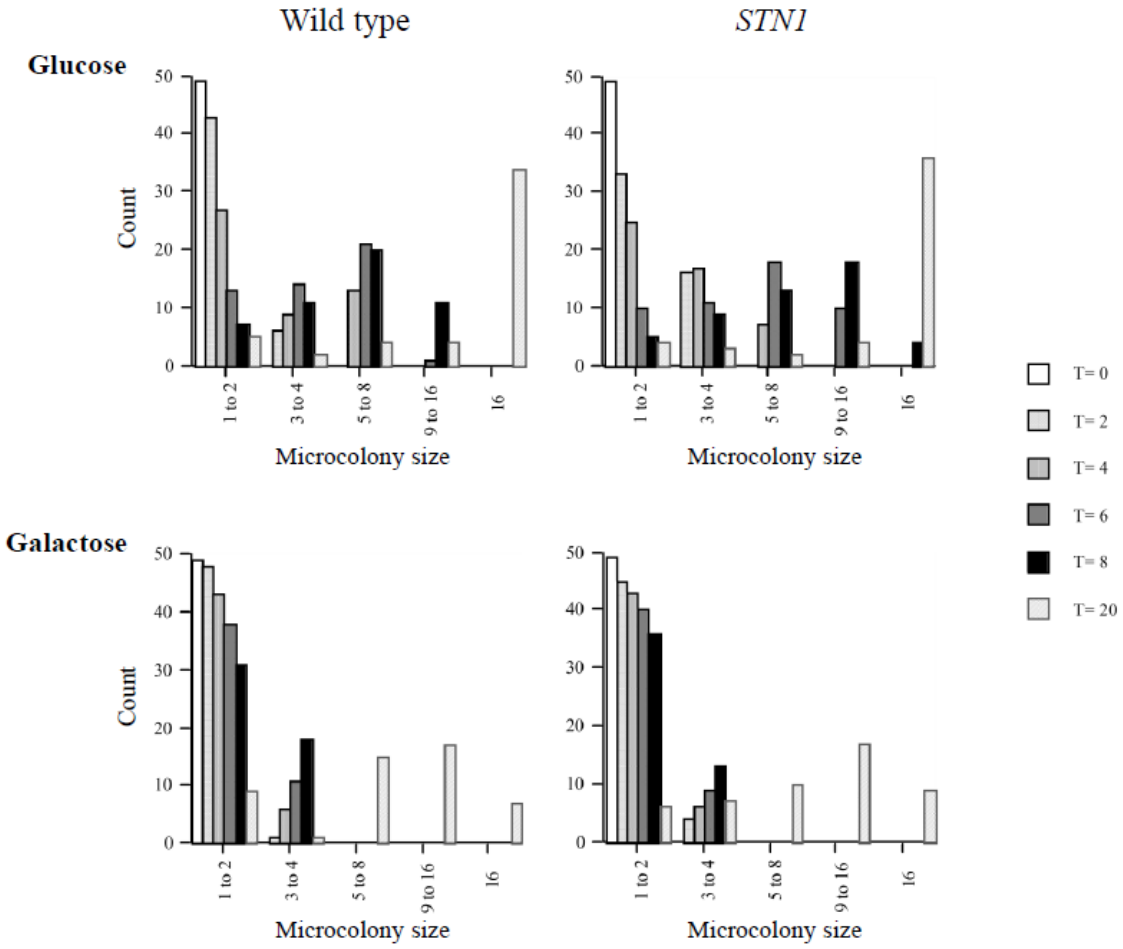

Figure 1-4: *STN1* overexpression does not interfere with the DNA damage checkpoint response

The DNA damage checkpoint response for cells overproducing Stn1 or vector control was analyzed. The strains contain and HO endonuclease recognition site, and the HO endonuclease under transcriptional control of a galactose inducible promoter. Strains were grown in selective media containing glucose to logarithmic phase, then plated onto either galactose plates to induce a double stranded break, or glucose control plates. 49 cells were isolated in a 7 x 7 grid, and their ability to form microcolonies was assessed at the indicated time points. Both WT and *STN1* overexpressing cells are able to arrest the cell cycle in response to a single DNA double strand break. Strains used in this figure: hc2230 (wild type), hc2232 (*STN1*). Plasmids used in this figure: pRS424 (vector), pVL1130 (*STN1*). Figure reproduced from Gasparyan *et al*, 2009 with permission from the publisher.

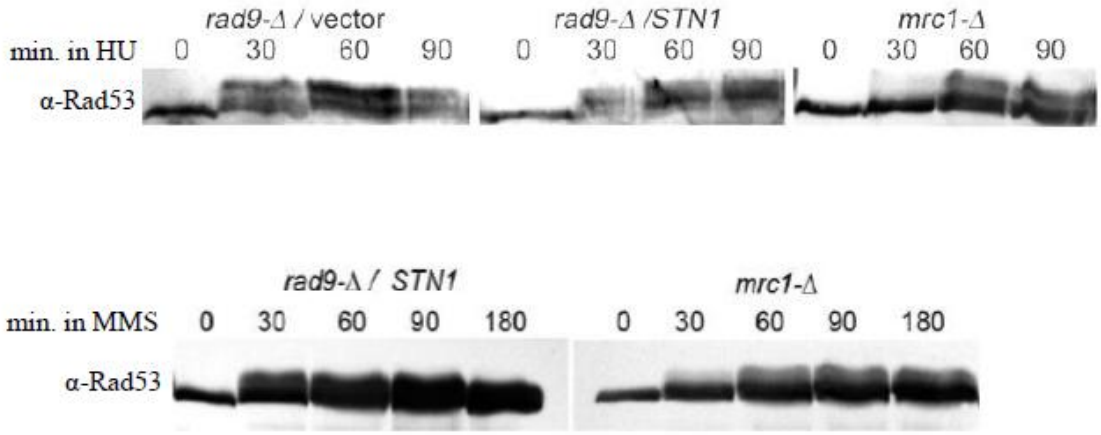

Figure 1-5: Stn1 overproducing cells can activate Rad53 in a timely manner in response to HU or MMS

Cultures of the indicated genotype were grown to logarithmic phase, arrested in G1, and released into media containing 200mM HU. Cells were lysed in 20% TCA, proteins were extracted, and separated on a 10% polyacrylamide gel. Western blot was performed probing against Rad53. The phosphorylated form of the protein migrates as a higher molecular weight species. Stn1 overproducing cells activate Rad53 with kinetics comparable to wild type controls. The *mrc1*Δ mutant control shows delayed activation of Rad53. Strains used in this figure: hc2112 (*rad9-Δ*/vector), hc2113 (*rad9-Δ*/*STN1*), mly89 (*mrc1-Δ*). Plasmids used in this figure: pCN416 (vector), pCN421 (*STN1*). Figure reproduced from Gasparyan *et al*, 2009 with permission from the publisher.

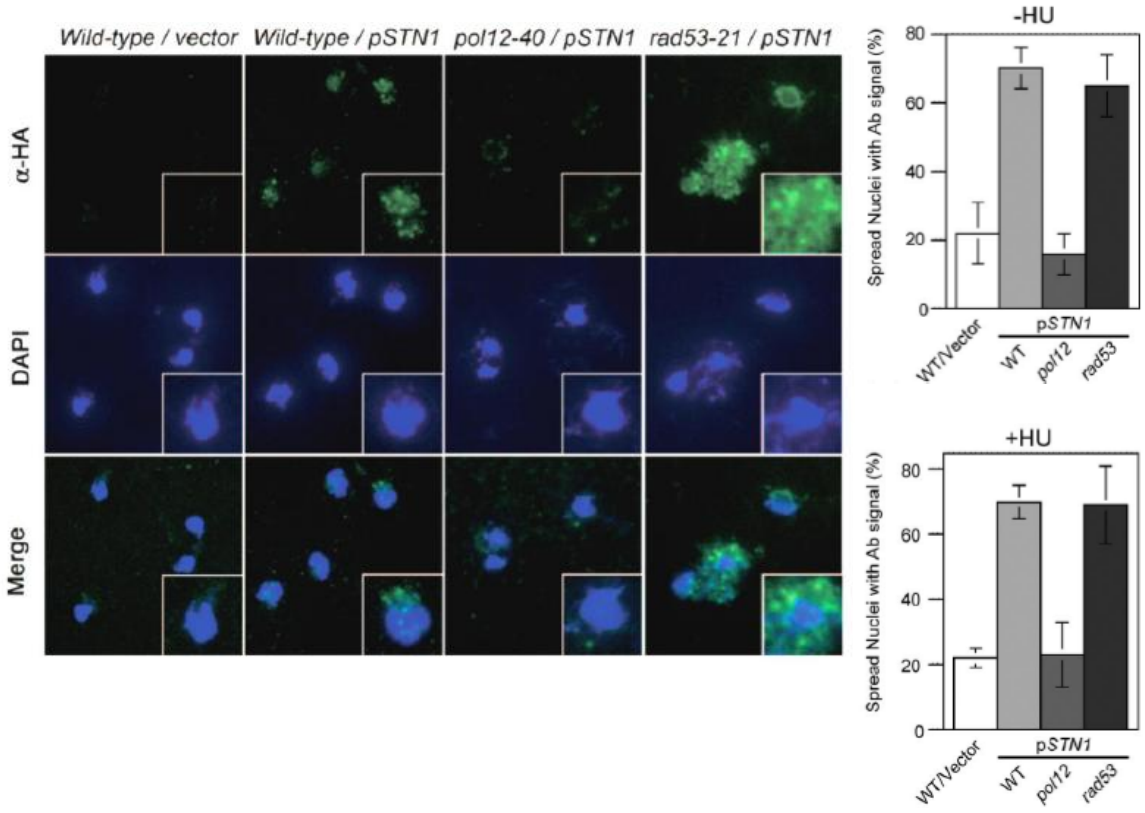

Figure 1-6: Overproduced Stn1 mislocalizes generally onto chromatin in a Pol12 dependent manner

Chromosome spreads were performed to assess misolcalization of overproduced Stn1. Cells of the indicated genotype were grown to logarithmic phase, lysed, and chromatin was spread on glass slides. Stn1 localization was monitored by immunostaining against HA, and DNA was stained with DAPI. For each sample, at least 100 nuclei were scored for the presence of signal over background, and the data was plotted on histograms. Overproduced Stn1 is shown to generally associate with chromatin; this association requires functional interaction with Pol-α. Strains used in this figure: hc160 (wild type), hc1741 (*pol12-40*), hc2062 (*rad53-21*). Plasmids used in this figure: pCN416 (vector), pCN421 (*STN1*). Figure reproduced from Gasparyan *et al*, 2009 with permission from the publisher.

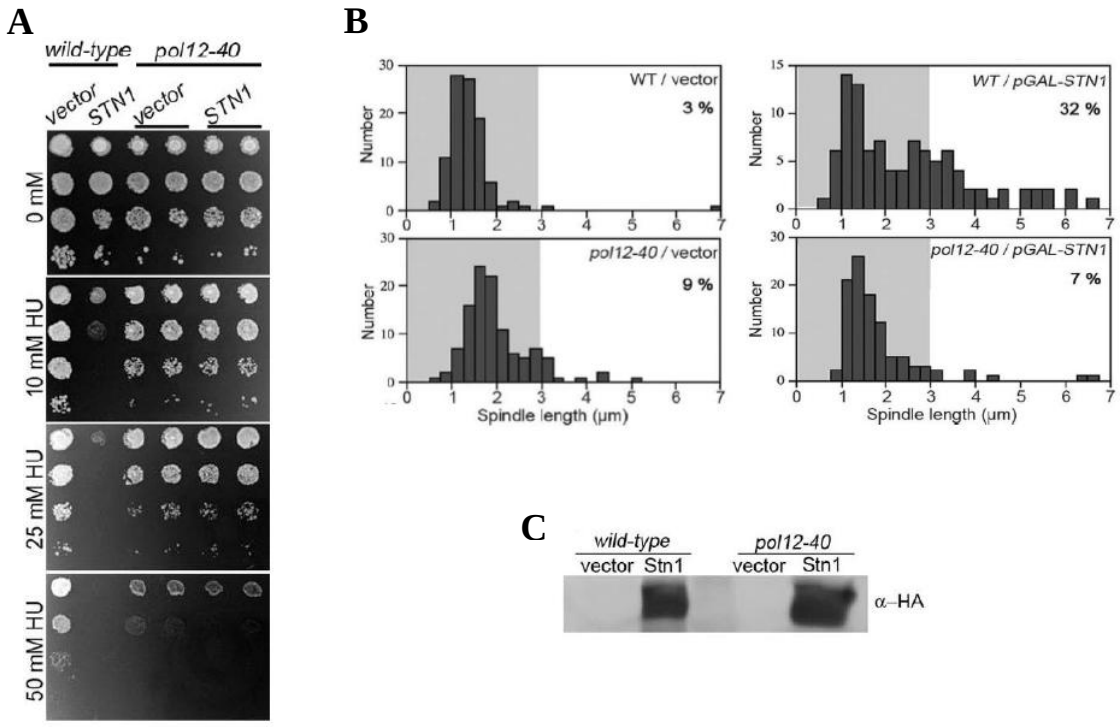

Figure 1-7: Compromising the Stn1-Pol12 interaction suppresses the S phase checkpoint defects caused by *STN1* overexpression

Disrupting the interaction between Stn1 and Pol12 suppresses the checkpoint defects caused by Stn1 overproduction. **(A)** Cells of the indicated genotype were grown to saturation in selective media for 3 days at 30°C, then 10-fold serial dilutions were stamped onto plates containing HU. Plates were incubated at 30°C for 3-4 days, then pictures were taken. **(B)** Cells were grown to logarithmic phase, arrested in G1, then released into media containing 200mM HU. After 2.5 hours, cells were fixed, spindles were stained with α-tubulin antibody, and DNA was stained with DAPI. The spindle lengths of at least 100 large budded cells from each sample were measured, and the data was plotted on histograms. **(C)** Stn1 levels were analyzed in wild type and *pol12-40* cells. Cells were grown to logarithmic phase, lysed by bead beating in Buffer A, proteins were extracted, and separated on a 10% polyacrylamide gel. Western blot was performed probing against HA. Stn1 accumulates to high levels in both wild type and *pol12-40* cells. Strains used in this figure: hc2208 (wild type/ vector), hc2209 (wild type/ *STN1*), hc2211 (*pol12-40*/ vector), hc2212 (*pol12-40*/ *STN1*). Plasmids used in this figure: pVL577 (vector), pCN177 (*STN1*), pPC64 (*pol12-40*). Figure reproduced from Gasparyan *et al*, 2009 with permission from the publisher.

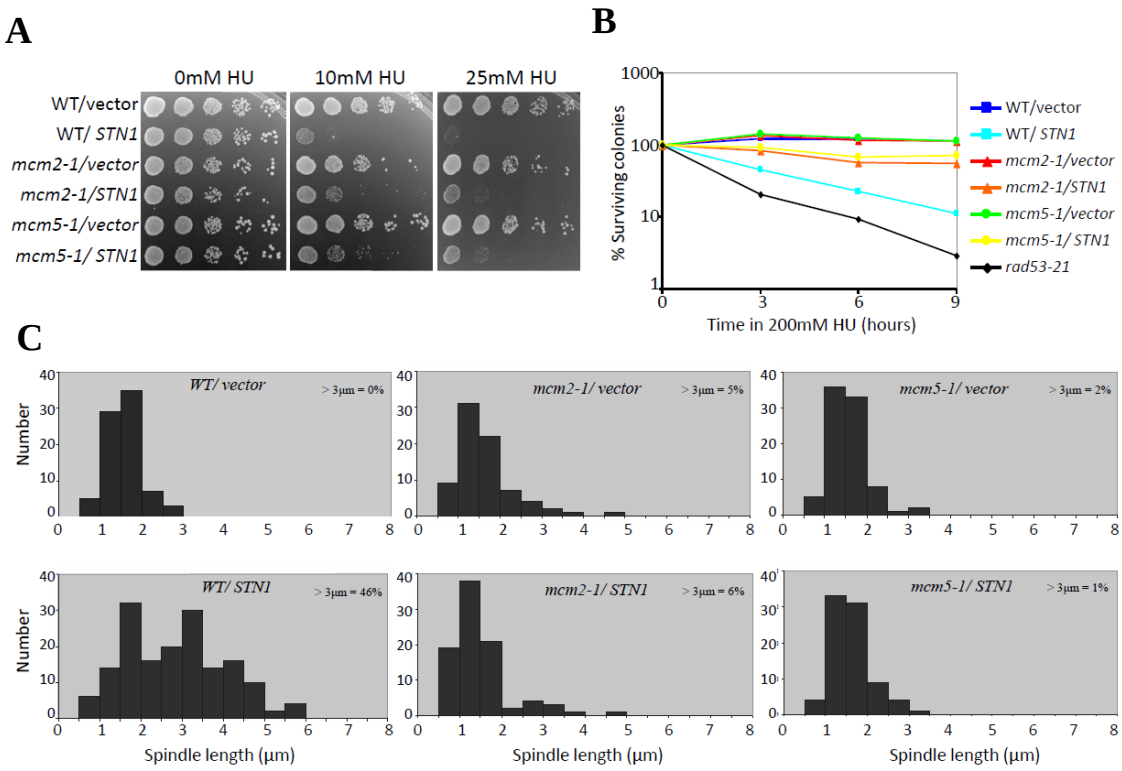

Figure 1-8: Loss of function *mcm* alleles can partially suppress the S phase checkpoint defects of *STN1* overexpression

Crippling the function of the MCM helicase complex partially suppresses the checkpoint defects caused by Stn1 overproduction. **(A)** Cells of the indicated genotype were grown to saturation in selective media for 3 days at 30°C, then 10-fold serial dilutions were stamped onto plates containing HU. Plates were incubated at 30°C for 3-4 days, then pictures were taken. **(B)** Viability of the indicated strains was determined after transient exposure to HU. Cells were grown to logarithmic phase, and treated with 200mM HU of the indicated times. Cells were then plated on media without drugs, and their ability to form colonies was assessed. **(C)** Cells were grown to logarithmic phase, arrested in G1, then released into media containing 200mM HU. After 2.5 hours, cells were fixed, and DNA was stained with DAPI. The position of the spindle poles was determined using a GFP tagged alleles of *SPC42*. The spindle lengths of at least 100 large budded cells from each sample were measured, and the data was plotted on histograms. Strains used in this figure: hc160 (wild type), hc2423 (*mcm2-1*), hc2424 (*mcm5-1*), hc27 (*rad53-21*). Plasmids used in this figure: pCN416 (vector), pCN421 (*STN1*).

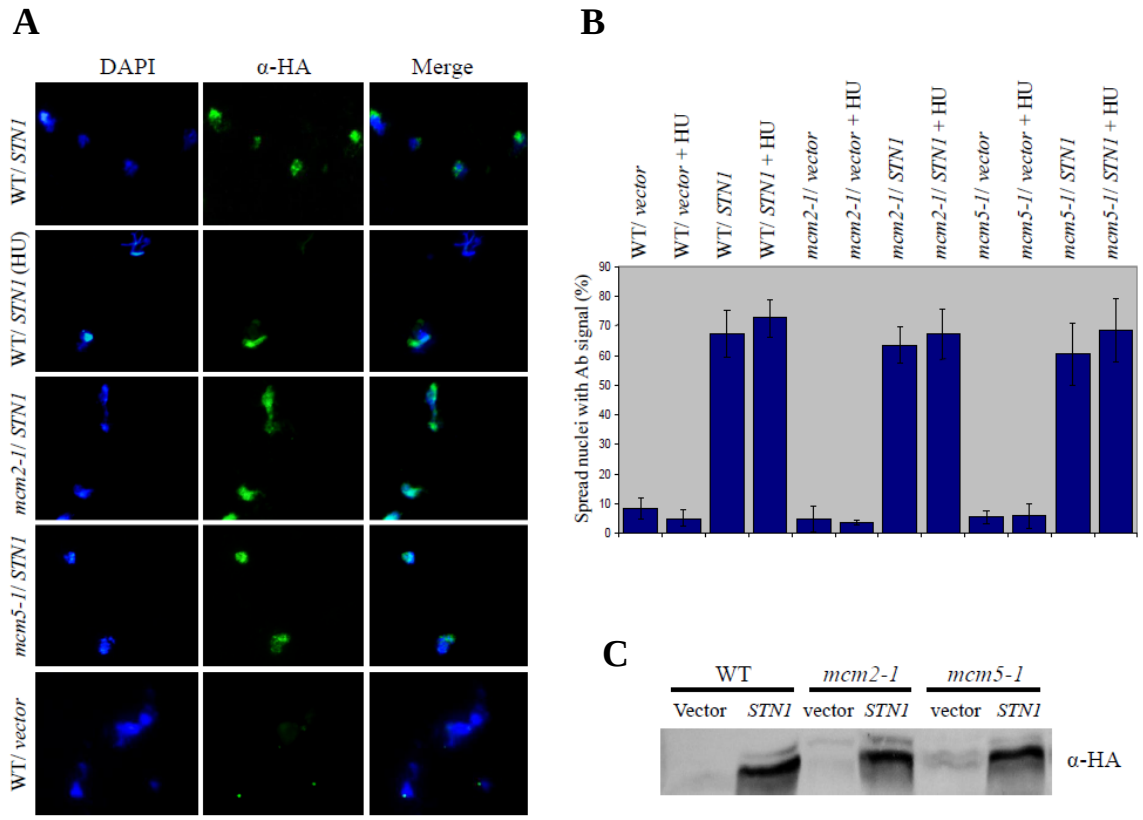

Figure 1-9: Overexpressed *STN1* still accumulates to high levels and associates with chromatin in *mcm* mutants

The protein levels and localization of Stn1 was monitored in *mcm* mutants. Chromosome spreads were performed to assess misolcalization of overproduced Stn1. Cells of the indicated genotype were grown to logarithmic phase, lysed, and chromatin was spread on glass slides. Stn1 localization was monitored by immunostaining against HA, and DNA was stained with DAPI. For each sample, at least 100 nuclei were scored for the presence of signal over background. **(A)** Representative micrographs of spreads showing Stn1 bound to chromatin. **(B)** Quantification of chromosome spread data. **(C)** Analysis of Stn1 levels wild type, *mcm2-1* and *mcm5-1* cells. Cells were grown to logarithmic phase, lysed by bead beating in Buffer A, proteins were extracted, and separated on a 10% polyacrylamide gel. Western blot was performed probing against HA. Stn1 accumulates to high levels in wild type and *mcm* cells. Strains used in this figure: hc160 (wild type), hc2423 (*mcm2-1*), hc2424 (*mcm5-1*). Plasmids used in this figure: pCN416 (vector), pCN421 (*STN1*).

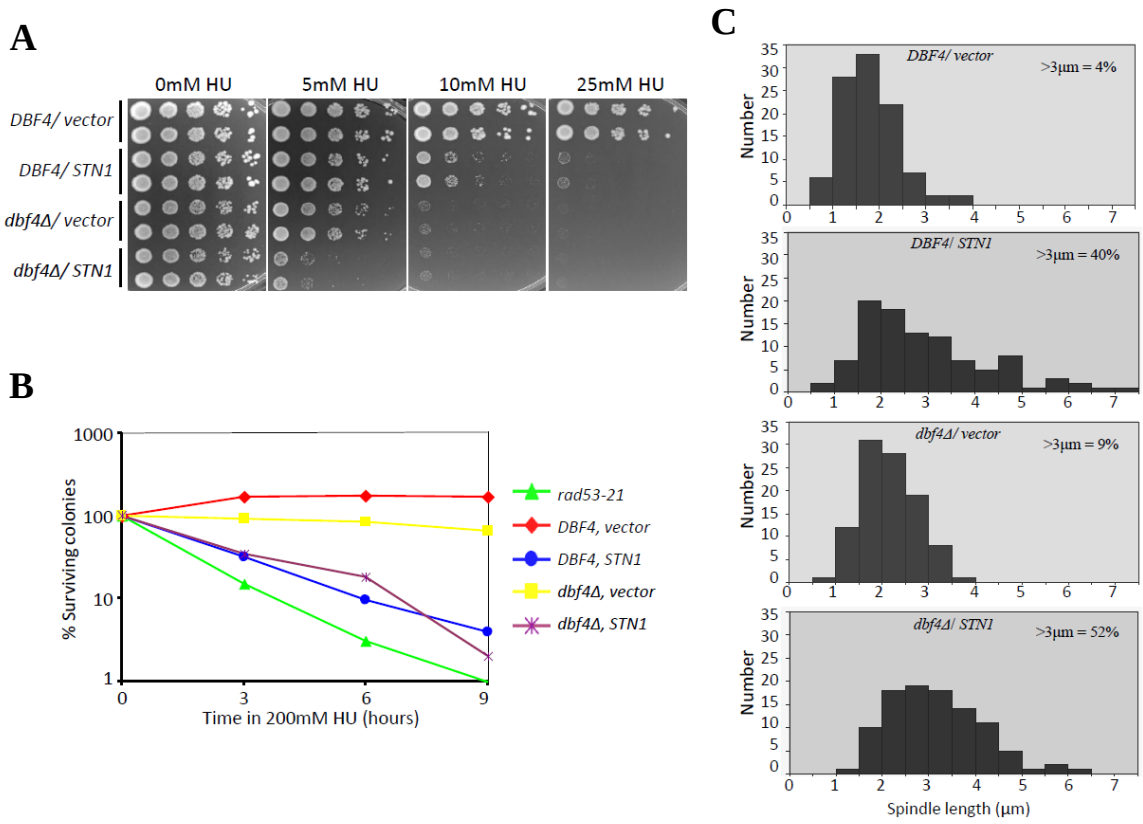

Figure 1-10: Stn1 overproduction can interfere with S phase checkpoint response in the absence of Dbf4

The *STN1* checkpoint defects are still observed in *dbf4*-Δ cells. *dbf4*-Δ cells are kept alive using the *mcm5*^{bob1} suppressor mutation. **(A)** Cells of the indicated genotype were grown to saturation in selective media for 3 days at 30°C, then 10-fold serial dilutions were stamped onto plates containing HU. Plates were incubated at 30°C for 3-4 days, then pictures were taken. **(B)** Viability of the indicated strains was determined after transient exposure to HU. Cells were grown to logarithmic phase, and treated with 200mM HU of the indicated times. Cells were then plated on media without drugs, and their ability to form colonies was assessed. **(C)** Cells were grown to logarithmic phase, arrested in G1, then released into media containing 200mM HU. After 2.5 hours, cells were fixed, and DNA was stained with DAPI. The position of the spindle poles was determined using a GFP tagged alleles of *SPC42*. The spindle lengths of at least 100 large budded cells from each sample were measured, and the data was plotted on histograms. Strains used in this figure: hc2405 (*DBF4*/vector), hc2406 (*DBF4/STN1*), hc2407 (*dbf4-Δ*/vector), hc2408 (*dbf4-Δ/STN1*), hc27 (*rad53-21*). Plasmids used in this figure: pCN416 (vector), pCN421 (*STN1*), pGO174 (*DBF4)*.

Table 1-1: List of strains used in chapter 1

Strain	Description	Reference
hc27	*MAT*a *ade2-1 ura3-1 his3-11,15 trp1-1 leu2-3,112 can1-100 CDC13myc($_{18x}$) rad53-21*	Gasparyan
hc29	*MAT*a *ade2-1 ura3-1 his3-11,15 trp1-1 leu2-3,112 can1-100 CDC13myc($_{18x}$) mec1-21*	Gasparyan
hc35	*MAT*a *ura3-52 lys2-801 ade2-101 trp1-Δ63 his3-Δ200 leu2-Δ1 stn1-Δ::kanMX2/* pVL1046	Petreaca[b]
hc160	*MAT*a *ura3-52 lys2-801 ade2-101 trp1-Δ63 his3-Δ200 leu2-Δ1*	Petreaca[a]
hc1741	*MAT*a *ura3-52 lys2-801 ade2-101 trp1-Δ63 his3-Δ200 leu2-Δ1 pol12-Δ::kanMX2/* pPC64	Chiu
hc2061	*MAT*a *ade2-1 ura3-1 his3-11,15 trp1-1 leu2-3,112 can1-100 CDC13myc($_{18x}$) rad53-21/* pCN416	Gasparyan
hc2062	*MAT*a *ade2-1 ura3-1 his3-11,15 trp1-1 leu2-3,112 can1-100 CDC13myc($_{18x}$) rad53-21/* pCN421	Gasparyan
hc2103	*MAT*a *ura3-52 lys2-801 ade2-101 trp1-Δ63 his3-Δ200 leu2-Δ1/* pCN422	Gasparyan
hc2104	*MAT*a *ura3-52 lys2-801 ade2-101 trp1-Δ63 his3-Δ200 leu2-Δ1/* pCN420	Gasparyan
hc2105	*MAT*a *ura3-52 lys2-801 ade2-101 trp1-Δ63 his3-Δ200 leu2-Δ1/* pCN424	Gasparyan
hc2106	*MAT*a *ura3-52 lys2-801 ade2-101 trp1-Δ63 his3-Δ200 leu2-Δ1/* pCN423	Gasparyan
hc2107	*MAT*a *ura3-52 lys2-801 ade2-101 trp1-Δ63 his3-Δ200 leu2-Δ1/* pCN419	Gasparyan
hc2108	*MAT*a *ura3-52 lys2-801 ade2-101 trp1-Δ63 his3-Δ200 leu2-Δ1/* pCN418	Gasparyan
hc2109	*MAT*a *ura3-52 lys2-801 ade2-101 trp1-Δ63 his3-Δ200 leu2-Δ1/* pCN421	Gasparyan
hc2110	*MAT*a *ura3-52 lys2-801 ade2-101 trp1-Δ63 his3-Δ200 leu2-Δ1/* pCN416	Gasparyan
hc2112	*MAT*a *ura3-52 lys2-801 ade2-101 trp1-Δ63 his3-Δ200 leu2-Δ1 rad9-Δ::His3/* pCN416	Gasparyan
hc2113	*MAT*a *ura3-52 lys2-801 ade2-101 trp1-Δ63 his3-Δ200 leu2-Δ1 rad9-Δ::His3/* pCN421	Gasparyan
hc2208	*MAT*a *ura3-52 lys2-801 ade2-101 trp1-Δ63 his3-Δ200 leu2-Δ1/* pVL577	Gasparyan
hc2209	*MAT*a *ura3-52 lys2-801 ade2-101 trp1-Δ63 his3-Δ200 leu2-Δ1/* pCN177	Gasparyan
hc2211	*MAT*a *ura3-52 lys2-801 ade2-101 trp1-Δ63 his3-Δ200 leu2-Δ1 pol12Δ::kanMX2/* pPC64, pVL577	Gasparyan

Table 1-1 (continued)

Strain	Description	Reference
hc2212	*MAT*a *ura3-52 lys2-801 ade2-101 trp1-*Δ*63 his3-*Δ*200 leu2-*Δ*1 pol12-*Δ*::kanMX2/* pPC64, pCN117	Gasparyan
hc2230	*MAT*a-*inc ura3-52 lys2-801 ade2-101 trp1-*Δ*63 his3-*Δ*200 leu2-*Δ*1 GAL-HO::LEU2 VII-L::ADE2-TG$_{1-3}$-HO site-LYS2/* pVL1130	Gasparyan
hc2232	*MAT*a-*inc ura3-52 lys2-801 ade2-101 trp1-*Δ*63 his3-*Δ*200 leu2-*Δ*1 GAL-HO::LEU2 VII-L::ADE2-TG$_{1-3}$-HO site-LYS2/* pRS415	Gasparyan
hc2405	*MAT*a *ura3-52 lys2-801 ade2-101 trp1-*Δ*63 his3-*Δ*200 leu2-*Δ*1 mcm5^{bob} SPC42GFP::TRP dbf4-*Δ*::KanMX2 /* pGO174, pCN416	This study
hc2406	*MAT*a *ura3-52 lys2-801 ade2-101 trp1-*Δ*63 his3-*Δ*200 leu2-*Δ*1 mcm5^{bob} SPC42GFP::TRP dbf4-*Δ*::KanMX2 /* pGO174, pCN421	This study
hc2407	*MAT*a *ura3-52 lys2-801 ade2-101 trp1-*Δ*63 his3-*Δ*200 leu2-*Δ*1 mcm5^{bob} SPC42GFP::TRP dbf4-*Δ*::KanMX2 /* pRS416, pCN416	This study
hc2408	*MAT*a *ura3-52 lys2-801 ade2-101 trp1-*Δ*63 his3-*Δ*200 leu2-*Δ*1 mcm5^{bob} SPC42GFP::TRP dbf4-*Δ*::KanMX2 /* pRS416, pCN421	This study
hc2413	*MAT*a *ade2-1 ura3-1 his3-11,15 trp1-1 leu2-3,112 can1-100 bar1-*Δ*::hisG ars608-*Δ*::HIS3 ars609-*Δ*::TRP1::BrdU–Inc/* pCN416	Gasparyan
hc2414	*MAT*a *ade2-1 ura3-1 his3-11,15 trp1-1 leu2-3,112 can1-100 bar1-*Δ*::hisG ars608-*Δ*::HIS3 ars609-*Δ*::TRP1::BrdU–Inc/* pCN421	Gasparyan
hc2423	*MAT*a *ade2-1 ura3-1 his3-11,15 trp1-1 leu2-3,112 can1-100 mcm2-1 SPC42GFP::TRP1*	This study
hc2424	*MAT*a *ade2-1 ura3-1 his3-11,15 trp1-1 leu2-3,112 can1-100 mcm5-1 SPC42GFP::TRP1*	This study
hc2425	*MAT*a *ade2-1 ura3-1 his3-11,15 trp1-1 leu2-3,112 can1-100 mcm2-1 SPC42GFP::TRP1/* pCN4165	This study
hc2426	*MAT*a *ade2-1 ura3-1 his3-11,15 trp1-1 leu2-3,112 can1-100 mcm2-1 SPC42GFP::TRP1/* pCN421	This study
hc2427	*MAT*a *ade2-1 ura3-1 his3-11,15 trp1-1 leu2-3,112 can1-100 mcm5-1 SPC42GFP::TRP1/* pCN416	This study
hc2428	*MAT*a *ade2-1 ura3-1 his3-11,15 trp1-1 leu2-3,112 can1-100 mcm5-1 SPC42GFP::TRP1/* pCN421	This study
mly89	*MATa ade2-1 ura3-1 his3-11,15 trp1-1 leu2-3,112 can1-100 mrc1-*Δ*::HIS5*	Lee

Table 1-2: List of plasmids used in chapter 1

Plasmid	Description	Reference
pCN1	*CEN LEU2 native promoter STN1*	Petreaca[b]
pCN177	*2μ URA3 GAL promoter STN1*	Gasparyan
pCN416	*2μ LEU2 ADH promoter vector*	Gasparyan
pCN418	*2μ LEU2 ADH promoter STN1$^{1-371}$*	Gasparyan
pCN419	*2μ LEU2 ADH promoter STN1$^{1-281}$*	Gasparyan
pCN420	*2μ LEU2 ADH promoter STN1$^{1-186}$*	Gasparyan
pCN421	*2μ LEU2 ADH promoter STN1*	Gasparyan
pCN422	*2μ LEU2 ADH promoter STN1$^{187-494}$*	Gasparyan
pCN423	*2μ LEU2 ADH promoter STN1$^{288-494}$*	Gasparyan
pCN424	*2μ LEU2 ADH promoter STN1$^{173-494}$*	Gasparyan
pGO174	*CEN URA3 native promoter DBF4*	Dohrmanm
pPC64	*CEN HIS3 native promoter pol12-40*	Chiu
pRS416	*CEN URA3 vector*	Sikorski
pRS424	*2μ TRP1 vector*	Sikorski
pVL576	*2μ LEU2 GAL promoter vector*	Gasparyan
pVL577	*2μ URA3 GAL promoter vector*	Gasparyan
pVL1046	*CEN URA3 native promoter STN1*	Petreaca[b]
pVL1051	*2μ LEU2 GAL promoter STN1*	Gasparyan
pVL1066	*2μ LEU2 native promoter STN1*	Pennock
pVL1130	*2μ TRP1 ADH promoter STN1*	Gasparyan

Chapter 2

Stn1 affects DNA replication and damage repair processes globally throughout the genome

Abstract

While investigating the mechanism by which Stn1 overproduction overrides the S phase checkpoint, we discovered that this phenotype requires both Pol-α and MCM helicase function, but is independent of the DDK complex. This finding led us to speculate that Stn1 can facilitate Pol-α and MCM dependent DNA synthesis throughout the genome, in a manner genetically downstream of, or in parallel to DDK function. If this model is correct, then we predict that Stn1 overproduction would suppress, or potentially even bypass DDK function. Indeed, we found that *STN1* is a dosage suppressor of the temperature sensitive *cdc7-1* and *dbf4-1* mutations. We show that this phenotype is not an indirect effect of S phase checkpoint disruption, but more likely results from Stn1 having an active role in controlling DNA metabolism. We also show that Stn1 overproduction improves the replication profiles of, and prevents DNA damage accumulation in the *cdc7-1* and *dbf4-1* mutants at high temperatures. These findings strengthen the hypothesis that Stn1 facilitates DNA replication or repair in a DDK independent pathway. As with the S phase checkpoint phenotype, all of the experiments up to this point have been in the context of overproduced Stn1. This again raises the possibility that the phenotypes we observe are an artifact, and do not represent the normal role of Stn1 in genome maintenance. To address this concern, we analyzed loss of function *stn1* alleles. We took a reciprocal approach, combining truncated *stn1* mutants with the *cdc7-1* and *dbf4-1* alleles. If our hypothesis is correct, then we would expect such double mutants to have synthetic interactions, and possibly be inviable. We discovered that *cdc7 stn1* and *dbf4 stn1* double mutants do in fact have a synthetic

phenotype, and display defects in DNA synthesis, as determined by FACS analysis. Surprisingly, analysis of origin firing and fork progression do not reveal any obvious replication defects. This finding led us to hypothesize that rather than promoting DNA replication throughout the genome, Stn1 may have a role in facilitating repair of stalled or damaged forks, especially in difficult to replicate areas. Consistent with this, we found that the loss of function Stn1 mutants have aberrant levels of single stranded DNA at the rDNA locus. Furthermore, these alleles have synthetic interactions with *rad6-Δ* and *rad52-Δ* mutants, implying that in the absence of fully functional Stn1, cells have an increased dependency on recombination and repair pathways for viability. Taken together, these results show that Stn1 facilitates DNA synthesis throughout the genome, by preventing the accumulation of, or stimulating the repair of DNA damage at difficult to replicate regions.

Introduction

While investigating Stn1's role in telomere capping and replication, we previously observed that increasing its dosage disrupts the S phase checkpoint (Gasparyan *et al*, 2009). We found that this phenotype results from the inability to repress late firing origins in response to replication inhibitor drugs such as HU or MMS. Furthermore, we showed that Stn1 interferes with checkpoint control of DNA replication in a Pol-α and MCM dependent, but DDK independent manner. The DDK complex, comprised of the Cdc7 kinase and Dbf4 regulatory subunits, is required for viability. The essential function of the DDK is thought to be phosphorylation of the MCM helicase complex, to initiate DNA replication. This is supported by the finding that specific mutations within components of the MCM helicase complex can completely bypass *CDC7* and *DBF4*. (Hardy *et al*, 1997; Hoang *et al*, 2007; Sheu and Stillman, 2010). Thus the DDK is thought to function directly upstream of the MCM complex in the initiation of DNA replication.

One of the major S phase checkpoint targets for repressing late origin firing in response to replication stress is Dbf4 (Lopez-Mosqueda *et al*, 2010; Zegerman and Diffley, 2010; Duch *et al*, 2011). When dNTP levels become limiting or replicative polymerases stall at site of lesions, the Rad53 checkpoint kinase is thought to phosphorylate Dbf4 (and Sld3) on multiple sites, thus rendering it inactive. This then shuts down DDK function, and the MCM helicases assembled on late origins remain inactive (See Figures 0-3 and 0-5). We have previously shown that Stn1 overproducing cells are able to activate Rad53 in a timely manner in response to both HU and MMS, but

the cells fail to repress firing of late origins (Gasparyan *et al*, 2009). Furthermore, we found that Stn1's ability to interfere with the S phase checkpoint does not required the DDK, but is partially dependent on MCM helicase function (Figures 1-8 and 1-10). These findings suggest that Stn1 interferes with checkpoint control of replication at a step upstream of MCM helicase function, but either downstream, or parallel to DDK function.

Since Stn1 does not require DDK function to disrupt the S phase checkpoint, we asked whether in can promote DNA replication through a DDK independent pathway. To investigate this possibility, we overexpressed Stn1 in the temperature sensitive *cdc7-1* and *dbf4-1* mutants, and analyzed their ability to survive and complete DNA synthesis at elevated temperatures. Here, we show that *STN1* is a dosage suppressor of both *cdc7-1* and *dbf4-1* temperature sensitivity. Additionally, we show that this phenotype is specific to Stn1 overproduction, as other genetic manipulations which also abrogate the S phase checkpoint do not suppress *cdc7-1* or *dbf4-1*. These findings, taken together with our previously published work, indicate that when Stn1 is overproduced, it promotes DNA synthesis in a manner that alleviates the need for fully functional DDK.

To further probe the role of Stn1 in DNA replication and its genetic interactions with the DDK, we generated *stn1 cdc7* and *stn1 dbf4* double mutants. The specific *stn1* mutants we selected for this analysis were two truncation alleles *stn1-186t* and *stn1-281t* generated in our lab. Both of these mutants show severe telomere length regulation defects, and elevated levels of telomeric ssDNA (Petreaca *et al*, 2007). Interestingly, the ssDNA in these mutants is resistant to treatment with bacterial Exo1 exonuclease, which specifically degrades terminal ssDNA. This result suggests that source of the telomeric

ssDNA in these mutants is not exclusively from nucleolytic degradation, but may be from incomplete synthesis on the lagging strand.

When these *stn1* truncation mutants are combined with either *cdc7-1* or *dbf4-1*, we observe a synthetic interaction. The double mutants display enhanced temperature sensitivity, and reduced cell cycle progression compared to single mutant controls. However, analysis of global origin firing and fork progression reveals no major defects, suggesting that the nature of the synthetic interaction may be related to excessive DNA damage, rather than replication problems *per se*. Indeed, we show that these *stn1* mutants do display damage at internal sites within the genome, accumulating excessive ssDNA at repetitive sequences. Furthermore, we show that these alleles have synthetic interactions when combined with various mutants in DNA repair or recombination pathways, suggesting that when Stn1 function is compromised, cells have an elevated requirement for DNA repair processes. Based on these observations, we discuss a model which integrates the findings from the *STN1* overproduction experiments, the genetic interactions with the DDK, and possible roles in DNA repair processes.

Results

STN1 is a dosage suppressor of *cdc7-1* and *dbf4-1*

The findings from Chapter 1 suggest that Stn1 interferes with the S phase checkpoint in a step upstream of MCM helicase activity, and either in parallel or downstream of DDK activity. Since a hallmark of S phase checkpoint defective cells is the inability to repress origin firing in the presence of replication stress, we began to speculate if Stn1 can promote DNA replication through a DDK independent pathway. To address this hypothesis, we tested if overproduced Stn1 could compensate for a defective DDK complex. We overexpressed *STN1* in the temperature sensitive *dbf4-1* and *cdc7-1* mutant backgrounds, and assessed the viability of these strains at elevated temperatures. Remarkably, increasing *STN1* dosage partially suppresses both the *dbf4-1* and *cdc7-1* mutations (Figure 2-1). The *cdc7-1* mutant is able to grow at temperatures of up to 30°C with overproduced Stn1, whereas it normally has a maximum permissive temperature of 28°C. Similarly, the *dbf4-1* mutant, which normally dies at temperatures above 30°C, is viable at 32°C with overproduced Stn1. At temperatures above 32°C, both *cdc7-1/ STN1* and *dbf4-1/ STN1* are inviable, indicating that Stn1 does not completely bypass DDK function (data not shown). This suggests that Stn1 does not necessarily promote DDK independent DNA replication, but may promote replication through a mechanism that partially relieves Cdc7 and Dbf4 requirement. It may do so through several different mechanisms, such as 1) loosening chromatin to facilitate replication initiation with reduced DDK activity; 2) altering the structure of the MCM helicases in a way that makes them more accessible to phosphorylation and activation by the DDK; 3) binding to

and stabilizing the DDK complex, thereby making it functional at elevated temperatures. There are several known genetic modifications which suppress, or even completely bypass the DDK via one of these mechanisms. For example, a point mutation within the *MCM5* gene or deletion of a inhibitory region of *MCM4* can bypass both *CDC7 and DBF4* by allowing the MCM complex to be active in the absence of DDK phosphorylation (Hardy *et al*, 1997; Hoang *et al*, 2007; Sheu and Stillman, 2010). In *S. pombe*, deletion of *MRC1* suppresses the temperature sensitivity of a hypomorphic allele of the *CDC7* ortholog, by alleviating the S phase checkpoint's block on replication origin firing (Matsumoto *et al*, 2011). It is also possible that Stn1 suppresses the *cdc7-1* and *dbf4-1* temperature sensitivity through a combination of these processes, or a different mechanism that we have not yet considered.

Stn1's suppression of *cdc7-1* and *dbf4-1* temperature sensitivity does not directly result from disrupting the S phase checkpoint

We next asked if *STN1* suppresses mutations in the DDK through the same mechanism by which it interferes with the replication checkpoint. Since mutations in *POL12* suppress *STN1*'s checkpoint phenotype, we wondered if functional Pol12 is required for Stn1's ability to suppress *cdc7-1* temperature sensitivity. To test this, we overexpressed *STN1* in the *cdc7-1 pol12-40* mutant background. The results show that Stn1 fails to suppress *cdc7-1* in this background (Figure 2-2). This suggests that functional Pol-α is required for both *STN1*'s ability to disrupt the S phase checkpoint, and suppress *cdc7-1* temperature sensitivity. However, this is only a correlative result, and

does not necessarily imply that the suppression is caused by checkpoint disruption. To address this, we tested if other mutations that abolish the S phase checkpoint can also suppress *cdc7-1* temperature sensitivity. We disrupted the replication checkpoint by deleting *mrc1*, or using the separation of function *mrc1-AQ* allele (Osborn and Elledge, 2003). These checkpoint deficient strains were crossed to the *cdc7-1* mutant, and plated at different temperatures. The data shows that *mrc1* deletion not only fails to suppress the *cdc7-1* temperature sensitivity, it makes cells even sicker (Figure 2-3). These observations indicate that Stn1's ability to suppress DDK mutations is not simply an indirect consequence of disrupting the S phase checkpoint; more likely, Stn1 has an active role in stimulating replication. This role may be beneficial in *cdc7-1* or *dbf1-1* mutants which are compromised for DNA replication, but becomes detrimental when cells are experiencing replication stress.

Stn1 enhances cell cycle progression of *cdc7-1* and *dbf4-1* mutants

To examine if *STN1*improves DNA replication in DDK mutants, we performed FACS analysis experiments. *cdc7-1*, *dbf4-1* and WT control cells overexpressing *STN1* or a vector control were arrested in G1 at 23°C, then released into S phase at 30°C. At semi-permissive temperatures, DDK mutants show a very slow replication profile caused by low efficiency firing of early origins (Bousset and Diffley, 1998; Donaldson *et al*, 1998). Although some replication can be detected by 2-dimensional gel electrophoresis, this amount is not sufficient to completely duplicate the genome, and thus cells are unable to grow at these temperatures. Our data is consistent with these reports, showing that both

cdc7-1 and *dbf4-1* have a slow progression through S phase, but fail to undergo mitosis within the time course of the experiment (Figure 2-4). When Stn1 is overexpressed in these strains, we observe a significantly improved replication profile. Both *cdc7-1* and *dbf4-1* mutants are able to complete S phase with kinetics comparable to WT control cells, and a population of post-mitotic G1 cells can be seen starting at 120 minutes (Figure 2-4). We also notice a large population of cells that appear to be arrested in G2/M with 2N DNA content at the end of the time course. These findings suggest that increased *STN1* dosage significantly improves the replication profile of *cdc7-1* and *dbf4-1* mutants; however it is unable to completely bypass DDK function.

STN1 suppresses Rad52 foci formation in *cdc7-1* and *dbf4-1* mutants

After showing that Stn1 improves the DNA replication profile of *cdc7-1* and *dbf4-1* cells, we tested if it could also suppress the accumulation of DNA damage in these strains. Previous work in *S. pombe* has shown that DDK mutants accumulate Rad52 repair foci at elevated temperatures, or after exposure to replication inhibitors (Matsumoto *et al*, 2005; Dolan *et al*, 2010). Although the exact source of damage which induces Rad52 foci formation is not completely understood, the prevailing view in the field hypothesizes that DDK mutants have increased incidence of fork collapse, leading to elevated levels of ssDNA. This could potentially serve as a substrate for Rad52 dependent recombination. Since *STN1* suppresses *cdc7-1* and *dbf4-1* temperature sensitivity and improves their replication profile, we asked if it can also suppress the accumulation of DNA damage in these mutants. We analyzed Rad52 foci formation in

these mutants, and found that *STN1* overexpression partially suppresses the accumulation of DNA damage at elevated temperatures (Figure 2-5). In both *cdc7-1* and *dbf4-1* strains released from G1 arrest to 36°C, approximately 50% of cells accumulated Rad52 foci at the 150 minute time point. In contrast, when *STN1* is overexpressed in the background, only 40% of *cdc7-1* cells and 30% of *dbf4-1* cells contain Rad52 foci. These findings imply that Stn1 either prevents DNA damage or facilitates its repair in the *cdc7-1* and *dbf4-1* mutants at elevated temperatures.

Synthetic interaction of *stn1 cdc7* and *stn1 dbf4* double mutants

Having shown that increased *STN1* dosage can suppress *cdc7-1* and *dbf4-1* temperature sensitivity and accumulation of DNA damage, we hypothesized that loss of function *stn1* mutants would have synthetic interactions when combined with *cdc7-1* and *dbf4-1*. To examine this, we used two truncation alleles, *stn1-186t* and *stn1-281t*, both of which perturb the telomere capping and length regulation functions of Stn1 (Petreaca *et al*, 2007). Double mutants were generated via mating and tetrad dissection, and strains were plated at various temperatures to test for synthetic interactions. The results show that all double mutant combinations (*cdc7-1 stn1-186t*, *cdc7-1 stn1-281t*, *dbf4-1 stn1-186t* and *dbf4-1 stn1-281t*) are more temperature sensitive than the single mutant controls (Figure 2-6). The *cdc7-1* single mutant is viable at 28°C, but both *cdc7-1 stn1-186t*, *cdc7-1 stn1-281t* double mutants are dead at that temperature. Similarly, the *dbf4-1* single mutant starts showing reduced viability at 30°C, whereas the *dbf4-1 stn1-186t* and *dbf4-1*

stn1-281t double mutants are dead at 28°C. This result is consistent with the observations that Stn1 improves viability and DNA replication efficiency in DDK mutants.

Analysis of telomere length and ssDNA in *stn1 cdc7* and *stn1 dbf4* double mutants

The synthetic interaction between Stn1 and the DDK could potentially be due to telomeric problems rather than defects in global DNA replication. To examine this possibility, we analyzed both the telomere length and integrity in *cdc7 stn1* and *dbf4 stn1* double mutants. Both the *stn1-186t* and *stn1-281t* mutants have extremely elongated, single-stranded telomeres (Figure 2-7, lanes 4-9; Figure 2-8, lanes 11 and 16), consistent with published results (Petreaca *et al*, 2007). The *cdc7-1* and *dbf4-1* single mutants have approximately wild type telomere length, and show no increase in telomeric ssDNA (Figure 2-7, lanes 10-12 and 19-21; Figure 2-8, lanes 2 and 3). The *cdc7 stn1* and *dbf4 stn1* double mutants have elongated telomeres and high levels of telomeric ssDNA, comparable to *stn1* single mutants, suggesting that the *stn1* phenotype is epistatic (Figure 2-7, lanes 13-18 and 22-27; Figure 2-8, lanes 12, 13, 17 and 18). These results imply that the synthetic interaction between Stn1 and the DDK is not likely caused by telomere related problems; however, we cannot formally exclude the possibility that in the double mutants, the terminal ssDNA extends beyond the telomeric repeats into subtelomeric sequences, further than in the *stn1* single mutants. A more quantitative approach, such as QAOS, will be required to conclusively determine the extent of the terminal single-stranded DNA in these strains.

stn1 cdc7 and *stn1 dbf4* double mutants show a delay in completion of S phase

Having demonstrated that *stn1 cdc7* and *stn1 dbf4* double mutants do not have any worse telomere length regulation or capping defects than the *stn1* single mutants, we next tested if the synthetic interaction could be caused by problems in general DNA replication. We performed FACS analysis on the *cdc7-1 stn1-186t*, *cdc7-1 stn1-281t*, *dbf4-1 stn1-186t* and *dbf4-1 stn1-281t* cells released from G1 arrest at 26°C. The results show that both the *stn1-186t* and *stn1-281t* single mutants are able to complete S phase with kinetics comparable to the wild type control, but a large fraction of cells arrest at the G2/M DNA damage checkpoint with 2N DNA content, as previously reported (Petreaca *et al*, 2007). The *cdc7-1* and *dbf4-1* single mutants complete S phase with slightly slower kinetics compared to the wild type control, reaching a 2N DNA content at approximately 120 minutes after release. In contrast, the *stn1 cdc7* double mutants show a dramatic reduction in S phase progression, reaching 2N DNA content 180 minutes after release (Figure 2-9). These results indicate that when DDK activity becomes compromised, cells require a fully functional Stn1 to complete S phase efficiently.

The *stn1 cdc7-1* double mutant can recover replication after transient exposure to high temperature

One interpretation of the results from Figure 2-9 is that when the *cdc7-1* mutants are exposed to high temperatures, they experience DNA damage resulting from replication fork problems, and Stn1 is required to repair the damage. To test this hypothesis, we asked if *cdc7 stn1* double mutants could recover from transient exposure

to high temperatures. Strains were arrested in G1 at 23°C, then split, with one half of the culture released at 23°C, while the second half was released at 34°C for 1 hour, then shifted back down to 23°C. Cell cycle progression was then monitored by FACS analysis. The samples released directly at 23°C show a normal cell cycle profile, completing S phase approximately 100 minutes after release (Figure 2-10). The double mutants do have a delay in G2/M, indicating activation of the DNA damage checkpoint caused by telomeric ssDNA (Petreaca *et al*, 2007). The cells initially released at 34°C show very little increase in DNA content in the first 60 minutes, consistent with an inability of the *cdc7* mutant to initiate origin firing (Bousset and Diffley, 1998; Donaldson *et al*, 1998). However, after shifting cells back down to 23°C, both the *cdc7* single mutant and the *cdc7 stn1* double mutants are able to recover, and complete S phase within 100 minutes (Figure 2-10). This observation suggests that Stn1 is not required to repair damage resulting from replication fork problems in *cdc7-1* mutants; rather, it may have an active role in promoting fork progression, which becomes essential when DDK function is compromised.

Analysis of replication fork progression in the *stn1-281t cdc7-1* double mutant

After discovering that *stn1 cdc7* double mutants are able to recover from transient exposure to elevated temperatures, we hypothesized that Stn1 may promote replication fork progression or origin firing when the DDK becomes compromised. Thus, we predicted that the *stn1 cdc7* double mutants would have reduced rate of replication fork progression or origin firing compared to single mutants. To analyze replication fork

dynamics in *stn1-281t cdc7-1* double mutants, we performed BrdU-ChIP microarray experiments in collaboration with the Oscar Aparicio lab at USC. In these experiments, cells were arrested in G1 at 23°C, then released at 28°C in either the presence or absence of 0.033% MMS, as indicated. Newly synthesized DNA was labeled with BrdU continuously for either 25, 40 or 60 minutes after release. The replication profile was then determined by immuno-precipitating the BrdU and hybridizing to a genomic microarrays, and comparing to G1 arrested unlabeled samples. The replication profile of Chromosome VI is shown for representation (Tittu Thomas provided technical assistance and performed computational analysis of data). The *stn1-281t cdc7-1* double mutant displays a BrdU incorporation profile comparable to the *cdc7-1* single mutant at all tested time points (Figure 2-11). Interestingly, at the 40 and 60 minute time points, the *cdc7-1* and *stn1-281t cdc7-1* strains show a greater amount of DNA replication compared to the *stn1-281t* and wild type control strains. However, this observation is consistent with published reports claiming that reduced origin firing in DDK mutants results in increased fork progression from early origins (Zhong *et al*, 2013). Taken together, these results indicate that the *stn1-281t cdc7-1* double mutant does not have a more severe defect in origin firing or fork progression than the *cdc7-1* single mutant.

Accumulation of single-stranded DNA at internal repetitive loci in *stn1* mutants

After finding that *stn1* mutants do not have origin firing and fork progression defects, we next considered the possibility of Stn1 being required to prevent the accumulation of single stranded DNA throughout the genome, especially at repetitive

sequences. These regions will have a higher rate of fork stalling and collapse events, which if left unrepaired, could lead to elevated levels of ssDNA (Kerrest *et al*, 2009; Anand *et al*, 2011). We hypothesized that Stn1 may be required to prevent fork collapse, or promote efficient restart of stalled forks to prevents excess ssDNA accumulation at repetitive regions in the genomes. If this were true, we would not expect to observe such fork progression issues on the BrdU-ChIP microarray data, since the microarray does not contain repetitive sequences.

To examine if *stn1* mutants accumulate aberrant ssDNA at repetitive loci, we performed random hexamer primed Klenow synthesis reactions on full length chromosomes, adapted from a published protocol (Feng *et al*, 2011). The synthesis reaction products were then denatured, run out on agarose gels, and Southern blots were performed. Probing against telomeric sequences reveals the presence ssDNA signal in the *stn1-281t* mutant sample, but not in the wild type or *mec1-21* controls (Figure 2-12 A). When the same blot was stripped and reprobed against rDNA sequences, ssDNA signal can be seen in both the *stn1-281t* and *mec1-21* strains, but not in the wild type control. We also attempted to probe against single copy loci in the genome, but no signal was observed indicating that this level of ssDNA may be below the threshold of detection for the assay. The ssDNA signal is dependent on addition of Klenow polymerase, as no products are detected in the absence of the enzyme. We also noticed a reduction in ssDNA signal upon HU addition in the *stn1-281t* sample, for both the rDNA and telomeric loci. However, no HU dependent reduction in signal was observed in the *mec1-21* strain. Our interpretation of this result is that in the presence of HU, the S phase

checkpoint represses synthesis of late replicating regions, such as the rDNA and telomeres, thus preventing the accumulation of ssDNA in the *stn1-281t* mutant.

We also examined the cell cycle dependency of ssDNA accumulation in *stn1* mutants. Cultures were arrested in G1, then released into the cell cycle synchronously. Samples were collected every 25 minutes, and subjected to Klenow synthesis reactions (Figure 2-12 B). Progression through the cell cycle for these strains was monitored by FACS analysis (Figure 2-12 C). The wild type control strains show very little ssDNA, with a faint signal appearing at the 50 and 75 minute time points, consistent with the late replication of telomeres and the rDNA locus (Raghuraman *et al*, 2001; Wyrick *et al*, 2001; Feng *et al*, 2006). Conversely, both the *stn1-186t* and *stn1-281t* mutants display elevated levels of ssDNA at telomeric and rDNA sequences, throughout the time course of the experiment (Figure 2-12 B). These findings suggest that Stn1 is required to prevent accumulation of ssDNA at repetitive genomic sequences throughout the cell cycle. This result may explain the synthetic interaction in *stn1 cdc7* and *stn1 dbf4* double mutants; however, the levels of single-stranded DNA at repetitive loci in the double mutants have not been determined yet. Therefore, we cannot draw any firm conclusions at this time.

Synthetic interactions between *stn1* and DNA repair mutants

The presence of ssDNA at repetitive sequences in *stn1* mutants led us to speculate that these strains may require the Rad6 dependent post-replicative repair (PRR) pathway for viability. To test this possibility, we attempted to generate *stn1 rad6* double mutants by mating haploids and dissecting tetrads. We were unable to recover any viable *stn1-*

281t rad6-Δ spores from the cross, suggesting that this double mutant combination is synthetic lethal. To confirm the synthetic lethality, the heterozygous diploid parent was transformed with a wild type *STN1* allele on a *URA3* marked plasmid. We were able to isolate *stn1-281t rad6-Δ*/ p*STN1* spores from this cross, but no viable *stn1-281t rad6-Δ* were recovered (Table 2-1). By plating the *stn1-281t rad6-Δ*/ p*STN1* strains on 5-FOA, we are able to counter-select for the plasmid bearing the wild type copy of *STN1*, thereby potentially yielding *stn1-281t rad6-Δ* double mutant colonies. No viable colonies were isolated on 5-FOA plates at either 23°C or 30°C, indicating that the *stn1-281t rad6-Δ* combination is synthetic lethal (Figure 2-13). This result suggests that when Stn1 function is compromised, cells require the PRR pathway for viability.

In addition to post-replicative repair, a major pathway for repairing damaged or unreplicated DNA is through recombination. The data from Figure 2-5 indicates that increasing *STN1* dosage reduces the levels of Rad52 foci accumulation in *cdc7-1* and *dbf4-1* mutants. Thus, we reasoned that in the loss of function *stn1* mutants or *stn1 cdc7* double mutants, Rad52 dependent recombinational repair may be required for viability. To explore the role of recombination, we crossed *stn1-186t cdc7-1* and *stn1-281t cdc7-1* double mutants to a *rad52-Δ* strain, and isolated strains of every genotype through tetrad dissection (Tables 2-2 and 2-3). Because we were able to isolate *stn1 rad52* double mutant and *cdc7 stn1 rad52* triple mutant spores from the cross, we conclude that recombination is not necessary for the viability of *stn1* and *cdc7 stn1* mutants; however, the frequency of *stn1 rad52* double mutant and *cdc7 stn1 rad52* triple mutant spores isolated from the crosses were much lower than expected, suggesting that Rad52 does

contribute to healthy growth of these strains. We next asked if the double or triple mutants would have a more severe growth defect than single mutant controls. We analyzed the growth of strains plated at different temperatures, and found that the *stn1 rad52* and *cdc7 stn1 rad52* are sicker than the controls (Figure 2-13). Both the *stn1-186t rad52-Δ* and *stn1-281t rad52-Δ* strains have smaller colonies and reduced logs of growth compared to the single mutants, especially at lower temperatures. Similarly, both *cdc7 stn1 rad52* triple mutants have reduced growth efficiency at 23°C compared to the double mutant controls; however, at higher temperatures, the effect of the *cdc7-1 stn1* synthetic interaction becomes epistatic, complicating the genetic analysis. These data imply that although recombination is not essential for the viability of *stn1* mutants, it does contribute to their healthy growth.

Discussion

Previously, we showed that when Stn1 is overproduced, it can interfere with the S phase checkpoint by overriding control of DNA replication. We found that this phenotype requires a fully functional MCM helicase complex, but is independent of DDK function. These findings are consistent with the observation that checkpoint regulates late origin firing via phosphorylation of Dbf4 (Lopez-Mosqueda *et al*, 2010; Zegerman and Diffley, 2010; Duch *et al*, 2011). Thus, even if Rad53 is able to target Dbf4 in response to replication stress to shut down DDK activity, Stn1 functions at a downstream step to override the checkpoint's control of replication origin firing. These observations led us to speculate if Stn1 can promote DDK independent replication. We discovered that *STN1* is a dosage suppressor of both *cdc7-1* and *dbf4-1* temperature sensitivity, and enhances DNA replication in these mutants. However, it cannot completely bypass their essential function.

In contrast to the overexpression results, we found that loss of function *stn1* mutations exacerbate the replication problems of *cdc7-1* and *dbf4-1* strains. However, analysis of origin firing and fork progression in the *cdc7-1 stn1-281t* double mutant did not reveal any obvious defects. Although this result was initially puzzling, it does make sense in the light of findings from *Xenopus* egg extracts which show that Stn1 promotes replication of a single-stranded plasmid, but not of a duplex one (Nakakoa *et al*, 2012). This, along with our findings that *STN1* can suppress but not bypass the DDK, suggest that rather than activate origin firing, Stn1 may stimulate *de novo* priming and synthesis

using a single-stranded template. This function would be directly analogous to Stn1's normal role at the telomere in C-strand synthesis (Figure 2-15).

How does Stn1 suppress DDK mutants? At elevated temperatures, DDK mutants do initiate firing of some origins; however, this level is not sufficient to replicate the entire genome, and thus, results in lethality (Bousset and Diffley, 1998; Donaldson *et al*, 1998). Stn1 may either activate additional origins, or stimulate replication by recruiting or activating Pol-α at single stranded templates. We favor the latter model for several reasons. First, this would be more in line with Stn1's role in telomere replication. Second, it can explain why Stn1 suppresses, but fails to bypass the DDK mutations. Third, it also explains why we don't see a reduction in origin firing in *stn1* or *cdc7 stn1* double mutants. Fourth, it provides a mechanism for why Stn1 overproduction reduces recombination foci in *cdc7-1* and *dbf4-1* mutants. Single stranded DNA is an intermediate in nearly all recombination processes. Thus, in DDK mutants, the limited levels of origin firing produce some replication forks, which eventually stall or collapse. These may ultimately be the source of the high levels of recombination that we observe. By promoting efficient re-priming and restart of these stalled forks, Stn1 may prevent the accumulation of ssDNA, and thereby decrease the levels of recombination in these mutants.

This model can also explain the elevated levels of ssDNA at the rDNA locus seen in the loss of function *stn1* mutants. The rDNA consists of multiple copies of *rRNA* genes oriented in tandem repeats. These genes are transcribed constitutively, resulting in the unidirectional movement of transcription forks through this region. During DNA synthesis, the replication fork is only allowed to move in the same direction as the

transcriptional forks, to limit torsional strain on the DNA molecule and minimize fork collisions. Thus, the unidirectional fork movement makes replication of the rDNA repeats especially challenging, and quite similar to replication of telomeres (Lucchini and Sogo, 1995). Studies have shown that when Pol-α levels are limiting, the rDNA repeat number becomes unstable, suggesting that cells use recombination mediated processes to complete synthesis (Casper *et al,* 2008). Here, we show that when Stn1 function is compromised, cells accumulate high levels of ssDNA at the rDNA repeats. This finding is consistent with Stn1 having a role in promoting Pol-α dependent re-priming of stalled forks, using single-stranded DNA as a template (Figure 2-15).

Lastly, this model may also explain the synthetic lethality of *stn1-281t rad6-Δ,* and the synthetic interaction between *stn1 rad52-Δ* mutants. Rad6 is a ubiquitin ligase that ubiquitilates PCNA in response to DNA lesions on the template strand during replication, to either promote the error prone translesion syntheis (TLS) pathway, or the error free homology-directed repair (HDR) pathway (Karras and Jentsch, 2010). Currently, it is not known whether *stn1* mutants require one or both of these pathways for viability. However, since both of these pathways, along with Rad52 dependent recombination, are involved in repair of damaged DNA to promote DNA synthesis, our genetic analysis suggests that Stn1 may also function in a parallel pathway. When cells encounter DNA damage on the template strand that stalls replication forks, they can either bypass the damage via TLS, switch to using an undamaged template via HDR after S phase. Our finding suggest that in addition to these conventional pathways, Stn1 may

allow re-priming and restart of the fork downstream of the lesion. Thus, knocking out multiple pathways makes cells extremely sick or inviable.

A more trivial interpretation of our results may be that the *RAD6* dependent PRR pathway is required for telomere maintenance in the absence of fully functional *STN1*. Although our analysis of *stn1 cdc7* and *stn1 dbf4* double mutants shows that loss of DDK function does not exacerbate the telomere maintenance phenotype of *stn1* mutants, we have not shown that *rad6-Δ* strains have similar effect. However, all of the data presented in Chapter 1 and 2 lead us to favor a model in which the synthetic lethality of the *rad6-Δ stn1-281t* double mutant results from defects in fork restart at internal sites in the genome, especially at repetitive sequences.

One final point of consideration is the cause of the ssDNA at the rDNA locus in *stn1* mutants. We can invoke two distinct models to account for this observation. In the first model, Stn1 may have an active role in preventing the accumulation of ssDNA, by promoting efficient synthesis through the rDNA repeats. In the second model, Stn1 functions as a facilitator of repair, promoting efficient restart of synthesis after forks encounter stalling lesions. Although our data cannot definitively discriminate between these two models, we favor the latter for two reasons. First, our BrdU microarray data suggests that *STN1* is not required for normal origin firing or fork movement. Second, this model is more consistent with Stn1's normal role in telomere replication; after telomerase extension of the G-strand, Stn1, along with Cdc13, are thought to recruit Pol-α to prime and synthesize the C-strand. Therefore, we hypothesize that the ssDNA

present at the rDNA in *stn1* mutants results from a failure to efficiently re-prime and restart DNA synthesis after a polymerase stalls at a lesion.

Materials and Methods

Strains and plasmids

All strains used in this chapter are listed in Table 2-4, and all plasmids used are listed in Table 2-5. Yeast strains were grown and propagated following standard procedures (Sherman, 2002).

Serial dilution plating assays

Cells of the indicated genotype were inoculated from single colonies grown on selective plates, and incubated for 3 days at 30°C (or 4 days at 23°C for temperature sensitive strains). For each strain, 10-fold serial dilutions from the same initial concentration of cells were done in a 96-well microtiter dish, and stamped onto appropriate plates. Plates were incubated for 3-4 days at the indicated temperatures.

FACS analysis

To measure DNA synthesis and cell cycle kinetics by FACS analysis, strains of the indicated genotype were synchronized in G1 by arresting with alpha factor pheromone at 23°C. The cells were then washed and released into fresh media at the indicated temperature. At each time point, 500μL of cells were collected and fixed in 70% ethanol overnight. Samples were rehydrated in 1mL of PBS for 1 hour, followed by 4 hour of treatment with 100μL of FACS buffer (0.2M Tris pH7.5, 20mM EDTA, 1mg/mL RNase) at 37°C. FACS buffer was then washed out, and cells were resuspended in 100μL of PBS with 50μg/mL of propidium iodide, at 4°C overnight. Samples were

then transferred to FACS tubes, and 900μL of PBS was added. Cells were briefly vortexed and sonicated at low power, and samples were run on a Becton Dickinson flow cytometer. Data acquisition and analysis was performed using Cellquest software.

Rad52-YFP foci measurements

Single colonies from cells of the indicated genotype containing the YFP-tagged *RAD52* construct (Lisby *et al*, 2001) were inoculated into 5mL of selective media supplemented with 100μg/mL of adenine, and grown to logarithmic phase at 23°C. Cultures were synchronized in G1 by arresting with alpha factor pheromone, then washed and released into fresh media at the indicated temperatures. At the indicated time points, 100μL of cells were collected, and fixed with 3.7% formaldehyde for 2 minutes. Samples were then washed twice with PBS, and resuspended in 100μL of PBS. Samples were mounted on slides, DNA was stained with DAPI, cover slips were applied, and cells were visualized by fluorescence microscopy. For each sample, 100 cells were scored for the presence of fluorescent foci. Images were acquired using the Metamorph software.

Telomeric single-stranded DNA analysis

Strains of the indicated genotype were inoculated in 30mL of YPD or selective media, and grown to logarithmic phase at 23°C. Cells were harvested and DNA was isolated using previously described protocols (Dionne and Wellinger, 1996), with minor modifications. The cells were lysed in 500μL of NIB buffer (17% glycerol, 50mM MOPS, 150mM K-AC, 2mM $MgCl_2$, 500μM spermidine, 150μM spermine) by bead beating.

Lysates were centrifuged for 20 minutes at 9200rpm in 4°C and resuspended in 500µL of TEN buffer (50mM Tris pH8, 50mM EDTA, 100mM NaCl). Sarkosyl was added to a final concentration of 1.5%, and samples were treated with 170µg of proteinase K (Sigma) for 1 hour at 37. DNA was then isolated by phenol/chloroform extraction, precipitated with 95% ethanol, washed with 70% ethanol, dried and resuspended in 100µL of TE.

DNA samples were digested with XhoI (New England BioLabs) at 37°C overnight, then precipitated with isopropanol, washed with 70% ethanol, and resuspended in 24µL of TE. To each sample, 1µL of P-32 radio-labeled single-stranded $C_{1-3}A$ probe was added. Samples were incubated at 37°C for 2 hours, followed by cooling on ice for 1 hour. DNA was then loaded on a large 0.75% agarose gel, and samples were run out at 22V for 18 hours at room temperature. The gel was then treated with 2x SSC for 30 minutes, dried for 12 minutes per side, wrapped in saran, and exposed to a phosphor-imager screen (Amersham) for 5 days. The screen was scanned and imaged using a Typhoon Fluorescence Imager (Amersham).

Under the conditions described above, telomeric DNA is kept in its native state, thereby allowing detection of single-stranded DNA. To determine the total telomeric DNA, the same gel was treated with 500mL of denaturing buffer (150mM NaCl, 0.5M NaOH) for 25 minutes at room temperature with gentle shaking, followed by treatment with 500mL of neutralizing buffer (150mM NaCl, 0.5M Tris pH8) for 20 minutes at room temperature with gentle shaking. The gel was then placed in a sealable bag, and immersed in 50mL of hybridization buffer (5x SSC, 1mM Na_2HPO_4, 50µM inorganic

pyrophosphate, 5x Denhardts solution, 40nM ATP, 20μg/mL salmon sperm DNA), to which 20μL of P-32 radio-labeled single-stranded $C_{1-3}A$ probe was added. The gel was incubated at 37°C overnight with gentle rocking. The following day, hybridization buffer and probe were removed, and the gel was washed with 500mL of 0.25x SSC 5 times, 30 minutes per wash, with gentle shaking at room temperature. The gel was then wrapped in saran, and exposed to a phosphor-imager screen (Amersham) for 2 days. The screen was scanned and imaged using a Typhoon Fluorescence Imager (Amersham).

BrdU-IP microarray experiments

BrdU-IP microarray experiments were performed in the laboratory of Dr. Oscar Aparicio at the University of Southern California, following previously described protocols (Vigiani *et al*, 2010), with minor modifications. The indicated strains containing the BrdU-Inc construct were synchronized in G1 by arresting with alpha factor pheromone. The cells were then washed and released into fresh media containing 800 μg/mL BrdU (Sigma) and 0.033% MMS where indicated. Cells were harvested at the indicated time points and lysed by bead-beating in lysis buffer (100mM Tris pH8.0, 50mM EDTA, 1% SDS). DNA was collected using standard phenol/chloroform extraction procedures, precipitated with 95% ethanol, resuspended 100μL of 1x TE, and sheared by sonication. Samples were treated with RNase for 1 hour at 37°C, proteinase K for 1 hour at 50°C. DNA was cleaned up over columns (Qiagen), eluted with 50μL of elution buffer, and the concentrations were measured on a nanodrop. For each sample, 1μg of DNA was used for the IP, and 1μg was saved as a "reference".

IP's were performed by combining 1μg of sample DNA, 50μg salmon sperm DNA, 10μL of 10x PBS and H_2O to a final volume of 100μL, heating samples to 95°C to denature DNA, cooling on ice, adding 900μL of IP buffer (1x PBS + 0.05% triton-X), 10μL of anti-BrdU antibody (Invitrogen) at a 1:500 dilution, and 20μL of protein A/G magnetic beads. Samples were incubated at 4°C for 2 hours with gentle rocking, washed 4 times with 1mL of IP buffer, and eluted with 50μL of elution buffer. Samples were cleaned up over columns (Qiagen), eluted with 10μL of elution buffer, and the concentrations were measured on a nanodrop. Samples were then amplified with the GenomePlex Whole Genome Amplification (WGA) kit (Sigma)

After amplification, samples were subjected to Klenow extension for 4 hours at 37°C. 500ng of each sample was conjugated with Cy5 fluorophore (GE Healthcare) to label immunoprecipitated DNA or Cy3 fluorophore (GE Healthcare) to label whole genomic "reference" DNA. 1 μg of "reference" DNA and 1 μg of immunoprecipitated sample were combined, dried in a SpeedVac (Thermo), resuspended in 10 mM EDTA, and denatured for 2 minutes. Samples were suspended in prewarmed (50°C) hybridization buffer (30% formamide, 5x SSC, 0.1% SDS, 100 μg/mL salmon sperm DNA), and hybridized to microarrays for 18 hours at 50°C. Slides were washed with gentle shaking in 1x SSC, 0.1% SDS, 1mM DTT for 5 min, submerged several times in 0.2x SSC, 1 mM DTT, and washed 2 times for 3 min in 0.1x SSC, 1mM DTT. Slides were dried by centrifugation for 45 seconds in a microcentrifuge and scanned in an Axon scanner using Genepix 5.0 to capture and save the images.

Telomere length analysis

To analyze telomere length of cells, single colonies from strain of the indicated genotype were inoculated in 10mL of YPD or selective media, and grown to saturation at either 30°C or 23°C for temperature sensitive strains. DNA was isolated using previously described protocols (Lundblad and Szostak, 1989), with minor modifications. Cells were harvested and spheroplasted in Zymolyase solution (0.9M sorbitol, 0.1M EDTA pH 7.6, 28mM BME, 0.3mg/ml Zymolyase 20T) for 1 hour at 37°C. The spheroplasted cells were then resuspended in 0.6mL of TE, to which 120µL of lysis solution (0.25mM EDTA pH8, 0.5M Tris base, 2.5% SDS) was added. Samples were incubated at 65°C for 30 minutes, then 200µL of 5M K-Ac was added, and the lysates were cooled on ice for 1-2 hours. Samples were then centrifuged for 15 minutes at 14,000rpm in 4°C, the supernatant was transferred to a new tube, and 550µL of isopropanol was added to precipitate nucleic acids. Samples were then washed with 70% ethanol, dried, and resuspended in 0.5mL of TE containing RNase overnight at 37°C. DNA was then re-precipitated with ethanol, resuspended in 40µL of TE, and digested with XhoI (New England BioLabs) at 37°C overnight.

Digested DNA was loaded and run on a large 0.8% agarose gel at 50V for 20 hours. The gel was then transferred to a nylon membrane (Hybond-XL from Amersham) overnight, and DNA was crosslinked with 120mJ of UV light (Stratagene). The membrane was blocked with Church's buffer (1% BSA, 1mM EDTA, 0.5M phosphate buffer, 7% SDS) overnight at 55°C with gentle rocking. Then 25µL of P-32 radiolabeled $TG_{1\text{-}3}/C_{1\text{-}3}A$ probe was added, and the blot was incubated overnight at 55°C with gentle

rocking. The following day, the blot was washed three times with 1L of washing solution (4x SSC, 0.1% SDS), and exposed to X-ray film for 2-5 days in -80°C, depending on signal strength. The film was developed on a developer (Mini-medical).

Klenow synthesis assay

Klenow synthesis experiments were done following previously published protocols (Feng *et al*, 2011), with minor modifications. Strains of the indicated genotype were grown to logarithmic phase at 30°C in YPD, and arrested with alpha factor pheromone, or treated with 200mM HU for 3 hours, as indicated. Cells were harvested, washed with 50mM EDTA, and the concentration of each sample was determined by hemocytometery. For each sample, ~10^9 cells were collected, and the volumes were adjusted to 500µL. The cell suspensions were warmed to 55°C, and mixed with 500µL of low melt agarose (Invitrogen) dissolved in 1x TBE at 1% concentration. The mixture was pipetted into plug molds, and allowed to solidify at room temperature for 15 minutes. 10 plugs were cast for each sample, and the solidified plugs were treated with 5mL of spheroplasting solution (1M sorbitol, 20mM EDTA, 10mM Tris pH7.5, 14mM BME, 0.5mg/mL Zymolyase 20T) for 4 hours at 37°C. Plugs were then washed with SDS solution (1% SDS, 100mM EDTA, 10mM Tris pH8) twice for 15 minutes each, and incubated in SDS solution at 37°C overnight with gentle rocking. The following day, plugs were washed with NDS solution (1% sarkosyl, 10mM Tris base, 0.5M EDTA pH9.5) 3 times for 30 minutes each, followed by 5 washes with TE for 30 minutes each, then stored in 4°C overnight.

The agarose plugs were then pre-equilibrated in 5mL of TMB buffer (50mM Tris pH6.8, 5mM $MgCl_2$, 10mM BME) for 30 minutes at room temperature, then samples were split into two. 5 plugs from each set were mixed with 400µL of TMB buffer, 10µL of dNTPs at 10µM concentration each, 10µL of random hexamer primers at 10µM concentration (Thermo Scientific), 100 units of exo$^-$ Klenow polymerase (New England BioLabs), and 50µL of 10x Klenow buffer. The other 5 were treated identically, but no Klenow polymerase was added. Samples were incubated at 37°C for 2 hours, then washed with TE. Plugs were then pre-equilibrated with 1x β-agarase buffer for 30 minutes on ice, heated to 65°C to melt agarose, and treated with 5 units of β-agarase (New England BioLabs) for 1 hour at 42°C. Salt concentration was adjusted to 0.5M NaCl, 0.8M LiCl, 0.3M NaO-Ac, samples were cooled on ice for 15 minutes, and DNA was precipitated with isopropanol. The DNA was then washed with cold 70% ethanol, dried, and resuspended in 40µL of TE.

The DNA samples were then denatured by addition of 10µL of 1M NaOH and 1µL of 0.5M EDTA followed by boiling at 95°C for 5 minutes. Samples were cooled on ice for 5 minutes, the loaded and run out on a large 1% agarose gel overnight at 50 volts. The gel was then transferred to a nylon membrane (Hybond-XL from Amersham) overnight, and DNA was crosslinked with 120mJ of UV light (Stratagene). The membrane was blocked with Church's buffer (1% BSA, 1mM EDTA, 0.5M phosphate buffer, 7% SDS) overnight at 55°C with gentle rocking. Then 25µL of P-32 radiolabeled $TG_{1\text{-}3}$ probe was added, and the blot was incubated overnight at 55°C with gentle rocking. The following day, the blot was washed three times with 1L of washing solution (4x SSC,

0.1% SDS), and exposed to X-ray film for 5 days in -80°C. The film was developed on a developer (Mini-medical). After development, the membrane was stripped of telomeric probe by immersing in boiling 0.1% SDS three times for 15 minutes each, then blocked with Church's buffer as before. 25μL of P-32 radiolabeled rDNA probe was added, and the blot was processed as before.

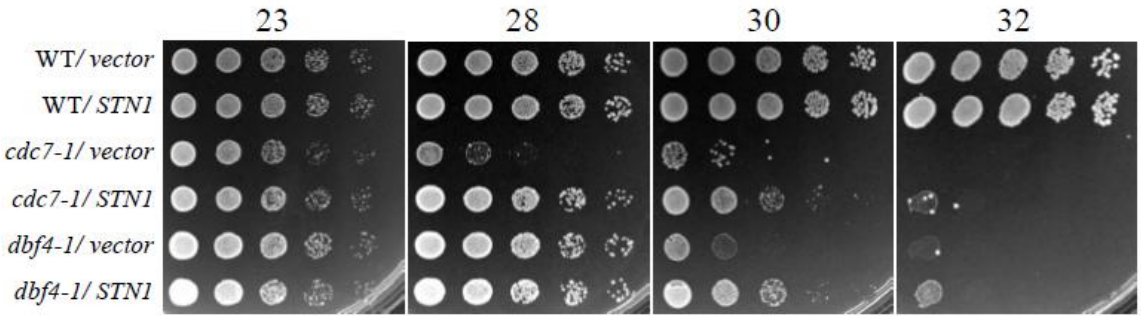

Figure 2-1: *STN1* is a dosage suppressor of *cdc7-1* and *dbf4-1*

Overexpression of *STN1* suppresses the temperature sensitivity of *cdc7-1* and *dbf4-1* mutants. Cells were grown to saturation in selective media for 3 days at 23°C, then 10-fold serial dilutions were stamped onto selective plates. Plates were incubated at the indicated temperatures for 3-4 days, then pictures were taken. Strains used in this figure: hc160 (wild type), hc15 (*cdc7-1*), jby999 (*dbf4-1*). Plasmids used in this figure: pCN416 (vector), pCN421 (*STN1*).

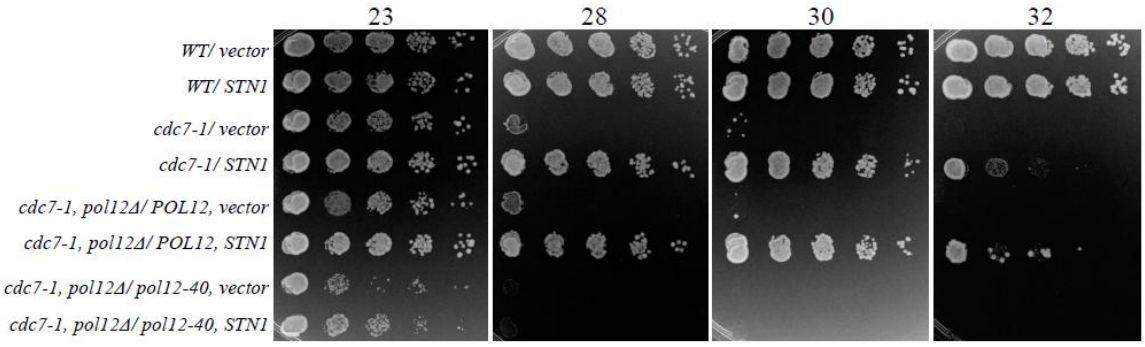

Figure 2-2: The Stn1-Pol12 interaction is necessary for suppression of *cdc7-1* temperature sensitivity

STN1 dosage suppression of *cdc7-1* requires interaction with Pol12. Cells were grown to saturation in selective media for 3 days at 23°C, then 10-fold serial dilutions were stamped onto selective plates. Plates were incubated at the indicated temperatures for 3-4 days, then pictures were taken. Strains used in this figure: hc160 (wild type), hc15 (*cdc7-1*), hc2318 (*cdc7-1*, *pol12-Δ*). Plasmids used in this figure: pCN416 (vector), pCN421 (*STN1*), pPC65 (*POL12*), pPC64 (*pol12-40*).

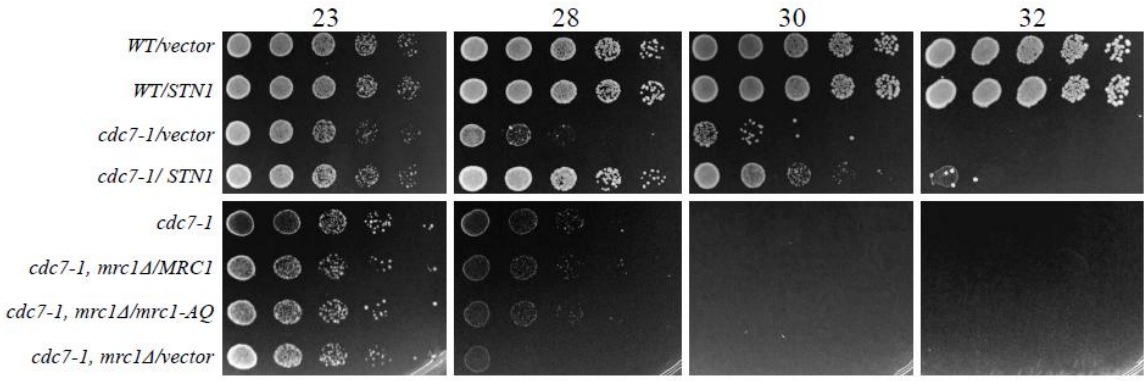

Figure 2-3: Blocking the S phase checkpoint response by *mrc1* deletion does not suppress *cdc7-1* temperature sensitivity

STN1 dosage suppression of *cdc7-1* is not directly caused by interfering with the S phase checkpoint. Blocking the checkpoint by mutating or deleting *mrc1* does not to suppress *cdc7-1* temperature sensitivity. The indicated strains were grown to saturation in selective media for 3 days at 23°C, then 10-fold serial dilutions were stamped onto selective plates. Plates were incubated at the indicated temperatures for 3-4 days, then pictures were taken. Strains used in this figure: hc160 (wild type), hc15 (*cdc7-1*), hc2312 (*cdc7-1*, *mrc1-Δ*). Plasmids used in this figure: pAO122 (*MRC1*), pAO139 (*mrc1-AQ*) pCN416 (vector), pCN421 (*STN1*), pRS415 (vector).

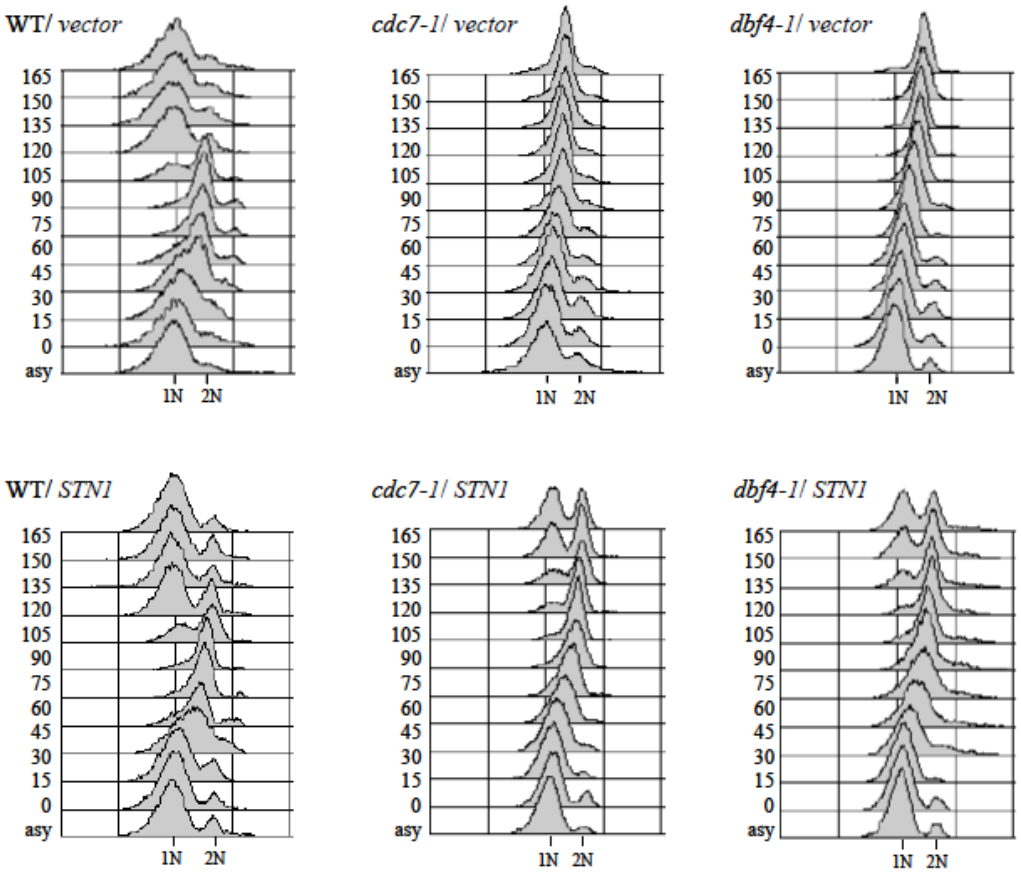

Figure 2-4: *STN1* overexpression suppresses *cdc7-1* and *dbf4-1* mutants by enhancing progression through S phase

cdc7-1 and *dbf4-1* mutants overproducing Stn1 are able to complete DNA synthesis at semi-permissive temperature. 10mL cultures were grown to logarithmic phase in selective media at 23°C, and arrested in G1. Cells were released into S phase at 30°C, and samples were collected every 15 minutes. DNA was stained with propidium iodide, and samples were subjected to FACS analysis. Strains used in this figure: hc160 (wild type), hc15 (*cdc7-1*), jby999 (*dbf4-1*). Plasmids used in this figure: pCN416 (vector), pCN421 (*STN1*).

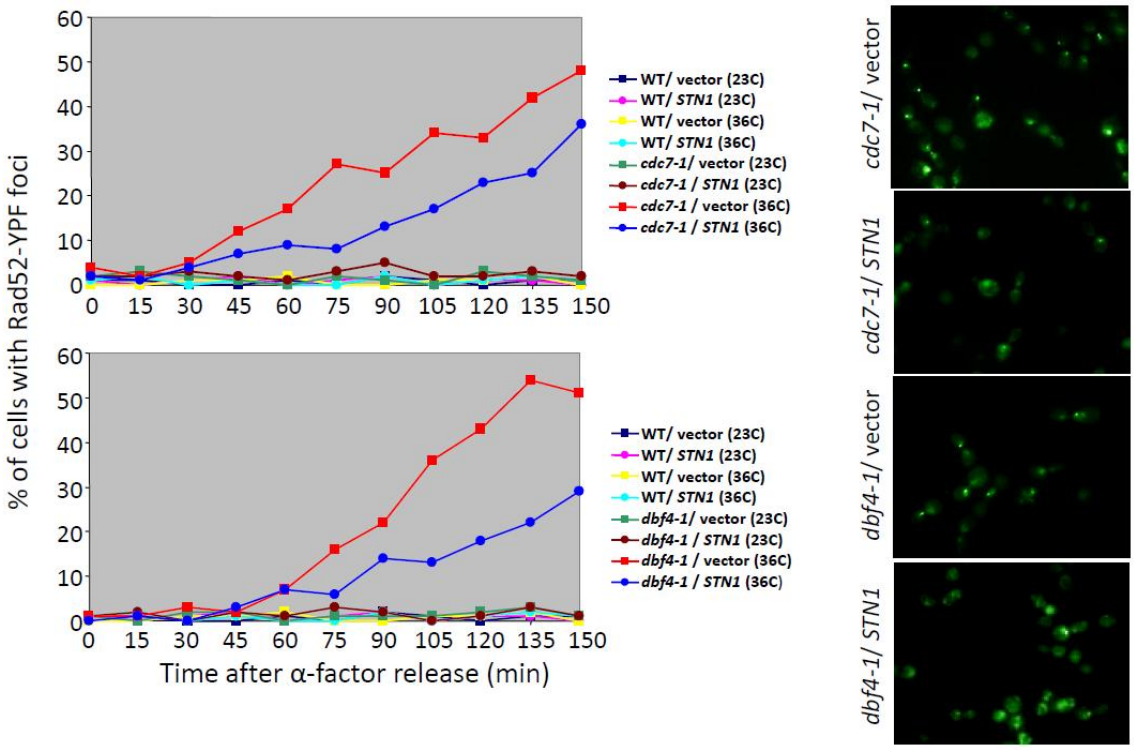

Figure 2-5: Stn1 overproduction suppresses accumulation of Rad52-YFP foci in *dbf4-1* and *cdc7-1* mutants at high temperature

Stn1 suppresses Rad52 foci formation in *cdc7-1* and *dbf4-1* mutants at high temperature. The indicated strains were grown in 10mL of selective media to logarithmic phase at 23°C, then arrested in G1. Cultures were divided, with one half released into S phase at 23°C while the second half was released at 36°C. Cells were collected at the indicated time points, and the presence of Rad52-YPF foci was scored for 100 cells from each sample by fluorescence microscopy. The data is plotted on the graphs, and representative micrographs are show from the 150 minute time point at 36°C. Strains used in this figure: hc2499 (*RAD52-YFP*), hc2391 (*cdc7-1, RAD52-YFP*), hc2393 (*dbf-1, RAD52-YFP*). Plasmids used in this figure: pCN416 (vector), pCN421 (*STN1*).

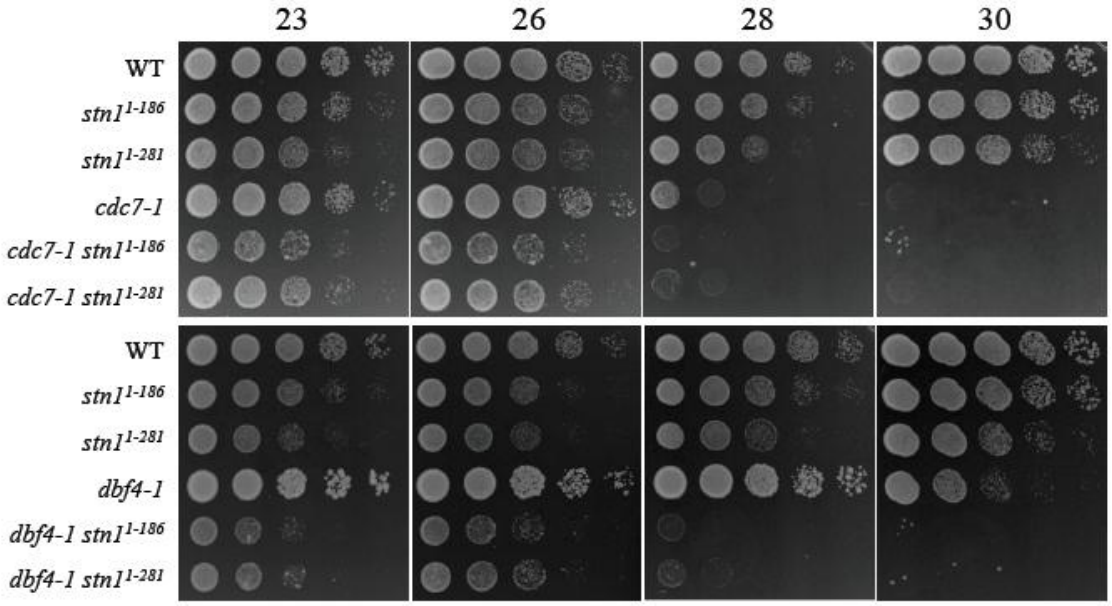

Figure 2-6: *stn1* truncation alleles display synthetic interactions with *cdc7-1* and *dbf4-1* mutants

cdc7-1 stn1 and *dbf4-1 stn1* double mutants display a synthetic growth phenotype. Cells were grown to saturation in for 3 days at 23°C, then 10-fold serial dilutions were stamped onto YPD plates. Plates were incubated at the indicated temperatures for 3-4 days, then pictures were taken. Strains used in this figure: hc160 (wild type), hc672 (*stn1-186t*), hc671 (*stn1-281t*), hc15 (*cdc7-1*), hc2572 (*cdc7-1*, *stn1-186t*), hc2571 (*cdc7-1*, *stn1-281t*), jby999 (*dbf4-1*), hc2569 (*dbf4-1*, *stn1-186t*), hc2567 (*dbf4-1*, *stn1-281t*).

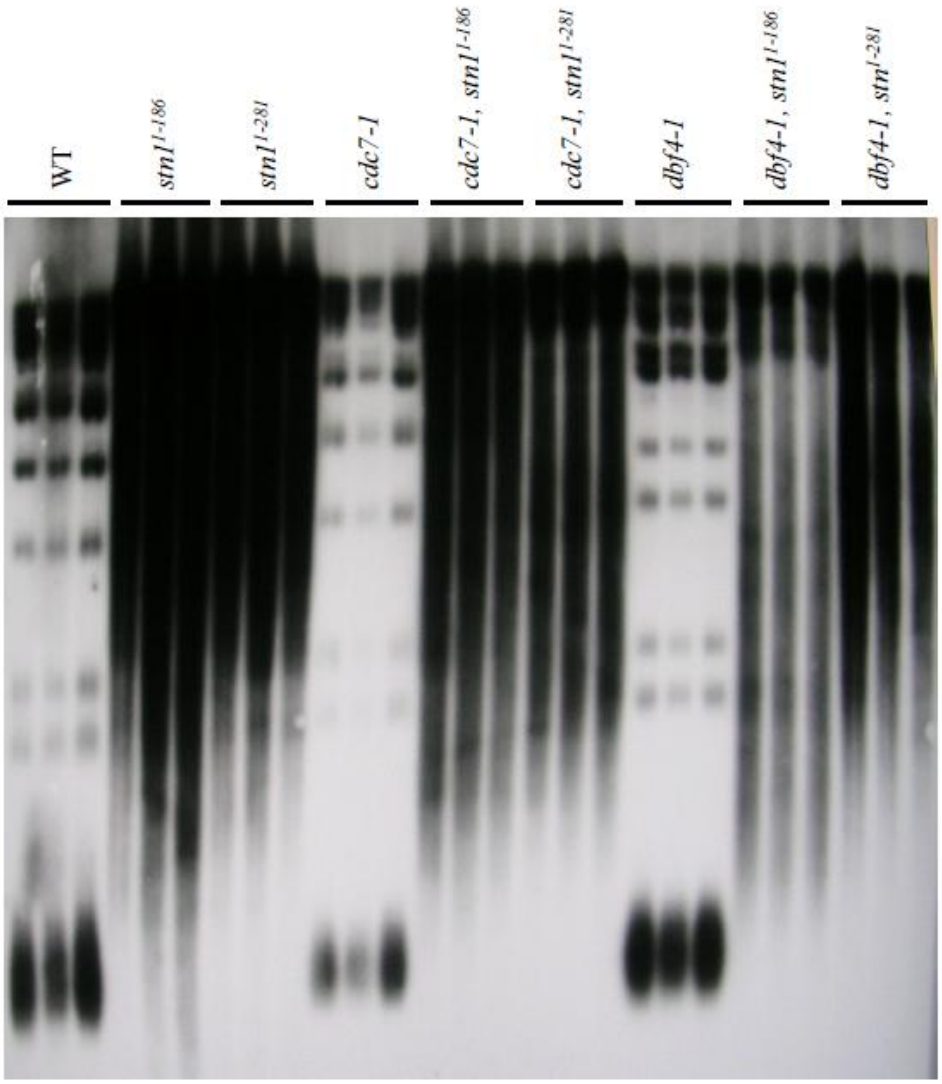

Figure 2-7: Telomere length of double mutants does not appear to be altered

Telomere length analysis of *cdc7-1 stn1* and *dbf4-1 stn1* double mutants shows that the *stn1* phenotype is epistatic. 10mL cultures were grown to saturation at 23°C for 3 days. DNA was isolated, digested, and run on a 0.8% agarose gel. Southern blot was performed probing against telomeric $TG_{1\text{-}3}/C_{1\text{-}3}A$ sequences. Strains used in this figure: hc160 (wild type), hc672 (*stn1-186t*), hc671 (*stn1-281t*), hc15 (*cdc7-1*), hc2572 (*cdc7-1*, *stn1-186t*), hc2571 (*cdc7-1*, *stn1-281t*), jby999 (*dbf4-1*), hc2569 (*dbf4-1*, *stn1-186t*), hc2567 (*dbf4-1*, *stn1-281t*).

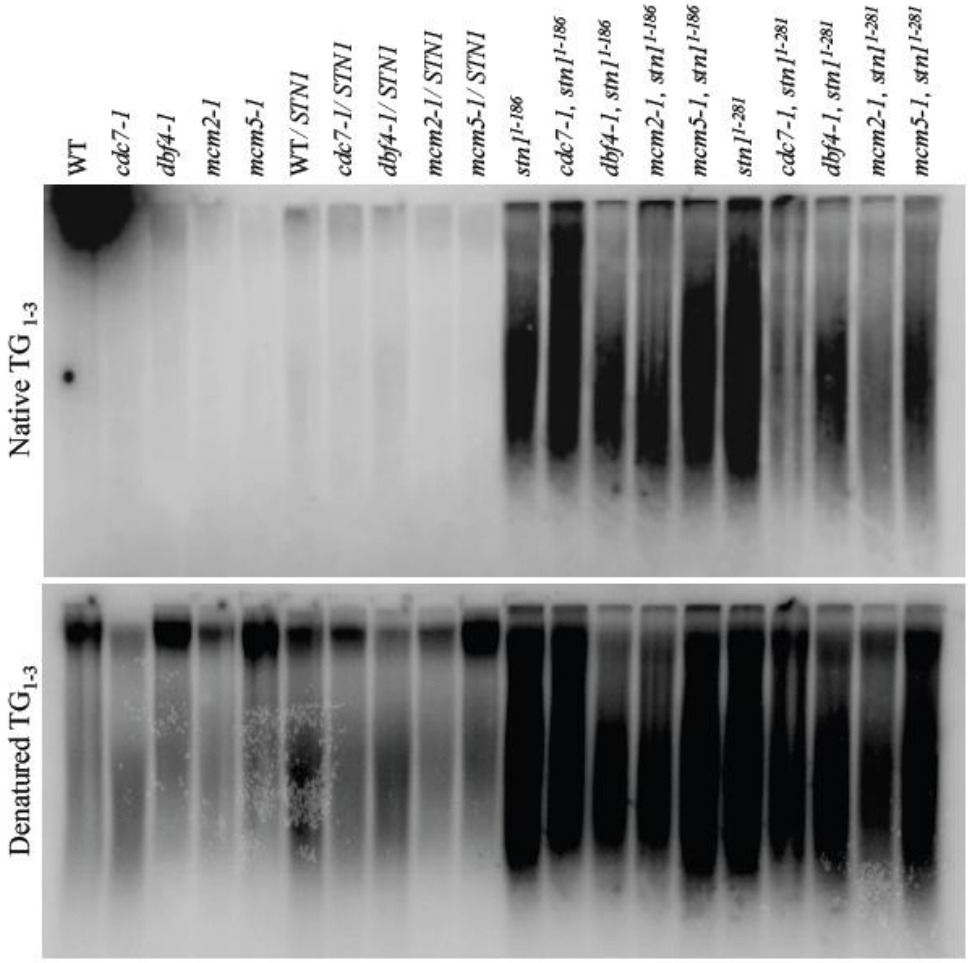

Figure 2-8: *stn1* DDK double mutants do not have increased telomeric ssDNA

Analysis of telomeric ssDNA shows that the *stn1* phenotype is epistatic in *cdc7-1*, *dbf4-1*, and *mcm* double mutants. 30mL cultures of each strain were grown to logarithmic phase at 23°C. DNA was isolated, digested, incubated with radiolabeled $C_{1-3}A$ probe, and run out on a 0.75% agarose gel under native conditions. The gel was dried and exposed to a phosphor-imager screen for 5 days. After developing the "native" image, the gel was denatured and re-probed with $C_{1-3}A$ probe to quantify the total telomeric DNA in each sample. Strains used in this figure: hc160 (wild type), hc15 (*cdc7-1*), jby999 (*dbf4-1*), hc2423 (*mcm2-1*), hc2424 (*mcm5-1*), hc672 (*stn1-186t*), hc2572 (*cdc7-1*, *stn1-186t*), hc2569 (*dbf4-1*, *stn1-186t*), hc2562 (*mcm2-1*, *stn1-186t*), hc2565 (*mcm5-1*, *stn1-186t*), hc671 (*stn1-281t*), hc2571 (*cdc7-1*, *stn1-281t*), hc2567 (*dbf4-1*, *stn1-281t*), hc2561 (*mcm2-1*, *stn1-281t*), hc2563 (*mcm5-1*, *stn1-281t*). Plasmids used in this figure: pCN416 (vector), pCN421 (*STN1*).

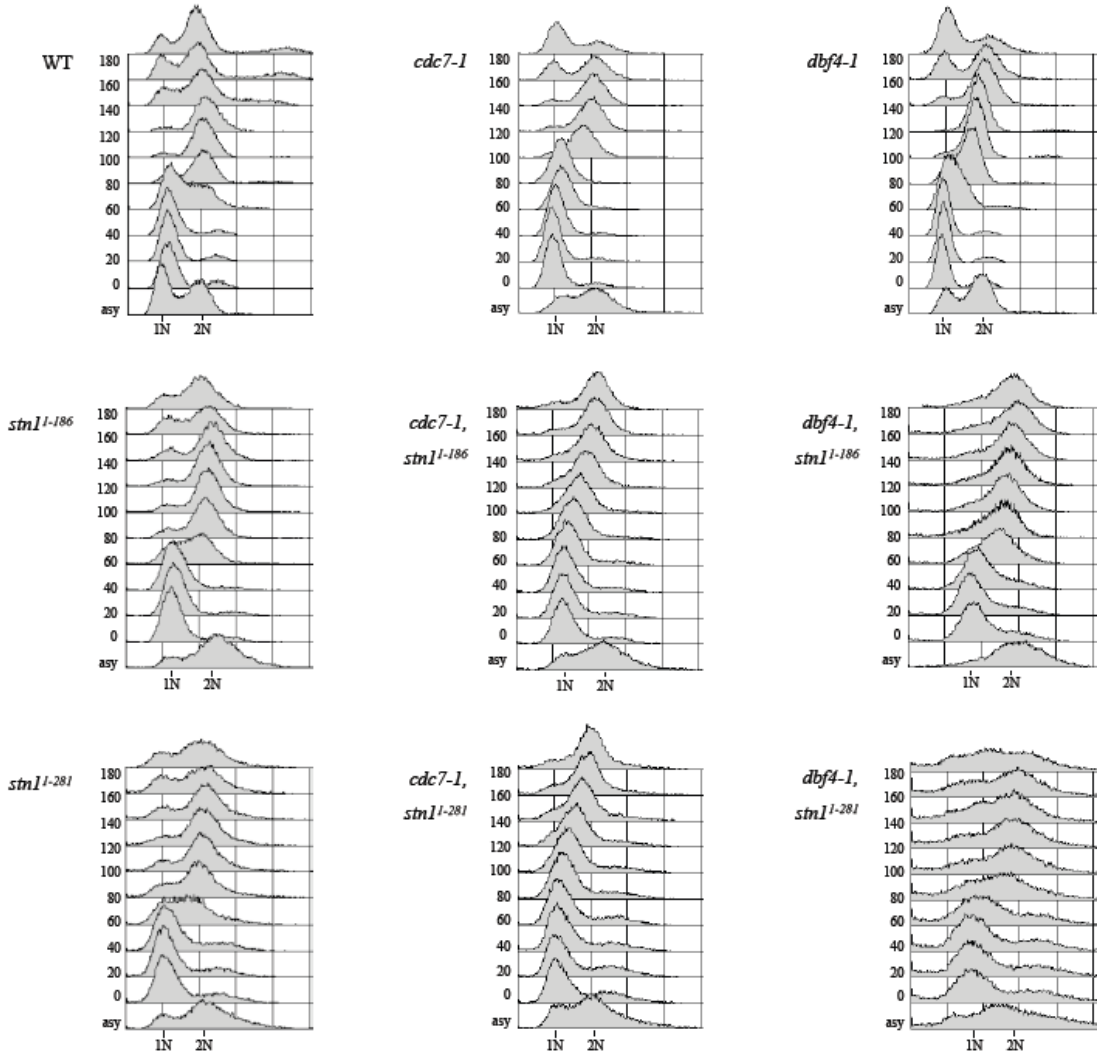

Figure 2-9: *stn1* DDK Double mutants show a delayed cell cycle progression

cdc7-1 stn1 and *dbf4-1 stn1* double mutants show a delay in completion of DNA synthesis at semi-permissive temperature. 10mL cultures were grown to logarithmic phase in selective media at 23°C, and arrested in G1. Cells were released into S phase at 28°C, and samples were collected every 20 minutes. DNA was stained with propidium iodide, and samples were subjected to FACS analysis. Strains used in this figure: hc160 (wild type), hc672 (*stn1-186t*), hc671 (*stn1-281t*), hc15 (*cdc7-1*), hc2572 (*cdc7-1*, *stn1-186t*), hc2571 (*cdc7-1*, *stn1-281t*), jby999 (*dbf4-1*), hc2569 (*dbf4-1*, *stn1-186t*), hc2567 (*dbf4-1*, *stn1-281t*).

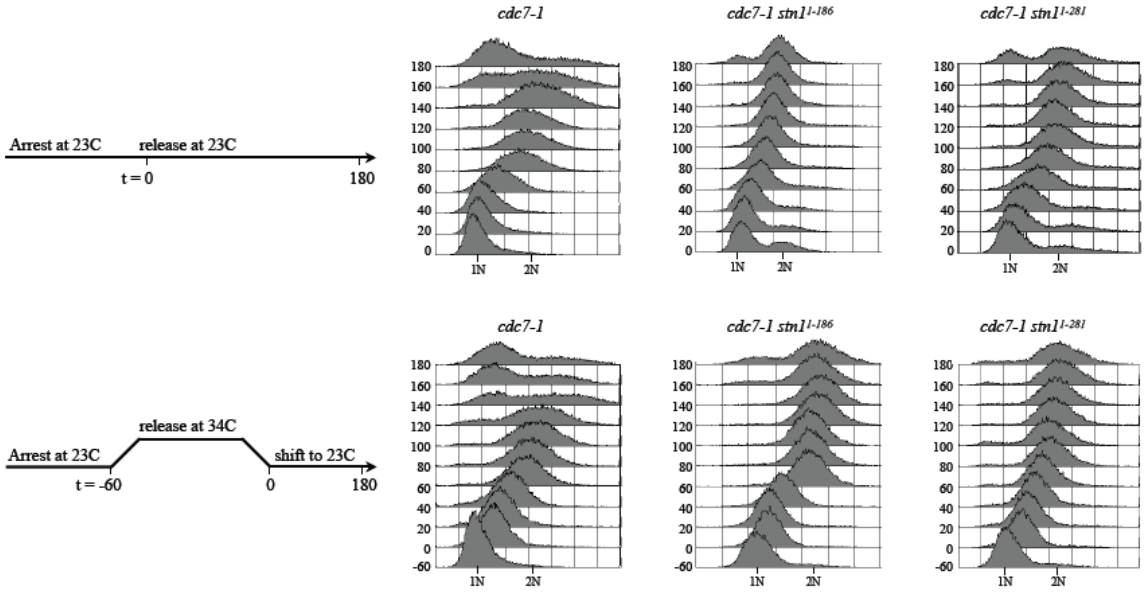

Figure 2-10: *cdc7-1 stn1* double mutants are able to recover replication after transient exposure to high temperature

cdc7-1 stn1 double mutants were grown to logarithmic phase in selective media at 23°C, and arrested in G1. The cultures were divided into two, with one half released at 23°C, while the second half was released at 34°C for 1 hour, followed by shifting down to 23°C (see schematic above). Samples were collected every 20 minutes. DNA was stained with propidium iodide, and samples were subjected to FACS analysis. The *cdc7-1 stn1* double mutants are able to recover from the transient shift to 34°C and complete DNA synthesis. Strains used in this figure: hc15 (*cdc7-1*), hc2572 (*cdc7-1*, *stn1-186t*), hc2571 (*cdc7-1*, *stn1-281t*).

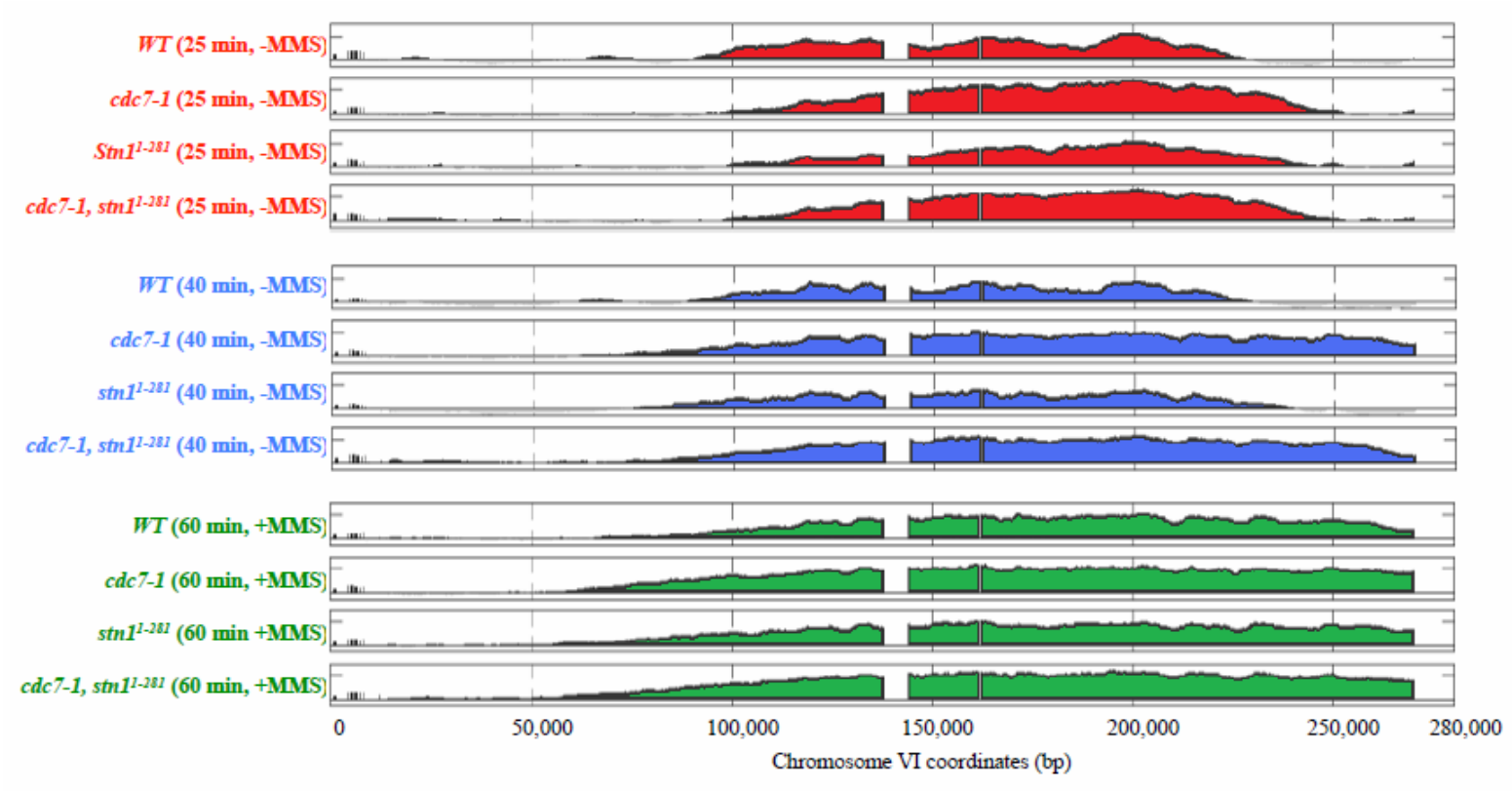
WT (25 min, -MMS)
cdc7-1 (25 min, -MMS)
Stn1^1-281 (25 min, -MMS)
cdc7-1, stn1^1-281 (25 min, -MMS)
WT (40 min, -MMS)
cdc7-1 (40 min, -MMS)
stn1^1-281 (40 min, -MMS)
cdc7-1, stn1^1-281 (40 min, -MMS)
WT (60 min, +MMS)
cdc7-1 (60 min, +MMS)
stn1^1-281 (60 min +MMS)
cdc7-1, stn1^1-281 (60 min, +MMS)
0
50,000
100,000
150,000
200,000
250,000
280,000
Chromosome VI coordinates (bp)

Figure 2-11: Origin firing and fork progression does not appear to be altered in the *cdc7-1 stn1-281t* double mutant

Strains of the indicated genotype were arrested in G1 at 23°C, and released into S phase at 28°C in either the absence or presence of 0.033% MMS, as indicated. Newly synthesized DNA was labeled with BrdU for either 0-25 minutes (red), 0-40 minutes (blue) or 0-60 (green) after release. Labeled DNA was immuno-precipitated with α-BrdU antibodies, and hybridized to a genomic microarray. The data for chromosome VI is shown. The peaks represent areas enriched for BrdU above background. The single and double mutants display origin firing and fork progression comparable to the wild type control. Strains used in this figure: hc2606 (wild type), hc2593 (*cdc7-1*), hc2592 (*stn1-281t*), hc2595 (*cdc7-1*,

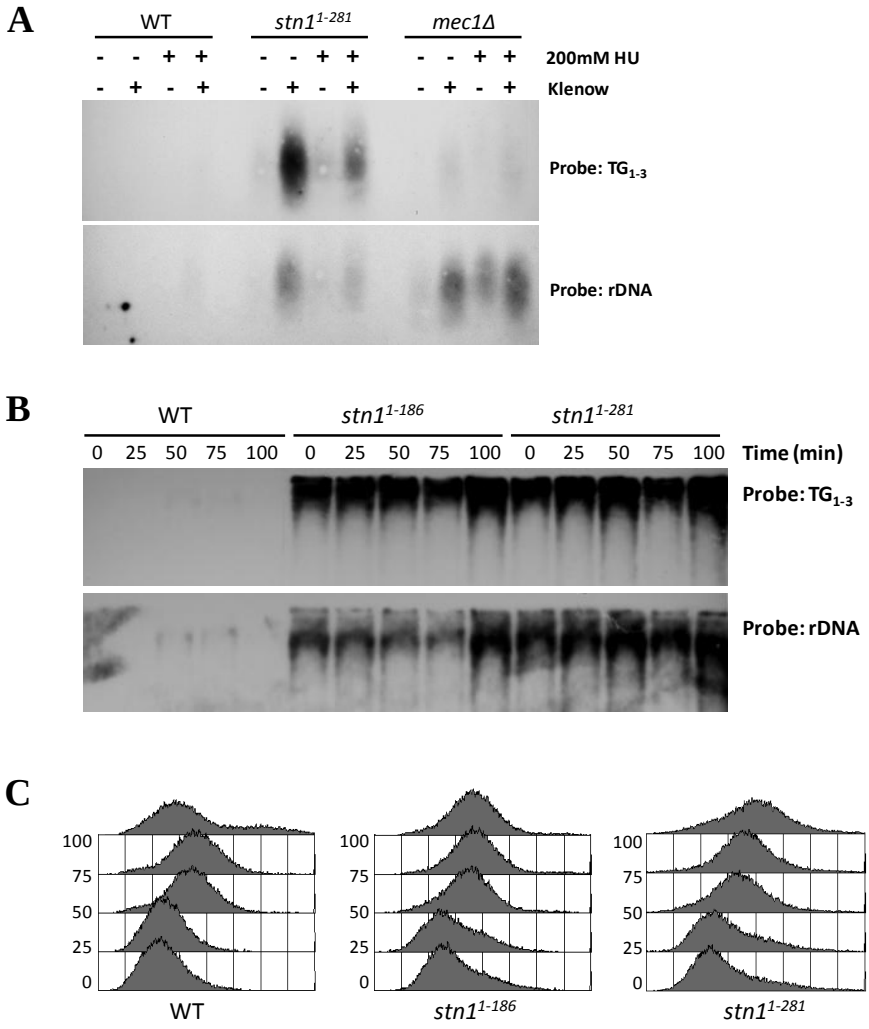

Figure 2-12: *stn1* mutants contain aberrant single-stranded DNA at non-telomeric repetitive regions in the genome

Stn1 prevents accumulation of single stranded DNA at repetitive loci in the genome. **(A)** Strains of the indicated genotype were grown to logarithmic phase at 30°C, and treated with HU where indicated. Samples were collected, suspended in agarose plugs, and chromosomal DNA was isolated. Using random hexameric primers, a Klenow reaction was performed to synthesize complementary DNA sequences across regions of ssDNA present on chromosomes. The samples were denatured and separated on a 1% agarose gel. Southern blot was performed probing against both telomeric and rDNA sequences. **(B)** Strains were arrested in G1 at 30°C, then released into fresh media. Samples were collected at the indicated time points, and subjected to a Klenow reaction as described above. **(C)** Aliquots of cells from the experiment in **(B)** were collected and subjected to FACS analysis. Strains used in this figure: hc160 (wild type), hc672 (*stn1-186t*), hc671 (*stn1-281t*), hc30 (*mec1-Δ*).

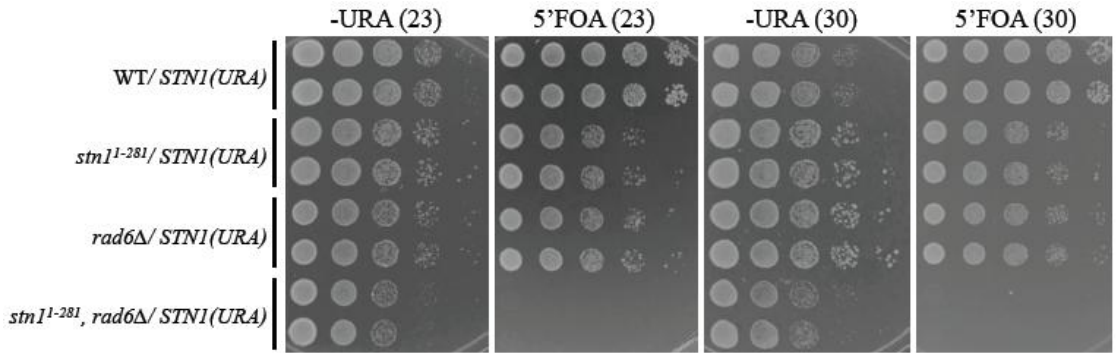

Figure 2-13: *stn1-281t* requires *RAD6*-dependent post replication repair for viability

The *stn1-281t* mutation is synthetic lethal when combined with *rad6*Δ. The double mutant strains were created by mating haploid single mutants, transforming the diploid parent with a plasmid containing wild type *STN1*, and dissecting tetrads. The resulting haploid offspring were genotyped, and two replicates of the appropriate genotype were selected. Cells were grown to saturation in selective media for 3 days at 23°C, then 10-fold serial dilutions were stamped onto either -URA plates to select for the *STN1* plasmid, or 5-FOA plates to force loss of the plasmid. Plates were incubated at the indicated temperatures for 3-4 days, then pictures were taken. Strains used in this figure: hc160 (wild type), hc671 (*stn1-281t*), jby285 (*rad6Δ*), hc2636 (*stn1-281t*, *rad6Δ*). Plasmids used in this figure: pVL1046 (*STN1*).

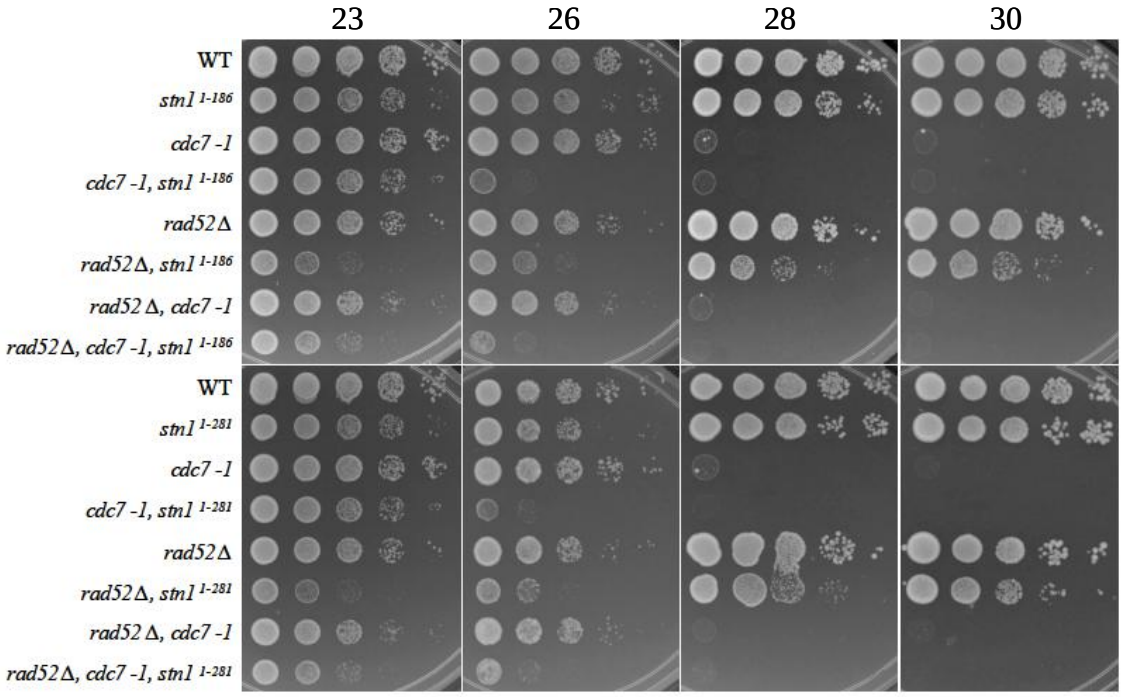

Figure 2-14: *stn1* and *cdc7-1 stn1* mutants have synthetic interactions with *rad52*

stn1 and *cdc7-1 stn1* mutants display a synthetic growth defect when combined with *rad52*Δ. Cells were grown to saturation in 5mL of YPD for 3 days at 23°C, then 10-fold serial dilutions were stamped onto YPD plates. Plates were incubated at the indicated temperatures for 3-4 days, then pictures were taken. Strains used in this figure: hc160 (wild type), hc672 (*stn1-186t*), hc15 (*cdc7-1*), hc2572 (*cdc7-1*, *stn1-186t*), hc861 (*rad52-Δ*), hc2644 (*rad52-Δ*, *stn1-186t*), hc2643 (*rad52-Δ*, *cdc7-1*), hc2640 (*rad52-Δ*, *cdc7-1*, *stn1-186t*), hc671 (*stn1-281t*), hc2571 (*cdc7-1*, *stn1-281t*), hc2645 (*rad52-Δ*, *stn1-281t*), hc2637 (*rad52-Δ*, *cdc7-1*, *stn1-281t*).

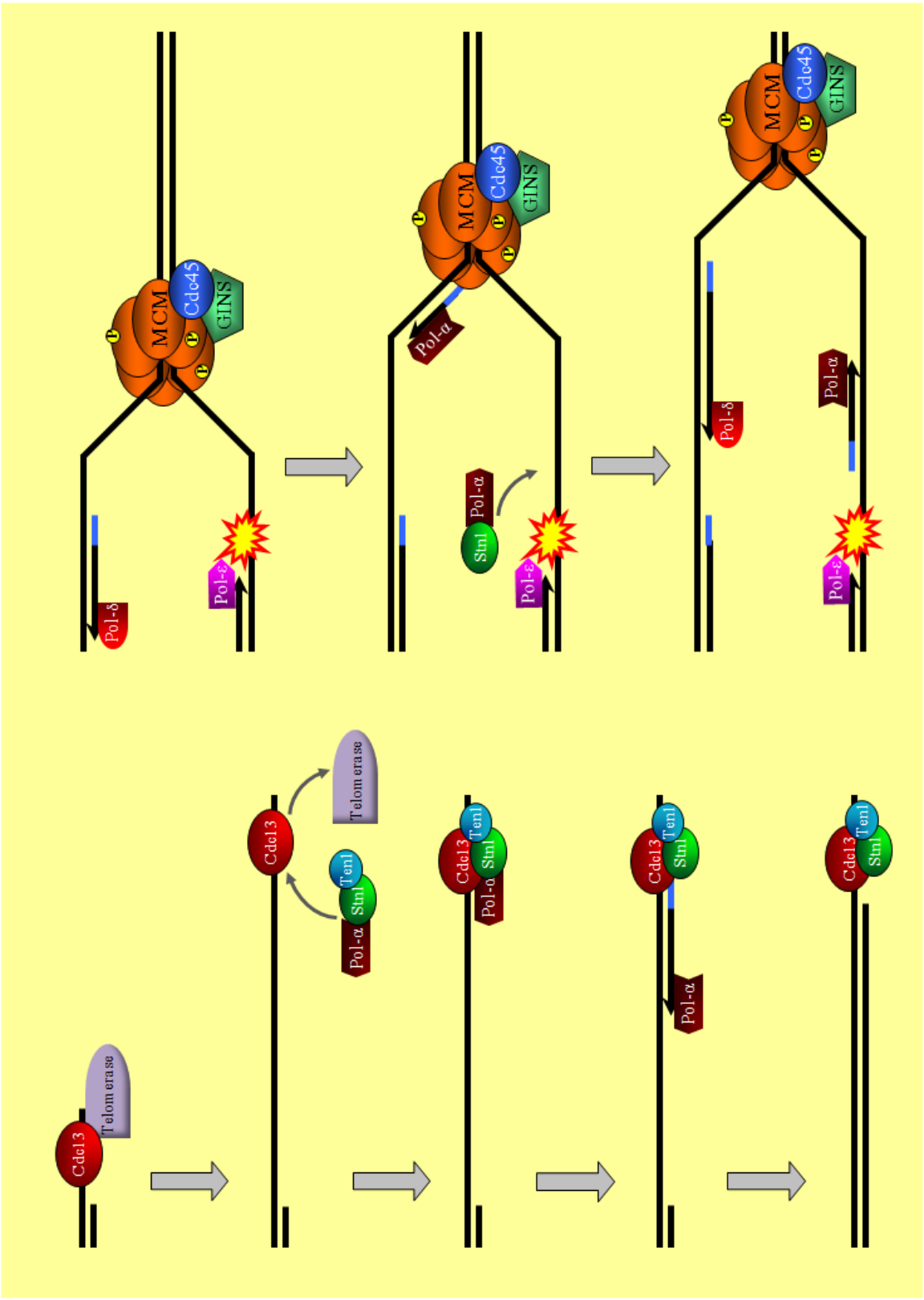
MCM
Cdc45
GINS
Pol-δ
Pol-ε
Pol-α
Stn1
Ten1
Cdc13
Telomerase

Figure 2-15: Model of Stn1's function in promoting DNA synthesis

Left- Stn1's function in telomere replication. Cdc13 is thought to first recruit telomerase to elongate the G-strand at critically short telomeres. Stn1, along with Ten1, then bring in Pol-α to the end, which is thought to negatively regulate telomerase. Once Pol-α is recruited to the end, it catalyzes "fill-in" synthesis of the C-strand to complete replication of the telomere. Right- Stn1's function in replication at non-telomeric sites. DNA lesions can cause fork stalling, leading to the uncoupling of the DNA polymerases from the MCM helicases and accumulation of single-stranded DNA. Stn1 can recruit or facilitate Pol-α activity ahead of lesions, to allow efficient synthesis throughout the genome.

Table 2-1: Tetrad analysis of *stn1-281t, rad6-Δ* cross

Parental genotype: *rad6-Δ::LEU2* / *RAD6* *stn1-281t::KanMX* / *STN1* pVL1046

Number of tetrads dissected: 24
Number of total spores: 96
Number of viable spores: 62

Genotype	**Viable spores**	**Frequency (viable)**	**Frequency (total)**	**Expected frequency**
WT	13	20.9	13.5	12.5
rad6-Δ	14	22.6	14.6	12.5
stn1-281t	8	12.9	8.3	12.5
rad6-Δ stn1-281t	0	0	0	12.5
WT/ p*STN1*	9	14.5	9.4	12.5
rad6-Δ/ p*STN1*	9	14.5	9.4	12.5
stn1-281t/ p*STN1*	4	6.5	4.2	12.5
rad6-Δ stn1-281t/ p*STN1*	5	8.1	5.2	12.5

Table 2-2: Tetrad analysis of *stn1-186t cdc7-1, rad52-Δ* cross

Parental genotype: *rad52-Δ::LYS2* / *RAD52* *stn1-186t::KanMX* / *STN1* *cdc7-1* / *CDC7*

Number of tetrads dissected: 22
Number of total spores: 88
Number of viable spores: 78

Genotype	Viable spores	Frequency (viable)	Frequency (total)	Expected frequency
WT	7	9.0	8.0	12.5
rad52-Δ	8	10.3	9.1	12.5
stn1-186t	18	23.1	20.5	12.5
cdc7-1	13	16.7	14.7	12.5
rad52-Δ stn1-186t	7	9.0	8.0	12.5
rad52-Δ cdc7-1	16	20.5	18.2	12.5
stn1-186t cdc7-1	4	5.1	4.5	12.5
rad52-Δ stn1-186t cdc7-1	5	6.4	5.7	12.5

Table 2-3: Tetrad analysis of *stn1-281t cdc7-1, rad52-Δ* cross

Parental genotype: *rad52-Δ::LYS2* *stn1-281t::KanMX* *cdc7-1*
RAD52 *STN1* *CDC7*

Number of tetrads dissected: 23
Number of total spores: 92
Number of viable spores: 58

Genotype	Viable spores	Frequency (viable)	Frequency (total)	Expected frequency
WT	5	8.6	5.4	12.5
rad52-Δ	6	10.3	6.5	12.5
stn1-281t	5	8.6	5.4	12.5
cdc7-1	17	29.3	18.4	12.5
rad52-Δ stn1-281t	4	6.9	4.3	12.5
rad52-Δ cdc7-1	11	19.0	12.0	12.5
stn1-281t cdc7-1	9	15.6	9.8	12.5
rad52-Δ stn1-281t cdc7-1	1	1.7	1.1	12.5

Table 2-4: List of strains used in chapter 2

Strain	Description	Reference
hc15	*MAT*a *ura3-52 lys2-801 ade2-101 trp1-Δ63 his3-Δ200 leu2-Δ1 cdc7-1*	This study
hc30	*MAT*a *ade2-1 ura3-1 his3-11,15 trp1-1 leu2-3,112 can1-100 CDC13myc($_{18x}$) mec1-Δ::HIS3 TRP1::GAP RNR1*	This study
hc160	*MAT*a *ura3-52 lys2-801 ade2-101 trp1-Δ63 his3-Δ200 leu2-Δ1*	Petreaca[a]
hc420	*MAT*a *ura3-52 lys2-801 ade2-101 trp1-Δ63 his3-Δ200 leu2-Δ1/* pVL1046	This study
hc667	*MATα ura3-52 lys2-801 ade2-101 trp1-Δ63 his3-Δ200 leu2-Δ1 stn1-186t::KanMX2*	Petreaca[b]
hc671	*MAT*a *ura3-52 lys2-801 ade2-101 trp1-Δ63 his3-Δ200 leu2-Δ1 stn1-281t::KanMX2*	Petreaca[b]
hc672	*MAT*a *ura3-52 lys2-801 ade2-101 trp1-Δ63 his3-Δ200 leu2-Δ1 stn1-186t::KanMX2*	Petreaca[b]
hc861	*MAT*a *ura3-52 lys2-801 ade2-101 trp1-Δ63 his3-Δ200 leu2-Δ1 rad52-Δ::LYS2*	This study
hc1090	*MATα ura3-52 lys2-801 ade2-101 trp1-Δ63 his3-Δ200 leu2-Δ1 stn1-281t::KanMX2*	Petreaca[b]
hc2109	*MAT*a *ura3-52 lys2-801 ade2-101 trp1-Δ63 his3-Δ200 leu2-Δ1/* pCN421	Gasparyan
hc2110	*MAT*a *ura3-52 lys2-801 ade2-101 trp1-Δ63 his3-Δ200 leu2-Δ1/* pCN416	Gasparyan
hc2220	*MAT*a *ura3-52 lys2-801 ade2-101 trp1-Δ63 his3-Δ200 leu2-Δ1 cdc7-1/* pCN416	This study
hc2222	*MAT*a *ura3-52 lys2-801 ade2-101 trp1-Δ63 his3-Δ200 leu2-Δ1 cdc7-1/* pCN421	This study
hc2225	*MAT*a *ade2-1 ura3-1 his3-11,15 trp1-1 leu2-3,112 can1-100 dbf4-1/* pCN416	This study
hc2227	*MAT*a *ade2-1 ura3-1 his3-11,15 trp1-1 leu2-3,112 can1-100 dbf4-1/* pCN421	This study
hc2312	*ura3-52 lys2-801 ade2-101 trp1-Δ63 his3-Δ200 leu2-Δ1 cdc7-1 mrc1-Δ::HIS5*	This study
hc2318	*MAT*a *ura3-52 lys2-801 ade2-101 trp1-Δ63 his3-Δ200 leu2-Δ1 cdc7-1 pol12Δ::kanMX2/* pPC64	This study
hc2319	*MAT*a *ura3-52 lys2-801 ade2-101 trp1-Δ63 his3-Δ200 leu2-Δ1 cdc7-1 pol12-Δ::kanMX2/* pPC64, pCN416	This study
hc2320	*MAT*a *ura3-52 lys2-801 ade2-101 trp1-Δ63 his3-Δ200 leu2-Δ1 cdc7-1 pol12-Δ::kanMX2/* pPC64, pCN421	This study
hc2391	*MAT*a *ura3-52 lys2-801 ade2-101 trp1-Δ63 his3-Δ200 leu2-Δ1 RAD52YFP cdc7-1/* pCN416	This study

Table 2-4 (continued)

Strain	Description	Reference
hc2392	*MAT*a *ura3-52 lys2-801 ade2-101 trp1-Δ63 his3-Δ200 leu2-Δ1 RAD52YFP cdc7-1/* pCN421	This study
hc2393	*MAT*a *ura3-52 lys2-801 ade2-101 trp1-Δ63 his3-Δ200 leu2-Δ1 RAD52YFP dbf4-1/* pCN416	This study
hc2394	*MAT*a *ura3-52 lys2-801 ade2-101 trp1-Δ63 his3-Δ200 leu2-Δ1 RAD52YFP dbf4-1/* pCN421	This study
hc2397	*MAT*a *ura3-52 lys2-801 ade2-101 trp1-Δ63 his3-Δ200 leu2-Δ1 cdc7-1 mrc1-Δ::HIS5/* pAO122	This study
hc2398	*MAT*a *ura3-52 lys2-801 ade2-101 trp1-Δ63 his3-Δ200 leu2-Δ1 cdc7-1 mrc1-Δ::HIS5/* pAO139	This study
hc2399	*MAT*a *ura3-52 lys2-801 ade2-101 trp1-Δ63 his3-Δ200 leu2-Δ1 cdc7-1 mrc1-Δ::HIS5/* pRS415	This study
hc2423	*MAT*a *ade2-1 ura3-1 his3-11,15 trp1-1 leu2-3,112 can1-100 mcm2-1 SPC42GFP::TRP1*	This study
hc2424	*MAT*a *ade2-1 ura3-1 his3-11,15 trp1-1 leu2-3,112 can1-100 mcm5-1 SPC42GFP::TRP1*	This study
hc2425	*MAT*a *ade2-1 ura3-1 his3-11,15 trp1-1 leu2-3,112 can1-100 mcm2-1 SPC42GFP::TRP1/* pCN416	This study
hc2426	*MAT*a *ade2-1 ura3-1 his3-11,15 trp1-1 leu2-3,112 can1-100 mcm2-1 SPC42GFP::TRP1/* pCN421	This study
hc2427	*MAT*a *ade2-1 ura3-1 his3-11,15 trp1-1 leu2-3,112 can1-100 mcm5-1 SPC42GFP::TRP1/* pCN416	This study
hc2428	*MAT*a *ade2-1 ura3-1 his3-11,15 trp1-1 leu2-3,112 can1-100 mcm5-1 SPC42GFP::TRP1/* pCN421	This study
hc2499	*MAT*a *ura3-52 lys2-801 ade2-101 trp1-Δ63 his3-Δ200 leu2-Δ1 RAD52YFP/* pCN416	This study
hc2500	*MAT*a *ura3-52 lys2-801 ade2-101 trp1-Δ63 his3-Δ200 leu2-Δ1 RAD52YFP/* pCN421	This study
hc2561	*MAT*a *ura3-52 lys2-801 ade2-101 trp1-Δ63 his3-Δ200 leu2-Δ1 mcm2-1 stn1-281t::KanMX2*	This study
hc2562	*MATα ura3-52 lys2-801 ade2-101 trp1-Δ63 his3-Δ200 leu2-Δ1 mcm2-1 stn1$^{1-86}$::KanMX2*	This study
hc2563	*MAT*a *ura3-52 lys2-801 ade2-101 trp1-Δ63 his3-Δ200 leu2-Δ1 mcm5-1 stn1-281t::KanMX2*	This study
hc2565	*MAT*a *ura3-52 lys2-801 ade2-101 trp1-Δ63 his3-Δ200 leu2-Δ1 mcm5-1 stn1$^{1-86}$::KanMX2*	This study
hc2567	*MAT*a *ura3-52 lys2-801 ade2-101 trp1-Δ63 his3-Δ200 leu2-Δ1 dbf4-1 stn1-281t::KanMX2*	This study
hc2569	*MAT*a *ura3-52 lys2-801 ade2-101 trp1-Δ63 his3-Δ200 leu2-Δ1 dbf4-1 stn1-186t::KanMX2*	This study

Table 2-4 (continued)

Strain	Description	Reference
hc2571	*MAT*a *ura3-52 lys2-801 ade2-101 trp1-Δ63 his3-Δ200 leu2-Δ1 cdc7-1 stn1-281t::KanMX2*	This study
hc2572	*MAT*a *ura3-52 lys2-801 ade2-101 trp1-Δ63 his3-Δ200 leu2-Δ1 cdc7-1 stn1-186t::KanMX2*	This study
hc2592	*MAT*a *ura3-52 lys2-801 ade2-101 trp1-Δ63 his3-Δ200 leu2-Δ1 stn1-281t::KanMX2 ars306-Δ::URA3::BrdU–Inc*	This study
hc2593	*MAT*a *ura3-52 lys2-801 ade2-101 trp1-Δ63 his3-Δ200 leu2-Δ1 cdc7-1 ars306-Δ::URA3::BrdU–Inc*	This study
hc2595	*MAT*a *ura3-52 lys2-801 ade2-101 trp1-Δ63 his3-Δ200 leu2-Δ1 cdc7-1 stn1-281t::KanMX2 ars306-Δ::URA3::BrdU–Inc*	This study
hc2606	*MAT*a *ura3-52 lys2-801 ade2-101 trp1-Δ63 his3-Δ200 leu2-Δ1 ars306-Δ::URA3::BrdU–Inc*	This study
hc2635	*MATα ura3-52 lys2-801 ade2-101 trp1-Δ63 his3-Δ200 leu2-Δ1 rad6-Δ::LEU2 stn1-281t::KanMX2/* pVL1046	This study
hc2636	*MAT*a *ura3-52 lys2-801 ade2-101 trp1-Δ63 his3-Δ200 leu2-Δ1 rad6-Δ::LEU2 stn1-281t::KanMX2/* pVL1046	This study
hc2637	*MAT*a *ura3-52 lys2-801 ade2-101 trp1-Δ63 his3-Δ200 leu2-Δ1 rad52-Δ::LYS2 cdc7-1 stn1-281t::KanMX2*	This study
hc2640	*MATα ura3-52 lys2-801 ade2-101 trp1-Δ63 his3-Δ200 leu2-Δ1 cdc7-1 rad52-Δ::LYS2 cdc7-1 stn1-186t::KanMX2*	This study
hc2643	*MATα ura3-52 lys2-801 ade2-101 trp1-Δ63 his3-Δ200 leu2-Δ1 rad52-Δ::LYS2 cdc7-1*	This study
hc2644	*MAT*a *ura3-52 lys2-801 ade2-101 trp1-Δ63 his3-Δ200 leu2-Δ1 rad52-Δ::LYS2 stn1-186t::KanMX2*	This study
hc2645	*MATα ura3-52 lys2-801 ade2-101 trp1-Δ63 his3-Δ200 leu2-Δ1 rad52-Δ::LYS2 stn1-281t::KanMX2*	This study
jby285	*MAT*a *ade2-1 ura3-1 his3-11,15 trp1-1 leu2-3,112 can1-100 rad6-Δ::LEU2*	This study
jby999	*MAT*a *ade2-1 ura3-1 his3-11,15 trp1-1 leu2-3,112 can1-100 dbf4-1*	Khalil
mly89	*MATa ade2-1 ura3-1 his3-11,15 trp1-1 leu2-3,112 can1-100 mrc1-Δ::HIS5*	Lee

Table 2-5: List of plasmids used in chapter 2

Plasmid	Description	Reference
pAO122	*CEN LEU2 native promoter MRC1*	Osborn
pAO139	*CEN LEU2 native promoter mrc1-AQ*	Osborn
pCN416	*2μ LEU2 ADH promoter vector*	Gasparyan
pCN421	*2μ LEU2 ADH promoter STN1*	Gasparyan
pPC64	*CEN HIS3 native promoter pol12-40*	Chiu
pPC65	*CEN HIS3 native promoter POL12*	Chiu
pRS415	*CEN LEU2 vector*	Sikorski
pVL1046	*CEN URA3 native promoter STN1*	Petreaca[b]

Chapter 3

New insights into the telomere capping and replication functions of Cdc13, Stn1, Ten1 and Pol12

Abstract

Interactions between the CST complex and Pol-α are thought to be important for telomere capping, length regulation and replication of chromosome ends. Multiple interactions have been discovered between CST and Pol-α; Cdc13 can directly bind Pol1, and Stn1 can bind Pol12. However, the functional consequences of these interactions are not fully understood. Moreover, it is not known if the interactions between the individual components within the CST complex are necessary for their telomere capping function, length regulation, or both processes. In this chapter, we analyze the role of interactions between the components of the CST complex, as well as their interactions with Pol-α. Earlier studies have shown that compromising Pol-α function leads to problems in chromosome end maintenance, including capping defects, telomere elongation, and failure to perform *de novo* telomere synthesis. In previous work from our lab, we generated an allele of *POL12*, *pol12-40* which has weakened interaction with Stn1. Here, we first show that *pol12-40* mutants are able to carry out *de novo* telomere synthesis. This suggests that the multiple interactions between CST and Pol-α may function redundantly. To explore this, we combined the *pol12-40* mutant with alleles of *cdc13* that are hypothesized to disrupt interaction with either Stn1 (*cdc13-5)* or Pol1 (*cdc13-50)*. We show that the *pol12-40 cdc13-5* double mutant has a severe telomere capping defect, and is sensitive to both HU and elevated temperatures. However, surprisingly, the *pol12-40 cdc13-50* double mutant has relatively mild phenotypes, suggesting that there may be yet additional interactions between CST and Pol-α. In support of this idea, we found that Ten1 can bind to Pol12, but it is not yet known if this interaction is direct. Our lab has

previously shown that Ten1 can also interact with Pol1, suggesting that in addition to its capping function, it may also be more intimately involved in replication of telomeres. The role of Ten1 in telomere maintenance is the least understood among the CST components. In the second half of this chapter, we utilize several temperature sensitive *ten1* alleles to gain further insight into its telomere length regulation and capping functions. We show that neither the Ten1-Stn1 nor the Ten1-Cdc13 interaction are necessary for viability, but do contribute to proper maintenance of telomere length. We also show that one of the *ten1* loss of function alleles can neither extend a critically short telomere, nor protect it against exonucleolytic degradation. Lastly, we utilize genetic analysis to determine which pathways contribute to the extreme telomere elongation phenotype of the *ten1* mutants. Our findings reveal that deletion of *rad9* or overexpression of *STN1* suppresses the telomere lengthening phenotype, but deletion of *exo1* does not. These results do not directly correlate with the suppression of temperature sensitivity, indicating that these phenotypes are not mechanistically linked. We conclude that Ten1 makes independent contributions to telomere capping, length regulation, and replication, and multiple processes have been disrupted in these mutants. Overall, the data from this chapter supports the hypothesis that multiple redundant interactions exist between the CST complex and Pol-α, which work in parallel to ensure proper telomere function.

Introduction

Telomeres maintain genomic stability via several distinct processes. They differentiate the natural ends of chromosomes from double stranded breaks, preventing inappropriate activation of checkpoint responses. In doing so, they also block inappropriate repair or recombination of chromosome ends. Additionally, telomeres facilitate replication of chromosome termini. The CST complex is thought to be directly involved in both the capping and replication of telomeres. Multiple reports have shown that mutations within any of the CST components can lead to accumulation of telomeric single-stranded DNA, resulting from a capping defect (Garvik *et al*, 1995; Grandin *et al*, 1997; Grandin *et al*, 2001; Petreaca *et al*, 2007; Xu *et al*, 2009). The role of CST in telomere replication is less well understood, but current models hypothesize that this is done in a two step process; first, Cdc13 recruits telomerase via interaction with the regulatory Est1 subunit, to extend the G-rich strand (Nugent *et al*, 1996; Evans and Lundblad, 1999; Qi and Zakian, 2000; Taggart *et al*, 2002). Then Pol-α is brought in via interactions with Cdc13 and Stn1 to fill-in the complementary C-rich strand (Qi and Zakian 2000; Grossi *et al*, 2004). Most of the evidence for this model is derived from genetic experiments, and the regulation of these processes is not fully understood.

Several observations from previous work in our lab suggest that the capping and replicative functions of telomeres are mechanistically linked. First, *stn1* loss of function mutants have elevated levels of telomeric single-stranded DNA. This phenotype has classically been interpreted as a capping defect, resulting in excessive, unregulated exonucleolytic degradation of the C-strand. However, after treating DNA isolated from

these *stn1* mutants with the bacterial Exo1 exonuclease to degrade terminal ssDNA, a large fraction of the signal remains (Petreaca *et al*, 2007). The presence of Exo1 resistant signal from these experiments implies that there is gapped single-stranded DNA in the telomeres of *stn1* mutants. The most likely source of such gapped structures is from incomplete synthesis of the C-strand, either during semi-conservative replication, or fill-in synthesis after telomerase extension of the G-strand.

Furthermore, catalytic deficient alleles of Pol-α have increased telomeric single-stranded DNA (Carson and Hartwell, 1985; Adams and Holm, 1996; Adams-Martin *et al*, 2000). The conventional interpretation of this phenotype has been that the ssDNA results from a failure to replicate the telomeric C-strand. Previous work from our lab revealed that these catalytically compromised Pol-α alleles have a synthetic interaction when combined with capping deficient *ten1* mutants (Xu *et al*, 2009). Additionally, *pol1* mutants which have reduced Cdc13 interaction are synthetic lethal in combination with these *ten1* alleles (Xu, 2009). These findings imply that Pol-α may contribute to telomere capping, or conversely, Ten1 may promote end replication. It is also possible that the synthetic lethality of these double mutants is an indirect consequence of disrupting two unrelated processes; however, given the established mechanistic links between Pol-α and the CST complex, it is much more likely that a single, essential function is being compromised in these strains.

Additional evidence supporting a mechanistic coupling of telomere capping and replication comes from *CDC13* bypass experiments. Simultaneous overexpression of the N-terminus of *STN1* along with full-length *TEN1* can bypass the essential capping

function of *CDC13* (Petreaca *et al*, 2006). However, this bypass pathway requires interaction between Stn1 and Pol12. These findings imply that either Pol12 has a direct role in telomere capping, or the interaction between Pol-α and Stn1/Ten1 during replication promotes their capping function. Both of these models point to a connection between telomere capping and replication.

These observations led us to hypothesize that interactions between the CST complex and Pol-α contribute to both telomere capping and length regulation. Because these two processes are related and require both CST and Pol-α function, we predict that disrupting interactions between these two complexes would cause defects in both telomere capping and replication. To probe the functional significance of the interactions between Pol-α and CST and the individual members within the CST complex, we utilized various alleles that have been proposed disrupt or weaken binding. The specific mutations we used were *pol12-40* to disrupt the Pol12-Stn1 interaction (Chiu, 2007), *cdc13-5* to disrupt the Cdc13-Stn1 interaction (Chandra *et al*, 2001), and *cdc13-50* to disrupt the Cdc13-Pol1 interaction (Qi and Zakian 2000). Our analysis reveals that although the *cdc13-5 pol12-40* double mutant has extremely high levels of telomeric ssDNA, the *cdc13-50 pol12-40* does not. This suggests that the *cdc13-50 pol12-40* mutant is largely competent for both telomere capping and replication. Given that both known Pol-α CST interactions have been compromised in this strain, this result was unexpected. These findings suggests that in addition to the Pol1-Cdc13 and Pol12-Stn1 association, there may be other interactions between components of the CST complex and Pol-α.

Our lab has in fact observed that Ten1 can co-immunoprecipitate with Pol1 (Xu, 2009). Here, we show Ten1 from yeast cell extracts can also associate with recombinant Pol12 produced from bacterial cells. However, this interaction appears to be indirect, since we fail to detect binding between bacterially expressed Ten1 and Pol12. In any case, this finding reinforces the notion that the CST complex and Pol-α interface via multiple points of contact, to modulate the interplay between telomere capping and replication. Although this model has been widely accepted within the telomere capping and replication fields, one of the significant unanswered questions that remains is whether CST is in fact a rigid complex that always functions as a heterotrimer, or do the individual components make independent contributions to telomere capping and replication? Our previously published *CDC13* bypass and *STN1* overexpression studies suggest that under some conditions, the individual members of CST can function autonomously. This led us to ask what is the contribution of each CST component, to both telomere capping and end replication.

The roles of Cdc13 and Stn1 it telomere maintenance have been characterized in much greater detail than that of Ten1. To ascertain Ten1's contribution to telomere capping and replication, Ling Xu generated several temperature sensitive alleles (Xu *et al*, 2009). Here, we utilize these reagents to explore which genetic pathways contribute to the telomere lengthening phenotype of *ten1* mutants. We show that there is no direct correlation between telomere length maintenance and temperature sensitivity. This finding suggests that Ten1 makes multiple independent contributions to telomere capping and replication. We will discuss the implications of these findings.

Results

The *pol12-40* mutant can heal a critically short telomere

Previous work from our lab identified a hypomorphic allele of *POL12*, *pol12-40*, which has a weakened Stn1 interaction. Phoebe Chiu has shown that recombinant pol12-40 expressed in *E. coli* pulls down the $Stn1^{1-186}$ protein from yeast lysates much less efficiently than wild type Pol12 (Chiu, 2007). Furthermore, *pol12-40* mutants display telomere elongation, and synthetic lethality in combination with *stn1* and *ten1* mutants, indicating that both Pol12's telomere length regulation and capping functions are compromised (Chiu, 2007; Xu, 2009). However, it is not known if the Pol12-Stn1 interaction is required for fill-in synthesis after telomerase elongates a critically short telomere. To answer this question, we utilized the *de novo* telomere addition assay (Diede and Gottschling, 1999). In this experiment, cells are arrested in G2 and a double stranded break is induced adjacent to a short telomeric seed, which can serve as a substrate for telomere elongation. This allows us to determine both the kinetics and extent of telomere elongation. The advantage of this assay is that since cells are arrested in G2, telomere extension can be studied as a separate event from semi-conservative replication. However, one important caveat to consider is that the extended product is a DNA break, and not a natural chromosome end.

We performed a telomere healing assay in the wild type and *pol12-40* mutant strains. The results show that both strains are able to extend the telomeric seed with comparable kinetics, and to a similar extent (Figure 3-1). We observe very efficient cutting of the locus in both strains, with nearly complete disappearance of the "pre-HO

cut" band at the 1 hour time point and a corresponding appearance of the "HO cut" band. We also see efficient healing of the telomeric seed starting at 3 hours, and increasing at the 4 hour time point in both strains. These results suggest that partially crippling the Pol12-Stn1 interaction does not affect for *de novo* telomere elongation.

Synthetic interaction between *cdc13 pol12* double mutants

After learning that the *pol12-40* mutant can heal a critically short telomere, we considered the possibility that multiple redundant interactions between CST and Pol-α contribute to efficient telomere length regulation and capping. To examine this hypothesis, we attempted to combine the *pol12-40* mutation with mutant alleles of the CST complex that weaken or eliminate interaction within the complex, or with Pol-α. All tested *pol12 stn1* and *pol12 ten1* double mutants displayed a synthetic lethal interaction, suggesting that these combinations had severe telomere capping defects (Chiu, 2007; Xu, 2009). Interestingly, all tested *cdc13* mutants were viable in combination with *pol12-40*.

We chose to characterize two specific *CDC13* alleles, *cdc13-5* and *cdc13-50*, which have significantly reduced interaction with Stn1 and Pol1, respectively (Chandra *et al*, 2001; Qi and Zakian 2000). We first tested for synthetic interaction in the *cdc13 pol12* double mutants. Cultures were grown to saturation at 30°C in YPD, then stamped onto plates and incubated at the indicated temperatures, or at 30°C with increasing concentrations of HU. The results show that the *cdc13-5 pol12-40* strain is both temperature sensitive and HU sensitive, but the *cdc13-50 pol12-40* strain has no synthetic interaction (Figure 3-2). The *pol12-40* single mutant does have a mild growth defect at

36°C, but the *cdc13-50* mutation does not exacerbate this phenotype. In contrast, the *cdc13-5 pol12-40* mutant shows a severe growth defect at 33°C, and dies at 36°C. This double mutant combination also show very weak growth on 50mM HU, and dies at 75mM, whereas the *cdc13-50 pol12-40* double mutant and all single mutants grow equivalent to wild type strains on all tested concentrations. These observations imply that cell can tolerate the disruption of multiple interactions between the CST and Pol-α components, but depending on the specific combination of alleles, they do suffer modest growth defects and sensitivity to DNA damaging agents.

Analysis of telomeric length and integrity in *cdc13 pol12* double mutants

The synthetic interaction between *cdc13-5* and *pol12-40* suggests that this mutant potentially has severe telomere maintenance problems, causing sensitivity to elevated temperatures and DNA damaging agents. To explore this possibility, we examined the telomere length and integrity of *cdc13-5 pol12-40* and, as a control, *cdc13-50 pol12-40* strains. To analyze telomere length, strains were propagated by inoculating a starting colony in liquid culture, growing to saturation, then removing small aliquots and re-inoculating into fresh media. This process was repeated for a total of 5 times, thereby allowing us to track changes in telomere length over generation time. The *pol12-40, cdc13-5* and *cdc13-50* single mutants all have elongated telomeres compared to the wild type control, consistent with previous findings (Chiu, 2007; Chandra *et al*, 2001; Qi and Zakian 2000). Interestingly, both *cdc13 pol12* double mutants also have elongated telomeres compared to the wild type, but neither combination shows an additive or

synergistic effect (Figure 3-3). Furthermore, all tested single and double mutants show an increase in telomere length over time, indicating these strains have a defect in a telomere length regulation pathway, rather than a new elongated steady-state length. Although these results show that the *cdc13-5 pol12-40* mutants do have a significant telomere length regulation problem, they are not sufficient to explain the synthetic interaction; the *cdc13-5* single mutant has approximately equivalent telomere length, but shows no temperature or HU sensitivity.

We next examined the structure of telomeres in the *cdc13 pol12* double mutants. Cultures were grown to logarithmic phase, and treated with nocodazole to arrest in G2, or allowed to grow asynchronously, as indicated. Because the *cdc13-5 pol12-40* double mutant is temperature sensitive, some of the cultures were shifted to 36°C transiently to assess if these strains have a temperature dependent increase in telomeric ssDNA. The final concentrations of each sample were equalized. The results show a dramatic increase in the levels of telomeric ssDNA in the *cdc13-5 pol12-40* double mutant, compared to wild type and single mutant control strains (Figure 3-4). We see elevated levels of ssDNA at 30°C, which further increases upon shifting cells to 36°C. We also note that cultures arrested in G2 have lower ssDNA signal than the equivalent asynchronously grown samples. This induction can potentially be attributed to the transient increase in ssDNA during S phase, as DNA is being replicated. However, we cannot exclude the possibility that cell-cycle regulated nucleases, which may be inactive during G2, are responsible for the increased ssDNA signal seen in asynchronous cells. The *cdc13-50 pol12-40* double mutants also show a higher telomeric ssDNA signal compared to the

controls samples, although the levels are significantly lower than in the *cdc13-5 pol12-40* strain. Taken together, these findings suggest that *cdc13 pol12* double mutants have a synergistic telomere capping defect, and the degree of this defect shows considerable allele specificity. Furthermore, we note that the temperature sensitivity of the *cdc13-5 pol12-40* strain correlates with the elevated levels of telomeric ssDNA at high temperatures. These results imply that the temperature sensitivity may be caused by a capping defect. However, the nature of the HU sensitivity in this strain is not currently understood.

Pol12 can associate with Ten1

There are at least two independent direct physical interactions between the CST complex and Pol-α; Cdc13 binds Pol1, and Stn1 binds Pol12 (Qi and Zakian 2000; Petreaca *et al*, 2006). Furthermore, work in our lab has shown that Ten1 can associate with Pol1 in a co-immunoprecipitation experiment, but it is not known if this binding is direct (Xu, 2009). After weakening the two known direct interactions between CST and Pol-α using the *pol12-40 cdc13-50* double mutant combination, we expected to observe a significant increase in telomeric ssDNA. We were surprised to find only a modest telomere length regulation and capping defect (Figures 3-3 and 3-4). Based on these observations, we hypothesized that there may be additional interactions between CST and Pol-α which contribute to the telomere capping and length regulation functions. To examine direct interactions, we decided to produce recombinant proteins from bacterial cells. Our lab has successfully expressed GST-Pol12 from the *E. coli* BL21 strain in the

past (Petreaca *et al*, 2006). We attempted to express recombinant versions of the CST proteins using a variety of different *E. coli* strains, but were only successful in producing FLAG-tagged Ten1 out of the Arctic Express strain (data not shown). This prompted us to test if Ten1 can interact with Pol12.

First, we asked if GST-Pol12 from *E. coli* can pull down FLAG-Ten1 expressed from yeast cells. Yeast cell lysates from FLAG-Ten1 or untagged control cells were incubated with bacterial cell lysates containing GST-Pol12 or GST, and a pulldown experiment was performed. The results indicate that Pol12 can interact with Ten1 expressed from yeast cells (Figure 3-5 A). We then asked if Pol12 can directly bind to Ten1 expressed from bacterial cells. Lysates from the Arctic Express strain of *E. coli* expressing recombinant FLAG-Ten1 were incubated with BL21 lysates expressing GST-Pol12 or GST, and a pulldown assay was performed. In this experiment, we fail to see binding between Pol12 and Ten1 (Figure 3-5 B). This may suggest that the interaction between Pol12 and Ten1 is indirect, being mediated through Stn1, Pol1, or Cdc13. However, it is also possible that the recombinant Ten1 expressed from bacteria is not completely functional, or requires post-translational modifications to associate with Pol12. Even if Ten1 does not directly associate with Pol12, it may do so via Pol1, providing a third physical contact between CST and Pol-α. Currently, we cannot conclusively establish whether Cdc13-Pol1 and Stn1-Pol12 binding are the only direct contacts between the CST complex and Pol-α, or if there are additional contributing interactions.

ten1 mutants fail to interact with Stn1 and Cdc13 in yeast two hybrid assay

The contribution of Ten1 to telomere capping and replication is the least characterized among the components of the CST complex. In the course of investigating the roles of the CST complex and Pol-α in telomere maintenance, Ling Xu used random PCR mutagenesis to generate four conditional *ten1* alleles (*ten1-101*, *ten1-103*, *ten1-105* and *ten1-106*). All four alleles have severely elongated telomeres with excessive ssDNA, suggesting that both the telomere capping and length regulation functions of Ten1 are compromised (Xu *et al*, 2009). This led us to ask if these hypomorphic *ten1* alleles are compromised for the ability to bind to Stn1 or Cdc13. We used the yeast two hybrid assay to test for interactions at both permissive and non-permissive temperatures. The results show that only the *ten1-105* mutant can interact with Stn1, at both permissive and restrictive temperatures (Figure 3-6 A). This was done in duplicate, using two independently transformed strains to confirm the reproducibility of the interaction. The three other *ten1* mutants fail to interact with Stn1 even at their permissive temperature. Furthermore, none of the *ten1* mutants showed detectable interaction with Cdc13 at any temperature (Figure 3-6 B). This finding implies that the interactions between Ten1-Cdc13 and Ten-Stn1 are not required for viability; however, they are critical for Ten1's telomere capping and length regulation functions.

Telomere length analysis of *ten1* mutants overproducing Stn1

Because the *ten1* loss of function mutants have reduced interaction with Stn1 and Cdc13, we asked if overproduction of these proteins could suppress the telomeric defects

of these mutants. Ling Xu found that while *CDC13* overexpression is toxic, *STN1* overexpression can suppress the temperature sensitivity of three out of four *ten1* mutants. The *ten1-101* and *ten1-103* mutants grew significantly better with increased Stn1 dosage, while the *ten1-105* mutant showed slight improvement in growth at elevated temperatures (Xu, 2009). This prompted us to examine if Stn1 overproduction can also suppress the severe telomere elongation phenotype of these *ten1* mutants. We overexpressed *STN1* off of high copy 2μ plasmids, using two different promoters: the constitutively active *ADH* promoter, and the galactose inducible *GAL* promoter. The results show a significant reduction in telomere length for the *ten1-101* and *ten1-103* mutants overexpressing *ADH-STN1*, and a modest reduction with *GAL-STN1* (Figure 3-7). The *ten1-105* mutant also has slightly shorter telomeres when Stn1 is overproduced using either the *ADH* or *GAL* promoter. These results directly correlate with the suppression of temperature sensitivity; the degree to which *STN1* suppresses temperature sensitivity is proportional to the reduction in telomere length.

The *ten1-105* mutant can neither heal a critically short telomere, nor protect it against nucleolytic degradation

To further probe the role of Ten1 in telomere replication and capping, we performed a telomere healing experiment using the *ten1-105* mutant. Previously, Ling Xu found that this allele cannot extend a critically short telomere at the non-permissive temperature of 36°C (Xu *et al*, 2009). Here, we also analyzed the ability of the *ten1-105* mutant elongate a critically short telomere, and simultaneously tested its ability to block

the end against exonucleolytic degradation, utilizing a plating approach. This method tracks the presence of two nutritional markers flanking the extendible telomere seed (Figure 3-8 A). The advantage of this strategy is that it allows monitoring of cutting efficiency, healing ability, and capping ability in one experiment. After induction of the HO cut, a calculated number of cells are initially plated on -Ade media at various time points. Then, after emergence of colonies, cells are replica-plated onto -Lys media and allowed to grow. The cutting efficiency can be determined by calculating the percentage of Ade^+ Lys^- colonies at each time point, while the ability to heal and prevent degradation can be ascertained by comparing the number of Ade^+ colonies at each time point to the number of Ade^+ colonies at the 0 time point. The results show that both *TEN1* and *ten1-105* cells are able to efficiently induce cutting of the HO locus at both 23°C and 36°C (Figure 3-8 B and C). Furthermore, both strains are able to protect and heal the short telomere seed at 23°C, as evidenced by the relatively high percent of Ade^+ colonies at the later time points. Conversely, the *ten1-105* mutant has a very low percent of Ade^+ colonies after cutting at 36°C, indicating that this strain is unable to both heal the telomere seed, and protect it against degradation.

To confirm that the *ten1-105* mutant cannot protect a critically short telomere against exonucleolytic degradation, we performed a duplex specific nuclease (DSN) digestion assay. The DSN enzyme displays very specific nuclease activity against duplex DNA, but virtually none against ssDNA (Figure 3-9 A and B). For these experiments, we induced an HO cut near the telomeric seed, collected samples at various time points, and isolated whole chromosomal DNA. The DNA was subjected to DSN digestion, followed

by dot blotting and probing against the *ADE2* locus (Figure 3-9 C) . Thus, if the *ten1-105* mutant cannot protect the telomeric seed, it will be resected, resulting in a single-stranded DNA molecule that is be resistant to DSN digestion. When we performed this experiment at 36°C, we find that the *ten1-105* strain retains high levels of DSN resistant *ADE2* DNA after inducing the HO cut, but the same locus is sensitive to DSN digestion in the control *TEN1* strain (Figure 3-9 D). In both strains, very weak signal is seen prior to HO induction, indicating that the *ADE2* locus is double-stranded prior to cutting. Based on these results, we conclude that at elevated temperatures the *ten1-105* is unable to prevent exonucleolytic degradation at a short telomeric seed.

Analysis of integrated *ten1-101* and *ten1-105* mutants

One caveat with our characterization of the hypomorphic *ten1* mutations is that up to this point, all experiments were conducted using a plasmid borne copies of the alleles covering the deletion of the endogenous *TEN1* gene. This may be problematic, as there can be selective pressure for cells to maintain multiple copies of the plasmid. This could potentially skew some of our results, leading to misinterpretation of the data. To circumvent this problem, we decided to integrate the *ten1-101* and *ten1-105* alleles. We cloned both mutant genes into an integrating vector, and targeted the construct to the native *TEN1* locus. We specifically used a strain in which the endogenous *TEN1* gene was replaced with *KanMX2*, and kept alive with a wild type copy of *TEN1* on a *URA3* marked plasmid, to facilitate screening for correct integrants. Using this approach, we

were able to successfully identify multiple correct integrants for both the *ten1-101* and *ten1-105* alleles.

After successful integration of the mutant *ten1* genes, we characterized their viability, temperature sensitivity, and telomere length. The integrants were struck out on 5-FOA plates to force loss of the covering wild type *TEN1* plasmid. After incubating plates at 23°C for 4 days, multiple viable colonies were observed, indicating that the integrated *ten1-101* and *ten1-105* mutants can complement the essential function of *TEN1* (data not shown). We next tested the temperature sensitivity of the integrated *ten1* mutants. Strains were grown to saturation, stamped onto YPD plates, and incubated at the indicated temperatures for 3-4 days. The results show that both integrated *ten1* mutants are temperature sensitive to approximately the same degree as strains carrying the mutant alleles on plasmids (Figure 3-10 A). Furthermore, integrants harboring a wild type copy of *TEN1* on a plasmid are able to grow at the elevated temperatures, confirming that the *ten1* temperature sensitivity is recessive.

We then analyzed the telomere length of the integrated *ten1* mutants. For each allele, two integrants were selected and struck out on 5-FOA to force loss of the covering plasmid. Then, two colonies from the 5-FOA plate, along with the parent, were subjected to telomere length analysis. The results reveal that both *ten1-101* and *ten1-105* integrants have elongated telomeres, and this phenotype is recessive to *TEN1* (Figure 3-10 B). We noticed that the telomere length of integrated strains is not as extremely elongated as the plasmid borne alleles, especially for the *ten1-101* mutant. However, this may be attributed to differential generation time; the telomeres of *ten1* mutants have been shown

to become longer as strains are propagated (Xu *et al*, 2009). From these results, we conclude that the integrated *ten1* mutants have the same phenotype as strains carrying the plasmid borne alleles.

Telomere length analysis of *ten1 rad9* and *ten1 exo1* double mutants

In the course of characterizing the *ten1* loss of function mutants, Ling Xu generated various double mutant combinations, testing for either suppression or enhancement of temperature sensitivity. From this analysis, she found that *exo1-Δ* can suppress all four ten1 mutants, while *rad9-Δ* suppresses three of the mutants, but has a synthetic interaction with *ten1-106* (Xu *et al*, 2009; Xu, 2009). Intriguingly, the *ten1 rad9* double mutants have a very low plating initial plating efficiency compared to the *ten1* single mutants, implying that the double mutants are in fact worse off than the singles (Xu *et al*, 2009). However, the arising colonies appear to be healthier, suggesting that they have undergone genomic rearrangements due to the selective pressure. We performed Southern blots to analyze the length, and indirectly, the structure of the telomeres in these strains. We hypothesized that because these double mutants are able to grow better at elevated temperatures, their telomeres should be shorter, and contain less single-stranded DNA than the *ten1* single mutants. The double mutants initially had a covering *TEN1* plasmid, which was shuffled out on 5-FOA. Changes in telomere length were monitored over time by serial propagation from these starting colonies. The results indicate that the *ten1 rad9* double mutants do have a modest suppression of the telomere elongation phenotype (Figure 3-11). The *ten1-106 rad9-Δ* combination has the longest

telomeres, which correlates with this mutant being the most temperature sensitive. The results from the *rad9* analysis demonstrate that the suppression of the temperature sensitivity correlates with a reduction in the severe telomere elongation phenotype of the *ten1* mutants. However, it is unlikely that the elongated telomeres are the root cause of the temperature sensitivity. We favor the model where these *ten1* mutants have sub-lethal levels of telomeric ssDNA, which activates a Rad9 dependent arrest. Thus, deletion of *RAD9* suppresses the temperature sensitivity by allowing these strains to divide and grow with sub-lethal levels of telomeric ssDNA, as has been previously reported for the *cdc13-1* mutant (Garvik *et al*, 1995). Thus, the reduction in telomere length in the *ten1 rad9* double mutants appears to be unrelated to the suppression of temperature sensitivity. In support of this model, we found that although deletion of *exo1* improves the viability of the *ten1* mutants, it does not suppress their telomere length phenotype (Figure 3-12). We hypothesize that *exo1* deletion partially suppresses the capping defect of the *ten1* mutants, thereby alleviating their temperature sensitivity without effecting telomere length. We will need to analyze the levels of telomeric ssDNA in these mutants to test this hypothesis.

Discussion

Previous work from our lab and others has shown that mutations within the CST complex are often synthetic lethal in combination with Pol-α mutations. The *pol12-40* mutation in particular was found to be lethal in combination with all tested *stn1* and *ten1* loss of function alleles (Chiu 2007, Xu 2009). We show here that *pol12-40 cdc13* double mutants are viable. We observed no additive or synergistic capping defect when *pol12-40* is combined with *cdc13-1*, nor an enhanced rate of senescence in combination with the *cdc13-2* mutation (data not shown). We also fail to see an additive or synergistic telomere length phenotype in combination with either *cdc13-5* or *cdc13-50* double mutants. However, we did find that the *cdc13-5 pol12-40* double mutant does have abnormally high levels of telomeric ssDNA, especially at elevated temperatures, and displays both temperature and HU sensitivity. Whether all of these phenotypes are directly related to each other is currently unknown. The temperature sensitivity may result from a severe capping defect. We speculate that at lower temperatures, there is enough Pol12 and Cdc13 function to overcome is capping deficiency to maintain cell viability; however, at elevated temperatures, the level of degradation may become intolerable, affecting essential genes upstream of the telomeric and subtelomeric sequences, and thus leading to lethality. Such a pattern is precisely what has been reported for capping deficient *ten1* alleles (Xu *et al*, 2009).

Why is the *cdc13-5 pol12-40* mutant sensitive to HU? We can envision two distinct models to account for this phenotype. In the first scenario, Cdc13 and Pol12 are required for recovery from HU induced replication stress throughout the genome. In the

second scenario, Cdc13 and Pol12 function specifically at telomeres to facilitate their replication. The presence of telomeric ssDNA in the *cdc13-5 pol12-40* double mutant might not arise exclusively from exonucleolytic degradation, but may be, at least in part, attributed to incomplete replication. Further experiments are needed to test this hypothesis. If the telomeric ssDNA is a result of replication problems in this strain, it may also explain the HU sensitivity, potentially providing a mechanistic link between all three phenotypes. However, it would still fail to discriminate between the two models described above. We would need to probe for the presence of non-telomeric ssDNA to make any conclusions about the extent of Cdc13 Pol12 function.

What is the role of *POl12* in telomere maintenance? The hypomorphic *pol12-40* mutant can provide some clues. The synthetic lethality of *stn1 pol12* has previously been interpreted as evidence for a telomere capping function of Pol12 (Grossi *et al*, 2004). Our data shows that the *pol12-40* mutant does not have increased telomeric ssDNA, consistent with previous observations (Chiu, 2007). This suggests that either *POL12* does not have an active role in capping telomeres against exonucleolytic degradation, or this function is not perturbed in the *pol12-40* mutant background. Is *POL12* required for fill-in synthesis of the C-strand after telomerase dependent extension? Our results indicate that *pol12-40* mutants are able to efficiently extend a critically short telomere with kinetics comparable to wild type cells, likely ruling out a fill-in synthesis defect. However, a caveat with this interpretation is that this experiment does not look at extension of a natural chromosome end; the extendible substrate is generated via double

strand break induction near a telomeric "seed". Thus, we cannot formally exclude the possibility that Pol12 has a role in C-strand fill-in synthesis after telomerase extension.

How does Pol12 function in telomere C-strand synthesis? It may do so by mediating interactions between the Pol-α primase complex and CST. Although Cdc13 and Pol1 have been shown to interact directly, it is not known whether this interaction is required to recruit Pol-α to the telomere (Qi and Zakian, 2000). The Cdc13-Pol1 interaction may simply stabilize Pol-α's association with the chromosome end after recruitment via Stn1-Pol12. It is also possible that Pol1 and Cdc13 first form a sub-complex elsewhere, which gets recruited to telomeres via interactions with Stn1-Pol12.

Are the Stn1-Pol12 and Cdc13-Pol1 interactions the only direct contacts between CST and Pol-α? We've shown here that bacterially produced Pol12 can associate with Ten1 from yeast lysate, but fails to bind Ten1 expressed from *e. coli* cells. This suggests that the Pol12-Ten1 interaction is indirect; however, it is possible that their association requires post-translational modifications, or bacterially expressed Ten1 cannot fold properly, or is unstable. Currently, we cannot conclusively determined if Pol12 and Ten1 directly bind, or if they associate indirectly via an intermediate bridging factor. An intriguing possibility is that the Pol12-Ten1 association is mediated via Pol1. Our lab has previously observed that Ten1 can co-immunoprecipitate with Pol1 (Xu, 2009). Thus, it is possible that Ten1-Pol1 or Ten1-Pol12 association represents a third direct contact between CST and Pol-α.

What is *TEN1*'s role in telomere maintenance? Initially, *TEN1* was identified as a dosage suppressor of *STN1*, and found to interact with Cdc13 and Stn1 via yeast two

hybrid analysis (Grandin *et al*, 2001). This led to the hypothesis that Ten1 functions as part of a complex with Cdc13 and Stn1 to cap telomeres. Our lab has also shown that loss of function *ten1* mutants display temperature sensitivity, and have extremely elongated, single-stranded telomeres (Xu *et al*, 2009). This indicates that *TEN1* functions in both telomere capping and length regulation, just as *CDC13* and *STN1* (Garvik *et al*, 1995; Grandin *et al*, 1997; Qi and Zakian, 2000; Chandra *et al*, 2001; Grossi *et al, 2004;* Petreaca *et al*, 2007). These findings are consistent with a model in which Cdc13, Stn1 and Ten1 function together as a single complex to cap telomeres, as well as coordinate telomerase dependent elongation and C-strand synthesis. We show here that all of our hypomorphic *ten1* alleles fail to interact with Cdc13, and three out of four fail to interact with Stn1, as determined by yeast two hybrid analysis. Interestingly, no interaction is detectable even at the permissive temperature, indicating that *TEN1*'s essential function does not require interaction with either Cdc13 or Stn1. This does not necessarily mean that Ten1 caps telomeres in an independent pathway from Cdc13 or Stn1. The *ten1* mutants do in fact have high levels of ssDNA at the permissive temperature (Xu *et al*, 2009). However, this level of damage is not high enough to cause lethality. In addition, increasing *STN1* dosage partially rescues the lethality of *ten1* mutants (Xu *et al*, 2009). Therefore, based on these observations we conclude that although Ten1 Stn1 interaction is not required for viability, these proteins appear to function together as a complex to efficiently cap telomeres.

Is the extreme telomere elongation phenotype of the *ten1* mutants related to their capping defect? Analysis of temperature sensitivity, viability, and telomere length in

various genetic mutant backgrounds initially suggested that these phenotypes are not linked. For example, both *rad9 ten1* and *exo1 ten1* double mutants can survive at higher temperatures that *ten1* single mutants (Xu *et al*, 2009). However, the telomere phenotypes of these strains are drastically different. Whereas deletion of *rad9* suppresses the telomere lengthening phenotype of *ten1* mutants, *exo1* deletion has no affect. One interpretation of this is that the telomere capping and length regulation phenotypes are not mechanistically related. However, an alternative model is that the improved viability and reduced telomeric ssDNA in the *rad9 ten1* double mutants directly leads to the shorter telomeres that we observe. The duplex nature of the chromosome termini allows efficient cutting to relieve the terminal restriction fragment in this strain, leading to the shorter telomeres seen on Southern blots. Thus, it is possible that the telomere capping and length regulation defects in the *ten1* mutants are directly related. Further work must be done to validate this hypothesis.

Materials and Methods

Strains and plasmids

All strains used in this chapter are listed in Table 3-1, and all plasmids used are listed in Table 3-2. Yeast strains were grown and propagated following standard procedures (Sherman, 2002).

Telomere healing assay (Southern blot)

The telomere healing experiments were performed following previously published protocols (Diede and Gottschling, 1999). 250mL cells containing an internal telomeric seed were grown to logarithmic phase in selective media at 30°C. Cultures were then transferred to YP-raffinose media, and arrested in G2 by addition of nocodazole at a final concentration of 15mg/L for 3 hours. Galactose was then added to a final concentration of 3% to induce expression of the HO endonuclease. Cells were harvested at the indicated time points, and DNA was isolated using previously described protocols (Lundblad and Szostak, 1989), with minor modifications. Cells were spheroplasted in Zymolyase solution (0.9M sorbitol, 0.1M EDTA pH 7.6, 28mM BME, 0.3mg/ml Zymolyase 20T) for 1 hour at 37°C. The spheroplasted cells were then resuspended in 0.6mL of TE, to which 120µL of lysis solution (0.25mM EDTA pH8, 0.5M Tris base, 2.5% SDS) was added. Samples were incubated at 65°C for 30 minutes, then 200µL of 5M K-Ac was added, and the lysates were cooled on ice for 1-2 hours. Samples were then centrifuged for 15 minutes at 14,000rpm in 4°C, the supernatant was transferred to a new tube, and 550µL of isopropanol was added to precipitate nucleic acids. Samples were then washed

with 70% ethanol, dried, and resuspended in 0.5mL of TE containing RNase overnight at 37°C. DNA was then re-precipitated with ethanol, resuspended in 50μL of TE, and digested with SpeI (New England BioLabs) at 37°C overnight.

Digested DNA was loaded and run on a large 0.8% agarose gel at 50V for 20 hours. The gel was then transferred to a nylon membrane (Hybond-XL from Amersham) overnight, and DNA was crosslinked with 120mJ of UV light (Stratagene). The membrane was blocked with Church's buffer (1% BSA, 1mM EDTA, 0.5M phosphate buffer, 7% SDS) overnight at 55°C with gentle rocking. Then 25μL of P-32 radiolabeled *ADE2* probe was added, and the blot was incubated overnight at 55°C with gentle rocking. The following day, the blot was washed three times with 1L of washing solution (4x SSC, 0.1% SDS), and exposed to X-ray film for 3 days in -80°C. The film was developed on a developer (Mini-medical).

Telomere length analysis

To analyze telomere length of cells, single colonies from strain of the indicated genotype were inoculated in 10mL of YPD or selective media, and grown to saturation at either 30°C or 23°C for temperature sensitive strains. DNA was isolated using previously described protocols (Lundblad and Szostak, 1989), with minor modifications. Cells were harvested and spheroplasted in Zymolyase solution (0.9M sorbitol, 0.1M EDTA pH 7.6, 28mM BME, 0.3mg/ml Zymolyase 20T) for 1 hour at 37°C. The spheroplasted cells were then resuspended in 0.6mL of TE, to which 120μL of lysis solution (0.25mM EDTA pH8, 0.5M Tris base, 2.5% SDS) was added. Samples were incubated at 65°C for 30 minutes,

then 200μL of 5M K-Ac was added, and the lysates were cooled on ice for 1-2 hours. Samples were then centrifuged for 15 minutes at 14,000rpm in 4°C, the supernatant was transferred to a new tube, and 550μL of isopropanol was added to precipitate nucleic acids. Samples were then washed with 70% ethanol, dried, and resuspended in 0.5mL of TE containing RNase overnight at 37°C. DNA was then re-precipitated with ethanol, resuspended in 40μL of TE, and digested with XhoI (New England BioLabs) at 37°C overnight.

Digested DNA was loaded and run on a large 0.8% agarose gel at 50V for 20 hours. The gel was then transferred to a nylon membrane (Hybond-XL from Amersham) overnight, and DNA was crosslinked with 120mJ of UV light (Stratagene). The membrane was blocked with Church's buffer (1% BSA, 1mM EDTA, 0.5M phosphate buffer, 7% SDS) overnight at 55°C with gentle rocking. Then 25μL of P-32 radiolabeled $TG_{1\text{-}3}/C_{1\text{-}3}A$ probe was added, and the blot was incubated overnight at 55°C with gentle rocking. The following day, the blot was washed three times with 1L of washing solution (4x SSC, 0.1% SDS), and exposed to X-ray film for 2-5 days in -80°C, depending on signal strength. The film was developed on a developer (Mini-medical).

Serial dilution plating assays

Cells of the indicated genotype were inoculated from single colonies grown on selective plates, and incubated for 3 days at 30°C (or 4 days at 23°C for temperature sensitive strains). For each strain, 10-fold serial dilutions from the same initial

concentration of cells were done in a 96-well microtiter dish, and stamped onto appropriate plates. Plates were incubated for 3-4 days at the indicated temperatures.

Telomeric single-stranded DNA analysis

Strains of the indicated genotype were inoculated into YPD or selective media, and grown to logarithmic phase at 30°C. Cultures were then split in two, with one half allowed to grow asynchronously, while the other half was arrested in G2 by addition of nocodazole at a final concentration of 15mg/L for 3 hours. The indicated cultures were then further split in two, with one half grown at 30°C, while the other half was shifted to 36°C for 2 hours. The initial cultures were inoculated in appropriate volumes such that the final volume of each sample was 30mL. After the indicated treatments, cells were harvested and DNA was isolated using previously described protocols (Dionne and Wellinger, 1996), with minor modifications. Cells were lysed in 500µL of NIB buffer (17% glycerol, 50mM MOPS, 150mM K-AC, 2mM $MgCl_2$, 500µM spermidine, 150µM spermine) by bead beating. Lysates were centrifuged for 20 minutes at 9200rpm in 4°C and resuspended in 500µL of TEN buffer (50mM Tris pH8, 50mM EDTA, 100mM NaCl). Sarkosyl was added to a final concentration of 1.5%, and samples were treated with 170µg of proteinase K (Sigma) for 1 hour at 37. DNA was then isolated by phenol/chloroform extraction, precipitated with 95% ethanol, washed with 70% ethanol, dried and resuspended in 100µL of TE.

DNA samples were digested with XhoI (New England BioLabs) at 37°C overnight, then precipitated with isopropanol, washed with 70% ethanol, and resuspended

in 24μL of TE. To each sample, 1μL of P-32 radio-labeled single-stranded $C_{1-3}A$ probe was added. Samples were incubated at 37°C for 2 hours, followed by cooling on ice for 1 hour. DNA was then loaded on a large 0.75% agarose gel, and samples were run out at 22V for 18 hours at room temperature. The gel was then treated with 2x SSC for 30 minutes, dried for 12 minutes per side, wrapped in saran, and exposed to a phosphor-imager screen (Amersham) for 2-5 days, depending on signal strength. After appropriate exposure, the screen was scanned and imaged using a Typhoon Fluorescence Imager (Amersham).

Under the conditions described above, telomeric DNA is kept in its native state, thereby allowing detection of single-stranded DNA. To determine the total telomeric DNA, the same gel was treated with 500mL of denaturing buffer (150mM NaCl, 0.5M NaOH) for 25 minutes at room temperature with gentle shaking, followed by treatment with 500mL of neutralizing buffer (150mM NaCl, 0.5M Tris pH8) for 20 minutes at room temperature with gentle shaking. The gel was then placed in a sealable bag, and immersed in 50mL of hybridization buffer (5x SSC, 1mM Na_2HPO_4, 50μM inorganic pyrophosphate, 5x Denhardts solution, 40nM ATP, 20μg/mL salmon sperm DNA), to which 20μL of P-32 radio-labeled single-stranded $C_{1-3}A$ probe was added. The gel was incubated at 37°C overnight with gentle rocking. The following day, hybridization buffer and probe were removed, and the gel was washed with 500mL of 0.25x SSC 5 times, 30 minutes per wash, with gentle shaking at room temperature. The gel was then wrapped in saran, and exposed to a phosphor-imager screen (Amersham) for 2 days. The screen was scanned and imaged using a Typhoon Fluorescence Imager (Amersham).

GST pulldown assays

To analyze the interaction between Pol12 and Ten1, chemo-competent BL21 *E. coli* cells (Invitrogen) were transformed with plasmid pPC23 encoding GST-Pol12, or pPC20 encoding GST. FLAG-Ten1 was expressed in either yeast cells transformed with plasmid pCN282, or chemo-competent Rosetta *E. coli* cells (Millipore) transformed with plasmid pHG42.

GST-Pol12 or GST expression was induced by inoculating cells into 5mL of LB-Amp liquid media and incubated at 37°C overnight. The following day, the 5mL cultures were added to 100mL of fresh LB-Amp media, and incubated at 37°C until the OD_{600} reached 0.4. IPTG was added to a final concentration of 1mM, and cultures were shifted to 16°C for 4 hours. Cells were pelleted by centrifugation at 14,000rpm for 20 minutes in 4°C, and resuspended in 1.5mL of lysis buffer (50mM KH_2PO_4 pH7.8, 400mM NaCl, 100mM KCl, 10% glycerol, 0.5% Triton X-100, 10mM imidazole). Cells were lysed by three cycles of freezing at -80°C for 20 minutes and thawing at 37°C for 1 minute, followed by 6 pulses of sonication for 10 seconds on medium power (Sonic Dismembrater Model 100 from Fisher Scientific). Lysates were centrifuged for 2 minutes at 14,000rpm in 4°C, supernatants were transferred to new tubes, and the protein concentrations were determined by Bradford assay (Bio-Rad). FLAG-Ten1 expression and preparation of lysates from bacterial cells was performed as described above. Yeast lysates were prepared by harvesting 50mL of logarithmically growing cells, and bead beating cells in 200µL of Buffer A (25mM HEPES pH 7.5, 5mM $MgCl_2$, 50mM KCl, 10% glycerol, 0.5% Triton X-100) supplemented with protease inhibitors (1µg/mL

leupeptin, 2μg/mL aprotinin, 15μg/mL benzamindine, 100μg/mL PMSF, 10μg/mL pepstatin). Samples were centrifuged for 15 minutes at 14,000rpm in 4°C, the supernatant was collected, and the protein concentrations were determined by Bradford assay (Bio-Rad).

500μg of GST or GST-Pol12 were incubated with 20μL of Glutathione Sepharose 4B beads (Amersham) at room temperature for 30 minutes in incubation buffer (20mM HEPES pH7.9, 100mM NaCl, 2.5mM $MgCl_2$, 0.1mM EDTA, 0.05% NP-40, 0.2% Triton X-100). After washing with wash buffer (150mM NaCl, 10% glycerol, 0.1% NP-40, 0.2% Triton X-100), beads were incubated with 500μg of either *E. coli* or yeast cell lysate expressing FLAG-Ten1. Samples were incubated at 4°C for 2 hours with gentle rocking. Beads were then washed twice with 1mL of wash buffer, and 25μL of Laemmli sample buffer (50mM Tris pH6.8, 2% SDS, 10% glycerol, 0.1M DTT, 0.01% bromophenol blue) were added to each sample. The samples were boiled at 95°C for 5 minutes, and run out on a 12% polyacrylamide gel. Proteins were transferred to a nitrocellulose membrane, and Western blots were performed using standard procedures. The primary antibody (mouse anti-FLAG, Sigma) was used at a 1:1,000 dilution in PBS containing 3% non-fat dry milk, while the secondary antibody (HRP-conjugated goat anti-mouse, Chemicon) was used at a 1:10,000 dilution in PBS containing 3% non-fat dry milk. After exposing and developing film, the blot was stripped by treating with 25mL of stripping solution (TBS with 2% SDS, 50mM Tris pH6.8, 100mM BME) for 30 minutes at 50°C, and re-probed for GST. The primary antibody (mouse anti-GST, Pierce) was used at a 1:1,000 dilution in PBS containing 3% non-fat dry milk, while the secondary

antibody (HRP-conjugated goat anti-mouse, Chemicon) was used at a 1:10,000 dilution in PBS containing 3% non-fat dry milk.

Yeast two hybrid experiments

Yeast two hybrid experiments were performed as previously described (James *et al*, 1996). Strain pj69-4a was transformed with the indicated yeast two hybrid plasmids using standard protocols (Gietz and Schiestl, 2007). Cells were inoculated into 5mL of selective media, and incubated for 3 days at 30°C. For each strain, 10-fold serial dilutions from the same initial concentration of cells were done in a 96-well microtiter dish, and stamped onto either control plates (-) or reporter plates (ADE, HIS). Plates were incubated for 3-4 days at the indicated temperatures. Growth on the reporter plates was used as an indicator of physical interaction between the two hybrid-fusion proteins.

Telomere healing assay (plating)

To test telomere healing efficiency by plating, 10mL of cells containing an internal telomeric seed were grown to logarithmic phase in selective media at 23°C. Cultures were then transferred to YP-raffinose media, and arrested in G2 by addition of nocodazole at a final concentration of 15mg/L for 3 hours. Galactose was then added to a final concentration of 3% to induce expression of the HO endonuclease. At the time of the induction, cultures were split into two, with one half shifted to 36°C while the other half was retained at 23°C. At the indicated time points, aliquots were collected, the cell concentrations were determined by hemocytometery. ~500 cells were plated onto -Ade

plates, and incubated at 23°C for 4 days. The colonies were then replica-plated onto -Lys -Ade plates and grown for 3 days at 23°C. The total number of colonies on each plate was counted, and the percentage of Ade^+ Lys^- colonies at each time point was calculated (plotted as lines on graph). This represents the cutting efficiency of the HO enzyme. To determine the "healing" efficiency, the total number of Ade^+ cells at each time point was divided by the number of Ade^+ colonies at time 0 hours (plotted as bars on graph).

Duplex Specific Nuclease (DSN) digestion assay

DSN digestion experiments were performed as previously described (Zhao *et al*, 2009), with minor modifications. First, the cutting efficiency of the DSN enzyme was determined using two methods. (A) 400ng of control template provided by the manufacturer was incubated with 1 unit of enzyme and 1x reaction buffer (Evrogen) at 65°C for 10 minutes. Reactions were then stopped by treating with 2x DSN stop solution (Evrogen), and DNA was run out on a 1% agarose gel. (B) 1μg samples of plasmid pRS415 were either retained as double-stranded molecules under native condition (ds-plasmid), or denatured to single-stranded molecules by addition of NaOH to a final concentration of 200mM, followed by heating at 95°C for 5 minutes (ss-plasmid). Samples were then treated with the indicated amounts of DSN nuclease for 10 minutes at 65°C, followed by inactivation with DSN stop buffer. The digested DNA was then diluted in 200μL of TE, and denatured by addition of NaOH to a final concentration of 400mM and EDTA at 10mM followed by heating at 95°C for 10 minutes. Samples were then cooled on ice for 5 minutes and blotted onto a nylon membrane (Hybond-XL from

Amersham) by dot-blotting. The DNA was crosslinked with 120mJ of UV light (Stratagene). The membrane was blocked with Church's buffer (1% BSA, 1mM EDTA, 0.5M phosphate buffer, 7% SDS) overnight at 55°C with gentle rocking. Then 25μL of P-32 radiolabeled *LEU2* probe was added, and the blot was incubated overnight at 55°C with gentle rocking. The following day, the blot was washed three times with 100mL of washing solution (4x SSC, 0.1% SDS), and exposed to X-ray film for 2 days in -80°C. The film was developed on a developer (Mini-medical).

To analyze the accumulation of ssDNA at a telomeric seed adjacent to an HO-induced double stranded break, 250mL of cells were grown to logarithmic phase in selective media at 23°C. Cultures were then transferred to YP-raffinose media, and arrested in G2 by addition of nocodazole at a final concentration of 15mg/L for 3 hours. Cultures were shifted to 36°C, and galactose was added to a final concentration of 3% to induce expression of the HO endonuclease. 50mL of cells were harvested at the indicated time points, and DNA was isolated using previously described protocols (Lundblad and Szostak, 1989), with minor modifications. Cells were spheroplasted in Zymolyase solution (0.9M sorbitol, 0.1M EDTA pH 7.6, 28mM BME, 0.3mg/ml Zymolyase 20T) for 1 hour at 37°C. The spheroplasted cells were then resuspended in 0.6mL of TE, to which 120μL of lysis solution (0.25mM EDTA pH8, 0.5M Tris base, 2.5% SDS) was added. Samples were incubated at 65°C for 30 minutes, then 200μL of 5M K-Ac was added, and the lysates were cooled on ice for 1-2 hours. Samples were then centrifuged for 15 minutes at 14,000rpm in 4°C, the supernatant was transferred to a new tube, and 550μL of isopropanol was added to precipitate nucleic acids. Samples were then washed

with 70% ethanol, dried, and resuspended in 0.5mL of TE containing RNase overnight at 37°C. DNA was then re-precipitated with ethanol, resuspended in 50μL of TE. 10% of the DNA was saved as an "input" control, and the remainder was digested with DSN and subjected to Southern blot analysis as described above. The probe used was against the *ADE2* locus.

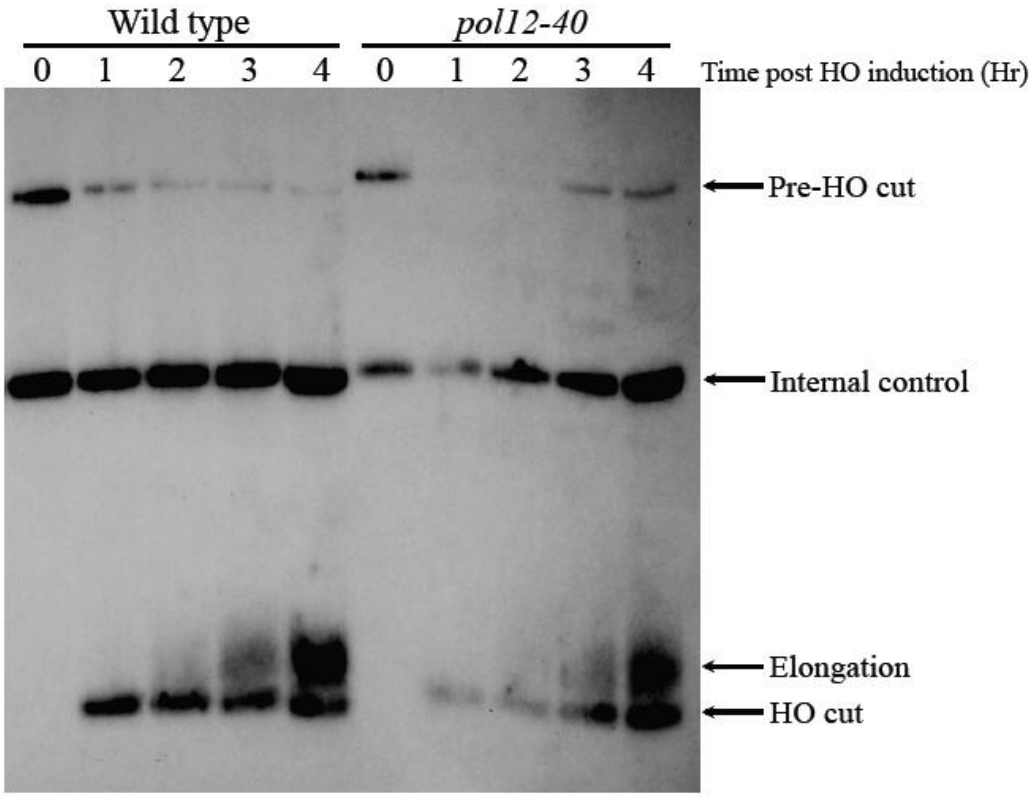

Figure 3-1: The *pol12-40* mutant can heal a critically short telomere

Telomere healing assay was performed with the *pol12-40* mutant strain. Strains were engineered with an short internal telomeric tract adjacent to the HO cleavage sequence, and galactose inducible HO endonuclease. Cells were grown to logarithmic phase in selective media, shifted to YP-raffinose, and arrested in G2. The double strand break was induced by addition of galactose. Cells were collected at the indicated time points, DNA was isolated and separated on an agarose gel. Southern blot was performed probing against the *ADE2* sequence. The *pol12-40* mutant is able to heal the critically short telomere with kinetics comparable to the wild type control. Strains used in this figure: ucc5706 (wild type), hc1931 (*pol12-40*). Plasmids used in this figure: pPC64 (*pol12-40*).

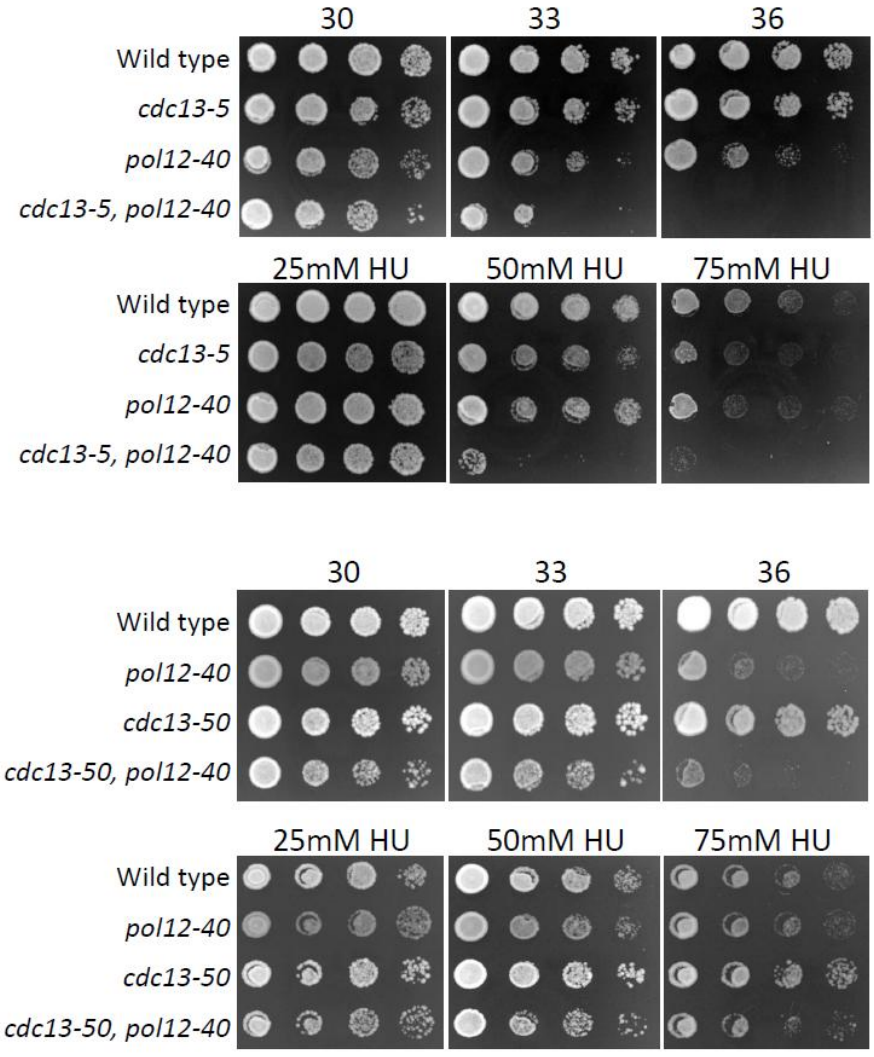

Figure 3-2: *pol12-40* displays allele specific synthetic interactions with various *cdc13* mutants

The *pol12-40* mutant has synthetic interactions with *cdc13-5*, but not with *cdc13-50*; the *cdc13-5 pol12-40* double mutant combination is both temperature sensitive and HU sensitive. Cells were grown to saturation in YPD for 3 days at 30°C, then 10-fold serial dilutions were stamped onto YPD plates or YPD-HU plates. Plates were incubated at the indicated temperatures (30°C for all HU plates) for 3-4 days, then pictures were taken. Strains used in this figure: hc160 (wild type), hc2046 (*cdc13-5*), hc1740 (*pol12-40*), hc2047 (*cdc13-5*, *pol12-40*), hc1781 (*cdc13-50*), hc1779 (*cdc13-50*, *pol12-40*). Plasmids used in this figure: pPC64 (*POL12*), pPC64 (*pol12-40*), pVL1033 (*cdc13-5*), pCN511 (*cdc13-50*).

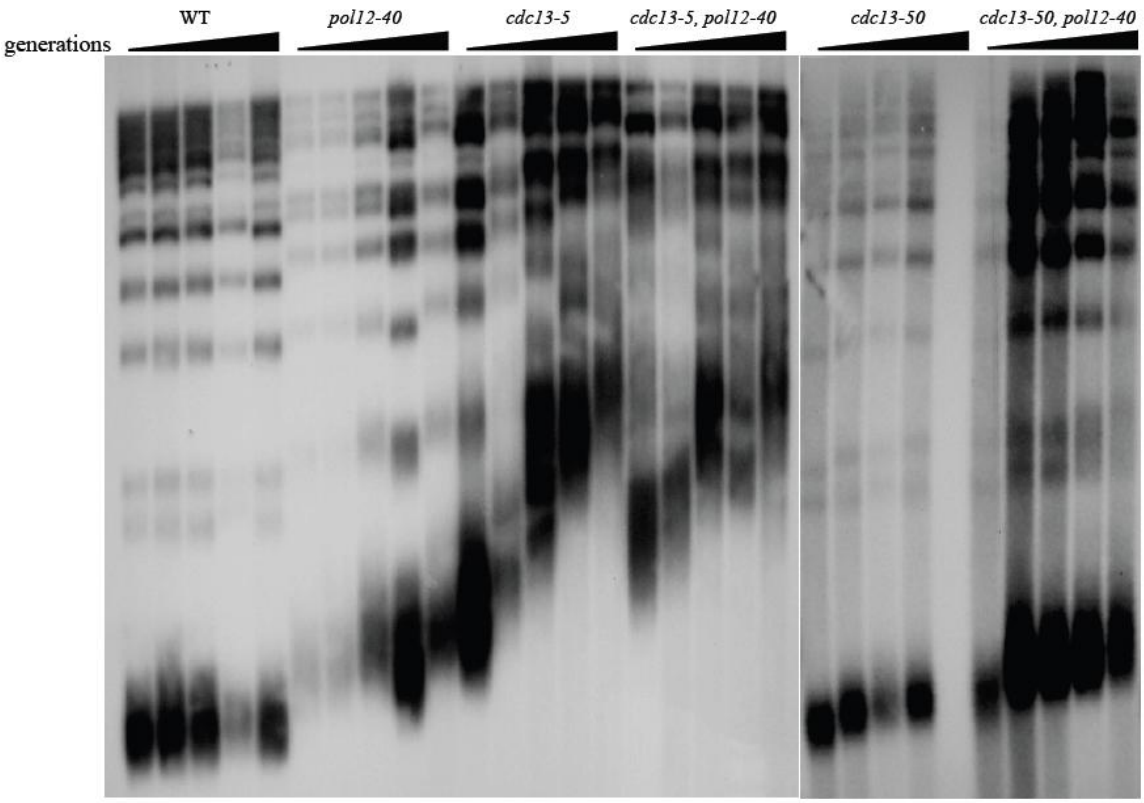

Figure 3-3: *cdc13 pol12-40* double mutants do not have an additive or synergistic telomere elongation phenotype

Telomere length of *pol12 cdc13* double mutants was analyzed by Southern blot. 10mL cultures were grown to saturation in YPD at 30°C for 3 days. 10μL of each saturated culture was then removed and added to 10mL of fresh media, and re-grown to saturation. This process was repeated to yield 5 total cultures from each strain. Each successive re-inoculation results in an increased number of generations of growth from the starting strain, allowing analysis of the dynamics of telomere length regulation over time. For each culture, DNA was isolated, digested, and run on a 0.8% agarose gel. Southern blot was performed probing against telomeric $TG_{1\text{-}3}/C_{1\text{-}3}A$ sequences. The *pol12 cdc13* double mutants do not show an additive or synergistic increase in telomere length compared to single mutants. Strains used in this figure: hc160 (wild type), hc1740 (*pol12-40*), hc2046 (*cdc13-5*), hc2047 (*cdc13-5*, *pol12-40*), hc1781 (*cdc13-50*), hc1779 (*cdc13-50*, *pol12-40*). Plasmids used in this figure: pPC64 (*POL12*), pPC64 (*pol12-40*), pVL1033 (*cdc13-5*), pCN511 (*cdc13-50*).

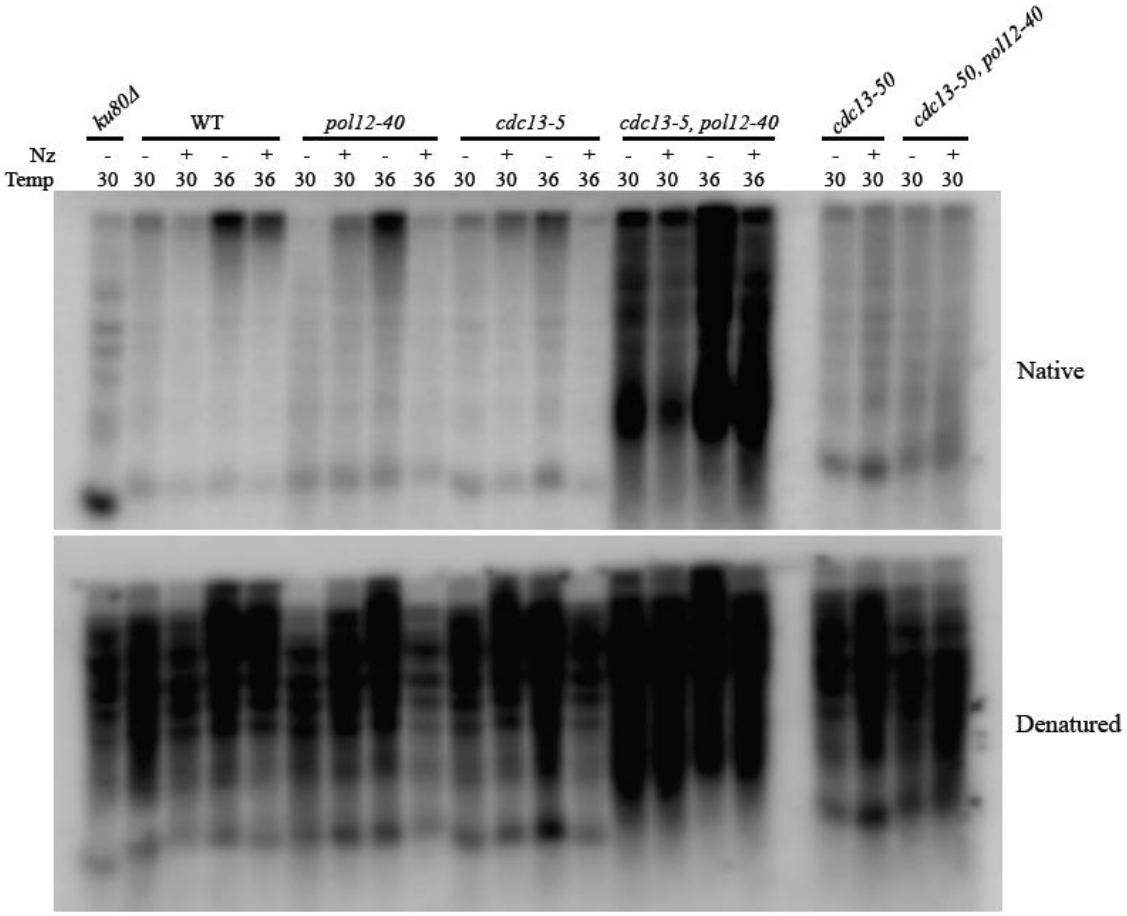

Figure 3-4: The *cdc13-5 pol12-40* double mutant has elevated levels of telomeric single-stranded DNA

The presence of telomeric ssDNA was assessed in *pol12 cdc13* double mutants. Strains were grown to logarithmic phase at 30°C, and either arrested in G2 with nocodazole or allowed to cycle asynchronously as indicated. For the indicated samples, cultures were shifted to 36°C for 2 hours, after which cells were harvested. DNA was isolated, digested, incubated with radiolabeled $C_{1\text{-}3}A$ probe, and run out on a 0.75% agarose gel under native conditions. The gel was dried and exposed to a phosphor-imager screen for 5 days. After developing the "native" image, the gel was denatured and re-probed with $C_{1\text{-}3}A$ probe to quantify the total telomeric DNA in each sample. The *cdc13-5 pol12-40* double mutant has significantly elevated levels of telomeric ssDNA compared to wild type and single mutant controls. Strains used in this figure: hc80 (*yku80-Δ*), hc160 (wild type), hc1740 (*pol12-40*), hc2046 (*cdc13-5*), hc2047 (*cdc13-5*, *pol12-40*), hc1781 (*cdc13-50*), hc1779 (*cdc13-50*, *pol12-40*). Plasmids used in this figure: pPC64 (*POL12*), pPC64 (*pol12-40*), pVL1033 (*cdc13-5*), pCN511 (*cdc13-50*).

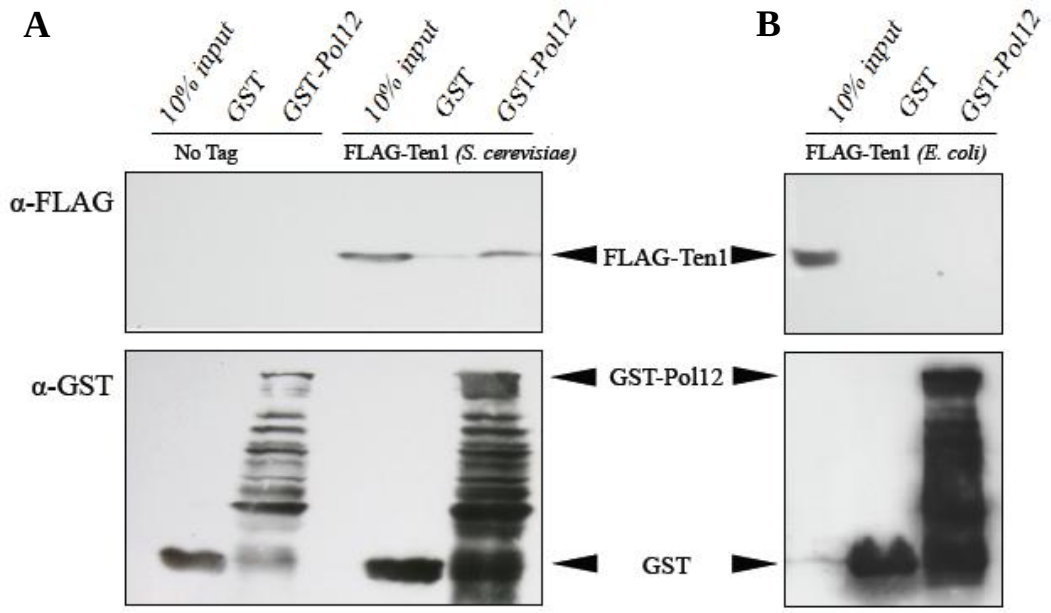

Figure 3-5: Ten1 interacts with Pol12 *in vivo*, but not *in vitro*

The physical interaction between Pol12 and Ten1 was tested through two different means. **(A)** GST-Pol12fusion protein or GST alone expressed from BL21 *E. coli* cells was incubated with yeast cell lysate containing FLAG-Ten1. **(B)** GST-Pol12 fusion protein or GST alone expressed from BL21 *E. coli* cells was incubated with FLAG-Ten1 expressed from Rosetta *E. coli* cells. In both experiments, Pol12 was pulled down with GST beads, and the presence of bound Ten1 was assessed by Western blot. Samples were separated on a 12% polyacrylamide gel, transferred to nylon membrane, and probed with anti-FLAG antibody. The membrane was then stripped and reprobed with anti-GST antibody. Ten1 expressed from yeast cells, but not from bacteria, interacts with Pol12. Strains used in this figure: hc160 (no tag), hc1880 (Flag-Ten1). Plasmids used in this figure: pPC20 (*GST*), pPC23 (*GST-POL12*), pCN282 (*FLAG-TEN1* from *S. cerevisiae*), pHG42 (FLAG-TEN1 from *E. coli*).

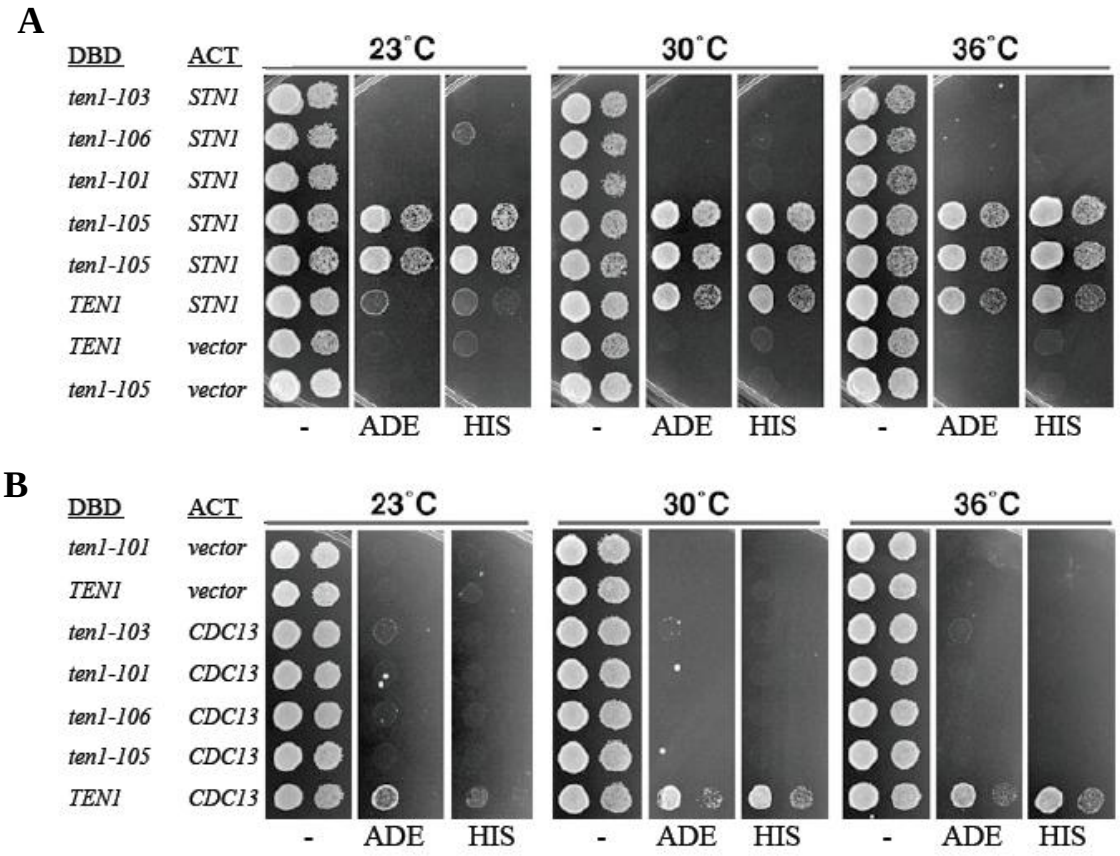

Figure 3-6: Temperature sensitive *ten1* mutants show reduced interaction with Stn1 and Cdc13 in yeast two hybrid assay

The interaction between several temperature sensitive *ten1* mutants was tested with Stn1 and Cdc13 using the yeast two hybrid assay. Plasmids encoding the indicated genes fused to either the DNA binding domain (DBD) or activation domain (AD) of Gal4 were transformed into strain pj69-4A containing the *HIS3*, *ADE2* and *lacZ* reporter genes under transcriptional control from a *GAL* promoter. Cells were grown to saturation in selective media for 4 days at 23°C, then 10-fold serial dilutions were stamped onto control plates (-) and reporter plates (ADE, HIS). Plates were incubated at the indicated temperatures for 3-4 days, then pictures were taken. **(A)** Only the *ten1-105* mutant reproducibly interacts with Stn1. **(B)** All *ten1* mutants show significantly reduced interaction with Cdc13, both at permissive and restrictive temperatures. Strains used in this figure: pj694a. Plasmids used in this figure: pCN124 (*TEN1*), pCN445 (*ten1-101*), pCN452 (*ten1-103*), pCN441 (*ten1-105*), pCN447 (*ten1-106*), pACT2.2 (vector), pCN181 (*STN1*), pVL835 (*CDC13*). Figure reproduced from Xu *et al*, 2009 with permission from the Genetics Society of America.

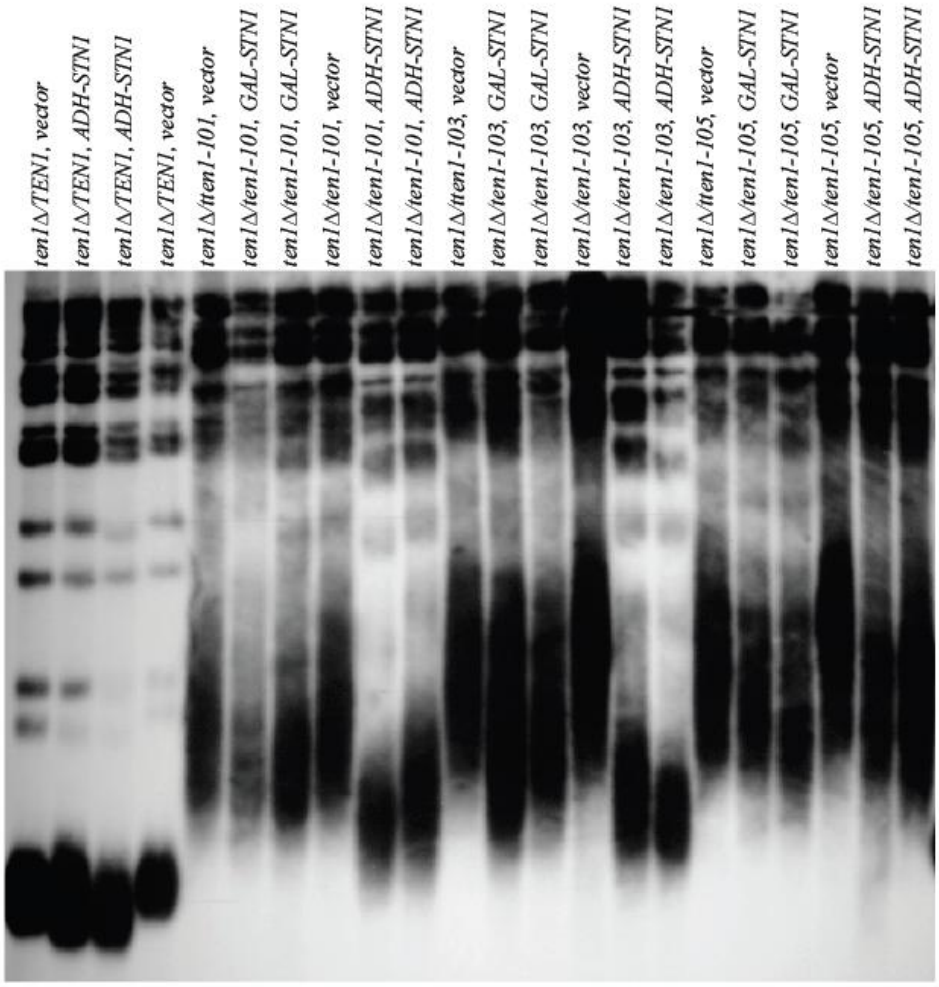

Figure 3-7: *STN1* overexpression partially suppresses the telomere lengthening phenotype of some *ten1* alleles

The telomere length of *ten1* mutants overproducing Stn1 was tested. Strains were transformed with plasmids encoding *STN1* expressed from either the *ADH* or *GAL* promoter, or with equivalent empty vector plasmids. Strains were inoculated into 10mL of selective media, and grown to saturation for 3 days at 30°C. For each culture, DNA was isolated, digested, and run on a 0.8% agarose gel. Southern blot was performed probing against telomeric $TG_{1\text{-}3}/C_{1\text{-}3}A$ sequences. Increasing the *STN1* dosage can partially suppress telomere elongation in the *ten1* mutants, but the effect shows allele specific variability. Strains used in this figure: hc1832 (*ten1*-Δ). Plasmids used in this figure: pCN250 (*TEN1-URA3*), pCN284 (*TEN1-TRP1*), pCN309 (*ten1-101*), pCN311 (*ten1-103*), pCN358 (*ten1-105*), pCN416 (*ADH*-vector), pCN421 (*ADH-STN1*), pVL576 (*GAL*-vector), pVL1051 (*GAL-STN1*).

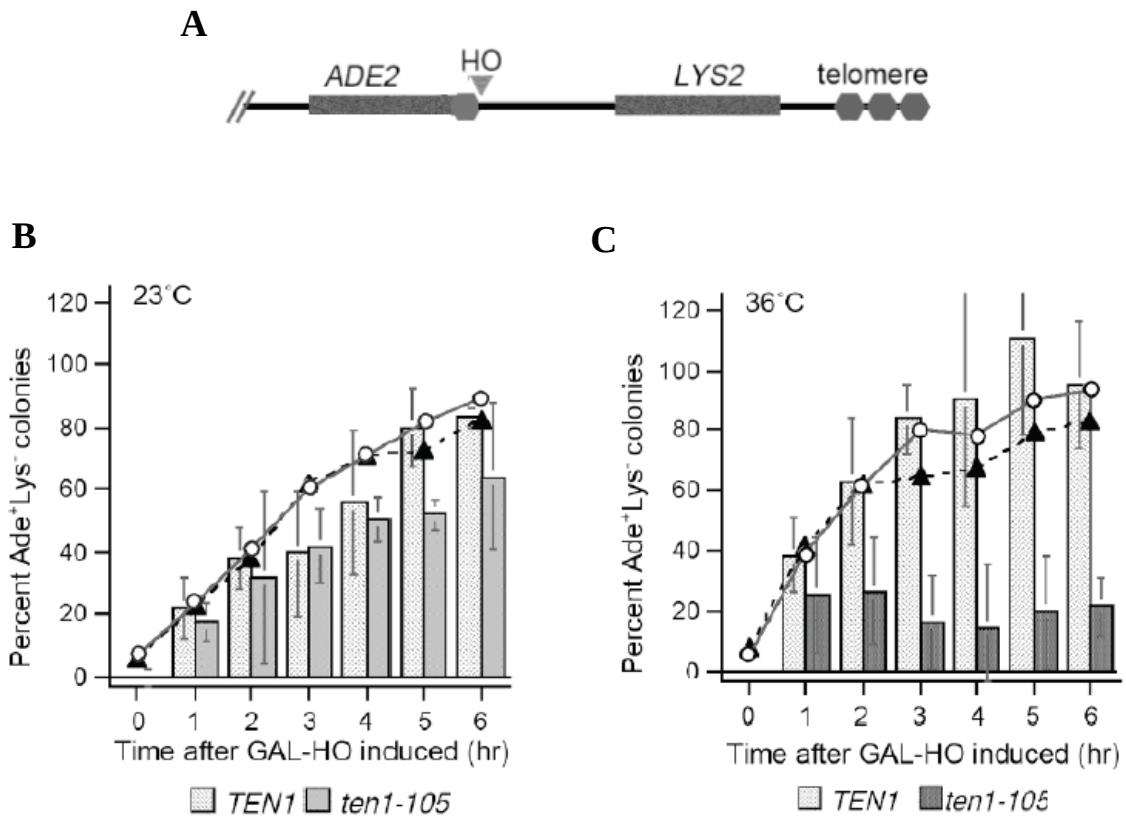

Figure 3-8: The *ten1-105* mutant cannot heal a critically short telomere adjacent to a double-stranded break at high temperatures

The ability of the *ten1-105* mutant to heal a critically short telomere was tested by plating. **(A)** Schematic representation of the chromosome arm containing a short internal telomeric sequence adjacent to a galactose inducible HO cut site. 10mL of cells were grown to logarithmic phase in selective media at 23°C. Cultures were then transferred to YP-raffinose media, and arrested in G2 with nocodazole for 3 hours. Galactose was added to induce expression of the HO endonuclease. At the time of the induction, cultures were split into two, with one half retained at 23°C **(B)** while the other half was shifted to 36°C **(C)**. At the indicated time points ~500 cells were plated onto -Ade plates, and incubated at 23°C for 4 days. The colonies were then replica-plated onto -Lys -Ade plates and grown for 3 days at 23°C. The total number of colonies on each plate was counted, and the percentage of Ade^+ Lys^- colonies at each time point was calculated (plotted as lines on graph). This represents the cutting efficiency of the HO enzyme. To determine the "healing" efficiency, the total number of Ade^+ cells at each time point was divided by the number of Ade^+ colonies at time 0 hours (plotted as bars on graph). Strains used in this figure: hc1943 (*TEN1*), hc1946 (*ten1-105*). Plasmids used in this figure: pCN284 (*TEN1*), pCN358 (*ten1-105*). Figure reproduced from Xu *et al*, 2009 with permission from the Genetics Society of America.

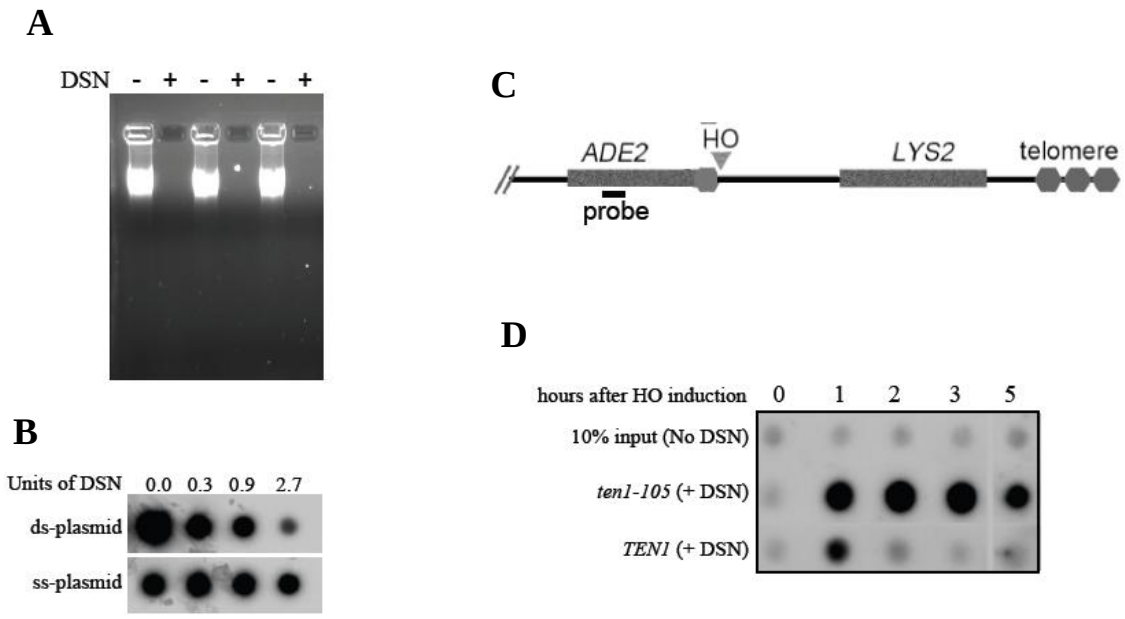

Figure 3-9: The *ten1-105* mutant cannot prevent resection of a critically short telomere adjacent to a double-stranded break at high temperatures

The ability of the *ten1-105* to protect a critically short telomere was assessed using a duplex specific nuclease (DSN). **(A)** Agarose gel showing a double stranded DNA template is sensitive to DSN digestion. **(B)** Southern blot of plasmid in either native conditions (ds-plasmid) or denatured (ss-plasmid) treated with DSN shows that the nuclease is highly specific for digesting only double stranded DNA. **(C)** Schematic representation of the chromosome arm containing a short internal telomeric sequence adjacent to a galactose inducible HO cut site. **(D)** The presence of ssDNA at a telomeric seed adjacent to an HO-induced double stranded break was analyzed with DSN. 250mL of cells were grown to logarithmic phase at 23°C. Cultures were then transferred to YP-raffinose media, and arrested in G2 with nocodazole for 3 hours. Cultures were shifted to 36°C, and galactose was added to induce expression of the HO endonuclease. 50mL of cells were harvested at the indicated time points, and DNA was isolated. 10% of the DNA was saved as an "input" control, and the remainder was digested with DSN. DNA samples were linked to a nylon membrane via dot blotting, then the membrane was subjected to Southern blot analysis. The probe used was against the *ADE2* locus. Strains used in this figure: hc1943 (*TEN1*), hc1946 (*ten1-105*). Plasmids used in this figure: pRS415 (ds/ss-plasmid), pCN284 (*TEN1*), pCN358 (*ten1-105*).

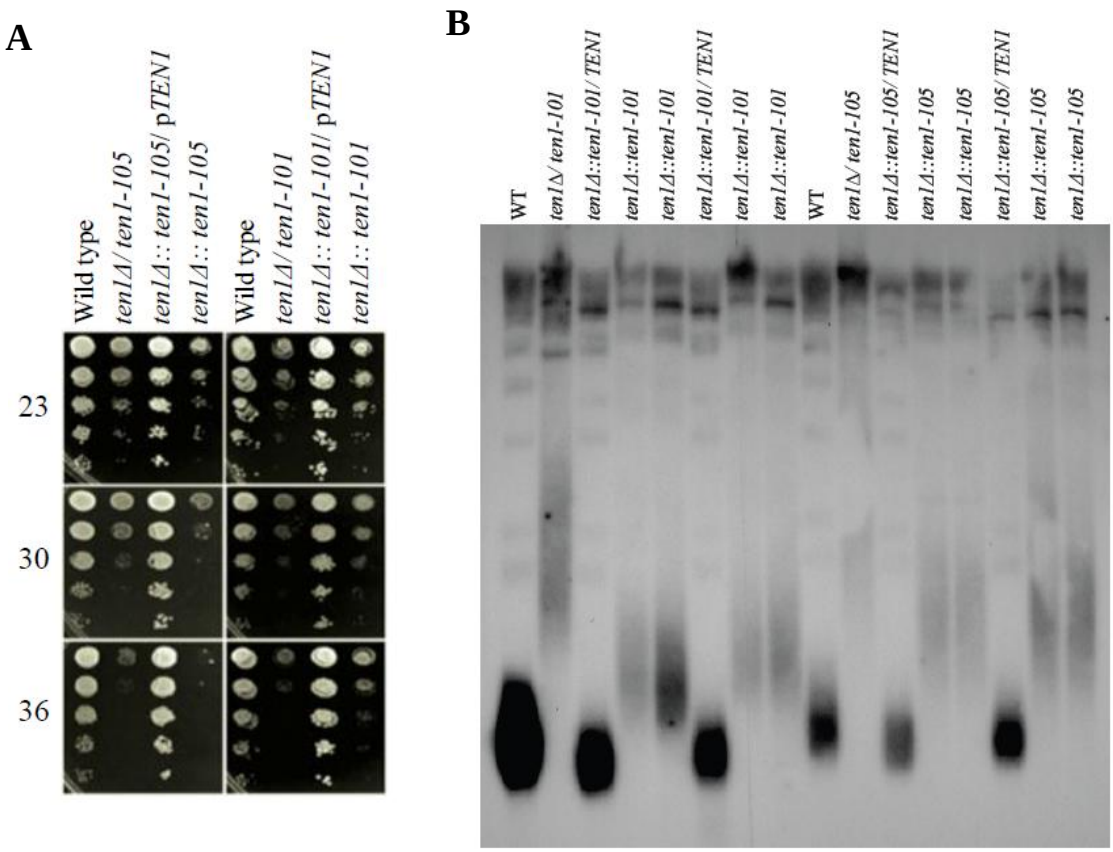

Figure 3-10: Integrated *ten1-101* and *ten1-105* mutants are temperature sensitive and have elongated telomeres

The phenotypes of integrated *ten1-101* and *ten1-105* were examined. Mutant alleles were targeted for integration at native *TEN1* locus in a *ten1*Δ strain, which was kept alive by a wild type copy of *TEN1* expressed from a *URA3* plasmid. After integration, the plasmid was shuffled out on 5-FOA. **(A)** Both integrated *ten1* mutants show temperature sensitivity comparable to strains expressing the mutant alleles from plasmids. **(B)** The telomere length of integrated ten1 mutants was analyzed. Two independent integrants were selected for each allele, and two independent colonies were isolated from the 5-FOA plates. 10mL cultures for each strain grown to saturation in YPD or selective media at 30°C for 3 days. DNA was isolated, digested, and run on a 0.8% agarose gel. Southern blot was performed probing against telomeric $TG_{1\text{-}3}/C_{1\text{-}3}A$ sequences. The integrated *ten1* mutants show telomere elongation comparable to expression of mutants from a plasmid. The telomere elongation phenotype is recessive. Strains used in this figure: hc160 (wild type), hc1832 (*ten1*-Δ), hc2246 (*ten1*-Δ*::ten1-101*), hc2241(*ten1*-Δ*::ten1-105*). Plasmids used in this figure: pCN250 (*TEN1*), pCN309 (*ten1-101*), pCN358 (*ten1-105*), pCN477 (integrating *ten1-101*), pCN476 (integrating *ten1-105*). Figure reproduced from Xu *et al*, 2009 with permission from the Genetics Society of America.

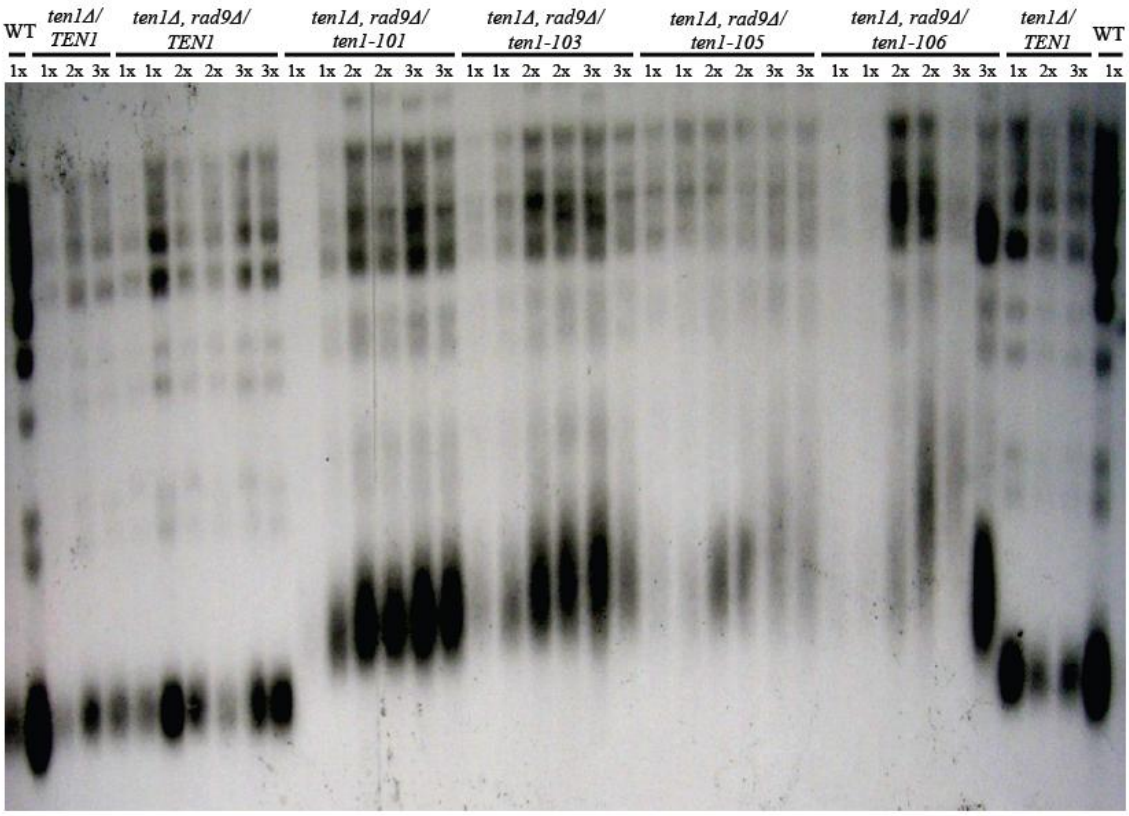

Figure 3-11: Deletion of *rad9* partially suppresses telomere lengthening phenotype of *ten1* mutants

The telomere length of *ten1 rad9* double mutants was tested. A *rad9*-Δ *ten1*-Δ/ p*TEN1* strain was constructed via mating. Mutant *ten1* alleles were transformed into the parental strain, and the plasmid encoding the wild type copy of *TEN1* was shuffled out on 5-FOA. 10mL cultures were grown to saturation in YPD at 30°C for 3 days. 10μL of each saturated culture was then removed and added to 10mL of fresh media, and re-grown to saturation. This process was repeated to yield 3 total cultures from each strain. Each successive re-inoculation results in an increased number of generations of growth from the starting strain, allowing analysis of the dynamics of telomere length regulation over time. For each culture, DNA was isolated, digested, and run on a 0.8% agarose gel. Southern blot was performed probing against telomeric $TG_{1\text{-}3}/C_{1\text{-}3}A$ sequences. Strains used in this figure: hc160 (wild type), hc1832 (*ten1*-Δ), hc1663 (*ten1*-Δ, *rad9*-Δ). Plasmids used in this figure: pCN250 (*TEN1-URA3*), pCN284 (*TEN1-TRP1*), pCN309 (*ten1-101*), pCN311 (*ten1-103*), pCN358 (*ten1-105*), pCN359 (*ten1-106*).

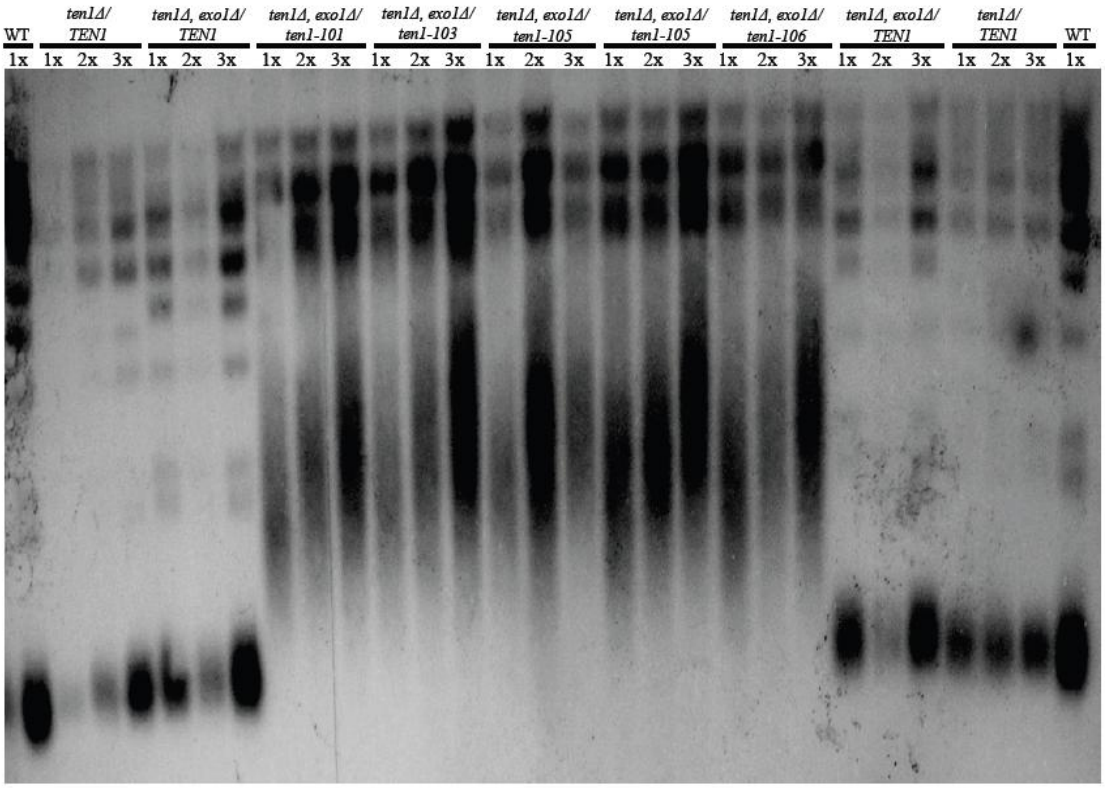

Figure 3-12: *exo1* deletion does not suppress *ten1* telomere length

The telomere length of *ten1 exo1* double mutants was tested. An *exo1*-Δ *ten1*-Δ/ p*TEN1* strain was constructed via mating. Mutant *ten1* alleles were transformed into the parental strain, and the plasmid encoding the wild type copy of *TEN1* was shuffled out on 5-FOA. 10mL cultures were grown to saturation in YPD at 30°C for 3 days. 10μL of each saturated culture was then removed and added to 10mL of fresh media, and re-grown to saturation. This process was repeated to yield 3 total cultures from each strain. Each successive re-inoculation results in an increased number of generations of growth from the starting strain, allowing analysis of the dynamics of telomere length regulation over time. For each culture, DNA was isolated, digested, and run on a 0.8% agarose gel. Southern blot was performed probing against telomeric $TG_{1\text{-}3}/C_{1\text{-}3}A$ sequences. Strains used in this figure: hc160 (wild type), hc1832 (*ten1*-Δ), hc1942 (*ten1*-Δ, *exo1*-Δ). Plasmids used in this figure: pCN250 (*TEN1-URA3*), pCN284 (*TEN1-TRP1*), pCN309 (*ten1-101*), pCN311 (*ten1-103*), pCN358 (*ten1-105*), pCN359 (*ten1-106*).

Table 3-1: List of strains used in chapter 3

Strain	Description	Reference
hc18	*MAT*a *ura3-52 lys2-801 ade2-101 trp1-*Δ*63 his3-*Δ*200 leu2-*Δ*1 CDC13myc($_{18x}$) yku80-*Δ*::KanMX2*	Xu[b]
hc35	*MAT*a *ura3-52 lys2-801 ade2-101 trp1-*Δ*63 his3-*Δ*200 leu2-*Δ*1 stn1-*Δ*::KanMX2/* pVL1046	Petreaca[b]
hc160	*MAT*a *ura3-52 lys2-801 ade2-101 trp1-*Δ*63 his3-*Δ*200 leu2-*Δ*1*	Petreaca[a]
hc1663	*MAT*a *ura3-52 lys2-801 ade2-101 trp1-*Δ*63 his3-*Δ*200 leu2-*Δ*1 rad9-*Δ*::HIS3 ten1-*Δ*::KanMX2/* pCN250	Xu[a]
hc1740	*MAT*a *ura3-52 lys2-801 ade2-101 trp1-*Δ*63 his3-*Δ*200 leu2-*Δ*1 pol12-*Δ*::KanMX2/* pPC64	Chiu
hc1779	*MAT*a *ura3-52 lys2-801 ade2-101 trp1-*Δ*63 his3-*Δ*200 leu2-*Δ*1 cdc13-*Δ*::LYS2 pol12-*Δ*::KanMX2/* pCN511, pPC64	Chiu
hc1781	*MAT*a *ura3-52 lys2-801 ade2-101 trp1-*Δ*63 his3-*Δ*200 leu2-*Δ*1 cdc13-*Δ*::LYS2 pol12-*Δ*::KanMX2/* pCN511, pPC65	Chiu
hc1832	*MAT*a *ura3-52 lys2-801 ade2-101 trp1-*Δ*63 his3-*Δ*200 leu2-*Δ*1 ten1-*Δ*::KanMX2/* pCN250	Xu[b]
hc1834	*MAT*a *ura3-52 lys2-801 ade2-101 trp1-*Δ*63 his3-*Δ*200 leu2-*Δ*1 rad9-*Δ*::HIS3 ten1-*Δ*::KanMX2/* pCN358	Xu[a]
hc1844	*MAT*a *ura3-52 lys2-801 ade2-101 trp1-*Δ*63 his3-*Δ*200 leu2-*Δ*1 rad9-*Δ*::HIS3 ten1-*Δ*::KanMX2/* pCN309	Xu[a]
hc1851	*MAT*a *ura3-52 lys2-801 ade2-101 trp1-*Δ*63 his3-*Δ*200 leu2-*Δ*1 rad9-*Δ*::HIS3 ten1-*Δ*::KanMX2/* pCN359	Xu[a]
hc1857	*MAT*a *ura3-52 lys2-801 ade2-101 trp1-*Δ*63 his3-*Δ*200 leu2-*Δ*1 rad9-*Δ*::HIS3 ten1-*Δ*::KanMX2/* pCN311	Xu[a]
hc1862	*MAT*a *ura3-52 lys2-801 ade2-101 trp1-*Δ*63 his3-*Δ*200 leu2-*Δ*1 ten1-*Δ*::KanMX2/* pCN309	Xu[b]
hc1863	*MAT*a *ura3-52 lys2-801 ade2-101 trp1-*Δ*63 his3-*Δ*200 leu2-*Δ*1 ten1-*Δ*::KanMX2/* pCN311	Xu[b]
hc1864	*MAT*a *ura3-52 lys2-801 ade2-101 trp1-*Δ*63 his3-*Δ*200 leu2-*Δ*1 ten1-*Δ*::KanMX2/* pCN358	Xu[b]
hc1946	*MAT*a*-inc ura3-52 lys2-801 ade2-101 trp1-*Δ*63 his3-*Δ*200 leu2-*Δ*1 GAL-HO::LEU2 VII-L::ADE2-TG$_{1\text{-}3}$-HO site-LYS2 rad52-*Δ*::LEU2 ten1-*Δ*::KanMX2/* pCN358	Xu[a]
hc1970	*MAT*a *ura3-52 lys2-801 ade2-101 trp1-*Δ*63 his3-*Δ*200 leu2-*Δ*1 exo1-*Δ*::KanMX2 ten1-*Δ*::KanMX2/* pCN309	Xu[b]
hc1971	*MAT*a *ura3-52 lys2-801 ade2-101 trp1-*Δ*63 his3-*Δ*200 leu2-*Δ*1 exo1-*Δ*::KanMX2 ten1-*Δ*::KanMX2/* pCN311	Xu[a]
hc1972	*MAT*a *ura3-52 lys2-801 ade2-101 trp1-*Δ*63 his3-*Δ*200 leu2-*Δ*1 exo1-*Δ*::KanMX2 ten1-*Δ*::KanMX2/* pCN358	Xu[b]

Table 3-1 (continued)

Strain	Description	Reference
hc1973	*MAT*a *ura3-52 lys2-801 ade2-101 trp1-*Δ*63 his3-*Δ*200 leu2-*Δ*1 exo1-*Δ*::KanMX2 ten1-*Δ*::KanMX2/* pCN359	Xu[a]
hc2046	*MAT*a *ura3-52 lys2-801 ade2-101 trp1-*Δ*63 his3-*Δ*200 leu2-*Δ*1 cdc13-*Δ*::LYS2 pol12-*Δ*::kanMX2/* pVL1033, pPC50	This study
hc2047	*MAT*a *ura3-52 lys2-801 ade2-101 trp1-*Δ*63 his3-*Δ*200 leu2-*Δ*1 cdc13-*Δ*::LYS2 pol12-*Δ*::kanMX2/* pVL1033, pPC64	This study
hc2241	*MAT*a *ura3-52 lys2-801 ade2-101 trp1-*Δ*63 his3-*Δ*200 leu2-*Δ*1 ten1-*Δ*::KanMX2-ten1-105-HIS3*	Xu[a]
hc2246	*MAT*a *ura3-52 lys2-801 ade2-101 trp1-*Δ*63 his3-*Δ*200 leu2-*Δ*1 ten1-*Δ*::KanMX2-ten1-101-HIS3*	Xu[a]
pj69-4a	*MATa trp1-901 leu2-3,112 ura3-52 his3-200 gal4-*Δ *gal80-*Δ *LYS2::GAL1-HIS3 GAL2-ADE2 met2::GAL7-lacZ*	James
ucc5706	*MAT*a-*inc ura3-52 lys2-801 ade2-101 trp1-*Δ*63 his3-*Δ*200 leu2-*Δ*1 GAL-HO::LEU2 VII-L::ADE2-TG*$_{1\text{-}3}$*-HO site-LYS2 rad52-*Δ*::hisG*	Diede[a]

Table 3-2: List of plasmids used in chapter 3

Plasmid	Description	Reference
pACT2.2	*2μ LEU2 ADH promoter GAL4 AD vector*	James
pCN124	*2μ TRP1 ADH promoter GAL4 DBD TEN1*	Petreaca[a]
pCN181	*2μ LEU2 ADH promoter GAL4 AD STN1*	Petreaca[a]
pCN250	*CEN URA3 native promoter TEN1*	Xu[b]
pCN282	*2μ URA3 GAL promoter FLAG-TEN1*	This study
pCN284	*CEN TRP1 native promoter TEN1*	Xu[b]
pCN309	*CEN TRP1 native promoter ten1-101*	Xu[b]
pCN311	*CEN TRP1 native promoter ten1-103*	Xu[b]
pCN358	*CEN TRP1 native promoter ten1-105*	Xu[b]
pCN359	*CEN TRP1 native promoter ten1-106*	Xu[b]
pCN416	*2μ LEU2 ADH promoter vector*	Gasparyan
pCN421	*2μ LEU2 ADH promoter STN1*	Gasparyan
pCN441	*2μ TRP1 ADH promoter GAL4 DBD ten1-105*	Xu[b]
pCN445	*2μ TRP1 ADH promoter GAL4 DBD ten1-101*	Xu[b]
pCN447	*2μ TRP1 ADH promoter GAL4 DBD ten1-106*	Xu[b]
pCN452	*2μ TRP1 ADH promoter GAL4 DBD ten1-103*	Xu[b]
pCN476	*integrating HIS3 KanMX2 native promoter ten1-105*	This study
pCN477	*integrating HIS3 KanMX2 native promoter ten1-101*	This study
pCN511	*CEN TRP1 native promoter cdc13-50*	Qi
pHG42	*pET3a-FLAG-TEN1*	This study
pPC20	*pET101/D-TOPO-GST*	Petreaca[a]
pPC23	*pGEX4T-1-GST-POL12*	Petreaca[a]
pPC50	*CEN HIS3 native promoter POL12*	Chiu
pPC64	*CEN HIS3 native promoter pol12-40*	Chiu
pPC65	*CEN HIS3 native promoter POL12*	Chiu
pRS415	*CEN LEU2 vector*	Sikorski
pVL438	*CEN URA3 native promoter CDC13*	Petreaca[a]
pVL576	*2μ LEU2 GAL promoter vector*	Gasparyan
pVL835	*2μ LEU2 ADH promoter GAL4 AD CDC13*$^{\Delta 585\text{-}677}$	Xu[b]
pVL903	*CEN LEU2 native promoter CDC13*	This study
pVL1033	*CEN LEU2 native promoter cdc13-5*	Chandra
pVL1046	*CEN URA3 native promoter STN1*	Petreaca[b]
pVL1051	*2μ LEU2 GAL promoter STN1*	Gasparyan
pVL1066	*2μ LEU2 native promoter STN1*	Pennock

Conclusion

Telomeres are essential for the maintenance of linear chromosomes. They cap the ends of chromosomes, protecting against degradation, recombination and end-to-end fusions, and help overcome the end replication problem. In budding yeast, the CST complex is intimately involved in both processes. All three CST components, Cdc13, Stn1 and Ten1 are essential for telomere capping. Loss of function mutations in any of them lead to elevated levels of telomeric ssDNA, suggesting that each is required to block against exonucleolytic degradation activities. Whether CST functions as a stable complex or each component works independently is not yet known. However, the multitude of genetic manipulations which allow bypass of Cdc13 function suggest that telomere capping is quite plastic and flexible. Our analyses here highlight *CDC13*'s, *POL12*'s, and *TEN1*'s role in telomere capping, demonstrating that each makes an essential, independent contribution to protecting chromosome ends.

The replicative function of the CST complex has been even more elusive. The current accepted model in the field proposes that Cdc13 first recruits telomerase to elongate the G-rich strand. Then, Pol-α is brought in via interactions between Cdc13-Pol1 and Stn1-Pol12 to fill in the complementary C-strand. How the switch off between these two processes occurs in still not known. A recent study proposed that CDK phosphorylation of Cdc13 modulates telomerase dependent extension and Stn1/Ten1 association with Cdc13 (Li *et al*, 2009). However, it is not known how this CDK phosphorylation event is regulated. Another study found that the Hsp82 molecular

chaperone mediates assembly and disassembly of Cdc13-telomerase, or CST on telomeres (DeZwaan *et al*, 2009). However, even in this study, the molecular mechanism which regulates different complex formation is undetermined, leading the authors to invoke a model where post-translational modifications are required. The lack of a detailed mechanistic understanding attests to the fact that there is still much to be learned about the regulation of these complex and dynamic processes. The coming years will be an exciting time in the telomere replication field.

An interesting new direction that the field is starting to move towards is exploring whether telomeric proteins affect DNA metabolism throughout the genome. Work performed in *S. pombe* within the last few years has revealed that both Rif1 and Taz1 control the timing of replication origin firing globally (Hayano *et al*, 2012; Tazumi *et al*, 2012). Mammalian *CTC1* and *STN1* were initially identified as DNA polymerase-alpha accessory factors (Goulian and Heard, 1990; Goulian *et al*, 1990; Casteel *et al*, 2009). More recently, a study has shown that knocking down STN1 in cultured human cells inhibits recovery from replication stress by preventing the activation of late firing and dormant origins (Stewart *et al*, 2012). Additionally, work done in *Xenopus* egg extracts has also shown that Stn1 is required for replication of a single-stranded plasmid (Nakaoka *et al*, 2012). These findings insinuate the tantalizing possibility that the functions of telomeric proteins are not strictly limited to chromosome ends.

Our work here demonstrates that the budding yeast Stn1 protein has a role in promoting DNA synthesis away from telomeres. We show that both overproduction and loss of function mutant alleles have an effect on DNA replication. The majority of our

understanding for this function is derived from genetic experiments. An interesting future direction for our lab will be to explore Stn1's role in DNA replication using more directed, biochemical assays. Findings from our future work will not only be of interest to investigators studying telomeres and DNA replication, but also to the DNA repair and checkpoint fields. Our work here shows that Stn1 functions at the crossroads of these interrelated processes, and is therefore likely to be an attractive area to study. From an evolutionary perspective, an interesting open question is how Stn1, and the entire CST complex arose. Did it start out as general replication protein which then became specialized for telomere related functions, or did it start as telomere specific factor that then evolved a new role in DNA metabolism elsewhere in the genome?

There are still much to learn about CST's roles in both telomere capping, and replication. The regulatory processes that control telomere capping, telomerase dependent extension and C-strand fill-in synthesis, and coordinate these events with semi-conservative DNA replication, as well as their regulation over the cell cycle are still poorly understood. Additionally, the functions of CST in global DNA metabolism are just beginning to be discovered. With so many unanswered questions, the telomere capping and replication field is at an incredibly exciting time in its history, ripe with ample opportunities for future investigators to expand our understanding. Analysis of CST's function in telomere maintenance and genome stability has become a particularly hot topic in recent years with the discovery that mutations within *CTC1* and *STN1* lead to a variety of human diseases (Angstadt *et al*, 2012; Armanios, 2012; Keller *et al*, 2012; Polvi *et al*, 2012; Romaniello *et al*, 2012; Gu and Chang, 2013; Walne *et al*, 2013). We

feel that our findings here lay the groundwork for future investigators to build upon. Although the initial motivating factor for our studies was to gain a better understanding of the fundamental processes that maintain genomic stability in eukaryotic cells, we believe that our work has the potential to be of significant clinical relevance. A detailed mechanistic understanding of Stn1's roles in telomere capping, replication, checkpoint control, and global DNA metabolism may help shed light on the root cause of diseases associated with mutations in the CST complex.

References

Adams AK, Holm C (1996) Specific DNA replication mutations affect telomere length in Saccharomyces cerevisiae. *Molecular and Cellular Biology* 16(9):4614-20.

Adams-Martin A, Dionne I, Wellinger RJ, Holm C (2000) The function of DNA polymerase alpha at telomeric G tails is important for telomere homeostasis. *Molecular and Cellular Biology* 20(3):786-96.

Alabert C, Bianco JN, Pasero P (2009) Differential regulation of homologous recombination at DNA breaks and replication forks by the Mrc1 branch of the S-phase checkpoint. *The EMBO Journal* 28(8):1131-41.

Alcasabas AA, Osborn AJ, Bachant J, Hu F, Werler PJ, Bousset K, Furuya K, Diffley JF, Carr AM, Elledge SJ (2001) Mrc1 transduces signals of DNA replication stress to activate Rad53. *Nature Cell Biology* 3(11):958-65.

Allen JB, Zhou Z, Siede W, Friedberg EC, Elledge SJ (1994) The SAD1/RAD53 protein kinase controls multiple checkpoints and DNA damage-induced transcription in yeast. *Genes and Development* 8(20):2401-15.

Amiard S, Depeiges A, Allain E, White CI, Gallego ME (2011) Arabidopsis ATM and ATR Kinases Prevent Propagation of Genome Damage Caused by Telomere Dysfunction. *Plant Cell* 23(12):4254-65.

Amiard S, Doudeau M, Pinte S, Poulet A, Lenain C, Faivre-Moskalenko C, Angelov D, Hug N, Vindigni A, Bouvet P, Paoletti J, Gilson E, Giraud-Panis MJ (2007) A topological mechanism for TRF2-enhanced strand invasion. *Nature Structural and Molecular Biology* 14(2):147-54.

Anand RP, Shah KA, Niu H, Sung P, Mirkin SM, Freudenreich CH (2011) Overcoming natural replication barriers: differential helicase requirements. *Nucleic Acids Research* 40(3):1091-105.

Anbalagan S, Bonetti D, Lucchini G, Longhese MP (2011) Rif1 supports the function of the CST complex in yeast telomere capping. *PLoS Genetics* 7(3).

Angstadt AY, Thayanithy V, Subramanian S, Modiano JF, Breen M (2012) A genome-wide approach to comparative oncology: high-resolution oligonucleotide aCGH of canine and human osteosarcoma pinpoints shared microaberrations. *Cancer Genetics* 205(11):572-87.

Aparicio OM (2013) Location, location, location: it's all in the timing for replication origins. *Genes and Development* 27(2):117-28.

Aparicio OM, Weinstein DM, Bell SP (1997) Components and dynamics of DNA replication complexes in S. cerevisiae: redistribution of MCM proteins and Cdc45p during S phase. *Cell* 91(1):59-69.

Armanios M (2012) An emerging role for the conserved telomere component 1 (CTC1) in human genetic disease. *Pediatric Blood and Cancer* 59(2):209-10.

Arnoult N, Saintome C, Ourliac-Garnier I, Riou JF, Londoño-Vallejo A (2009) Human POT1 is required for efficient telomere C-rich strand replication in the absence of WRN. *Genes and Development* 23(24):2915-24.

Bachant J, Jessen SR, Kavanaugh SE, Fielding CS (2005) The yeast S phase checkpoint enables replicating chromosomes to bi-orient and restrain spindle extension during S phase distress. *Journal of Cell Biology* 168(7):999-1012.

Bae NS, Baumann P (2007) A RAP1/TRF2 complex inhibits nonhomologous end-joining at human telomeric DNA ends. *Molecular Cell* 26(3):323-34.

Bailis JM, Luche DD, Hunter T, Forsburg SL (2008) Minichromosome maintenance proteins interact with checkpoint and recombination proteins to promote s-phase genome stability. *Molecular and Cellular Biology* 28(5):1724-38.

Bando M, Katou Y, Komata M, Tanaka H, Itoh T, Sutani T, Shirahige K (2009) Csm3, Tof1, and Mrc1 form a heterotrimeric mediator complex that associates with DNA replication forks. *The Journal of Biological Chemistry* 284(49):34355-65.

Basenko EY, Cesare AJ, Iyer S, Griffith JD, McEachern MJ (2010) Telomeric circles are abundant in the stn1-M1 mutant that maintains its telomeres through recombination. *Nucleic Acids Research* 38(1):182-9.

Bashkirov VI, King JS, Bashkirova EV, Schmuckli-Maurer J, Heyer WD (2000) DNA repair protein Rad55 is a terminal substrate of the DNA damage checkpoints. *Molecular and Cellular Biology* 20(12):4393-404.

Baumann P, Cech TR (2000) Protection of telomeres by the Ku protein in fission yeast. *Molecular Biology of the Cell* 11(10):3265-75.

Baumann P, Cech TR (2001) Pot1, the putative telomere end-binding protein in fission yeast and humans. *Science* 292(5519):1171-5.

Bell SP, Stillman B (1992) ATP-dependent recognition of eukaryotic origins of DNA replication by a multiprotein complex. *Nature* 357(6374):128-34.

Bianchi A, Shore D (2007) Early replication of short telomeres in budding yeast. *Cell*. 128(6):1051-62.

Bianchi A, Shore D (2007) Increased association of telomerase with short telomeres in yeast. *Genes and Development* 21(14):1726-30.

Boltz KA, Leehy K, Song X, Nelson AD, Shippen DE (2012) ATR cooperates with CTC1 and STN1 to maintain telomeres and genome integrity in Arabidopsis. *Molecular Biology of the Cell* 23(8):1558-68.

Bonetti D, Clerici M, Anbalagan S, Martina M, Lucchini G, Longhese MP (2010) Shelterin-like proteins and Yku inhibit nucleolytic processing of Saccharomyces cerevisiae telomeres. *PLoS Genetics* 6(5).

Booth C, Griffith E, Brady G, Lydall D (2001) Quantitative amplification of single-stranded DNA (QAOS) demonstrates that cdc13-1 mutants generate ssDNA in a telomere to centromere direction. *Nucleic Acids Research* 29(21):4414-22.

Bousset K, Diffley JF (1998) The Cdc7 protein kinase is required for origin firing during S phase. *Genes and Development* 12(4):480-90.

Branzei D, Foiani M (2010) Maintaining genome stability at the replication fork. *Nature Reviews: Molecular Cell Biology* 11(3):208-19.

Broccoli D, **Smogorzewska A**, **Chong L**, **de Lange T** (1997) Human telomeres contain two distinct Myb-related proteins, TRF1 and TRF2. *Nature Genetics* 1997 17(2):231-5.

Burgers PM (2009) Polymerase dynamics at the eukaryotic DNA replication fork. *The Journal of Biological Chemistry* 284(7):4041-5.

Carson MJ, Hartwell L (1985) CDC17: an essential gene that prevents telomere elongation in yeast. *Cell* 42(1):249-57.

Casper AM, Mieczkowski PA, Gawel M, Petes TD (2008) Low levels of DNA polymerase alpha induce mitotic and meiotic instability in the ribosomal DNA gene cluster of Saccharomyces cerevisiae. *PLoS Genetics* 4(6)

Casteel DE, Zhuang S, Zeng Y, Perrino FW, Boss GR, Goulian M, Pilz RB (2009) A DNA Polymerase-α-Primase cofactor with homology to replication protein A-32 regulates DNA replication in mammalian Cells. *The Journal of Biological Chemistry* 284(9):5807-18.

Cech TR, Lingner J (1997) Telomerase and the chromosome end replication problem. *Ciba Foundation Symposium* 211:20-8.

Chai W, Du Q, Shay JW, Wright WE (2006) Human telomeres have different overhang sizes at leading versus lagging strands. *Molecular Cell* 21(3):427-35.

Chakhparonian M, Wellinger RJ (2003) Telomere maintenance and DNA replication: how closely are these two connected? *Trends in Genetics* 19(8):439-46.

Chandra A, Hughes TR, Nugent CI, Lundblad V (2001) Cdc13 both positively and negatively regulates telomere replication. *Genes and Development* 15(4):404-14.

Chang M, Arneric M, Lingner J (2007) Telomerase repeat addition processivity is increased at critically short telomeres in a Tel1-dependent manner in Saccharomyces cerevisiae. *Genes and Development* 21(19):2485-94.

Chen LY, Redon S, Lingner J (2012) The human CST complex is a terminator of telomerase activity. *Nature* 488(7412):540-4.

Chen S, de Vries MA, Bell SP (2007) Orc6 is required for dynamic recruitment of Cdt1 during repeated Mcm2-7 loading. *Genes and Development* 21(22):2897-907.

Chen SH, Zhou H (2009) Reconstitution of Rad53 activation by Mec1 through adaptor protein Mrc1. *The Journal of Biological Chemistry* 284(28):18593-604.

Chen Y, Hennessy KM, Botstein D, Tye BK (1992) CDC46/MCM5, a yeast protein whose subcellular localization is cell cycle-regulated, is involved in DNA replication at autonomously replicating sequences. *Proceedings of the National Academy of Sciences* 89(21):10459-63.

Chen Y, Rai R, Zhou ZR, Kanoh J, Ribeyre C, Yang Y, Zheng H, Damay P, Wang F, Tsujii H, Hiraoka Y, Shore D, Hu HY, Chang S, Lei M (2011) A conserved motif within RAP1 has diversified roles in telomere protection and regulation in different organisms. *Nature Structural and Molecular Biology* 18(2):213-21.

Chow TT, Zhao Y, Mak SS, Shay JW, Wright WE (2012) Early and late steps in telomere overhang processing in normal human cells: the position of the final RNA primer drives telomere shortening. *Genes and Development* 26(11):1167-78.

Chui HC (2007) Dissertation. University of California, Riverside, Graduate program in Cell, Molecular and Developmental Biology.

Cifuentes-Rojas C, Kannan K, Tseng L, Shippen DE (2011) Two RNA subunits and POT1a are components of Arabidopsis telomerase. *Proceedings of the National Academy of Sciences* 108(1):73-78.

Colgin LM, Baran K, Baumann P, Cech TR, Reddel RR (2003) Human POT1 facilitates telomere elongation by telomerase. *Current Biology* 13(11):942-6.

Cooper JP, Nimmo ER, Allshire RC, Cech TR (1997) Regulation of telomere length and function by a Myb-domain protein in fission yeast. *Nature* 385(6618):744-7.

Cortez D, Guntuku S, Qin J, Elledge SJ (2001) ATR and ATRIP: partners in checkpoint signaling. *Science* 294(5547):1713-6.

Cosgrove AJ, Nieduszynski CA, Donaldson AD (2002) Ku complex controls the replication time of DNA in telomere regions. *Genes and Development* 16(19):2485-90.

Costanzo V, Shechter D, Lupardus PJ, Cimprich KA, Gottesman M, Gautier J (2003) An ATR- and Cdc7-dependent DNA damage checkpoint that inhibits initiation of DNA replication. *Molecular Cell* 11(1):203-13.

Cotta-Ramusino C, Fachinetti D, Lucca C, Doksani Y, Lopes M, Sogo J, Foiani M (2005) Exo1 processes stalled replication forks and counteracts fork reversal in checkpoint-defective cells. *Molecular Cell* 17(1):153-9.

Crabbe L, Verdun RE, Haggblom CI, Karlseder J (2004) Defective telomere lagging strand synthesis in cells lacking WRN helicase activity. *Science* 306(5703):1951-3.

Dahlén M, Sunnerhagen P, Wang TS (2003) Replication proteins influence the maintenance of telomere length and telomerase protein stability. *Molecular and Cellular Biology* 23(9):3031-42.

Dahmann C, Diffley JF, Nasmyth KA (1995) S-phase-promoting cyclin-dependent kinases prevent re-replication by inhibiting the transition of replication origins to a pre-replicative state. *Current Biology* 5(11):1257-69.

Dai X, Huang C, Bhusari A, Sampathi S, Schubert K, Chai W (2010) Molecular steps of G-overhang generation at human telomeres and its function in chromosome end protection. *The EMBO Journal* 29(16):2788-801.

Dai X, Huang C, Chai W (2012) CDK1 differentially regulates G-overhang generation at leading- and lagging-strand telomeres in telomerase-negative cells in G 2 phase. *Cell Cycle* 11(16):3079-86.

de Lange T (2009) How telomeres solve the end-protection problem. *Science* 326(5955):948-52.

Dehé PM, Rog O, Ferreira MG, Greenwood J, Cooper JP (2012) Taz1 Enforces Cell-Cycle Regulation of Telomere Synthesis. *Molecular Cell* 46(6):797-808.

Denchi EL, de Lange T (2007) Protection of telomeres through independent control of ATM and ATR by TRF2 and POT1. *Nature* 448(7157):1068-71.

De Piccoli G, Katou Y, Itoh T, Nakato R, Shirahige K, Labib K (2012). Replisome stability at defective DNA replication forks is independent of S phase checkpoint kinases. *Molecular Cell* 45(5):696-704.

Desany BA, Alcasabas AA, Bachant JB, Elledge SJ (1998) Recovery from DNA replicational stress is the essential function of the S-phase checkpoint pathway. *Genes and Development* 12(18):2956-70.

Devault A, **Gueydon E**, **Schwob E** (2008) Interplay between S-cyclin-dependent kinase and Dbf4-dependent kinase in controlling DNA replication through phosphorylation of yeast Mcm4 N-terminal domain. *Molecular Biology of the Cell* 19(5):2267-77.

Dewar JM, **Lydall D** (2010) Pif1- and Exo1-dependent nucleases coordinate checkpoint activation following telomere uncapping. *The EMBO Journal* 29(23):4020-34.

DeZwaan DC, Toogun OA, Echtenkamp FJ, Freeman BC (2009)The Hsp82 molecular chaperone promotes a switch between unextendable and extendable telomere states. *Nature Structural and Molecular Biology* 16(7):711-6.

Diede SJ, Gottschling DE (1999) Telomerase-mediated telomere addition in vivo requires DNA primase and DNA polymerases alpha and delta. *Cell* 99(7):723-33.

Diede SJ, Gottschling DE (2001) Exonuclease activity is required for sequence addition and Cdc13p loading at a de novo telomere. *Current Biology* 11(17):1336-40.

Diffley JF, Cocker JH, Dowell SJ, Rowley A (1994) Two steps in the assembly of complexes at yeast replication origins in vivo. *Cell* 78(2):303-16.

Dionne I, Wellinger RJ (1996) Cell cycle-regulated generation of single-stranded G-rich DNA in the absence of telomerase. *Proceedings of the National Academy of Sciences* 93(24):13902-7.

Dionne I, Wellinger RJ (1998) Processing of telomeric DNA ends requires the passage of a replication fork. *Nucleic Acids Research* 26(23):5365-71.

Dohrmann PR, Oshiro G, Tecklenburg M, Sclafani RA (1999) RAD53 regulates DBF4 independently of checkpoint function in Saccharomyces cerevisiae. *Genetics* 151(3):965-77.

Dolan WP, Le AH, Schmidt H, Yuan JP, Green M, Forsburg SL (2010) Fission yeast Hsk1 (Cdc7) kinase is required after replication initiation for induced mutagenesis and proper response to DNA alkylation damage. *Genetics* 185(1):39-53.

Donaldson AD, Fangman WL, Brewer BJ (1998) Cdc7 is required throughout the yeast S phase to activate replication origins. *Genes and Development* 12(4):491-501.

Donovan S, Harwood J, Drury LS, Diffley JF (1997) Cdc6p-dependent loading of Mcm proteins onto pre-replicative chromatin in budding yeast. *Proceedings in the National Academy of Sciences* 94(11):5611-6.

Drosopoulos WC, Kosiyatrakul ST, Yan Z, Calderano SG, Schildkraut CL (2012) Human telomeres replicate using chromosome-specific, rather than universal, replication programs. *Journal of Cell Biology* 197(2):253-66.

Duch A, Palou G, Jonsson ZO, Palou R, Calvo E, Wohlschlegel J, Quintana DG (2011). A Dbf4 mutant contributes to bypassing the Rad53-mediated block of origins of replication in response to genotoxic stress. *The Journal of Biological Chemistry* 286(4):2486-91.

Duncker BP, Shimada K, Tsai-Pflugfelder M, Pasero P, Gasser SM (2002) An N-terminal domain of Dbf4p mediates interaction with both origin recognition complex (ORC) and Rad53p and can deregulate late origin firing. *Proceedings of the National Academy of Sciences* 99(25):16087-92.

Elledge SJ (1996) Cell cycle checkpoints: preventing an identity crisis. *Science* 274(5293):1664-72.

Enoch T, Carr AM, Nurse P (1992) Fission yeast genes involved in coupling mitosis to completion of DNA replication. *Genes and Development* 6(11):2035-46.

Evans SK, Lundblad V (1999) Est1 and Cdc13 as comediators of telomerase access. *Science* 286(5437):117-20.

Fan X, Price CM (1997) Coordinate regulation of G- and C strand length during new telomere synthesis. *Molecular Biology of the Cell* 8(11):2145-55.

Faure V, Coulon S, Hardy J, Géli V (2010) Cdc13 and telomerase bind through different mechanisms at the lagging- and leading-strand telomeres. *Molecular Cell* 38(6):842-52.

Feldser DM, Hackett JA, Greider CW (2003) Telomere dysfunction and the initiation of genome instability. *Nature Reviews*: *Cancer* 3(8):623-7.

Feng W, Bachant J, Collingwood D, Raghuraman MK, Brewer BJ (2009) Centromere replication timing determines different forms of genomic instability in Saccharomyces cerevisiae checkpoint mutants during replication stress. *Genetics* 183(4):1249-60.

Feng W, Collingwood D, Boeck ME, Fox LA, Alvino GM, Fangman WL, Raghuraman MK, Brewer BJ (2006) Genomic mapping of single-stranded DNA in hydroxyurea-challenged yeasts identifies origins of replication. *Nature Cell Biology* 8(2):148-55.

Feng W, **Di Rienzi SC**, **Raghuraman MK**, **Brewer BJ** (2011) Replication stress-induced chromosome breakage is correlated with replication fork progression and is preceded by single-stranded DNA formation. *G3 (Bethesda)* 1(5):327-35.

Ferguson BM, Fangman WL (1992) A position effect on the time of replication origin activation in yeast. *Cell* 68(2):333-9.

Ferreira MG, Cooper JP (2001)The fission yeast Taz1 protein protects chromosomes from Ku-dependent end-to-end fusions. *Molecular Cell* 7(1):55-63.

Fisher TS, Taggart AK, Zakian VA (2004) Cell cycle-dependent regulation of yeast telomerase by Ku. *Nature Structural and Molecular Biology* 11(12):1198-205.

Fisher TS, Zakian VA (2005) Ku: a multifunctional protein involved in telomere maintenance. *DNA Repair 4*(11):1215-26.

Frank CJ, Hyde M, Greider CW (2006) Regulation of telomere elongation by the cyclin-dependent kinase CDK1. *Molecular Cell* 24(3):423-32.

Friedman KL, Diller JD, Ferguson BM, Nyland SV, Brewer BJ, Fangman WL (1996) Multiple determinants controlling activation of yeast replication origins late in S phase. *Genes and Development* 10(13):1595-607.

Froget B, **Blaisonneau J**, **Lambert S**, **Baldacci G** (2008) Cleavage of stalled forks by fission yeast Mus81/Eme1 in absence of DNA replication checkpoint. *Molecular Biology of the Cell* 19(2):445-56.

Gao H, Cervantes RB, Mandell EK, Otero JH, Lundblad V (2007) RPA-like proteins mediate yeast telomere function. *Nature Structural and Molecular Biology* 14(3):208-14.

Gambus A, **van Deursen F**, **Polychronopoulos D**, **Foltman M**, **Jones RC**, **Edmondson RD**, **Calzada A**, **Labib K** (2009) A key role for Ctf4 in coupling the MCM2-7 helicase to DNA polymerase alpha within the eukaryotic replisome. *The EMBO Journal* 28(19):2992-3004.

Garvik B, Carson M, Hartwell L (1995) Single-stranded DNA arising at telomeres in cdc13 mutants may constitute a specific signal for the RAD9 checkpoint. *Molecular and Cellular Biology* 15(11):6128-38.

Gasparyan HJ, Xu L, Petreaca RC, Rex AE, Small VY, Bhogal NS, Julius JA, Warsi TH, Bachant J, Aparicio OM, Nugent CI (2009) Yeast telomere capping protein Stn1 overrides DNA replication control through the S phase checkpoint. *Proceedings of the National Academy of Sciences* 106(7) 2206-11.

Gelinas AD, Paschini M, Reyes FE, Héroux A, Batey RT, Lundblad V, Wuttke DS (2009) Telomere capping proteins are structurally related to RPA with an additional telomere-specific domain. *Proceedings of the National Academy of Sciences* 106(46):19298-303.

Gietz RD, Schiestl RH (2007) High-efficiency yeast transformation using the LiAc/SS carrier DNA/PEG method. *Nature Protocols* 2(1):31-4.

Gilson E, Géli V (2007) How telomeres are replicated. *Nature Reviews: Molecular Cell Biology* 8(10):825-38.

Giraud-Panis MJ, Teixeira MT, Géli V, Gilson E (2010) CST meets shelterin to keep telomeres in check. *Molecular Cell* 39(5):665-76.

Goulian M, Heard CJ (1990) The mechanism of action of an accessory protein for DNA polymerase alpha/primase. *The Journal of Biological Chemistry* 265(22):13231-9.

Goulian M, Heard CJ, Grimm SL (1990) Purification and properties of an accessory protein for DNA polymerase alpha/primase. *The Journal of Biological Chemistry* 265(22):13221-30.

Grandin N, Damon C, Charbonneau M (2001) Ten1 functions in telomere end protection and length regulation in association with Stn1 and Cdc13. *The EMBO Journal* 20(5):1173-83.

Grandin N, Reed SI, Charbonneau M (1997) Stn1, a new Saccharomyces cerevisiae protein, is implicated in telomere size regulation in association with Cdc13. *Genes and Development* 11(4):512-27.

Gravel S, Larrivée M, Labrecque P, Wellinger RJ (1998) Yeast Ku as a regulator of chromosomal DNA end structure. *Science* 280(5364):741-4.

Greider CW, Blackburn EH (1985) Identification of a specific telomere terminal transferase activity in Tetrahymena extracts. *Cell* 43(2):405-13.

Griffith JD, Comeau L, Rosenfield S, Stansel RM, Bianchi A, Moss H, de Lange T (1999) Mammalian telomeres end in a large duplex loop. *Cell* 97 (4):503-14.

Grossi S, Puglisi A, Dmitriev PV, Lopes M, Shore D (2004) Pol12, the B subunit of DNA polymerase alpha, functions in both telomere capping and length regulation. *Genes and Development* 18(9):992-1006.

Gu P, Chang S (2013) Functional characterization of human CTC1 mutations reveals novel mechanisms responsible for the pathogenesis of the telomere disease Coats plus. *Aging Cell*.

Gu P, Min JN, Wang Y, Huang C, Peng T, Chai W, Chang S (2012) CTC1 deletion results in defective telomere replication, leading to catastrophic telomere loss and stem cell exhaustion. *The EMBO Journal* 31(10):2309-21.

Hardy CF, Dryga O, Seematter S, Pahl PM, Sclafani RA (1997) mcm5/cdc46-bob1 bypasses the requirement for the S phase activator Cdc7p. *Proceedings of the National Academy of Sciences* 94(7):3151-5.

Hardy CF, Sussel L, Shore D (1992) A RAP1-interacting protein involved in transcriptional silencing and telomere length regulation. *Genes and Development* 6(5):801-14.

Hartwell LH, Weinert TA (1989) Checkpoints: controls that ensure the order of cell cycle events. *Science* 1989 246(4930):629-34.

Hayano M, Kanoh Y, Matsumoto S, Renard-Guillet C, Shirahige K, Masai H (2012) Rif1 is a global regulator of timing of replication origin firing in fission yeast. *Genes and Development* 26(2):137-50.

Hayflick L (1965) The limited in vitro lifetime of human diploid cell strains. *Experimental Cell Research* 37:614-36.

Hector RE, Shtofman RL, Ray A, Chen BR, Nyun T, Berkner KL, Runge KW (2007) Tel1p preferentially associates with short telomeres to stimulate their elongation. *Molecular Cell* 27(5):851-8.

Heller RC, **Kang S**, **Lam WM**, **Chen S**, **Chan CS**, **Bell SP** (2011) Eukaryotic origin-dependent DNA replication in vitro reveals sequential action of DDK and S-CDK kinases. *Cell* 146(1):80-91.

Henderson ER, Blackburn EH (1989) An overhanging 3' terminus is a conserved feature of telomeres. *Molecular and Cellular Biology* 9(1):345-8.

Henning KA, Moskowitz N, Ashlock MA, Liu PP (1998) Humanizing the yeast telomerase template. *Proceedings of the National Academy of Sciences* 95(10):5667-71.

Herzberg K, Bashkirov VI, Rolfsmeier M, Haghnazari E, McDonald WH, Anderson S, Bashkirova EV, Yates JR 3rd, Heyer WD (2006) Phosphorylation of Rad55 on serines 2, 8, and 14 is required for efficient homologous recombination in the recovery of stalled replication forks. *Molecular and Cellular Biology* 26(22):8396-409.

Hirano Y, Fukunaga K, Sugimoto K (2009) Rif1 and rif2 inhibit localization of tel1 to DNA ends. *Molecular Cell* 33(3):312-22.

Hoang ML, Leon RP, Pessoa-Brandao L, Hunt S, Raghuraman MK, Fangman WL, Brewer BJ, Sclafani RA (2007) Structural changes in Mcm5 protein bypass Cdc7-Dbf4 function and reduce replication origin efficiency in Saccharomyces cerevisiae. *Molecular and Cellular Biology* 27(21):7594-602

Hockemeyer D, Palm W, Else T, Daniels JP, Takai KK, Ye JZ, Keegan CE, de Lange T, Hammer GD (2007) Telomere protection by mammalian Pot1 requires interaction with Tpp1. *Nature Structural and Molecular Biology* 14(8):754-61.

Homesley L, Lei M, Kawasaki Y, Sawyer S, Christensen T, Tye BK (2000) Mcm10 and the MCM2-7 complex interact to initiate DNA synthesis and to release replication factors from origins. *Genes and Development* 14(8):913-26.

Horvath MP (2011) Structural anatomy of telomere OB proteins. *Critical Reviews in Biochemistry and Molecular Biology* 46(5):409-35.

Hu J, Sun L, Shen F, Chen Y, Hua Y, Liu Y, Zhang M, Hu Y, Wang Q, Xu W, Sun F, Ji J, Murray JM, Carr AM, Kong D (2012)The intra-S phase checkpoint targets Dna2 to prevent stalled replication forks from reversing. *Cell* 149(6):1221-32.

Huang C, Dai X, Chai W (2012) Human Stn1 protects telomere integrity by promoting efficient lagging-strand synthesis at telomeres and mediating C-strand fill-in. *Cell Research* 22(12):1681-95.

Hughes TR, Evans SK, Weilbaecher RG, Lundblad V (2000) The Est3 protein is a subunit of yeast telomerase. *Current Biology* 10(13):809-12.

Iadonato SP, **Gnirke A** (1996) RARE-cleavage analysis of YACs. *Methods in Molecular Biology* 54:75-85.

Ivessa AS, Zhou JQ, Schulz VP, Monson EK, Zakian VA (2003) Saccharomyces Rrm3p, a 5' to 3' DNA helicase that promotes replication fork progression through telomeric and subtelomeric DNA. *Genes and Development* 16(11):1383-96.

Ivessa AS, Zhou JQ, Zakian VA (2001) The Saccharomyces Pif1p DNA helicase and the highly related Rrm3p have opposite effects on replication fork progression in ribosomal DNA. *Cell* 100(4):479-89.

Iyer S, Chadha AD, McEachern MJ (2005) A mutation in the STN1 gene triggers an alternative lengthening of telomere-like runaway recombinational telomere elongation and rapid deletion in yeast. *Molecular and Cellular Biology* 25(18):8064-73.

Jacob F, Brenner S, Cuzin F (1963) On the regulation of DNA replication in bacteria. *Cold Spring Harbor Symposia on Quantitative Biology* 28:329–48.

James P, Halladay J, Craig EA (1996) Genomic libraries and a host strain designed for highly efficient two-hybrid selection in yeast. *Genetics* 144(4):1425-36.

Kanoh J, Ishikawa F (2001) spRap1 and spRif1, recruited to telomeres by Taz1, are essential for telomere function in fission yeast. *Current Biology* 11(20):1624-30.

Karras GI, Jentsch S (2010) The RAD6 DNA damage tolerance pathway operates uncoupled from the replication fork and is functional beyond S phase. *Cell* 141(2):255-67.

Katou Y, Kanoh Y, Bando M, Noguchi H, Tanaka H, Ashikari T, Sugimoto K, Shirahige K (2003) S-phase checkpoint proteins Tof1 and Mrc1 form a stable replication-pausing complex. *Nature* 424(6952):1078-83.

Keller RB, Gagne KE, Usmani GN, Asdourian GK, Williams DA, Hofmann I, Agarwal S (2012) CTC1 Mutations in a patient with dyskeratosis congenita. *Pediatric Blood and Cancer* 59(2):311-4.

Kerrest A, Anand RP, Sundararajan R, Bermejo R, Liberi G, Dujon B, Freudenreich CH, Richard GF (2009) SRS2 and SGS1 prevent chromosomal breaks and stabilize triplet repeats by restraining recombination. *Nature Structural and Molecular Biology* 16(2):159-67.

Khalil AM, Julius JA, Bachant J (2007) One step construction of PCR mutagenized libraries for genetic analysis by recombination cloning. *Nucleic Acids Research* 35(16):e104.

Knott SR, **Peace JM**, **Ostrow AZ**, **Gan Y**, **Rex AE**, **Viggiani CJ**, **Tavaré S**, **Aparicio OM**. (2012) Forkhead transcription factors establish origin timing and long-range clustering in S. cerevisiae. *Cell* 148(1-2):99-111.

Knott SR, **Viggiani CJ**, **Tavaré S**, **Aparicio OM** (2009) Genome-wide replication profiles indicate an expansive role for Rpd3L in regulating replication initiation timing or efficiency, and reveal genomic loci of Rpd3 function in Saccharomyces cerevisiae. *Genes and Development* 23(9):1077-90.

Labib K (2010) How do Cdc7 and cyclin-dependent kinases trigger the initiation of chromosome replication in eukaryotic cells? *Genes and Development* 24(12):1208-19.

Labib K, De Piccoli G (2011). Surviving chromosome replication: the many roles of the S-phase checkpoint pathway. *Philosophical Transactions of the Royal Society of London. Series B, Biological Sciences* 366(1584):3554-61.

Larrivée M, LeBel C, Wellinger RJ (2004) The generation of proper constitutive G-tails on yeast telomeres is dependent on the MRX complex. *Genes and Development* 18(12):1391-6.

Larrivée M, Wellinger RJ (2006) Telomerase- and capping-independent yeast survivors with alternate telomere states. *Nature Cell Biology* 8(7):741-7.

Lee MT (2010) Dissertation. University of California, Riverside, Graduate program in Biochemistry and Molecular Biology.

Lei M, Podell ER, Cech TR (2004) Structure of human POT1 bound to telomeric single-stranded DNA provides a model for chromosome end-protection. *Nature Structural and Molecular Biology* 11(12):1223-9.

Leman AR, **Dheekollu J**, **Deng Z**, **Lee SW**, **Das MM**, **Lieberman PM**, **Noguchi E** (2012) Timeless preserves telomere length by promoting efficient DNA replication through human telomeres. *Cell Cycle* 11(12):2337-47.

Lendvay TS, Morris DK, Sah J, Balasubramanian B, Lundblad V (1996) Senescence mutants of Saccharomyces cerevisiae with a defect in telomere replication identify three additional EST genes. *Genetics* 144(4):1399-412.

Li S, Makovets S, Matsuguchi T, Blethrow JD, Shokat KM, Blackburn EH (2009) Cdk1-dependent phosphorylation of Cdc13 coordinates telomere elongation during cell-cycle progression. *Cell* 136(1):50-61.

Lian HY, Robertson ED, Hiraga S, Alvino GM, Collingwood D, McCune HJ, Sridhar A, Brewer BJ, Raghuraman MK, Donaldson AD (2011) The effect of Ku on telomere replication time is mediated by telomere length but is independent of histone tail acetylation. *Molecular Biology of the Cell* 2(10):1753-65.

Liang C, Weinreich M, Stillman B (1995) ORC and Cdc6p interact and determine the frequency of initiation of DNA replication in the genome. *Cell* 81(5):667-76.

Lin JJ, Zakian VA (1996) The Saccharomyces CDC13 protein is a single-strand TG_{1-3} telomeric DNA-binding protein in vitro that affects telomere behavior in vivo. *Proceedings of the National Academy of Sciences* 93(24):13760-5.

Lin YC, Hsu CL, Shih JW, Lin JJ (2001) Specific binding of single-stranded telomeric DNA by Cdc13p of Saccharomyces cerevisiae. *The Journal of Biological Chemistry* 276(27):24588-93.

Lingner J, Cech TR, Hughes TR, Lundblad V (1997) Three Ever Shorter Telomere (EST) genes are dispensable for in vitro yeast telomerase activity. *Proceedings of the National Academy of Sciences* 94(21):11190-5.

Lingner J, Cooper JP, Cech TR (1995) Telomerase and DNA end replication: no longer a lagging strand problem? *Science* 269(5230):1533-4.

Lingner J, Hughes TR, Shevchenko A, Mann M, Lundblad V, Cech TR (1997) Reverse transcriptase motifs in the catalytic subunit of telomerase. *Science* 276(5312): 561-7.

Lisby M, Rothstein R, Mortensen UH (2001) Rad52 forms DNA repair and recombination centers during S phase. *Proceedings of the National Academy of Sciences* 98(15):8276-82.

Loayza D, de Lange T (2003) POT1 as a terminal transducer of TRF1 telomere length control. *Nature* 423(6943):1013-8.

Lopes M, Cotta-Ramusino C, Pellicioli A, Liberi G, Plevani P, Muzi-Falconi M, Newlon CS, Foiani M (2001) The DNA replication checkpoint response stabilizes stalled replication forks. *Nature* 412(6846):557-61.

Lopez-Mosqueda J, Maas NL, Jonsson ZO, Defazio-Eli LG, Wohlschlegel J, Toczyski DP (2010) Damage-induced phosphorylation of Sld3 is important to block late origin firing. *Nature* 467(7314):479-83.

Lou H, Komata M, Katou Y, Guan Z, Reis CC, Budd M, Shirahige K, Campbell JL (2008) Mrc1 and DNA polymerase epsilon function together in linking DNA replication and the S phase checkpoint. *Molecular Cell* 32(1):106-17.

Lucchini R, Sogo JM (1995) Replication of transcriptionally active chromatin. *Nature* 374(6519):276-80.

Luciano P, Coulon S, Faure V, Corda Y, Bos J, Brill SJ, Gilson E, Simon MN, Géli V (2012) RPA facilitates telomerase activity at chromosome ends in budding and fission yeasts. *The EMBO Journal* 31(8):2034-46.

Lundblad V, Szostak JW (1989) A mutant with a defect in telomere elongation leads to senescence in yeast. *Cell* 57(4):633-43.

Lustig AJ, Kurtz S, Shore D (1990) Involvement of the silencer and UAS binding protein RAP1 in regulation of telomere length. *Science* 250(4980):549-53.

Majka J, Binz SK, Wold MS, Burgers PM (2006) Replication protein A directs loading of the DNA damage checkpoint clamp to 5'-DNA junctions. *The Journal of Biological Chemistry* 281(38):27855-61.

Majka J, Niedziela-Majka A, Burgers PM (2006) The checkpoint clamp activates Mec1 kinase during initiation of the DNA damage checkpoint. *Molecular Cell* 24(6):891-901.

Makovets S, Herskowitz I, Blackburn EH (2004) Anatomy and dynamics of DNA replication fork movement in yeast telomeric regions. *Molecular and Cellular Biology* 24(9):4019-31.

Mandell EK, Gelinas AD, Wuttke DS, Lundblad V (2011) Sequence-specific binding to telomeric DNA is not a conserved property of the Cdc13 DNA binding domain. *Biochemistry* 50(29):6289-91.

Mantiero D, Mackenzie A, Donaldson A, Zegerman P (2011) Limiting replication initiation factors execute the temporal programme of origin firing in budding yeast. *The EMBO Journal* 30(23):4805-14.

Marcand S, Brevet V, Gilson E (1999) Progressive cis-inhibition of telomerase upon telomere elongation. *The EMBO Journal* 18(12):3509-19.

Marcand S, Brevet V, Mann C, Gilson E (2000) Cell cycle restriction of telomere elongation. *Current Biology* 10(8):487-90.

Marcand S, Gilson E, Shore D (1997) A protein-counting mechanism for telomere length regulation in yeast. *Scienc*e 275(5302):986-90.

Marcand S, Pardo B, Gratias A, Cahun S, Callebaut I (2008) Multiple pathways inhibit NHEJ at telomeres. *Genes and Development* 22(9):1153-8.

Marcand S, Wotton D, Gilson E, Shore D (1997) Rap1p and telomere length regulation in yeast. *Ciba Foundation Symposium* 211:76-93.

Maringele L, Lydall D (2002) EXO1-dependent single-stranded DNA at telomeres activates subsets of DNA damage and spindle checkpoint pathways in budding yeast yku70Delta mutants. *Genes and Development* 16(15):1919-33.

Martín V, Du LL, Rozenzhak S, Russell P (2007) Protection of telomeres by a conserved Stn1-Ten1 complex. *Proceedings of the National Academy of Sciences* 104(35):14038-43.

Martínez P, Thanasoula M, Muñoz P, Liao C, Tejera A, McNees C, Flores JM, Fernández-Capetillo O, Tarsounas M, Blasco MA (2009) Increased telomere fragility and fusions resulting from TRF1 deficiency lead to degenerative pathologies and increased cancer in mice. *Genes and Development* 23(17):2060-75.

Masai H, Matsui E, You Z, Ishimi Y, Tamai K, Arai K (2000) Human Cdc7-related kinase complex. In vitro phosphorylation of MCM by concerted actions of Cdks and Cdc7 and that of a critical threonine residue of Cdc7 by Cdks. *The Journal of Biological Chemistry* 275(37):29042-52.

Masai H, **Matsumoto S**, **You Z**, **Yoshizawa-Sugata N**, **Oda M** (2010) Eukaryotic chromosome DNA replication: where, when, and how? *Annual Review of Biochemistry* 79:89-130.

Masai H, **Taniyama C**, **Ogino K**, **Matsui E**, **Kakusho N**, **Matsumoto S**, **Kim JM**, **Ishii A**, **Tanaka T**, **Kobayashi T**, **Tamai K**, **Ohtani K**, **Arai K** (2006) Phosphorylation of MCM4 by Cdc7 kinase facilitates its interaction with Cdc45 on the chromatin. *The Journal of Biological Chemistry* 281(51):39249-61.

Matsumoto S, Hayano M, Kanoh Y, Masai H (2011) Multiple pathways can bypass the essential role of fission yeast Hsk1 kinase in DNA replication initiation. *The Journal of Cell Biology* 195(3):387-401.

Matsumoto S, Ogino K, Noguchi E, Russell P, Masai H (2005) Hsk1-Dfp1/Him1, the Cdc7-Dbf4 kinase in Schizosaccharomyces pombe, associates with Swi1, a component of the replication fork protection complex. *The Journal of Biological Chemistry* 280(52):42536-42.

McClintock, B (1938) The production of homozygous deficient tissues with mutant characteristics by means of the aberrant mitotic behavior of ring-shaped chromosomes. *Genetics* 23(4):315–376.

McClintock B (1941) The stability of broken ends of chromosomes in Zea mays. *Genetics* 26(2):234-82.

Meselson M, Stahl FW (1958) The replication of DNA in Escherichia coli. *Proceedings of the National Academy of Sciences* 44(7):671-82.

Michelson RJ, Rosenstein S, Weinert T (2005) A telomeric repeat sequence adjacent to a DNA double-stranded break produces an anticheckpoint. *Genes and Development* 19(21):2546-59.

Mieczkowski PA, Mieczkowska JO, Dominska M, Petes TD (2003) Genetic regulation of telomere-telomere fusions in the yeast Saccharomyces cerevisiae. *Proceedings of the National Academy of Sciences* 100(19):10854-9.

Miller KM, Ferreira MG, Cooper JP (2005) Taz1, Rap1 and Rif1 act both interdependently and independently to maintain telomeres. *The EMBO Journal* 2005 24(17):3128-35.

Miller KM, Rog O, Cooper JP (2006) Semi-conservative DNA replication through telomeres requires Taz1. *Nature* 440(7085):824-8.

Mitton-Fry RM, Anderson EM, Hughes TR, Lundblad V, Wuttke DS (2002) Conserved structure for single-stranded telomeric DNA recognition. *Science* 296(5565):145-7.

Mitton-Fry RM, Anderson EM, Theobald DL, Glustrom LW, Wuttke DS (2004) Structural basis for telomeric single-stranded DNA recognition by yeast Cdc13. *Journal of Molecular Biology* 338(2):241-55.

Miyake Y, Nakamura M, Nabetani A, Shimamura S, Tamura M, Yonehara S, Saito M, Ishikawa F (2009) RPA-like mammalian Ctc1-Stn1-Ten1 complex binds to single-stranded DNA and protects telomeres independently of the Pot1 pathway. *Molecular Cell* 36(2):193-206.

Miyoshi T, Kanoh J, Saito M, Ishikawa F (2008) Fission yeast Pot1-Tpp1 protects telomeres and regulates telomere length. *Science* 320(5881):1341-4.

Mizuno K, Lambert S, Baldacci G, Murray JM, Carr AM (2009) Nearby inverted repeats fuse to generate acentric and dicentric palindromic chromosomes by a replication template exchange mechanism. *Genes and Development* 23(24):2876-86.

Moser BA, Chang YT, Kosti J, Nakamura TM (2011) Tel1ATM and Rad3ATR kinases promote Ccq1-Est1 interaction to maintain telomeres in fission yeast. *Nature Structural and Molecular Biology* 18(12):1408-13.

Moser BA, Subramanian L, Chang YT, Noguchi C, Noguchi E, Nakamura TM (2009) Differential arrival of leading and lagging strand DNA polymerases at fission yeast telomeres. *The EMBO Journal* 28(7): 810-20.

Mordes DA, **Nam EA**, **Cortez D** (2008) Dpb11 activates the Mec1-Ddc2 complex. *Proceedings of the National Academy of Sciences* 105(48):18730-4.

Morin I, Ngo HP, Greenall A, Zubko MK, Morrice N, Lydall D (2008) Checkpoint-dependent phosphorylation of Exo1 modulates the DNA damage response. *The EMBO Journal* 27(18):2400-10.

Muller HJ (1938) The remaking of chromosomes. *The Collecting Net* 13:181-95.

Nakaoka H, Nishiyama A, Saito M, Ishikawa F (2012) Xenopus laevis Ctc1-Stn1-Ten1 (xCST) complex is involved in priming DNA synthesis on single-stranded DNA template in Xenopus egg extract. *The Journal of Biological Chemistry* 287(1):619-27.

Navadgi-Patil VM, Burgers PM (2008) Yeast DNA replication protein Dpb11 activates the Mec1/ATR checkpoint kinase. *The Journal of Biological Chemistry* 283(51):35853-9.

Navas TA, Zhou Z, Elledge SJ (1995) DNA polymerase epsilon links the DNA replication machinery to the S phase checkpoint. *Cell* 80(1):29-39.

Naylor ML, Li JM, Osborn AJ, Elledge SJ (2009) Mrc1 phosphorylation in response to DNA replication stress is required for Mec1 accumulation at the stalled fork. *Proceedings of the National Academy of Sciences* 106(31):12765-70.

Ngo HP, Lydall D (2010) Survival and growth of yeast without telomere capping by Cdc13 in the absence of Sgs1, Exo1, and Rad9. *PLoS Genetics* 6(8).

Nugent CI, Bosco G, Ross LO, Evans SK, Salinger AP, Moore JK, Haber JE, Lundblad V (1998) Telomere maintenance is dependent on activities required for end repair of double-strand breaks. *Current Biology* 8(11):657-60.

Nugent CI, Hughes TR, Lue NF, Lundblad V (1996) Cdc13p: a single-strand telomeric DNA-binding protein with a dual role in yeast telomere maintenance. *Science* 274(5285):249-52.

Ogi H, Wang CZ, Nakai W, Kawasaki Y, Masumoto H (2008) The role of the Saccharomyces cerevisiae Cdc7-Dbf4 complex in the replication checkpoint. *Gene* 414(1-2):32-40.

Olovnikov AM (1973) A theory of marginotomy: The incomplete copying of template margin in enzymic synthesis of polynucleotides and biological significance of the phenomenon. *Journal of Theoretical Biology* 41(1):181-90.

Osborn AJ, Elledge SJ (2003) Mrc1 is a replication fork component whose phosphorylation in response to DNA replication stress activates Rad53. *Genes and Development* 17(14):1755-67.

Paciotti V, Clerici M, Lucchini G, Longhese MP (2000) The checkpoint protein Ddc2, functionally related to S. pombe Rad26, interacts with Mec1 and is regulated by Mec1-dependent phosphorylation in budding yeast. *Genes and Development* 14(16):2046-59.

Palm W, de Lange T (2008) How shelterin protects mammalian telomeres. *Annual Review of Genetics* 42:301-34.

Pardo B, Marcand S (2005) Rap1 prevents telomere fusions by nonhomologous end joining. *The EMBO Journal* 24(17):3117-27.

Paschini M, Mandell EK, Lundblad V (2010) Structure prediction-driven genetics in Saccharomyces cerevisiae identifies an interface between the t-RPA proteins Stn1 and Ten1. *Genetics* 185(1):11-21.

Patel PK, **Arcangioli B**, **Baker SP**, **Bensimon A**, **Rhind N** (2006) DNA replication origins fire stochastically in fission yeast. *Molecular Biology of the Cell* 17(1):308-16.

Paulovich AG, Hartwell LH (1995) A checkpoint regulates the rate of progression through S phase in S. cerevisiae in response to DNA damage. *Cell* 82(5):841-7.

Pavlov YI, Frahm C, Nick McElhinny SA, Niimi A, Suzuki M, Kunkel TA (2006) Evidence that errors made by DNA polymerase alpha are corrected by DNA polymerase delta. *Current Biology* 16(2):202-7.

Pellicioli A, Lucca C, Liberi G, Marini F, Lopes M, Plevani P, Romano A, Di Fiore PP, Foiani M (1999) Activation of Rad53 kinase in response to DNA damage and its effect in modulating phosphorylation of the lagging strand DNA polymerase. *The EMBO Journal* 18(22):6561-72.

Pennock E, Buckley K, Lundblad V (2001) Cdc13 delivers separate complexes to the telomere for end protection and replication. *Cell* 104(3):387-96.

Petreaca RC, Chiu HC, Eckelhoefer HA, Chuang C, Xu L, Nugent CI (2006) Chromosome end protection plasticity revealed by Stn1p and Ten1p bypass of Cdc13p. *Nature Cell Biology* 8(7):748-55.

Petreaca RC, Chiu HC, Nugent CI (2007) The role of Stn1p in Saccharomyces cerevisiae telomere capping can be separated from its interaction with Cdc13p. *Genetics* 177(3):1459-74.

Pfander B, **Diffley JF** (2011) Dpb11 coordinates Mec1 kinase activation with cell cycle-regulated Rad9 recruitment. *The EMBO Journal* 30(24):4897-907.

Pobiega S, Marcand S (2010) Dicentric breakage at telomere fusions. *Genes and Development* 24(7):720-33.

Poli J, Tsaponina O, Crabbé L, Keszthelyi A, Pantesco V, Chabes A, Lengronne A, Pasero P (2012) dNTP pools determine fork progression and origin usage under replication stress. *The EMBO Journal* 31(4):883-94.

Polotnianka RM, Li J, Lustig AJ (1998) The yeast Ku heterodimer is essential for protection of the telomere against nucleolytic and recombinational activities. *Current Biology* 8(14):831-4.

Polvi A, Linnankivi T, Kivelä T, Herva R, Keating JP, Mäkitie O, Pareyson D, Vainionpää L, Lahtinen J, Hovatta I, Pihko H, Lehesjoki AE (2012) Mutations in CTC1, encoding the CTS telomere maintenance complex component 1, cause cerebroretinal microangiopathy with calcifications and cysts. *American Journal of Human Genetics* 90(3):540-9.

Price CM, Boltz KA, Chaiken MF, Stewart JA, Beilstein MA, Shippen DE (2010) Evolution of CST function in telomere maintenance. *Cell Cycle* 9(16):3157-65.

Puglisi A, Bianchi A, Lemmens L, Damay P, Shore D (2008) Distinct roles for yeast Stn1 in telomere capping and telomerase inhibition. *The EMBO Journal* 27(17):2328-39.

Pursell ZF, Isoz I, Lundström EB, Johansson E, Kunkel TA (2007) Yeast DNA polymerase epsilon participates in leading-strand DNA replication. *Science* 317(5834):127-30.

Qi H, Zakian VA (2000) The Saccharomyces telomere-binding protein Cdc13p interacts with both the catalytic subunit of DNA polymerase alpha and the telomerase-associated est1 protein. *Genes and Development* 14(14):1777-88.

Raghuraman MK, Winzeler EA, Collingwood D, Hunt S, Wodicka L, Conway A, Lockhart DJ, Davis RW, Brewer BJ, Fangman WL (2001) Replication dynamics of the yeast genome. *Science* 294(5540):115-21.

Ray S, Karamysheva Z, Wang L, Shippen DE, Price CM (2002) Interactions between telomerase and primase physically link the telomere and chromosome replication machinery. *Molecular and Cellular Biology* 22(16):5859-68.

Ribes-Zamora A, Mihalek I, Lichtarge O, Bertuch AA (2007) Distinct faces of the Ku heterodimer mediate DNA repair and telomeric functions. *Nature Structural and Molecular Biology* 14(4):301-7.

Ricke RM, **Bielinsky AK** (2006) conserved Hsp10-like domain in Mcm10 is required to stabilize the catalytic subunit of DNA polymerase-alpha in budding yeast. *The Journal of Biological Chemistry* 281(27):18414-25.

Romaniello R, Arrigoni F, Citterio A, Tonelli A, Sforzini C, Rizzari C, Pessina M, Triulzi F, Bassi MT, Borgatti R (2012) Cerebroretinal Microangiopathy With Calcifications and Cysts Associated With CTC1 and NDP Mutations. *Journal of Child Neurology*.

Sabatinos SA, Green MD, Forsburg SL (2012) Continued DNA synthesis in replication checkpoint mutants leads to fork collapse. *Molecular and Cellular Biology* 32(24):4986-97.

Sabourin M, Tuzon CT, Zakian VA (2007) Telomerase and Tel1p preferentially associate with short telomeres in S. cerevisiae. *Molecular Cell* 27(4):550-61.

Sampathi S, Chai W (2011) Telomere replication: poised but puzzling. *Journal of Cellular and Molecular Medicine* 15(1):3-13.

Sanchez Y, Desany BA, Jones WJ, Liu Q, Wang B, Elledge SJ (1996) Regulation of RAD53 by the ATM-like kinases MEC1 and TEL1 in yeast cell cycle checkpoint pathways. *Science* 271(5247):357-60.

Sandell LL, Zakian VA (1993) Loss of a yeast telomere: arrest, recovery, and chromosome loss. *Cell* 75(4):729-39.

Santocanale C, Diffley JF (1998) A Mec1- and Rad53-dependent checkpoint controls late-firing origins of DNA replication. *Nature* 395(6702):615-8.

Sarthy J, Bae NS, Scrafford J, Baumann P (2009) Human RAP1 inhibits non-homologous end joining at telomeres. *The EMBO Journal* 28(21):3390-9.

Segurado M, Diffley JF (2008) Separate roles for the DNA damage checkpoint protein kinases in stabilizing DNA replication forks. *Genes and Development* 22(13):1816-27.

Segurado M, Tercero JA (2009) The S-phase checkpoint: targeting the replication fork. *Biology of the Cell* 101(11):617-27.

Sfeir A, Kabir S, van Overbeek M, Celli GB, de Lange T (2010) Loss of Rap1 induces telomere recombination in the absence of NHEJ or a DNA damage signal. *Science* 327(5973):1657-61.

Sfeir A, Kosiyatrakul ST, Hockemeyer D, MacRae SL, Karlseder J, Schildkraut CL, de Lange T (2009) Mammalian telomeres resemble fragile sites and require TRF1 for efficient replication. *Cell* 138(1):90-103.

Shampay J, Szostak JW, Blackburn EH (1984) DNA sequences of telomeres maintained in yeast. *Nature* 310(5973):154-7.

Sheu YJ, **Stillman B** (2006) Cdc7-Dbf4 phosphorylates MCM proteins via a docking site-mediated mechanism to promote S phase progression. *Molecular Cell* 24(1):101-13.

Sheu YJ, Stillman B (2010) The Dbf4-Cdc7 kinase promotes S phase by alleviating an inhibitory activity in Mcm4. *Nature*. 2010 Jan 7;463(7277):113-7.

Sherman F (2002) Getting started with yeast. *Methods is Enzymology* 350:3-41.

Shirahige K, Hori Y, Shiraishi K, Yamashita M, Takahashi K, Obuse C, Tsurimoto T, Yoshikawa H (1998) Regulation of DNA-replication origins during cell-cycle progression. *Nature* 395(6702):618-21.

Shore D, Nasmyth K (1987) Purification and cloning of a DNA binding protein from yeast that binds to both silencer and activator elements. *Cell* 51(5):721-32.

Sikorski RS, Hieter P (1989) A system of shuttle vectors and yeast host strains designed for efficient manipulation of DNA in Saccharomyces cerevisiae. *Genetics* 122(1):19-27.

Singer MS, **Gottschling DE** (1994) TLC1: template RNA component of Saccharomyces cerevisiae telomerase. *Science* 266(5184):404-9.

Smogorzewska A, van Steensel B, Bianchi A, Oelmann S, Schaefer MR, Schnapp G, de Lange T (2000) Control of human telomere length by TRF1 and TRF2. *Molecular and Cellular Biology* 20(5):1659-68.

Sogo JM, Lopes M, Foiani M (2002) Fork reversal and ssDNA accumulation at stalled replication forks owing to checkpoint defects. *Science* 297(5581):599-602.

Song X, Leehy K, Warrington RT, Lamb JC, Surovtseva YV, Shippen DE (2008) STN1 protects chromosome ends in Arabidopsis thaliana. *Proceedings of the National Academy of Sciences* 105(50):19815-20.

Stellwagen AE, Haimberger ZW, Veatch JR, Gottschling DE (2003) Ku interacts with telomerase RNA to promote telomere addition at native and broken chromosome ends. *Genes and Development* 17(19):2384-95.

Stewart JA, Chaiken MF, Wang F, Price CM (2011) Maintaining the end: Roles of telomere proteins in end-protection, telomere replication and length regulation. *Mutation Research* 730(1-2):12-9.

Stewart JA, Wang F, Chaiken MF, Kasbek C, Chastain PD 2nd, Wright WE, Price CM (2012) Human CST promotes telomere duplex replication and general replication restart after fork stalling. *The EMBO Journal* 31(17):3537-49.

Stinchcomb DT, **Struhl K**, **Davis RW** (1979) Isolation and characterisation of a yeast chromosomal replicator. *Nature* 282(5734):39-43.

Sun J, Yu EY, Yang Y, Confer LA, Sun SH, Wan K, Lue NF, Lei M (2009) Stn1-Ten1 is an Rpa2-Rpa3-like complex at telomeres. *Genes and Development* 23(24):2900-14.

Sun J, Yang Y, Wan K, Mao N, Yu TY, Lin YC, DeZwaan DC, Freeman BC, Lin JJ, Lue NF, Lei M (2011) Structural bases of dimerization of yeast telomere protein Cdc13 and its interaction with the catalytic subunit of DNA polymerase α. *Cell Research* 21(2):258-74.

Sun Z, Fay DS, Marini F, Foiani M, Stern DF (1996) Spk1/Rad53 is regulated by Mec1-dependent protein phosphorylation in DNA replication and damage checkpoint pathways. *Genes and Development* 10(4):395-406.

Sun Z, Hsiao J, Fay DS, Stern DF (1998) Rad53 FHA domain associated with phosphorylated Rad9 in the DNA damage checkpoint. *Science* 281(5374):272-4.

Surovtseva YV, Churikov D, Boltz KA, Song X, Lamb JC, Warrington R, Leehy K, Heacock M, Price CM, Shippen DE (2009) Conserved telomere maintenance component 1 interacts with STN1 and maintains chromosome ends in higher eukaryotes. *Molecular Cell* 36(2):207-18.

Szostak JW, Blackburn EH (1982) Cloning yeast telomeres on linear plasmid vectors. *Cell* 29(1):245-55.

Szyjka SJ, Aparicio JG, Viggiani CJ, Knott S, Xu W, Tavaré S, Aparicio OM (2008) Rad53 regulates replication fork restart after DNA damage in Saccharomyces cerevisiae. *Genes and Development* 22(14):1906-20.

Szyjka SJ, Viggiani CJ, Aparicio OM (2005) Mrc1 is required for normal progression of replication forks throughout chromatin in S. cerevisiae. *Molecular Cell* 19(5):691-7.

Taggart AK, Teng SC, Zakian VA (2002) Est1p as a cell cycle-regulated activator of telomere-bound telomerase. *Science* 297(5583):1023-6.

Takata H, Tanaka Y, Matsuura A (2005) Late S phase-specific recruitment of Mre11 complex triggers hierarchical assembly of telomere replication proteins in Saccharomyces cerevisiae. *Molecular Cell* 17(4):573-83.

Takayama Y, Kamimura Y, Okawa M, Muramatsu S, Sugino A, Araki H (2003) GINS, a novel multiprotein complex required for chromosomal DNA replication in budding yeast. *Genes and Development* 17(9):1153-65.

Tanaka S, Diffley JF (2002) Interdependent nuclear accumulation of budding yeast Cdt1 and Mcm2-7 during G1 phase. *Nature Cell Biology* 4(3):198-207.

Tanaka S, Umemori T, Hirai K, Muramatsu S, Kamimura Y, Araki H (2007) CDK-dependent phosphorylation of Sld2 and Sld3 initiates DNA replication in budding yeast. *Nature* 445(7125):328-32.

Tazumi A, Fukuura M, Nakato R, Kishimoto A, Takenaka T, Ogawa S, Song JH, Takahashi TS, Nakagawa T, Shirahige K, Masukata H (2012) Telomere-binding protein Taz1 controls global replication timing through its localization near late replication origins in fission yeast. *Genes and Development* 26(18):2050-62.

Teixeira MT, Arneric M, Sperisen P, Lingner J (2000) Telomere length homeostasis is achieved via a switch between telomerase- extendible and -nonextendible states. *Cell* 117(3):323-35.

Tercero JA, Diffley JF (2001) Regulation of DNA replication fork progression through damaged DNA by the Mec1/Rad53 checkpoint. *Nature* 412(6846):553-7.

Theobald DL, Wuttke DS (2004) Prediction of multiple tandem OB-fold domains in telomere end-binding proteins Pot1 and Cdc13. *Structure* 12(10):1877-9.

Tomita K, Cooper JP. (2008) Fission yeast Ccq1 is telomerase recruiter and local checkpoint controller. *Genes and Development* 22(24):3461-74.

Tomita K, Kibe T, Kang HY, Seo YS, Uritani M, Ushimaru T, Ueno M (2004) Fission yeast Dna2 is required for generation of the telomeric single-strand overhang. *Molecular Cell Biology* 24(21):9557-67.

Tomita K, Matsuura A, Caspari T, Carr AM, Akamatsu Y, Iwasaki H, Mizuno K, Ohta K, Uritani M, Ushimaru T, Yoshinaga K, Ueno M (2003) Competition between the Rad50 complex and the Ku heterodimer reveals a role for Exo1 in processing double-strand breaks but not telomeres. *Molecular Cell Biology* 23(15):5186-97.

Tong AH, Evangelista M, Parsons AB, Xu H, Bader GD, Pagé N, Robinson M, Raghibizadeh S, Hogue CW, Bussey H, Andrews B, Tyers M, Boone C (2001) Systematic genetic analysis with ordered arrays of yeast deletion mutants. *Science* 294(5550):2364-8.

Tseng SF, Shen ZJ, Tsai HJ, Lin YH, Teng SC (2009) Rapid Cdc13 turnover and telomere length homeostasis are controlled by Cdk1-mediated phosphorylation of Cdc13. *Nucleic Acids Research* 37(11):3602-11.

van Steensel B, de Lange T (1997) Control of telomere length by the human telomeric protein TRF1. *Nature* 385(6618):740-3.

van Steensel B, Smogorzewska A, de Lange T. (1998) TRF2 protects human telomeres from end-to-end fusions. *Cell* 92(3):401-13.

Vega LR, Mateyak MK, Zakian VA (2003) Getting to the end: telomerase access in yeast and humans. *Nature Reviews: Molecular Cell Biology* 4(12):948-59.

Verdun RE, Karlseder J (2007) Replication and protection of telomeres. *Nature* 447(7147):924-31.

Viggiani CJ, Knott SR, Aparicio OM (2010) Genome-wide analysis of DNA synthesis by BrdU immunoprecipitation on tiling microarrays (BrdU-IP-chip) in Saccharomyces cerevisiae. *Cold Spring Harbor Protocols* 2010(2):pdb.prot5385.

Vodenicharov MD, Laterreur N, Wellinger RJ (2010) Telomere capping in non-dividing yeast cells requires Yku and Rap1. *The EMBO Journal* 29(17):3007-19.

Vodenicharov MD, Wellinger RJ (2006) DNA degradation at unprotected telomeres in yeast is regulated by the CDK1 (Cdc28/Clb) cell-cycle kinase. *Molecular Cell* 24(1):127-37.

Walne AJ, Bhagat T, Kirwan M, Gitiaux C, Desguerre I, Leonard N, Nogales E, Vulliamy T, Dokal IS (2013) Mutations in the telomere capping complex in bone marrow failure and related syndromes. *Haematologica* 98(3):334-8.

Wan M, Qin J, Songyang Z, Liu D (2009) OB fold-containing protein 1 (OBFC1), a human homolog of yeast Stn1, associates with TPP1 and is implicated in telomere length regulation. *The Journal of Biological Chemistry* 284(39):26725-31.

Wang F, Podell ER, Zaug AJ, Yang Y, Baciu P, Cech TR, Lei M (2007) The POT1-TPP1 telomere complex is a telomerase processivity factor. *Nature* 445(7127):506-10.

Wang F, Stewart JA, Kasbek C, Zhao Y, Wright WE, Price CM (2012) Human CST Has Independent Functions during Telomere Duplex Replication and C-Strand Fill-In. *Cell Reports* 2(5):1096-103.

Watson JD (1972) Origin of concatemeric T7 DNA. *Nature: New Biology* 239(94):197-201.

Watson JD, Crick FH (1953) Molecular structure of nucleic acids; a structure for deoxyribose nucleic acid. *Nature* 71(4356):737-8.

Webb CJ, Zakian VA (2012) Schizosaccharomyces pombe Ccq1 and TER1 bind the 14-3-3-like domain of Est1, which promotes and stabilizes telomerase-telomere association. *Genes and Development* 26(1):82-91.

Weinert TA, Kiser GL, Hartwell LH (1994) Mitotic checkpoint genes in budding yeast and the dependence of mitosis on DNA replication and repair. *Genes and Development* 8(6):652-65.

Weinreich M, Stillman B (1999) Cdc7p-Dbf4p kinase binds to chromatin during S phase and is regulated by both the APC and the RAD53 checkpoint pathway. *The EMBO Journal* 18(19):5334-46.

Wellinger RJ, Sen D (1997) The DNA structures at the ends of eukaryotic chromosomes. *European Journal of Cancer* 33(5):735-49.

Wellinger RJ, Wolf AJ, Zakian VA (1993) Saccharomyces telomeres acquire single-strand TG1-3 tails late in S phase. *Cell* 72(1):51-60.

Wotton D, Shore D (1997) A novel Rap1p-interacting factor, Rif2p, cooperates with Rif1p to regulate telomere length in Saccharomyces cerevisiae. *Genes and Development* 11(6):748-60.

Wu L, Multani AS, He H, Cosme-Blanco W, Deng Y, Deng JM, Bachilo O, Pathak S, Tahara H, Bailey SM, Deng Y, Behringer RR, Chang S (2006) Pot1 deficiency initiates DNA damage checkpoint activation and aberrant homologous recombination at telomeres. *Cell* 126(1):49-62.

Wu P, Takai H, de Lange T (2012) Telomeric 3' Overhangs Derive from Resection by Exo1 and Apollo and Fill-In by POT1b-Associated CST. *Cell* 150(1):39-52.

Wyrick JJ, Aparicio JG, Chen T, Barnett JD, Jennings EG, Young RA, Bell SP, Aparicio OM (2001) Genome-wide distribution of ORC and MCM proteins in S. cerevisiae: high-resolution mapping of replication origins. *Science* 294(5550):2357-60.

Xin H, Liu D, Wan M, Safari A, Kim H, Sun W, O'Connor MS, Songyang Z (2007) TPP1 is a homologue of ciliate TEBP-beta and interacts with POT1 to recruit telomerase. *Nature* 445(7127):559-62.

Xu L (2009) Dissertation. University of California, Riverside, Graduate program in Cell, Molecular and Developmental Biology.

Xu L, Petreaca RC, Gasparyan HJ, Vu S, Nugent CI (2009) TEN1 is essential for CDC13-mediated telomere capping. *Genetics* 183(3):793-810.

Yabuuchi H, **Yamada Y**, **Uchida T**, **Sunathvanichkul T**, **Nakagawa T**, **Masukata H** (2006) Ordered assembly of Sld3, GINS and Cdc45 is distinctly regulated by DDK and CDK for activation of replication origins. *The EMBO Journal* 25(19):4663-74.

Yamazaki H, Tarumoto Y, Ishikawa F (2012) Tel1(ATM) and Rad3(ATR) phosphorylate the telomere protein Ccq1 to recruit telomerase and elongate telomeres in fission yeast. *Genes and Development* 26(3):241-6.

Yan H, Gibson S, Tye BK (1991) Mcm2 and Mcm3, two proteins important for ARS activity, are related in structure and function. *Genes and Development* 5(6):944-57.

Yan S, Michael WM (2009) TopBP1 and DNA polymerase-alpha directly recruit the 9-1-1 complex to stalled DNA replication forks. *The Journal of Cell Biology* 184(6):793-804.

Yan S, Michael WM (2009) TopBP1 and DNA polymerase alpha-mediated recruitment of the 9-1-1 complex to stalled replication forks: implications for a replication restart-based mechanism for ATR checkpoint activation. *Cell Cycle* 8(18):2877-84.

Ye J, Lenain C, Bauwens S, Rizzo A, Saint-Léger A, Poulet A, Benarroch D, Magdinier F, Morere J, Amiard S, Verhoeyen E, Britton S, Calsou P, Salles B, Bizard A, Nadal M, Salvati E, Sabatier L, Wu Y, Biroccio A, Londoño-Vallejo A, Giraud-Panis MJ, Gilson E (2010) TRF2 and apollo cooperate with topoisomerase 2alpha to protect human telomeres from replicative damage. *Cell* 142(2):230-42.

Ye JZ, Donigian JR, van Overbeek M, Loayza D, Luo Y, Krutchinsky AN, Chait BT, de Lange T (2004) TIN2 binds TRF1 and TRF2 simultaneously and stabilizes the TRF2 complex on telomeres. *The Journal of Biological Chemistry* 279(45):47264-71.

Zegerman P, Diffley JF (2007) Phosphorylation of Sld2 and Sld3 by cyclin-dependent kinases promotes DNA replication in budding yeast. *Nature* 445(7125):281-5.

Zegerman P, Diffley JF (2010) Checkpoint-dependent inhibition of DNA replication initiation by Sld3 and Dbf4 phosphorylation. *Nature* 467(7314):474-8.

Zhang W, Durocher D (2010) De novo telomere formation is suppressed by the Mec1-dependent inhibition of Cdc13 accumulation at DNA breaks. *Genes and Development* 24(5):502-15.

Zhao X, Muller EG, Rothstein R (1998). A suppressor of two essential checkpoint genes identifies a novel protein that negatively affects dNTP pools. *Molecular Cell* 2(3):329-40.

Zhao Y, Hoshiyama H, Shay JW, Wright WE (2008) Quantitative telomeric overhang determination using a double-strand specific nuclease. *Nucleic Acids Research* 36(3):e14.

Zhao Y, Sfeir AJ, Zou Y, Buseman CM, Chow TT, Shay JW, Wright WE (2009) Telomere extension occurs at most chromosome ends and is uncoupled from fill-in in human cancer cells. *Cell* 138(3):463-75.

Zhong Y, Nellimoottil T, Peace JM, Knott SR, Villwock SK, Yee JM, Jancuska JM, Rege S, Tecklenburg M, Sclafani RA, Tavaré S, Aparicio OM (2013) The level of origin firing inversely affects the rate of replication fork progression. *The Journal of Cell Biology* 201(3):373-83.

Zhou Z, Elledge SJ (1993) DUN1 encodes a protein kinase that controls the DNA damage response in yeast. *Cell* 75(6):1119-27.

Zou L, Elledge SJ (2003) Sensing DNA damage through ATRIP recognition of RPA-ssDNA complexes. *Science* 300(5625):1542-8.

Zubko MK, Lydall D (2006) Linear chromosome maintenance in the absence of essential telomere-capping proteins. *Nature Cell Biology* 8(7):734-40.